

PATHOPHYSIOLOGY AND TOXICOKINETIC STUDIES OF BLUE-GREEN ALGAE
INTOXICATION IN THE SWINE MODEL

20030129086

ANNUAL REPORT

Val R. Beasley
Wanda M. Haschek-Hock
Wayne W. Carmichael
William O. Cook
Andrew M. Dahlem
Stephen B. Hooser
Randall A. Lovell
Nik A. Mahmood
William M. Valentine

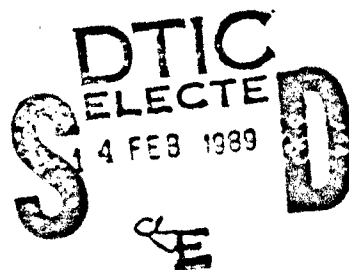
AUGUST 31, 1987

Supported by

U.S. ARMY MEDICAL RESEARCH AND DEVELOPMENT COMMAND
Fort Detrick, Frederick, Maryland 21701-5012

Contract No. DAMD17-85-C-5241

University of Illinois
2001 South Lincoln Avenue
Urbana, IL 61801



Approved for public release; distribution unlimited

The findings in this report are not to be construed as an official Department
of the Army position unless so designated by other authorized documents.

89 2 13 273

AD-A203 948

REPORT DOCUMENTATION PAGE				Form Approved OMB No. 0704-0188	
1a. REPORT SECURITY CLASSIFICATION UNCLASSIFIED			1b. RESTRICTIVE MARKINGS		
2a. SECURITY CLASSIFICATION AUTHORITY			3. DISTRIBUTION/AVAILABILITY OF REPORT Approved for public release; distribution unlimited.		
2b. DECLASSIFICATION/DOWNGRADING SCHEDULE			5. MONITORING ORGANIZATION REPORT NUMBER(S)		
4. PERFORMING ORGANIZATION REPORT NUMBER(S)			7a. NAME OF MONITORING ORGANIZATION		
6a. NAME OF PERFORMING ORGANIZATION University of Illinois		6b. OFFICE SYMBOL (If applicable)	7b. ADDRESS (City, State, and ZIP Code)		
6c. ADDRESS (City, State, and ZIP Code) 2001 South Lincoln Avenue Urbana, Illinois 61801			9. PROCUREMENT INSTRUMENT IDENTIFICATION NUMBER DAMD17-85-C-5241		
8a. NAME OF FUNDING/SPONSORING ORGANIZATION U.S. Army Medical Research & Development Command		8b. OFFICE SYMBOL (If applicable)	10. SOURCE OF FUNDING NUMBERS		
8c. ADDRESS (City, State, and ZIP Code) Fort Detrick Frederick, Maryland 21701-5012			PROGRAM ELEMENT NO. 61102A	PROJECT NO. 3M1 61102BS12	TASK NO. AA
8d. ADDRESS (City, State, and ZIP Code) Fort Detrick Frederick, Maryland 21701-5012			WORK UNIT ACCESSION NO. 006		
11. TITLE (Include Security Classification) (U) Pathophysiology and Toxicokinetic Studies of Blue-Green Algae Intoxication in the Swine Model					
12. PERSONAL AUTHOR(S) V.R. Beasley, W.M. Haschek-Hock, W.W. Carmichael, W.O. Cook, A.M. Dahlem, S.B. Hooser, R.A. Lovell, N.A. Mahmood, and W.M. Valentine					
13a. TYPE OF REPORT Annual		13b. TIME COVERED FROM 9/1/86 TO 8/31/87		14. DATE OF REPORT (Year, Month, Day) 1987 August 31	
15. PAGE COUNT 250					
16. SUPPLEMENTARY NOTATION					
17. COSATI CODES			18. SUBJECT TERMS (Continue on reverse if necessary and identify by block number)		
FIELD	GROUP	SUB-GROUP	Blue-green algae, phycotoxin, microcystin, cyanoginosin		
06	16		anatoxin-a(s), pathophysiology, radiolabelled toxin,		
06	20		analysis, RA 1		
19. ABSTRACT (Continue on reverse if necessary and identify by block number) Microcystin-A (MCYST-A) is isolated from algal extracts on an ODS column, followed by silica gel separation. Purity is checked with silica gel TLC with 2 detection reagents and reverse phase HPLC with UV at 238 nm. Mobile phases developed to enable MCYST-B to be used as an internal standard for MCYST-A analyses include: methanol/0.05% trifluoroacetic acid (6:4); or methanol/1M sodium sulfate (1:1). Plasma and urine samples containing MCYST-A were placed on ODS columns, washed with water, and 15% methanol in water. Toxin was eluted with methanol and membrane filters were used to remove protein precipitates from plasma extracts before HPLC. Recovery was 92% from urine and 63% from plasma. MCYST-A was radiolabelled with ³ H or ¹⁴ C by addition of labeled glutamic acid to growing <i>M. aeruginosa</i> .					
20. DISTRIBUTION/AVAILABILITY OF ABSTRACT <input type="checkbox"/> UNCLASSIFIED/UNLIMITED <input checked="" type="checkbox"/> SAME AS RPT. <input type="checkbox"/> DTIC USERS			21. ABSTRACT SECURITY CLASSIFICATION Unclassified		
22a. NAME OF RESPONSIBLE INDIVIDUAL Mary Frances Bostian			22b. TELEPHONE (Include Area Code) 301-663-7325		22c. OFFICE SYMBOL SGRD-RMI-S

MCYST-A has low acute oral toxicity in laboratory animals. In vivo isolated intestinal loops of the rat permit modelling of absorption, which appears more efficient in the ileum than the jejunum. Cholestyramine decreased the toxic effect of MCYST-A. Pancreatic enzymes and bovine serum albumin caused similar reductions in toxicity, suggesting nonspecific protein binding. Saturation at the N-methyldehydroalanine of MCYST-A lessens hepatotoxicity to i.p. dosed mice.

Primary ultrastructural lesions in hepatocytes observed after injection of rats with MCYST-A include plasma membrane invagination, and loss of microvilli, dissociation, and rounding. Plasma membrane changes occur within 10 min. of i.p. dosing. Sinusoidal endothelial damage may be secondary. Sinusoidal endothelial disruption advances more rapidly in mice, permitting more severe intrahepatic hemorrhage and shock.

In swine given a lethal dose of MCYST-A, increases in portal venous pressure occur before large reductions in mean aortic pressure. Reductions in hepatic perfusion occur before declines in renal perfusion and mean aortic pressure.

Mean tissue arginase activities of swine were: liver 34.01, pancreas 5.43, kidney 3.24, salivary gland 0.52, jejunal mucosa 0.47, and quadriceps 0.10 IU/g. Other tissues tested were ≤ 0.03 IU/g. Mean serum arginase activity was 2.29 IU/L, and half-lives were 128.5 min. in a gilt and 85.8 min. in a barrow. Serum arginase exceeded 240 IU/L 14 hr after a sublethal IV dose (16 ug/kg) of MCYST-A, and returned to near baseline values by 24 hr. Within 5.5 hr, the serum arginase activity of a pig given a lethal IV dose (24 ug/kg) was 1,450 IU/L.

Liver weights increased 51% and kidney weights 20% within 200 minutes of an i.p. LD₁₀₀ min of MCYST-A in naive mice. Administration of a LD₂₃ of MCYST-A resulted in significantly increased survivability and survival time when an LD₁₀₀ min of MCYST-A was given 3 days later. Survivors were weak, recumbent, anorexic, and jaundiced and had marked gross liver lesions. Histologically these lesions were undergoing a rapid reparative process.

After injection of antx-a(s), no inhibition of brain cholinesterase (ChE) was observed in mice. ChE in plasma, red blood cells, and diaphragm tissue were inhibited longer than with pyridostigmine but similar to paraoxon. RBC ChE was highly susceptible to persistent in vivo inhibition by antx-a(s).

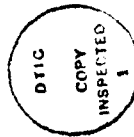
Ethanol acidified with acetic acid and 2 concentrations of trifluoroacetic acid were evaluated for extraction of antx-a(s) in place of gel filtration. The 3 new extraction solvents decreased pigments in the extracts. Extracts obtained with acidified ethanol had 50% more activity than those obtained with trifluoroacetic acid. With the Amberlite IRP 64 column, approximately 80% pure antx-a(s) was obtained. Using purified antx-a(s), the equilibrium (k_d), "phosphorylation" (k_p), and inhibition (k_i) constants for inhibition of electric eel and human erythrocyte ChEs were determined. Data were consistent with formulation of a reversible Michaelis complex followed by an irreversible complex. Antx-a(s) was more potent than DFP. The toxin was a more potent inhibitor of human erythrocyte ChE as compared to electric eel ChE.

- 1/2

FOREWORD

In conducting research using animals, the investigator(s) adhered to the "Guide for the Care and Use of Laboratory Animals," prepared by the Committee on Care and Use of Laboratory Animals of the Institute of Laboratory Animal Resources Commission on Life Sciences, National Research Council (DHHS, PHS, NIH Publications No. 86-23, Revised 1985).

Citations of commercial organizations and trade names in this report do not constitute an official Department of the Army endorsement or approval of the products or services of these organizations.



Accession For	
NTIS CRA&I	<input checked="checked" type="checkbox"/>
DTIC TAB	<input type="checkbox"/>
Unannounced	<input type="checkbox"/>
Justification	
By	
Distribution	
Availability Codes	
Dist	Avail and/or Special
A-1	

4/3/86

TABLE OF CONTENTS

	<u>Page</u>
FOREWORD	1
SUMMARY	5
I. Studies on the intestinal absorption of microcystin-A in rats . . .	12
II. Improved purification method for cyclic peptides produced by cyanobacteria	32
III. Structure/toxicity relationship of the N-methyldehydroalanine moiety of microcystin-A	44
IV. Development of urine and plasma extraction methods for microcystin-A	53
V. Oral toxicity of microcystin-A	59
VI. The effect of glutathione depletion on the IP toxicity of microcystin-A	63
VII. Visualization of rat hepatocytes within the pulmonary vasculature via microscopic radiography	65
VIII. Biosynthetic radiolabeling of microcystin-A	67
IX. Evaluation of enzyme release by primary cultures of hepatocytes following exposure to microcystin-A.	70
X. Sequential hepatic, pulmonary, and renal ultrastructural changes induced by microcystin-A (cyanoginosin LR) in rats	72
XI. Effects of microcystin-A on hepatic, and renal blood flow, and mean aortic pressure in intravenously dosed swine	96
XII. Arginase activity in twelve tissues and serum, serum arginase half-life and changes in serum arginase activity following administration of microcystin-A (cyanoginosin LR) in swine	123
XIII. Toxicity of one or two intraperitoneal doses of microcystin-A in two strains of male mice	138
XIV. Inhibition of brain cholinesterase and reversibility of plasma, red blood cell, and diaphragm cholinesterase in mice after injection of anatoxin-a(s) compared to carbamate and organophosphorous agents	157
XV. Neurobehavioral effects of nicotine, atropine, paraoxon, and physostigmine on Long-Evans rats	171
XVI. Anatoxin-a(s) purification and inhibition of electric eel and human erythrocyte acetylcholinesterase	186

SUMMARY

→ The need to conserve toxin and the goal of creating a model for naturally occurring toxicosis caused us to evaluate the oral administration of microcystin-A (MCYST-A) to rodents. But in practice, purified MCYST-A has demonstrated low acute toxicity when administered to laboratory animals by the oral route. Development of an in vivo isolated intestinal loop preparation in the rat has provided a model system for investigating the enteric absorption site of MCYST-A on toxicity. Using this system, MCYST-A toxicity was observed to be greater from the ileum than the jejunum as measured by increased liver weight. Also, cholestyramine was evaluated as a therapeutic agent and found to decrease the toxicity of MCYST-A when administered with the toxin into the isolated ileal loop preparation. Pancreatic enzymes and protein-binding were examined as 2 possible causes for the low oral toxicity of MCYST-A. Pancreatic enzymes added to MCYST-A in the ileum or incubated with the toxin before introduction into the ileum lowered its toxicity. Addition of bovine serum albumin to MCYST-A placed in the isolated ileal loop caused a similar reduction in toxicity suggesting that nonspecific protein-binding may play a role in the tolerance of laboratory animals to orally administered toxin. *Keywords:*

Methodology for the extraction of MCYST-A from algae cells has been improved. Separation on an ODS column followed by silica gel separation and normal phase silica gel thin-layer chromatography with 2 detection reagents and reverse phase HPLC with UV detection at 238 nm is now being used. The combination of reversed phase and normal phase separations excludes more of the co-existing contaminants in toxin fractions than did previous methods. This procedure also eliminates costly and time consuming gel filtration steps. This method has been used to produce purified toxin equivalent to 0.2% to 0.3% of the weight of lyophilized cells in 3 to 4 days.

Phytotoxins, Microsistis, Microsistis aeruginosa

The contribution of the unsaturation present in the N-methyl dehydroalanine residue to toxicity was determined for MCYST-A. Selective saturation at this site resulted in a 50% reduction in toxicity as assessed by increases of liver weight in mice. A decrease of 75% was observed for a similar saturation of the N-methyl aminobutyric acid of Modularia toxin (1986 annual report). These results verify the importance of the dehydroamino acids in the toxicity of algal cyclic peptide hepatotoxins.

Preliminary experiments to extract MCYST-A from swine urine and plasma have been performed. MCYST-A was added to plasma and urine at 10 µg/ml and 20 µg/ml, respectively. The plasma and urine were then subjected to separation by Bond Elut (ODS) columns washed with water, then 15% methanol in water, and the toxin was eluted with methanol and analyzed by HPLC. Filtration through Acro 0.2 µm membrane filters was used to remove insoluble protein precipitates in plasma extracts before analysis by HPLC. Recovery from urine was 92% and from plasma 63%. This technique is now being applied to urine from swine dosed with MCYST-A.

Mobile phases have been developed to achieve separation of MCYST-A from MCYST-B. These phases are methanol--0.05% trifluoroacetic acid in a ratio of 6:4; or methanol--1M sodium sulfate in a ration of 1:1. This separation will enable the use of MCYST-B as an internal standard for MCYST-A for both methods development and metabolism studies.

Radiolabeling of MCYST-A with ³H or ¹⁴C by addition of labeled glutamic acid to the growth media of MCYST-A has been accomplished. A proportional relationship between the amount of labeled glutamic acid and the resultant specific activity of the toxin produced was observed. Incorporation of tritiated L glutamic acid resulted in toxin with a lower specific activity

than incorporation of D-L mixtures of ^{14}C -labeled glutamic acid. This addition of isotopically labeled glutamic acid to growth media for production of radioactive labeled toxin provides an alternative to synthetic labeling.

Transmission electron microscopy has revealed hepatic, renal, and pulmonary ultrastructural changes occurring in rats as a consequence of MCYST-A toxicosis. Primary ultrastructural lesions observed after MCYST-A administration include changes in the plasma membrane of hepatocytes and coincide with the hepatocyte dissociation and rounding observed by light microscopy. Changes in the plasma membrane of hepatocytes occur within 10 minutes of intraperitoneal administration of a lethal dose of MCYST-A. These initial ultrastructural changes could be due to primary effects on the plasma membrane or some component of the cellular cytoskeleton. The fact that hepatocyte changes precede all other ultrastructural alterations observed in this organ suggests that this cell is a primary site of action and that sinusoidal endothelial damage occurs secondarily. The differences in sequential hepatic ultrastructural changes observed in rats, compared to those reported for mice, provide a possible explanation for the longer survival time of rats. Sinusoidal endothelial disruption advances more rapidly in mice than in rats permitting more severe intrahepatic hemorrhage and an earlier onset of terminal circulatory shock.

Hepatic and renal perfusion in swine following administration of a lethal or sublethal toxic dose of MCYST-A are being measured using the temperature pulse decay method. Aortic diastolic and systolic pressures and mean venous pressure in the jugular and portal vein are also being monitored. Preliminary analysis of the data indicates an increase in portal venous pressure occurring prior to the large fall in mean aortic pressure in animals administered a

lethal dose of MCYST-A. Reductions in hepatic perfusion in pigs given lethal doses tend to occur before the decline in renal perfusion and mean aortic pressure.

The arginase activity in 12 tissues and serum, serum arginase half-life, and increases in serum arginase activity following IV administration of a sublethal and lethal dose of MCYST-A in swine were determined. Mean tissue arginase activity of 6 swine measured by a direct colorimetric method were as follows: liver 34.01, pancreas 5.43, kidney 3.24, salivary gland 0.52, jejunal mucosa 0.47, quadriceps 0.10, and all other tissues (lung, diaphragm, brain, adrenal, spleen, and heart) were equal to or less than 0.03 IU/g. The mean serum arginase activity in these 6 swine was 2.29 IU/L. Following an IV injection of 2.0 ml/kg of a porcine liver extract containing 145 IU arginase activity/ml, the serum arginase half-life was 128.5 minutes in a gilt and 85.8 minutes in a barrow. MCYST-A induced marked increases in serum arginase activity which were dose-dependent with respect to latency and magnitude. The serum arginase activity exceeded 240 IU/L 14 hours after a sublethal IV dose (16 µg/kg) of MCYST-A, and returned to near baseline values by 24 hours postdosing. The lethal IV dose (24 µg/kg) of MCYST-A produced a serum arginase activity of approximately 1,450 IU/L, and death within 5.5 hours of administration. Serum arginase activity never exceeded 22 IU/L during the 24-hour postdosing period in a gilt administered the ethanol/saline vehicle.

Swiss Webster (SW) mice were administered various ip doses of MCYST-A to establish dose-response curves and to determine whether a sublethal dose of the toxin would provide protection against an LD₁₀₀ min given subsequently. Liver weights increased 51%; and kidney weights increased 20% within 200 minutes following administration of an LD₁₀₀ min of MCYST-A in naive mice.

Grossly and histologically the marked increase in liver weight appeared to be caused primarily by intrahepatic hemorrhage. In C₅₇ mice, administration of an LD₂₃ of MCYST-A resulted in significantly increased survivability and survival time when an LD₁₀₀ min of MCYST-A was given 3 days later. Survivors of the LD₂₃/LD₁₀₀ min regimen had 96-hour postdosing liver weights not significantly different from those of mice which died acutely after the same hepatotoxin treatments. These survivors showed weakness, recumbency, anorexia, and jaundice and had marked gross liver lesions. Histologically these lesions were undergoing rapid reparative processes.

The in vivo effect of anatoxin-a(s) [antx-a(s)] on mouse brain acetyl-cholinesterase activity and the reversibility of antx-a(s)-induced inhibition of mouse plasma, red blood cell, and diaphragm cholinesterase have been characterized. The effects of antx-a(s) upon certain of these parameters were compared to the effects of physostigmine salicylate, pyridostigmine bromide, and paraoxon. No inhibition of whole brain acetylcholinesterase was observed in mice that died or those killed 24 hours after an injection of antx-a(s) suggesting that antx-a(s) does not act centrally. Antx-a(s) inhibited cholinesterases in plasma, red blood cells, and diaphragm tissue longer than pyridostigmine with a duration of action similar to paraoxon. Red blood cell acetylcholinesterase was the most susceptible to persistent in vivo inhibition by antx-a(s). The results of this investigation indicate that antx-a(s) is a peripheral acting, irreversible inhibitor of cholinesterase.

Figure-8 maze activity, accelerating rotarod performance, grip strength, and startle response have been used as neurobehavioral endpoints in rats intraperitoneally administered atropine sulfate, nicotine, paraoxon, and physostigmine. These tests have been conducted as a means of standardizing

instrumentation and for future comparison to antx-a(s). With atropine, nicotine, and physostigmine, the neurobehavioral tests detected decrements that were reversible in nature. Physostigmine and nicotine caused decrements in exploratory activity in the figure-8 maze that were indicative of centrally acting toxicants. At the doses used, paraoxon affected sensory and exploratory behavior without detectable effects upon neuromuscular or balancing performance. Completion of these experiments will provide a data base for these known toxicants for comparison with antx-a(s).

Ethanol acidified with acetic acid and 2 concentrations of trifluoroacetic acid have been evaluated for extraction of antx-a(s). In addition, cation exchange has been used in place of gel filtration for the first purification step. The 2 new extraction solvents decreased the concentrations of pigments in the extracts. Extracts obtained with acidified ethanol showed 50% greater activity than those obtained with trifluoroacetic acid. Two cationic exchange columns, containing Dowex 50 and benzene sulfonic acid, produced samples with too high a salt content for further purification with HPLC. With the Amberlite IRP 64 column, it was possible to obtain antx-a(s) of approximately 80% purity. This process took 2 weeks and produced an average of 0.1 mg of toxin from 10 grams of lyophilized Anabaena flos-aqua cells.

Using purified antx-a(s), the equilibrium (k_d), "phosphorylation" (k_2), and inhibition (k_i) constants for inhibition of electric eel and human erythrocyte acetylcholinesterases were determined. The data indicates an initial formation of a reversible Michaelis complex followed by the formation of an irreversible complex. This is similar to the inhibition observed with known irreversible organophosphorus compounds. Antx-a(s) was found to be a more potent inhibitor than the organophosphorus compound DFP, to have a higher

affinity, and to produce greater inhibition of human erythrocyte acetylcholinesterase than of electric eel acetylcholinesterase.

I. STUDIES ON THE INTESTINAL ABSORPTION OF MICROCYSTIN-A IN RATS

Andrew M. Dahlem, Aslam S. Hassan, Bernard S. Buetow

ABSTRACT

Rats were used to evaluate a model system for studying the hepatotoxicity caused by microcystin-A (MCYST-A), a cyclic peptide toxin produced by Microcystis aeruginosa, and for evaluating the in vivo therapeutic potential of cholestyramine resin (CTR) which was found to bind the toxin in vitro. Also, the effect of pancreatic enzymes and protein binding on the toxicity of MCYST-A was examined in order to investigate factors which might contribute to the observed low oral toxicity of purified toxin.

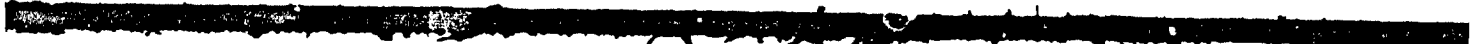
Female rats were randomly assigned to 1 of 2 groups and treated with either toxin or an equivalent volume of saline vehicle instilled directly into the lumen of an in situ isolated ileal loop. Male rats were dosed with toxin as described above, and then randomly selected animals were dosed with either cholestyramine resin (CTR) (50 mg/rat) or an equivalent volume of vehicle infused into the ileal loop. In a related experiment, toxin was infused into either the isolated ileum or a similarly isolated section of the jejunum and the resultant toxic effect was evaluated. Additionally, 18 fasted male Harlan Sprague-Dawley rats were randomly assigned to 1 of 3 groups. Group 1 was given microcystin-A (MCYST-A) at a dose of 2.5 mg/kg in H₂O administered directly into a segment of isolated ileum. Group 2 animals were given a rat acetone pancreas extract (50 mg) which had been preincubated for 2 hours in 0.1 M phosphate buffer at 37° before being infused into an ileal segment. Group 3 animals were given the 2.5 mg/kg dose of MCYST-A after it had been preincubated in an enzyme solution identical to that given to group 2 animals

(ratio of toxin:pancreas extract protein of 1:50). Finally, 12 male Harlan Sprague-Dawley rats were randomly assigned to 1 of 2 test groups and dosed either with MCYST-A at 2.5 mg/kg or with MCYST-A at 2.5 mg/kg after its preincubation for 2 hours with bovine serum albumin (BSA) in a ratio of toxin to protein of 1:50. Toxin was administered via the ileal loop as described above.

The animals in all studies were killed 6 hours postdosing and hepatotoxicity was assessed by change in liver weight as a percent of whole body weight. In all groups given toxin alone, there was a significant increase in liver weight. No sex-related differences in the response to the toxin were evident. Liver weights of the toxin plus CTR treated rats were similar to those in vehicle-treated rats. When the toxin was administered into an isolated jejunal loop, liver weight was significantly less than that resulting from an equivalent dose administered via the ileal loop. Rats given toxin alone had relative liver weights which were significantly greater than those given toxin preincubated with pancreatic extract; and the relative liver weights of the latter animals were significantly greater than those given pancreatic extract alone. The relative liver weights of rats dosed with toxin alone were significantly greater than those of animals given toxin preincubated with BSA.

INTRODUCTION

Toxic blooms of blue-green algae have been reported to cause livestock deaths in many countries throughout the world (Carmichael, 1981; Schwimmer and Schwimmer, 1968). More recently human toxicosis has been implicated following the occurrence of cyanobacterial blooms in municipal water supplies (Falconer et al., 1983). One species often associated with toxic bloom formation is



Microcystis aeruginosa (Carmichael, 1982; Watanabe et al., 1980). Isolation and analysis of toxic materials from Microcystis cells has identified monocyclic heptapeptides containing several unusual amino acids (Botes, 1984; Krishnamurthy, 1986). Microcystin-A (cyanoginosin-LR, toxin BE-2) is the principal toxic peptide produced by a laboratory isolate of M. aeruginosa strain PCC-7820. This toxin (Figure 1) has a molecular weight of 994 daltons, and produces characteristic toxic effects when injected into laboratory animals. A reproducible feature of the toxicosis is elevation in liver weight due to hepatocyte necrosis with destruction of sinusoidal endothelium and extensive hemorrhage into the hepatic parenchyma (Falconer et al., 1981; Jackson et al., 1984).

In preliminary studies we had previously attempted to produce hepatotoxic effects using purified toxin or doses of lyophilized cell suspension administered orally. However, even at oral doses greater than 30 times the IP or IV LD₁₀₀ (300 µg/kg IP, rat), we were unable to produce any toxic effects. Therefore, the objective of this study was to design an in vivo model system to study the absorption of the toxin from various segments of the gastrointestinal tract as assessed by significant increases in liver weight as a percent of whole body weight in rats. Additionally, since the toxin is an anion, we tested the hypothesis that an anion exchange resin, cholestyramine (CTR), would bind it and thereby reduce its hepatotoxic potential. Finally, since the toxin is unprotected by the cell membrane when administered in purified form, we tested the hypothesis that pancreatic enzyme degradation was responsible for the apparent low oral toxicity.

MATERIALS AND METHODS

Toxin

M. aeruginosa strain PCC-7820 is in continuous culture in the laboratories of Wright State University, Dayton, Ohio. Algae for this experiment was grown on BG-11 media (Carmichael, 1984) and harvested following conclusion of log phase algal growth. The cells were filtered and dried, and the toxin extracted as described by Krishnamurthy et al. (1986). Toxin purity was evaluated on Whatman KGF normal phase high performance silica TLC plates (American Scientific Products, McGaw Park, IL) as described by Harada et al. (1987) and additionally by HPLC with UV detection at 240 nm. Toxin purity was assessed to be > 95% by all methods described. The peptide was then subjected to fast atom bombardment/mass spectrometry using a ZAB 10 kv mass spectrometer. The toxin was embedded in "magic bullet" matrix (1:3, dithiothreitol-dithioerythritol). The source temperature was 30°C and the target was bombarded with xenon atoms at 9 kv. A characteristic mass of 995 (M + H⁺) was observed (Figure 2).

In vitro Studies

CTR resin (Bristol-Myers, Evansville, IN) was combined with deionized water (50 mg/ml) and mixed on a rocker mixer for 2 hours prior to the addition of toxin. Varying amounts of MCYST-A were added in triplicate to tubes containing 50 mg CTR. All the samples were then mixed on a rocker mixer for 15 minutes. Next, the samples were filtered through a 0.2 µ Acro LC13 disposable filter membrane (Gelman, Ann Arbor, MI). The filtrate was then injected into a Spectra Physics 8800 ternary gradient HPLC system equipped with a Whatman Partisphere C-18 column (4.6 x 120 mm) using a flow rate of 1.0 ml/min and UV detection at 240 nm. The mobile phase was 0.01 M ammonium

acetate (pH 6) and acetonitrile in a ratio of 75:25. The detection limit was 0.02 µg/ml.

Animal Experiments

Sprague-Dawley rats of either sex (Harlan Industries, Indianapolis, IN) weighing between 93 to 144 g, were used for all experiments. Food and water were available ad libitum for at least a 1-week acclimation period. Prior to the study, the animals were subjected to an overnight fast (16 hours) in cages with wire mesh floors to avoid any contact with bedding material. Water was available at all times.

Rats were anesthetized with ether, weighed to the nearest 0.1 g, and placed in dorsal recumbency on a heating pad. The abdomen was opened using a midline incision. To isolate an in situ ileal loop (Figure 3), a ligature was placed around the ileum approximately 5 cm proximal to the ileo-cecal junction (ligature A). Ten to 15 cm proximal to ligature A, a second ligature was placed around the ileum (ligature B). A small incision was made on the antimesenteric side of the isolated ileal segment immediately proximal to ligature A, and 2 ml of normal saline followed by 1 ml of air was instilled gently near ligature B to flush the intestinal contents out through the antimesenteric incision. A third ligature (ligature C) was then used to tie off the area of intestine containing the antimesenteric incision and a fourth ligature (ligature D) was tied around the 30 g needle which had been introduced into the intestinal lumen in order to administer the test solution into the loop. Following the injection, the needle was removed, the intestinal segment was examined for leakage, and returned to the body cavity. The abdominal incision was closed with 9 mm Autoclip wound clips (Clay Adams, Parsippany, NJ). To isolate an in situ jejunal loop, ligature A was tied 5 cm

distal to the ligament of Treitz and ligature B was placed approximately 10 to 15 cm distal to ligature-A. The loop was flushed, toxin injected, and additional ligatures tied as described above.


In the case of CTR treatment, the experiment was identical to that described with regard to the toxin administration into the ileal loop, except that ligature D was tied around an 18-gauge needle and experimental solutions were administered through a 3-way stopcock. Thirty seconds postadministration of toxin, either 50 mg of CTR in 0.5 ml of H₂O, or an equivalent volume of saline was administered.

In the case of either the pancreatic acetone extract (PAX) or the bovine serum albumin (BSA), the experiment was identical to that described above for toxin administration except that either the PAX or BSA was preincubated with toxin for 3 hours prior to administration.

In all cases, care was taken not to ligate the blood supply to the segment of interest, and intestinal loops were removed at the end of the study and examined to make certain leakage had not occurred. Following surgery, the animals were allowed to recover from the anesthesia. All rats were killed with ether at 6 hours after treatment. The livers were immediately removed, blotted dry, and weighed. The liver weight was expressed as a percent of total body weight. Differences between selected groups were analyzed using the Student's one-tailed t-test for unpaired means; a level of $\alpha = 0.05$ was chosen to identify significant differences.

RESULTS

Within 6 hours after infusion of a single dose of MCYST-A (5 mg/kg) into the isolated ileum, the animals experienced labored breathing and appeared to be in a state of circulatory shock. As shown in Figure 4, there was a



significant increase in liver weight of the rats given the toxin when compared to vehicle-treated controls. There were no differences in liver weights between male and female rats given the same dose of toxin (5 mg/kg) into the ileal loop (females, 7.2 ± 0.2 [N = 4] vs. males, 7.0 ± 0.2 [N = 5]; mean \pm SEM).

When the toxin was infused into the ileal loop at a dose of 2.5 mg/kg body weight, the liver weights were significantly greater than controls, but significantly less than in animals dosed in the same manner at 5 mg/kg body weight. As shown in Figure 5, in this dose range, there was a linear relationship between toxin dose and liver weight. When toxin at 5 mg/kg body weight was instilled into the jejunal loop, liver weight was significantly lower than that obtained with an equivalent dose of toxin infused into the ileal loop (ileum, 7.0 ± 0.2 [N = 5] vs. jejunum, 6.0 ± 0.1 [N = 3], mean \pm SEM). Interestingly, the liver weight in animals dosed at 2.5 mg/kg via the ileal loop was virtually the same as that found in animals given 5 mg/kg via the jejunal loop (Figure 6).

Cholestyramine resin was found to bind MCYST-A over the range of CTR to toxin ratios tested in vitro (Table 1). Furthermore, rats treated via the ileal loop with toxin at 5 mg/kg followed by CTR had liver weights which were very similar to those of vehicle-treated controls and significantly less than in animals dosed with toxin alone at 5 mg/kg (Figure 7).

Animals given toxin alone had relative liver weights ($7.11 \pm .646$, mean \pm SEM) which were significantly greater than those of animals given pancreatic extract alone ($4.28 \pm .414$, mean \pm SEM) or toxin preincubated with these enzymes ($5.8 \pm .818$, mean \pm SEM). The relative liver weights of rats given the toxin with the enzymes were significantly greater than those of rats given the enzymes alone.

The relative liver weights of rats dosed with toxin alone ($7.69 \pm .288$, mean \pm SEM) were significantly greater in those of rats given toxin preincubated with BSA ($5.98 \pm .446$, mean \pm SEM).

DISCUSSION

When injected IP or IV, either M. aeruginosa cell extracts or purified MCYST-A toxin produce hepatic lesions in rats similar to those observed in other species of animals involved in field cases resulting from ingestion. Despite an ip LD₅₀ of 200 µg/kg in preliminary studies, laboratory animals gavaged with MCYST-A at 5 mg/kg did not appear clinically affected and no gross liver damage was apparent up to 24 hours after dosing. To our knowledge, orally induced toxicosis has not been produced in laboratory rats or mice with pure peptide toxin. Similarly, when lyophilized cell suspensions were administered orally at doses up to 12 mg toxin equivalent/kg, no detectable acute toxicity was evident. The limited availability and prohibitive cost of the toxin limits testing with extremely high oral doses of purified material, and limitations of the rat stomach size prevents administration of higher oral doses using cell suspensions. Therefore, a model was developed to study the effects of toxin absorbed via the intestinal tract. The rat isolated in situ ileal loop/MCYST-A preparation is reproducible when monitored for hepatotoxic effects. Our results indicate that, while the rat appears to be a less-than-satisfactory animal model for studying the oral toxicity of MCYST-A, it can be conveniently used to monitor intestinal absorption by utilizing in situ isolated intestinal loops.

Experiments with CTR binding of MCYST-A in vitro and in vivo suggest that CTR may prove therapeutically effective in cases of animal ingestion of toxic waterblooms. CTR is widely available and it apparently limits intestinal

absorption of MCYST-A. Since CTR itself is not absorbed, it would not contribute to the xenobiotic load of affected animals.

The observation that the degree of toxicity was dependent on whether the toxin was infused into the jejunum or ileum, is notable since it suggests that the ileum may be a "preferential" site for toxin absorption. Due to differences in mucosal structure, the surface area of the jejunum is far greater than an equivalent length of ileum, but a more severe hepatotoxic effect was observed with toxin administration via the latter. There is in vitro evidence suggesting that MCYST-A is transported into hepatocytes by interacting with specific carriers for bile acids (Runnegar et al., 1981). Specific carriers for bile acids are also located in the ileum (Hofmann, 1983). If the hypothesis of Runnegar et al. (1981) is correct, it may help to explain why equivalent doses of the toxin produce greater effects when introduced into the ileum as compared to the jejunum. Thus, if MCYST-A is transported by specific bile acid carriers into the hepatocyte, it is also possible that MCYST-A could be transported by the bile acid carriers in the ileum. In contrast to the ileum, bile acids are absorbed principally by passive diffusion in the jejunum (Hofmann, 1983). By analogy, absorption of MCYST-A from the jejunum may also occur by passive diffusion. Thus, for a given dose of MCYST-A, a greater degree of toxicity would be expected when infused into the ileum than when infused into the jejunum as observed in the present study.

In the case of orally-induced toxicosis resulting from ingestion of algal bloom material, it was felt that the Microcystis cell membrane and associated structures might protect the toxin molecule from pancreatic enzymes; and these enzymes might degrade the toxin when administered (free of cells) via the oral

route whether in the purified state or in lyophilized material. Preincubation of MCYST-A with pancreatic enzymes produced a marked decrease in the observed toxic effect of this compound, but significant toxicity remained. It was felt that an even greater decrease in toxicity of MCYST-A should have been observed if enzymatic degradation were a major factor contributing to the detoxification of MCYST-A.

The reduction in toxicity reflected in the BSA experiment indicated that nonspecific protein binding may have been responsible for the decrease in toxicity observed in the pancreatic extract experiment. This data coupled with in vitro data from pepsin, trypsin, and chymotrypsin experiments recently performed in our laboratory (not presented) lead us to believe that enzyme degradation is not likely to be the primary factor causing the low oral toxicity of MCYST-A. Protein binding, however, appears to be quite significant in reducing the amount of free toxin.

In summary, this study has: 1) established a reproducible model for studying the intestinal absorption of MCYST-A, 2) demonstrated that CTR-resin may be a useful therapeutic agent in cases involving known ingestion of MCYST-A containing algae, 3) provided evidence suggesting site specificity in the intestinal absorption of MCYST-A, and 4) demonstrated that pancreatic enzyme degradation may not be a primary cause of the low oral toxicity observed with purified MCYST-A in rats.

REFERENCES

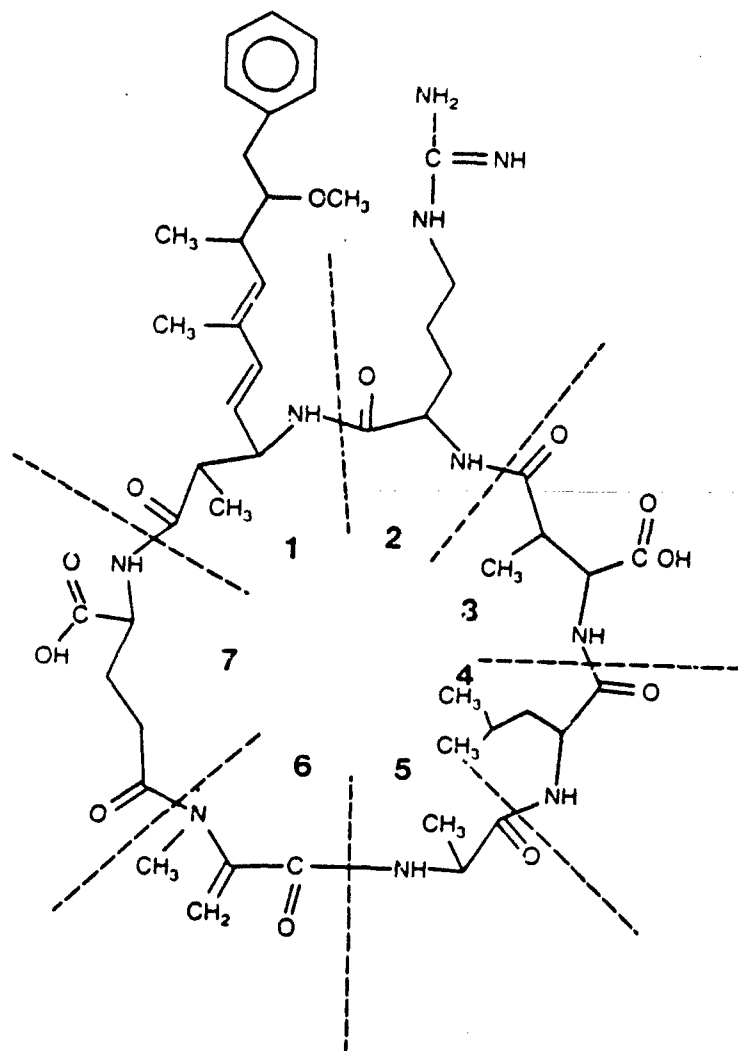
- Botes, D. P., Tuinman, A. A., Wessels, P. L., Viljoen, C. C., Kruger, H., Williams, D. H., Santikarn, S., Smith, R. J., and Hammond, S. J.: The structure of cyanoginosin-LA, a cyclic heptapeptide toxin from the cyanobacterium Microcystis aeruginosa. J. Chem. Soc. Perkin Trans. I:2311:2318, 1984.
- Carmichael, W. W.: Freshwater blue-green algae (Cyanobacteria) toxins--a review. In Carmichael, W. W. (Ed.), The Water Environment, Algal Toxins and Health. Plenum Press, New York, 1-13, 1981.
- Carmichael, W. W.: Chemical and toxicological studies of the toxic freshwater cyanobacteria Microcystis aeruginosa, Anabaena flos-aquae and Aphanizomenon flos-aquae. S. Afr. J. Sci. 78:367-372, 1982.
- Carmichael, W. W.: Isolation, culture and toxicity testing of toxic freshwater cyanobacteria (blue-green algae). Proc. of I.S.H.C. Symposium, Leningrad, USSR, Gordon and Breach Pub., New York, 1984.
- Falconer, I. R., Jackson, A. R. B., Langley, J., and Runnegar, M. T.: Liver pathology in mice in poisoning by the blue-green alga Microcystis aeruginosa. Aust. J. Biol. Sci. 34:179-187, 1981.
- Falconer, I. R., Beresford, A. M., and Runnegar, M. T. C.: Evidence of liver damage by toxin from a bloom of blue-green algae, Microcystis aeruginosa. Med. J. Aust. 1:511-514, 1983.
- Harada, K.-I., Suzuki, M., Dahlem, A. M., Beasley, V. R., Carmichael, W. W., and Rinehart, K. L., Jr.: A rapid and simple purification method for peptides produced by cyanobacteria. In press, Toxicon.

- Hofmann, A. F.: The enterohepatic circulation of bile acids in health and disease. In Sleisenger, M. H., and Fordtran, J. S. (Eds.), Gastrointestinal Disease. W. B. Saunders Publishing Co., Philadelphia, PA, 115-134, 1983.
- Krishnamurthy, T., Carmichael, W. W., and Sarver, E. W.: Toxic peptides from freshwater cyanobacteria (blue-green algae). I. Isolation, Purification and Characterization of Peptides from Microcystis aeruginosa and Anabaena flos-aquae. Toxicon. 24(9):865-873, 1986.
- Jackson, A. R. B., Falconer, I. R., and Runnegar, M. T. C.: Clinical and pathological changes in sheep experimentally poisoned by the blue-green alga Microcystis aeruginosa. Vet. Pathol. 21:102-113, 1984.
- Runnegar, M. T., Falconer, I. R., and Silver, J.: Deformation of isolated rat hepatocytes by a peptide hepatotoxin from the blue-green alga Microcystis aeruginosa. Arch. Pharmacol. 317:268-272, 1981.
- Schwimmer, D., and Schwimmer, M.: Medical aspects of phycology. In Jackson, D. (Ed.), Algae, Man, and the Environment. Syracuse University Press, Syracuse, 270-358, 1968.
- Watanabe, M. F., and Oishi, S.: Toxicities of Microcystis aeruginosa collected from some lakes, reservoirs, ponds and a moat in Tokyo and adjacent regions. Japan J. Limnol. 41:5-9, 1980.
-

Table 1. Binding of microcystin-A to cholestyramine resin in vitro. All analyses were run in triplicate at each level of testing.

Cholestyramine (mg)	Microcystin-A (μ g)	% Toxin Removed
50	25	> 99.0
50	50	> 99.0
50	100	> 99.0
50	200	> 99.0
25	200	> 99.0
25	400	> 99.0
0	50	10.9 \pm 3.1
0	100	4.9 \pm 4.6
50	0	0.0

Figure 1. Structure of microcystin-A produced by Microcystis aeruginosa strain 7820.



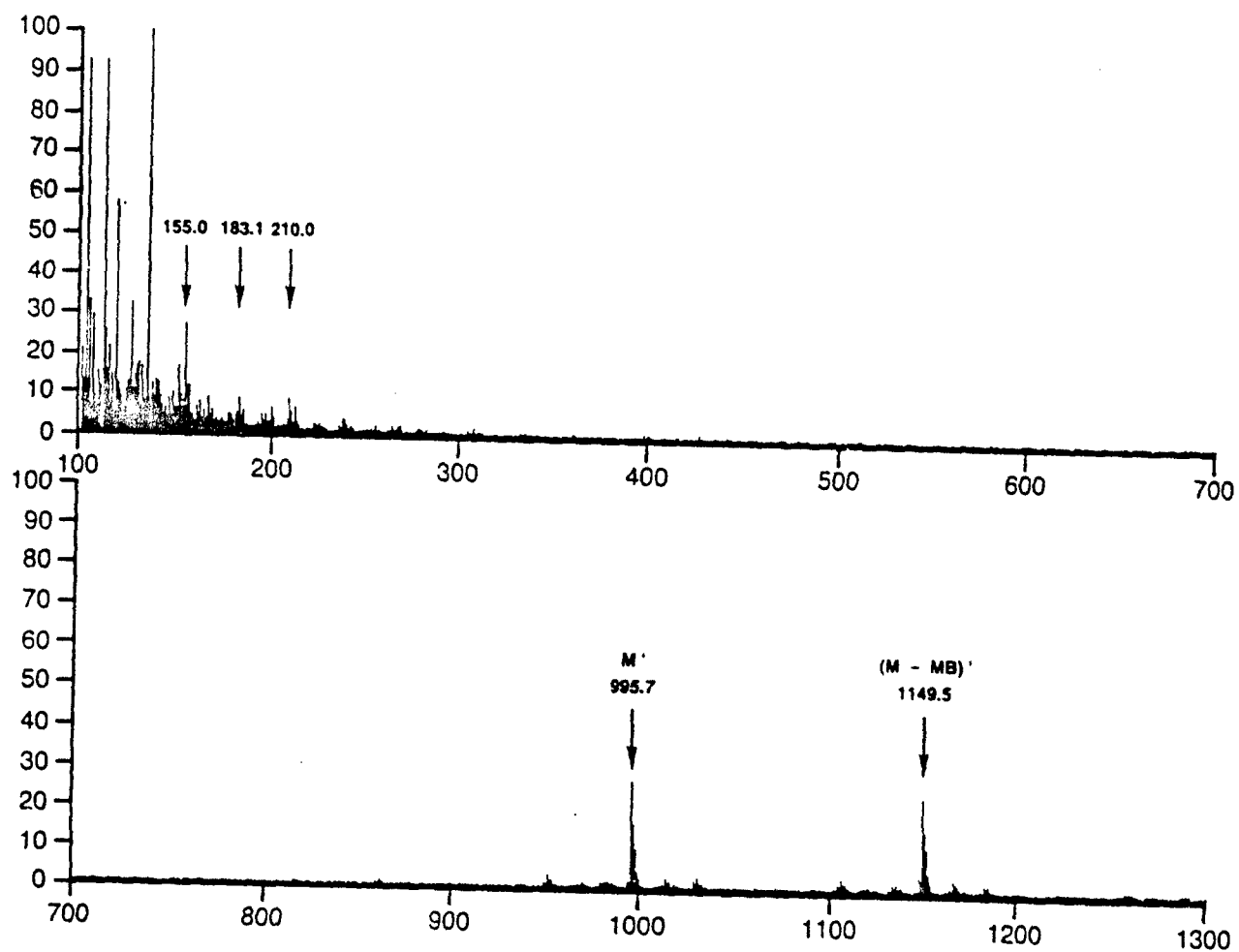
Microcystin - A

Molecular weight 994

1. Adda
2. Arginine
3. β -Methylaspartic Acid
4. Leucine
5. Alanine
6. Methyldehydroalanine
7. Glutamic Acid

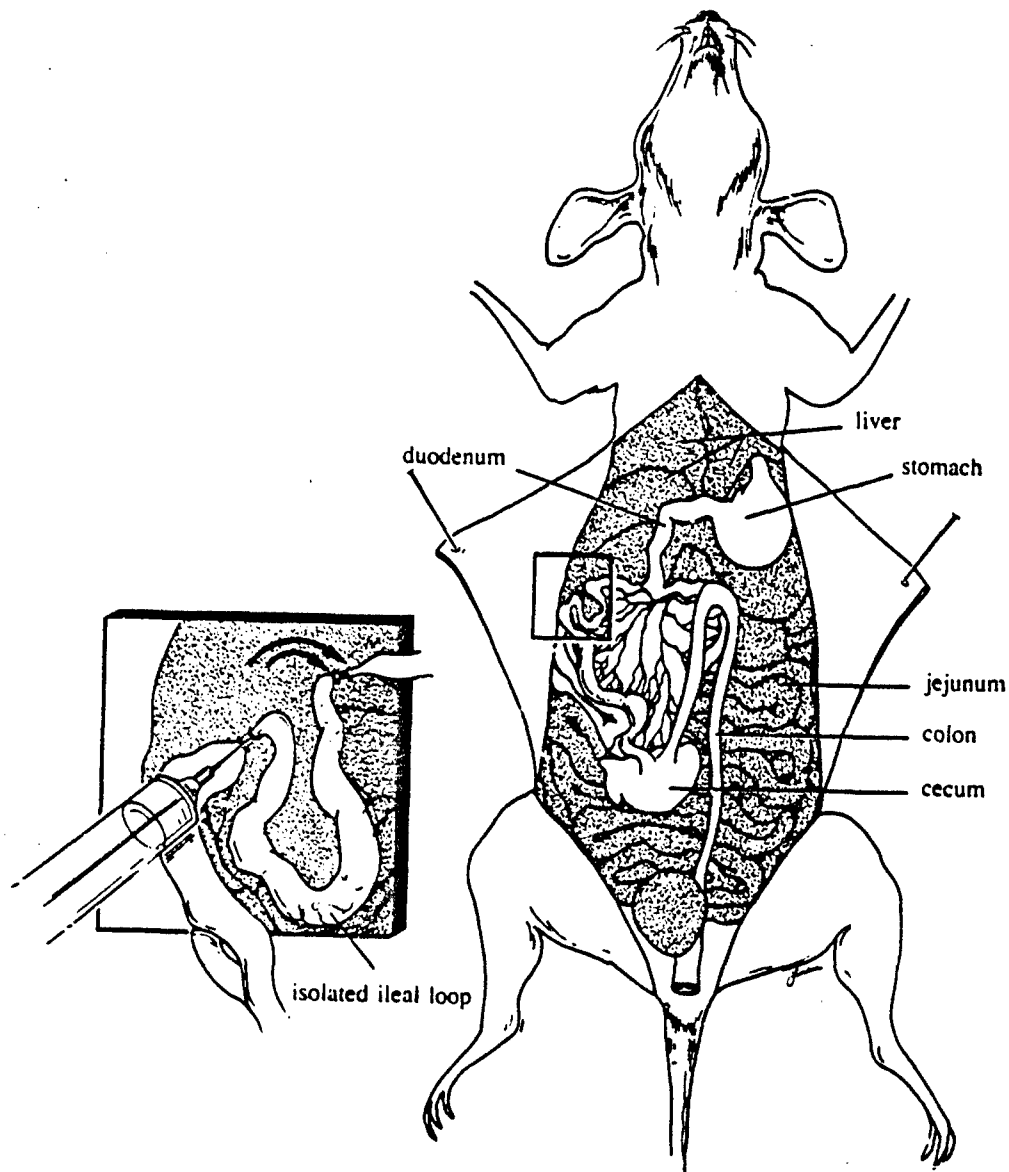
Section I

Figure 2. Fast atom bombardment/mass spectroscopy of microcystin-A (M) in magic bullet matrix (MB).



Section I

Figure 3. Diagram of in situ isolated rat ileum. The small antimesenteric incision is between the 2 ligatures indicated by the arrows.



Section I

Figure 4. Comparison of liver weights as a percent of body weight (mean \pm SEM) from animals treated with microcystin-A or vehicle via the ileal loop. Rats were dosed either with the toxin (5 mg/kg; N = 4) or equivalent volume of vehicle (N = 4). Livers were removed and weighed 6 hours following treatment. *Significantly ($p < 0.05$) less than toxin-treated animals.

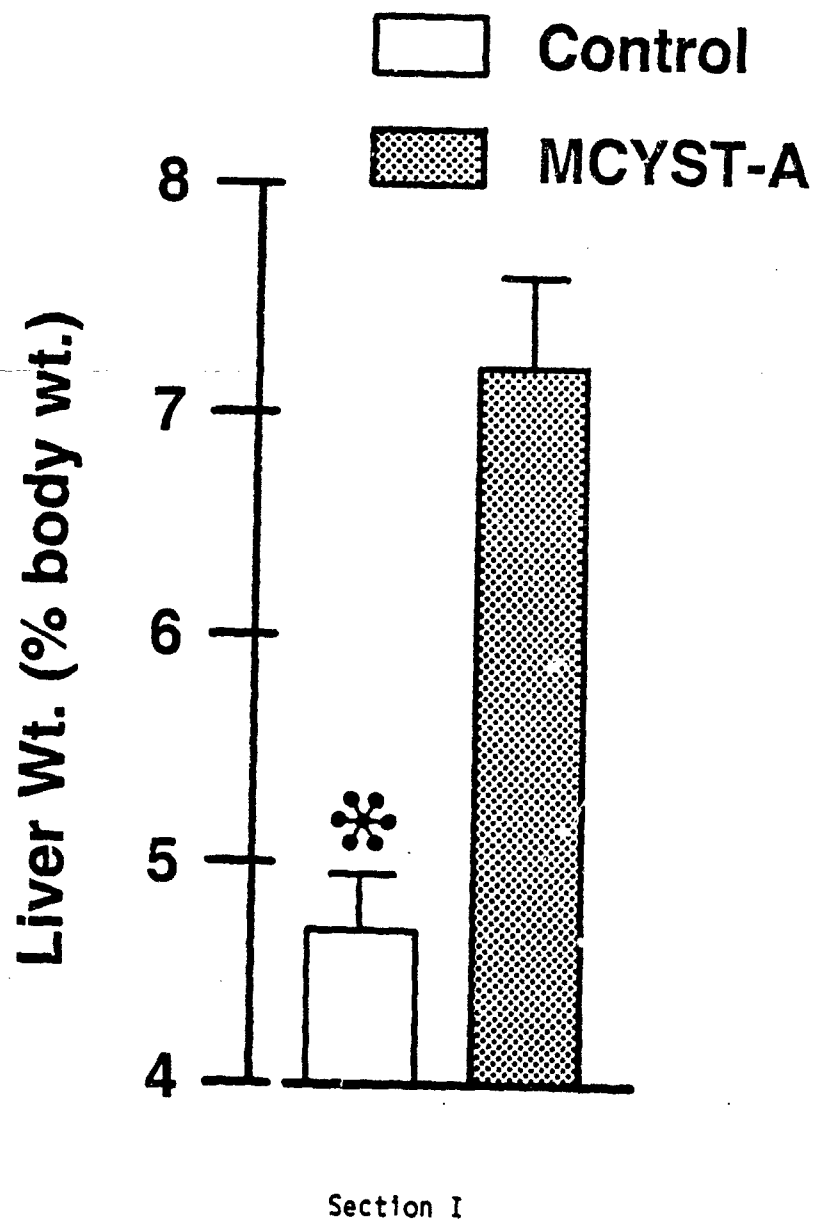
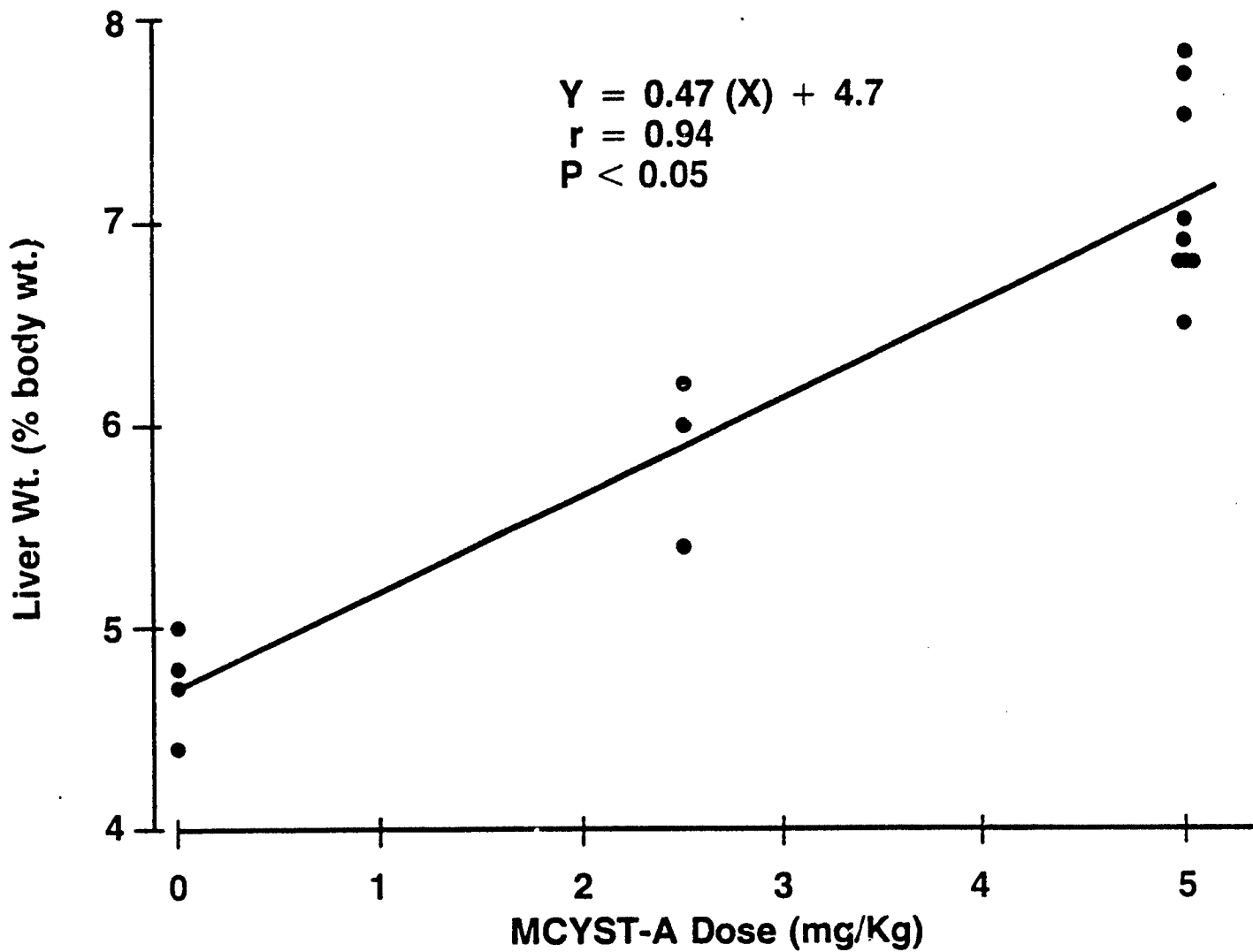


Figure 5. Linear regression analysis of liver weights from animals given vehicle, or microcystin-A at either 2.5 mg/kg body weight or 5 mg/kg body weight via the ileal loop. The straight line is the line of "best fit" according to the method of least squares. Each point represents the value from 1 animal.



Section I

Figure 6. Comparison of liver weights as a percent of body weight (mean \pm SEM) at 6 hours after ileal or jejunal infusion of microcystin-A. Toxin was infused into the ileal (2.5 mg/kg body weight; N = 3) or jejunal loop (5 mg/kg body weight; N = 3).

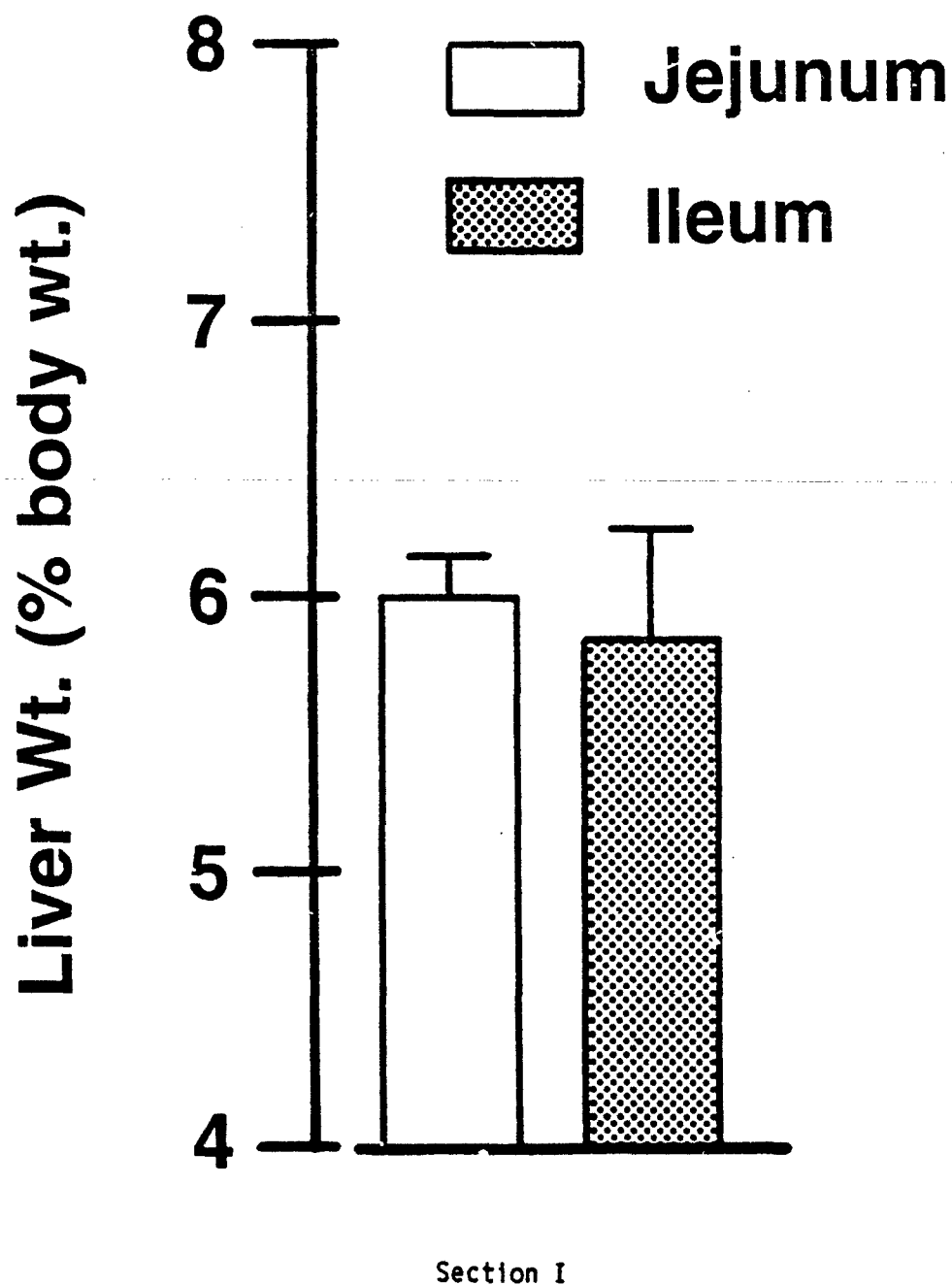
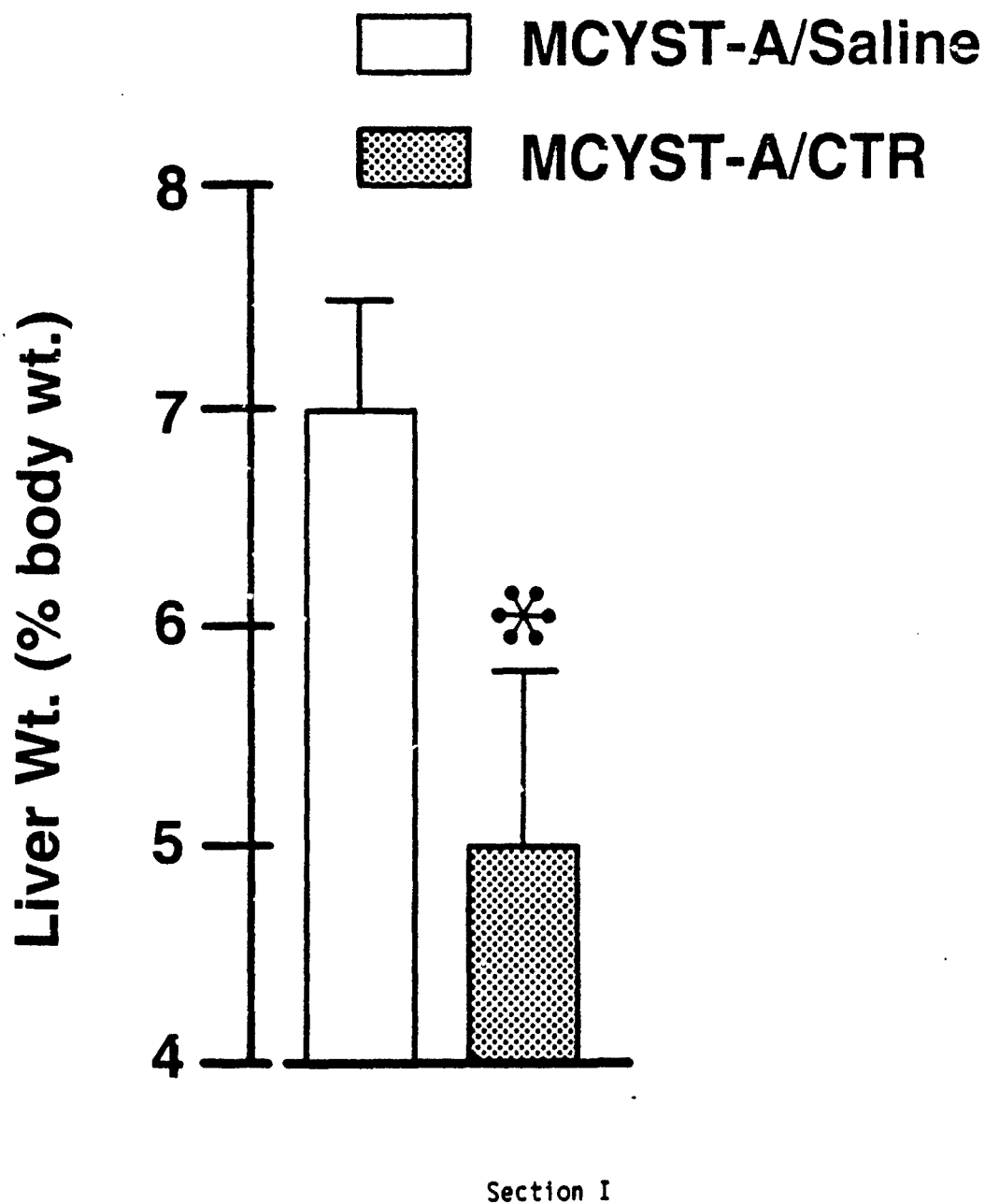


Figure 7. Comparison of liver weights as a percent of body weight (mean \pm SEM) from animals given microcystin-A plus saline (N = 5) or microcystin-A plus CTR (N = 4) via the ileal loop. Livers were removed and treated as described in Figure 3. *Significantly ($p < 0.05$) less than toxin/saline treated group.



II. IMPROVED PURIFICATION METHOD FOR CYCLIC PEPTIDES PRODUCED BY CYANOBACTERIA

Andrew M. Dahlem, Ken-Ichi Harada

ABSTRACT

An alternative purification method was established for toxic peptides from cyanobacteria. This method consists of octadecylsilane-silica gel separation, normal phase silica gel thin layer chromatography with 2 detection reagents and reverse phase HPLC with UV (238 nm) detection. The method has been successfully applied to the isolation of toxic peptides from the Monroe and M-228 strains of Microcystis aeruginosa. Use of this method reduces toxin extraction and separation time, provides additional means of detection of toxin and impurities, and thereby enables rapid and repeatable isolation of peptide toxins from cyanobacteria.

INTRODUCTION

Toxic blooms of cyanobacteria are a characteristic feature of some nutrient-filled fresh and brackish waters. Four genera, Microcystis (Elleman et al., 1978; Botes et al., 1982; Krishnamurthy et al., 1986), Anabaena (Krishnamurthy et al., 1986), Oscillatoria (Ostensvik et al., 1981) and Nodularia (Edler et al., 1985), are known to produce potent hepatotoxins. The principal species under investigation, M. aeruginosa, has been frequently cited in animal poisoning incidents. Toxins of interest from this species have low molecular weights (about 1,000 daltons) and are cyclic peptide hepatotoxins of relatively high toxicity (LD₅₀: 35 to 59 µg/kg IP mouse; Carmichael, 1987).

Isolation and purification methods for the cyclic peptide toxins, as well as development of methods to assess the purity of toxins supplied, are

essential prior to toxicology studies to assess such parameters as minimum lethal dose (MLD), no effect dose (NED), LD₅₀, and pathophysiologic functions. These algae toxins display very steep dose/effect curves between a dose which will not cause death, and potentially lethal doses. For these reasons, the integrity of toxin must be precisely known so that toxicity, bioavailability, and related studies can be valid and reproducible.

MATERIALS AND METHODS

Organisms

Two M. aeruginosa strains were used. One was from a surface bloom collected from a farm pond in Monroe, Wisconsin USA (Galey et al., 1987), designated as the Monroe strain, and another was from culture strain (M-228) originally collected from Lake Suwa in Japan (Watanabe and Oishi, 1983). Cells in all cases were lyophilized prior to toxin extraction.

Toxin Extraction

Ten g of dried cells (10 g) of the Monroe strain of Microcystis were extracted with 200 ml of 5% acetic acid (aq) for 1 hour while stirring. The extract was centrifuged at 10,000 rpm and then the supernatant (about 600 ml) was applied directly to 30 g of reversed phase silica gel (Micro Bead Silica gel 5D [100-200 mesh] ODS-W, Fuji-Davison Chemical Ltd., Tokyo, Japan). The column containing the toxin was rinsed with water (850 ml), followed by water:methanol (8:2, 400 ml). Elution from the column with methanol (400 ml) gave 110 mg of the toxin-containing fraction. Similarly, 90 mg of the toxic fraction was obtained from 5 g of the M-228 cells.

Thin Layer Chromatography

HPLC grade methanol was used to dissolve the toxin to give a final concentration of 5 µg/µl. Samples were applied to silica gel TLC plates

(Kieselgel 60F254, E. Merck, Darmstadt, FRG) with glass microcaps in amounts of 5, 10, and 25 µg and application was verified by observation under short wave UV prior to development (toxin absorbs short wave UV). The TLC plates were placed in pre-equilibrated TLC chambers and the solvent path was 13 cm.

Mobile Phase for TLC

See Pages 4-5, Annual Report, 1986.

Detection

See Page 5, Annual Report, 1986.

Silica Gel Chromatography

The biologically active fraction (210 mg) from the Monroe strain was subjected to a silica gel column (made by slurry packing 15 g of silica gel [Kieselgel 60, 230 to 400 mesh, E. Merck, Darmstadt, FRG]) using chloroform:methanol:water (65:35:10), and fractions were collected. Each column fraction was then spotted on TLC, and fractions containing toxin only were combined to yield 43 mg of the toxin. The second silica gel (20 g) column chromatographic purification of the active fraction gave 20 mg of almost pure toxin (above 95% purity by TLC) using chloroform:methanol:water (65:25:5) as an eluting solvent system. Similarly, the active fraction (90 mg) from the M-228 strain was chromatographed on silica gel using chloroform:methanol:water (65:25:5) to give 4 mg of one toxin (MW 994) and 13 mg of another toxin (MW 1044).

HPLC

HPLC separations of crude and purified toxins were accomplished under reversed phased isocratic conditions with a Nucleosil 5 C₁₈ (150 x 4.6 mm, Chemco Scientific Co., Osaka, Japan) column and a mobile phase of methanol:0.05% trifluoroacetic acid in water (6:4). The flow rate was 1 ml/min and UV absorbance at 238 nm was used for detection.

Purity Evaluation

See Page 5, Annual Report, 1986.

Mass Spectrometry

Secondary ion mass spectrometry (SIMS) was performed using a double focusing Hitachi M-80B mass spectrometer fitted with a high-field magnet, SIMS source, and M-0101 data system. Operating conditions were: primary ion, Xe⁺; accelerating voltage, 8 kv (primary) and 3 kv (secondary); source temperature, 35°C. Samples were dissolved in methanol at a concentration of 10 µg/µl. Each sample solution (0.5 to 1 µl) was loaded on a silver target. About 1 µl of matrix material, glycerol or "magic bullet" (dithiothreitol-dithioerythritol [3:1]), was added to the sample on the target.

RESULTS AND DISCUSSION

Several toxic peptides have been isolated from freshwater cyanobacteria. Among them the structures of 5 toxins have already been characterized by Botes and coworkers. They are monocyclic heptapeptides (microcystins) and contain a common moiety composed of a novel amino acid, 3-amino-9-methoxy-10-phenyl-2,6,8-trimethyl-deca-4,6-dienoic acid (Adda), as well as N-methyl-dehydroalanine (Medha), D-alanine, D-erythro-β-methyl-isoaspartic acid, and D-isoglutamic acid, in addition to 2 variant L-amino acids (Botes et al., 1984; Botes et al., 1985). Other toxic peptides from this species appear to have similar structures.

Isolation and purification of these toxins have been carried out mainly using gel filtration and HPLC with UV detection. Although gel filtration is a mild and effective method, it only provides a semi-pure toxin extract and requires more time than the procedure reported in this study, due primarily to the large volumes of water which must be evaporated. To efficiently isolate

toxic peptides from cyanobacteria, we devised a new extraction, separation and purification method and applied it to the isolation of the toxins from the Monroe and M-228 strains (Figure 1).

In the extraction step we employed octadecylsilanized (ODS) silica gel. Algae cells were air-dried and the dried cells were extracted with 5% acetic acid (aq) for 30 minutes 3 times. The combined extract was centrifuged at 10,000 rpm and the supernatant was applied directly to the preconditioned ODS-column. The centrifugation process is essential for smooth passage of the supernatant. ODS-cartridges have been successfully used for purification of the toxins by 2 groups (Krishnamurthy et al., 1986; Brooks and Codd, 1986). In our procedure, an additional washing step was added prior to elution with methanol. The column which contained the toxin is rinsed with water, followed by water:methanol (8:2) to remove as many polar contaminants as possible. These rinses were not toxic to mice and so were discarded. The toxin was then eluted from the column with methanol and the solute was evaporated to dryness. To purify toxin from a small amount of lyophilized Microcystis cells, commercially available ODS-cartridges such as Sep-Pak, Bond Elute and Baker 10 are recommended.

Methods have been developed previously for the isolation and purification of these toxic peptides, but to date, all methods have relied on purity evaluation based on HPLC with UV absorption. Even though toxin with relatively high purity can be obtained by this method, non-UV-absorbing impurities have been detected occasionally in "purified" material.

The TLC method developed in our laboratories and described in our 1986 Annual Report was also applicable to silica gel column chromatography without significant modification. This column chromatography procedure is rapid,

inexpensive, efficient, and can repeatedly provide toxin of purity greater than 95%. The silica column method began with the slurry packing of fine silica gel (230 to 400 mesh) using either of the 2 mobile phases used for the TLC method. Each fraction from the column was spotted on TLC, and then those fractions containing toxin were combined. The purified toxins retained their biological activity (IP LD₅₀ in mice, about 60 µg/kg), and their behavior on TLC (Figure 2). Even more precise resolution would be expected by the use of less polar solvent systems such as chloroform:methanol:water (65:25:5) and ethyl acetate:isopropyl alcohol:water (6:3:7). When toxin of greater purity is required, the use of a Sephadex LH-20 column with methanol, or preparative HPLC using a C-18 column and methanol:0.05% trifluoroacetic acid (aq) (6:4) is quite effective. Figure 3 shows typical high performance liquid chromatograms of the methanol fraction after ODS clean-up from M-228 cells.

Fast atom bombardment (FAB) and secondary ion mass spectrometry (SIMS) are powerful techniques for obtaining molecular weight information on nonvolatile compounds. Because the ions at m/z 995 and 1045, 1149 and 1159 are assignable to $(M+H)^+$ and $(M+H+matrix)^+$, respectively, the molecular weights of the toxins are determined to be 994 and 1044. These correspond with cyanoginosins LR and YR (Botes et al., 1985), also known as microcystins A and B (Carmichael, 1987).

A rapid and simple purification method for toxic peptides produced by cyanobacteria is described. Our procedures include ODS-silica gel extraction, with thin-layer silica gel separation and 2 detection methods, as well as HPLC with UV (235 nm) detection. This combination of reversed phase and normal phase separations excludes more of the contaminants in toxin fractions than did previous methods. Also, these procedures eliminate costly and time-consuming gel filtration steps and greatly reduce the time required in

evaporation of large amounts of water. As a result, the method can be used to obtain 0.2% to 0.3% of the purified toxin from these lyophilized cells in a total of 3 or 4 days.

ACHNKOWLEGEMENT

We are grateful to Dr. M. F. Watanabe for providing the M-228 cell materials.

REFERENCES

- Botes, D. P., Kruger, H., and Viljoen, C. C.: Isolation and characterization of four toxins from the blue-green algae Microcystis aeruginosa. Toxicon. 20:945, 1982.
- Botes, D. P., Tuinman, A. A., Wessels, P. L., Viljoen, C. C., Kruger, H., Williams, D. H., Santikarn, S., Smith, R. J., and Hammond, S. J.: The structure of cyanoginosin-LA, a cyclic heptapeptide toxin from the cyanobacterium Microcystis aeruginosa. J. Chem. Soc. Perkin Trans. 1:2311, 1984.
- Botes, D. P., Wessels, P. L., Kruger, H., Runnegar, M. T. C., Santikarn, S., Smith, R. J., Barna, J. C. J., and Williams, D. H.: Structural studies on cyanoginosins-LR, -YR, -YA, and -YM, peptide toxins from Microcystis aeruginosa. J. Chem. Soc. Perkin Trans. 1:2747, 1985.
- Brooks, W. P., and Codd, G. A.: Extraction and purification of toxic peptides from natural blooms and laboratory isolate of the cyanobacterium Microcystis aeruginosa. Lett. Appl. Microbio. 2:1, 1986.
- Carmichael, W. W.: Toxins of freshwater algae: Handbook of natural product toxins, Tu, A. T. (Ed.). Marcel-Dekker Inc., In press.
- Edler, L., Ferno, S., Lind, M. G., Lundberg, R., and Nilsson, P. O.: Mortality of dogs associated with a bloom of the cyanobacterium Nodularia spumigena in the Baltic Sea. Ophelia 24:103, 1985.
- Elleman, T. C., Falconer, I. R., Jackson, A. R. B., and Runnegar, M. T.: Isolation, characterization and pathology of the toxin from a Microcystis aeruginosa (Anacystis cyanea) bloom. Aust. J. Biol. Sci., 31:209, 1978.
- Galey, F. D., Beasley, V. R., Carmichael, W. W., Kleppe, G., Hooser, S. B. and Haschek, W. M.: Blue-green algae (Microcystis aeruginosa) hepatotoxicosis in dairy cows. Am. J. Vet. Res., 48:1415, 1987.

- Krishnamurthy, T., Carmichael, W. W., and Sarver, E. W.: Toxic peptides from freshwater cyanobacteria (blue-green algae). I. Isolation, purification and characterization of peptides from Microcystis aeruginosa and Anabaena flos-aquae. Toxicon. 24:865, 1986.
- Poon, G. K., Priestley, I. M., Hunt, S. M., Fawell, J. K., and Codd, G. A.: Purification procedure for peptide toxins from the cyanobacterium Microcystis aeruginosa involving high-performance thin-layer chromatography. J. Chromatogr. 387:551, 1987.
- Ostensvik, O., Skulberg, O. M., and Soli, N. O.: Toxicity studies with blue-green algae from Norwegian inland waters. In the water environment: Algal toxins and health, W. W. Carmichael (Ed.). Plenum Press, New York, pp. 315, 1981.
- Watanabe, M. F., and Oishi, S.: A highly toxic strain of blue-green alga Microcystis aeruginosa isolated from Lake Suwa. Bull. Japan Soc. Sci. Fish 49:1759, 1983.

Figure 1. Extraction and purification procedure for peptide toxins from cyanobacteria.

Lyophilized cells

Extract with 5% AcOH (aq) 30 minutes,
three times.

Centrifuge at 9300 g.

Supernatant

ODS-column

- 1) wash with H₂O followed by
MeOH:H₂O (2:8)
- 2) elute with MeOH
- 3) evaporate to dryness

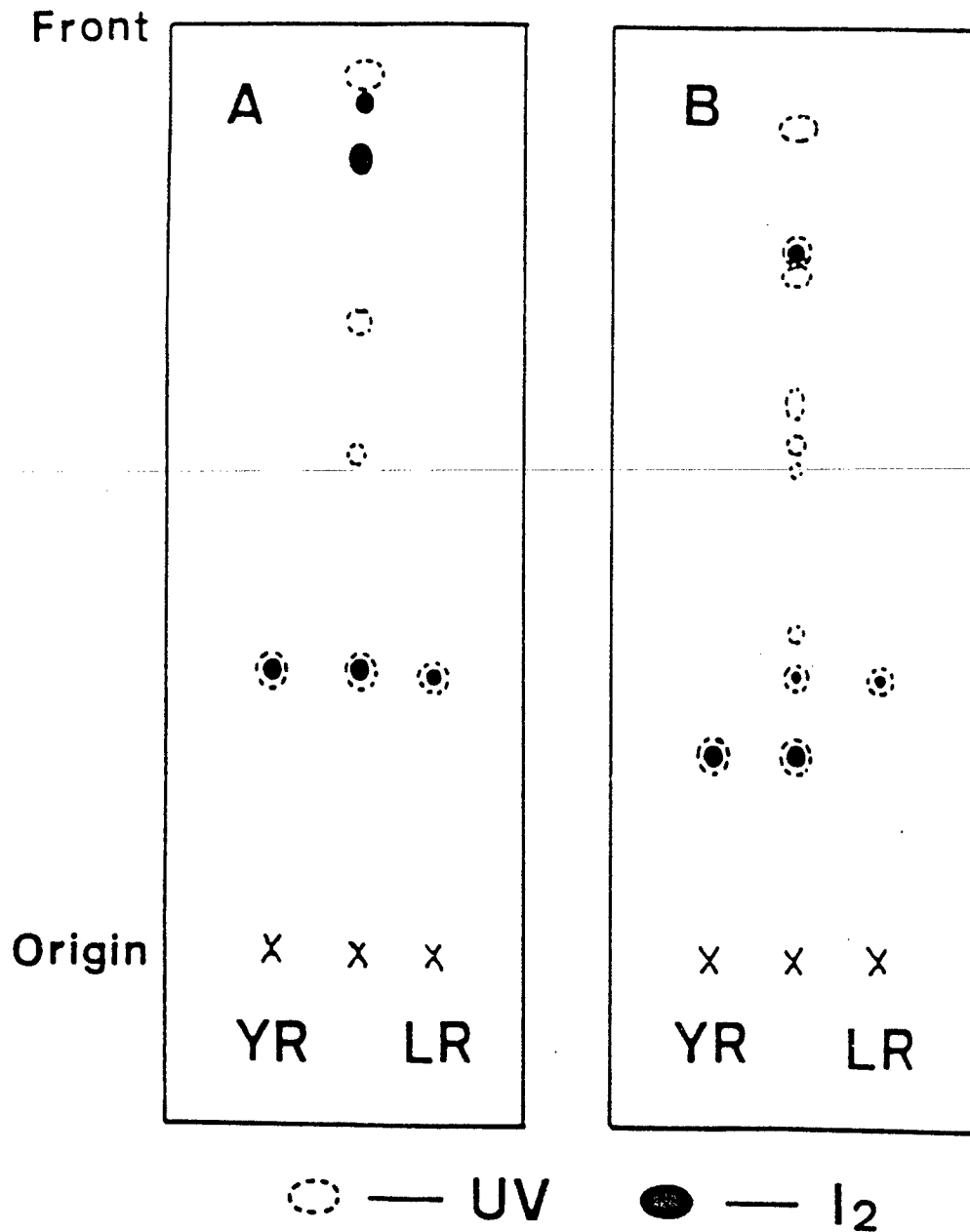
Residue

- a) Silica gel column with
CHCl₃:MeOH:H₂O (65:35:10)
or
AcOEt:1-PrOH:H₂O (4:3:7)
- b) HPLC
MeOH:0.05% TFA (aq) (6:4)
1 ml/min, 238 nm

Purified toxins

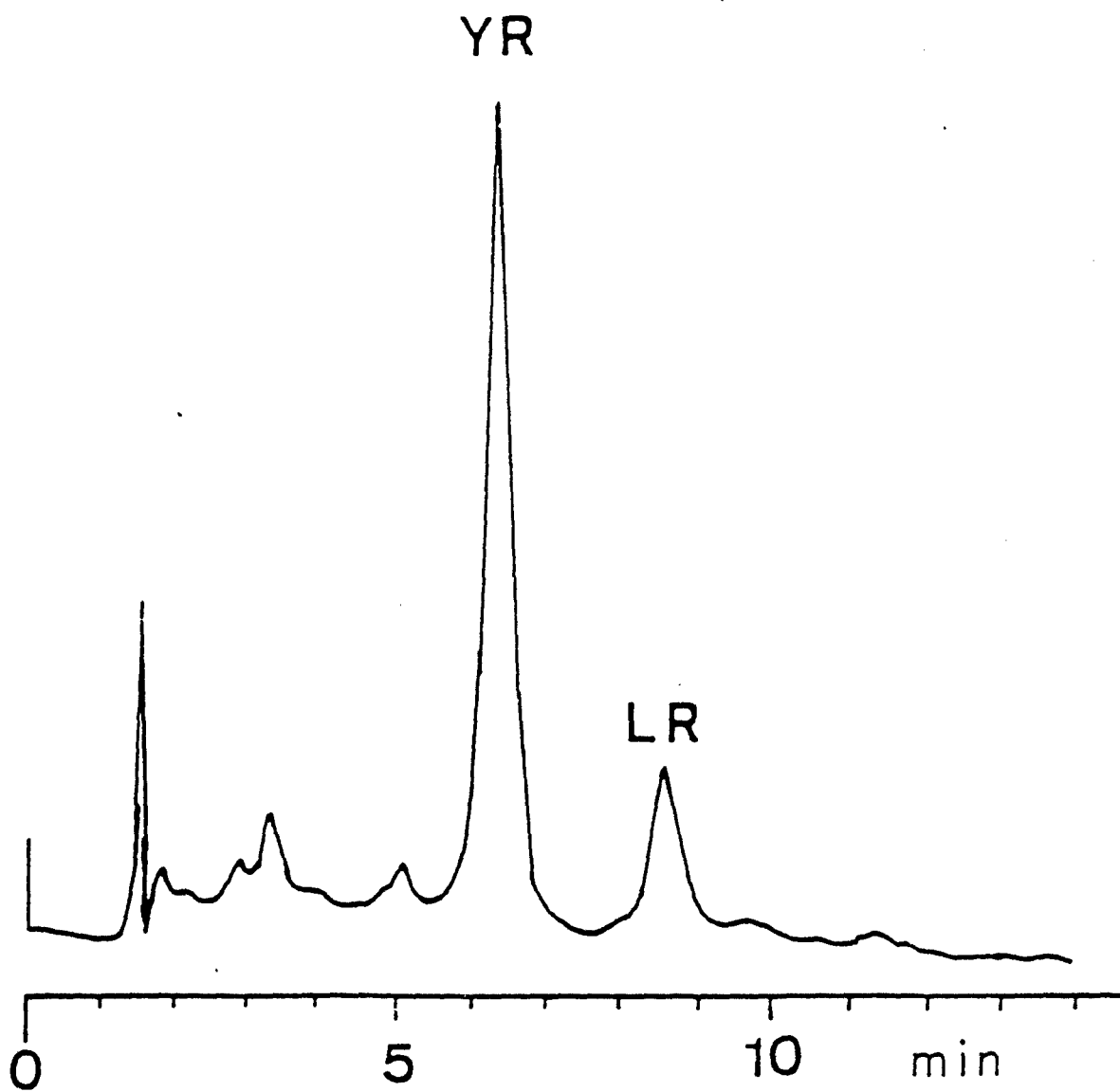
Section II

Figure 2. Thin layer chromatograms of the methanol fraction after ODS clean-up from M-228 cells and purified cyanoginosins LR and YR using (A) chloroform:methanol:water (65:35:10) and (B) ethyl acetate:isopropyl alcohol:water (4:3:7) with UV and iodine detections.



Section II

Figure 3. High performance liquid chromatograms of the methanol fraction after ODS clean-up from M-228 cells.



Section II

III. STRUCTURE/TOXICITY RELATIONSHIP OF THE N-METHYLDEHYDROALANINE MOIETY OF MICROCYSTIN-A

Andrew M. Dahlem, Ken-Ichi Harada, Kenneth L. Rinehart, Stephen B. Hooser

ABSTRACT

In our last annual report we documented the importance of the double bonds in the toxicity of a cyclic peptide toxin from Nodularia spumigena. In a related experiment, the same sodium borohydride treatment which was used previously to saturate the N-methylaminobutyric acid of the Nodularia toxin was employed with microcystin-A, (MCYST-A) a cyclic peptide toxin from Microcystis aeruginosa. Selective saturation at the N-methyldehydroalanine portion of MCYST-A resulted in a 50% reduction in the toxicity of this compound. This experiment demonstrated that the dehydroamino acid of MCYST-A is also important in the observed toxicity of this compound, and that the altered toxin remains hepato-specific and extremely potent even after saturation of this moiety.

INTRODUCTION

To understand the biochemical mechanisms of action of algal peptide hepatotoxins, it is important to identify factors responsible for their high toxicity through the use of structure/toxicity relationships of the functional moieties of parent compounds and derivatives.

The first structural moieties which we have investigated in these peptide hepatotoxins are the dehydroamino acids. The bioactivity associated with other naturally occurring peptide molecules are directly related to the presence of dehydroamino acids (Gross et al., 1967). For example, the antibiotics nisin and subtilin produced by bacteria contain alpha-beta

unsaturated amino acids which are believed to be essential to their antibiotic activity. One working hypothesis for the biological action of cyclic peptide hepatotoxins containing dehydroamino acids is that the toxins may impair essential sulfhydryl groups by reacting across the double bond in their alpha, beta unsaturated amino acids. The present and previous studies indicate that the dehydroamino acids in the cyclic peptides produced by Nodularia spumigena, and Microcystis aeruginosa contribute to the toxicity of these compounds.

MATERIALS AND METHODS

Toxin

Purified microcystin-A (MCYST-A) was prepared from algae grown in the laboratories of Dr. Wayne W. Carmichael at Wright State University, Dayton, Ohio. The purity of the toxin material utilized was determined to be greater than 95% by HPLC and TLC evaluation prior to animal administration.

Chemicals and Solvents

All solvents were distilled in glass. All chemicals were of analytical grade.

Toxin Derivative Formation

MCYST-A (5.2 mg) was reacted with sodium borohydride (21 mg) in methanol to produce 2.2 mg (greater than 95% pure) of the dihydro derivative of MCYST-A (confirmed by fast atom bombardment mass spectroscopy). The compound formed is a toxin derivative with saturation of the double bond in the dehydroalanine portion of MCYST-A.

TLC

See the procedure section of the 1986 Annual Report, page 11. The iodine vapor was followed by 20% sulfuric acid in methanol and heat (110°C).

HPLC

See the 1986 Annual Report, page 11. The detection wavelength was set at 240 nm.

Confirmations of Structures

See the 1986 Annual Report, page 11. "Magic bullet matrix" (1:3 dithiothreitol:dithioerythritol) was used as before. The parent ion of 997 was observed ($M+H^++2$ hydrogen). No intact parent compound was detected.

Mouse Bioassay

Female Balb/c mice were randomly assigned to 3 groups (6/group) and injected intraperitoneally with: 1) MCYST-A at doses of 25, 50, or 100 $\mu\text{g/kg}$ (positive controls); 2) with the dihydro derivative of MCYST-A at 25, 50, 100, 200, 300, or 400 $\mu\text{g/kg}$ (test group); or 3) with the saline vehicle (negative controls). Mice were observed for 24 hours, the mortality of each group was recorded. Mice which survived the observation period were killed by cervical dislocation. At the time of death or euthanasia, livers and kidneys were removed, weighed, and fixed by immersion in 10% neutral buffered formalin. Tissues were routinely processed, embedded in paraffin, and stained with hematoxylin and eosin for histologic examination.

STATISTICAL ANALYSIS

A one-way analysis of variance was used to analyze this data; a level of $\alpha = .05$ was chosen to detect statistically significant differences.

RESULTS AND DISCUSSION

A fast atom bombardment mass spectrum for dihydromicrocystin is shown in Figure 1. The chromatograms of microcystin-A and dihydromicrocystin are shown in Figure 2.

Table 1 shows the means and standard deviations for liver and kidney weights expressed as a percentage of mouse whole body weight for the various

treatment groups. When the relative liver weights of microcystin and dihydromicrocystin-dosed animals that died were compared, no significant difference was found. Similarly, when the relative liver weights of microcystin and dihydromicrocystin-dosed animals that survived were compared, no significant difference was found. However, when animals that died in either group were compared with those that lived, the relative liver weights of the former were greater than those of the latter. The nature of the variance and the similarity among controls and survivors was suggestive of a near "all or none effect." The kidney data showed no significant difference between the survivors and nonsurvivors with MCYST-A but significantly greater fractional kidney weights were observed in the survivors vs. the nonsurvivors with dihydro MCYST-A. The lack of a significant difference in kidney weights of survivors vs. nonsurvivors in the MCYST-A-dosed mice may possibly be due to the fact that nonsurvivors did not live long enough to accumulate hepatocyte debris in the kidneys.

No lesions were seen in mice treated with MCYST-A at 25 µg/kg or in the dihydro derivative mice treated at 25, 50, or 100 µg/kg. Livers from animals dosed with MCYST-A at 50 µg/kg were characterized by mild lesions consisting of occasional, scattered, single cell necrosis of hepatocytes immediately (1 to 2 layers) adjacent to the central vein. Mice dosed with MCYST-A at 100 µg/kg, and those dosed with dihydro MCYST-A at 200, 300, or 400 µg/kg all had similar microscopic hepatic lesions. These consisted of severe, widespread centrilobular and midzonal hepatocyte dissociation, rounding, degeneration and necrosis with massive intralesional hemorrhage. In the more mildly affected adjacent areas, many hepatocytes contained one to several large, clear intracytoplasmic vacuoles.

The acute toxicity of dihydro MCYST-A appears to be approximately one-half that of MCYST-A. Similar pathology was observed in animals which died acutely from dihydro MCYST-A and MCYST-A. Relative organ weights were also similar in animals from both groups which died acutely, and were also similar when the survivors of the 2 groups were compared. This data may be compared to a similar experiment performed with a cyclic pentapeptide hepatotoxin from Nodularia spumigena and its dihydrogenated and hexahydrogenated derivatives. (See the annual report for 1986.) In the case of Nodularia toxin, saturation of the dehydroamino acid contained within its structure produced a more marked decrease in toxicity. In addition, the dihydrogenation of Nodularia toxin produced a change in the liver lesions observed in animals surviving 24 hours after toxin administration. A similar alteration in lesions was not observed in the case of the MCYST-A dihydro derivative. The dehydroamino acid present in Nodularia toxin is N-methylaminobutyric acid instead of N-methyldehydroalanine present in MCYST-A. It is also important to note that, while toxicity is decreased by saturation of the dehydro moieties, these compounds still remain quite potent and continue to display marked specificity for the liver as a target organ.

REFERENCE

Gross, E., and Morall, J. L.: The presence of dehydroalanine in the antibiotic nisin and its relationship to activity. J. Amer. Chem. Soc. 89:11, 1967.

Table 1. Mean values of fractional organ weights of mice given intraperitoneal injections of microcystin-A or its dihydro derivative (n = 6 for all treatment groups).

	% Liver Weight ¹	% Kidney Weight ¹	24-Hour Mortality (Dead/Live)
<u>Dosage Dihydro</u>			
25 µg/kg	5.60 ± 0.41	1.42 ± 0.10	0/6
50 µg/kg	5.25 ± 0.30	1.37 ± 0.08	0/6
100 µg/kg	5.18 ± 0.25	1.42 ± 0.07	0/6
200 µg/kg	8.87 ± 0.80	1.66 ± 0.14	6/6
300 µg/kg	8.80 ± 0.69	1.57 ± 0.10	6/6
400 µg/kg	8.73 ± 0.67	1.67 ± 0.08	6/6
<u>Dosage MCYST-A</u>			
25 µg/kg	5.33 ± 0.31	1.28 ± 0.15	0/6
50 µg/kg	5.62 ± 0.41	1.55 ± 0.29	0/6
100 µg/kg	7.92 ± 0.50	1.53 ± 0.08	6/6
<u>Vehicle Treated</u>			
0 µg/kg	5.08 ± 0.44	1.42 ± 0.08	0/6

¹Expressed as mean ± Standard Deviation of organ percentage of animal whole body weight.

21-HYDRO-CYANOGLINGOSIN LR GLY-1NHCL
 SAMPLE NO. 1 3592 SCAN NO. 1 5.12 TIME (MIN): 0.4

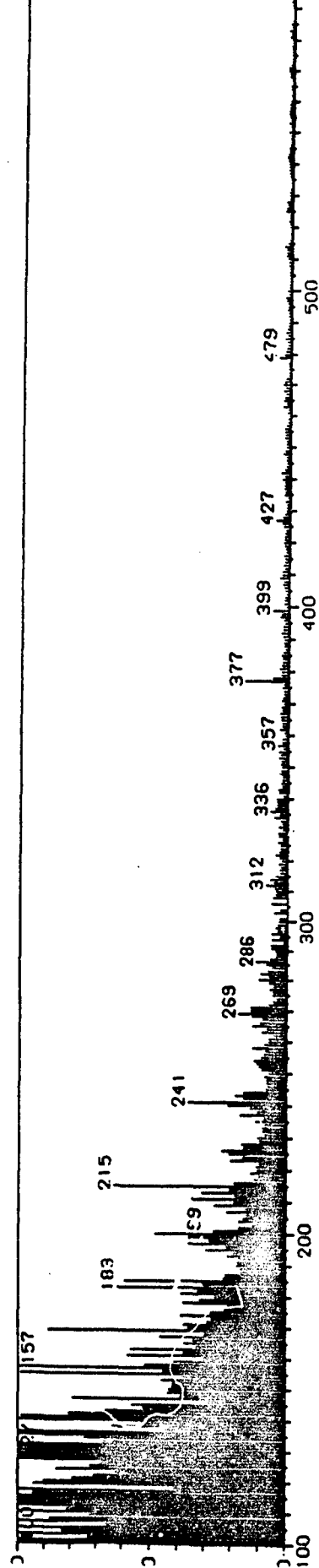
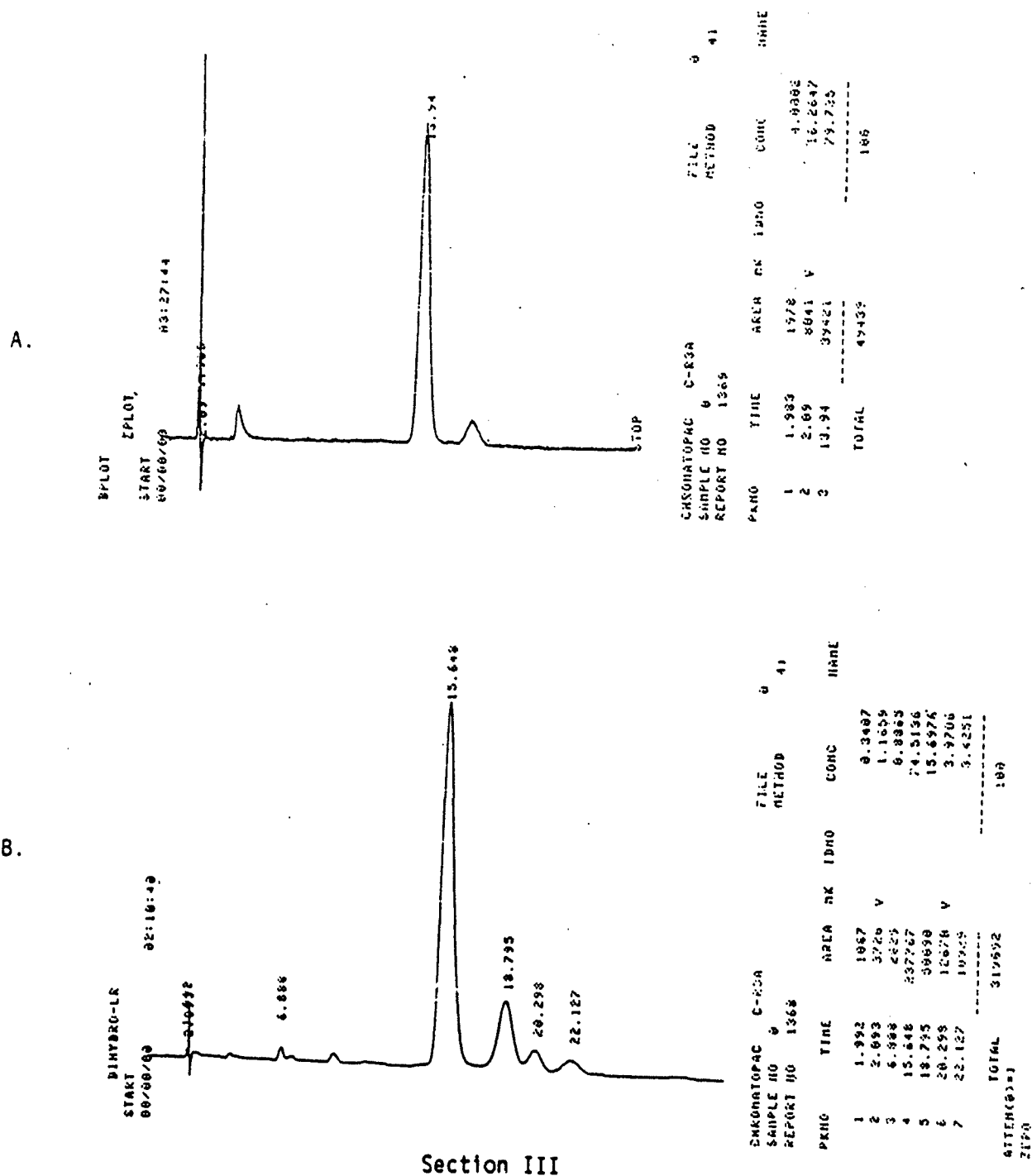


Figure 1. FAB-mass spectrum of dihydromicrocystin.

Figure 2. HPLC chromatograms for microcystin-A (A) and dihydromicrocystin (B). (Column = nucleosil 5C₁₈ [0.46X 150 mm]; mobile phase of MeOH-0.05 M phosphate (58:42), pH = 3; flow rate = 1 ml/min; UV detection at 238 nm.)



IV. DEVELOPMENT OF URINE AND PLASMA EXTRACTION METHODS FOR MICROCYSTIN-A

Andrew M. Dahlem, Ken-Ichi Harada, and Leslie Waite

INTRODUCTION

Microcystin-A (MCYST-A) was extracted from swine urine and plasma using disposable reverse phase cartridges and quantitated by high performance liquid chromatography (HPLC) with UV detection.

PROCEDURES AND RESULTS

Swine urine (4 ml) was amended with MCYST-A (80 µg) and placed on preconditioned Bond Elut octadecylsilane (ODS) cartridges. The cartridge was then washed with water (2 x 2 ml) followed by 15% methanol in water (2 x 2 ml). The MCYST-A was eluted from the cartridge with 6 ml of methanol. The eluate was evaporated to dryness using a rotary evaporator and then transferred to autosampler vials and subjected to HPLC analysis. The HPLC conditions were: a mobile phase of acetonitrile--0.1 M ammonium acetate, pH 5, in a ratio of 22.5:77.5. The flow rate was 1.5 ml/min and detection was by UV absorption at 238 nm.

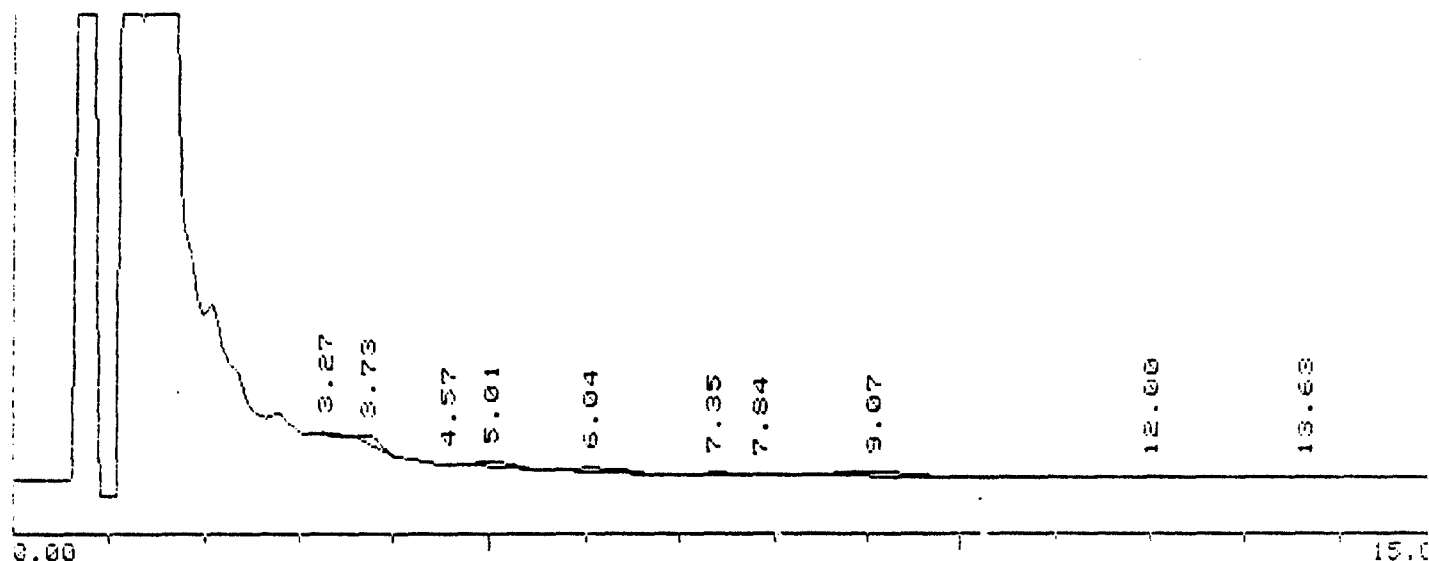
Swine plasma was subjected to the same solid phase extraction described above except that 2 ml of plasma was amended with 20 µg of MCYST-A and extracted. Additional physical separation was sometimes necessary to remove an insoluble protein precipitate before HPLC analysis. The methanol eluate was filtered through Acro 0.2 µm membrane filters then evaporated on a rotary evaporator, transferred to autosampler vials and subjected to HPLC analysis under the conditions described above. Chromatograms for control urine, amended urine, control plasma, and amended plasma are shown in Figures 1-4. Recoveries of toxin from amended samples were 92% for urine and 63% for plasma (means of 3 samples each).

DISCUSSION

Octadecylsilane solid phase extraction columns have a high affinity for MCYST-A, and thus are applicable to extraction of toxin from the biological matrices examined to date. It is not yet known how extensively MCYST-A will be excreted into the urine of affected animals, but samples from toxin-dosed animals are currently under investigation. The plasma extraction efficiency was lower than that for urine and may result from nonspecific protein binding in the plasma. Additional treatment of plasma, including acid precipitation and heat will be used prior to extraction in order to free protein-bound MCYST-A for detection on HPLC.

Figure 1. Chromatogram of control urine.

LY1.RAW URINE.FIL FIGURINE.CFG PW = 6 PT = 70 OF = 10% AT = 256.
 SAMPLE: LY1 AT 08/10/87 15:41:24 FILENAME: MATRIX1 FROM /1.A/
 DISK FILE: LY1.RAW PEAK WIDTH = 6 ATTENUATION = 256.0



DISK FILE: LY1.RAW FROM / 1.A/ INJECTED AT: 08/10/87 15:41:24

MATRIX CH= A PS= 1
 FILE 2 METHOD 0 RUN 4 INDEX 4

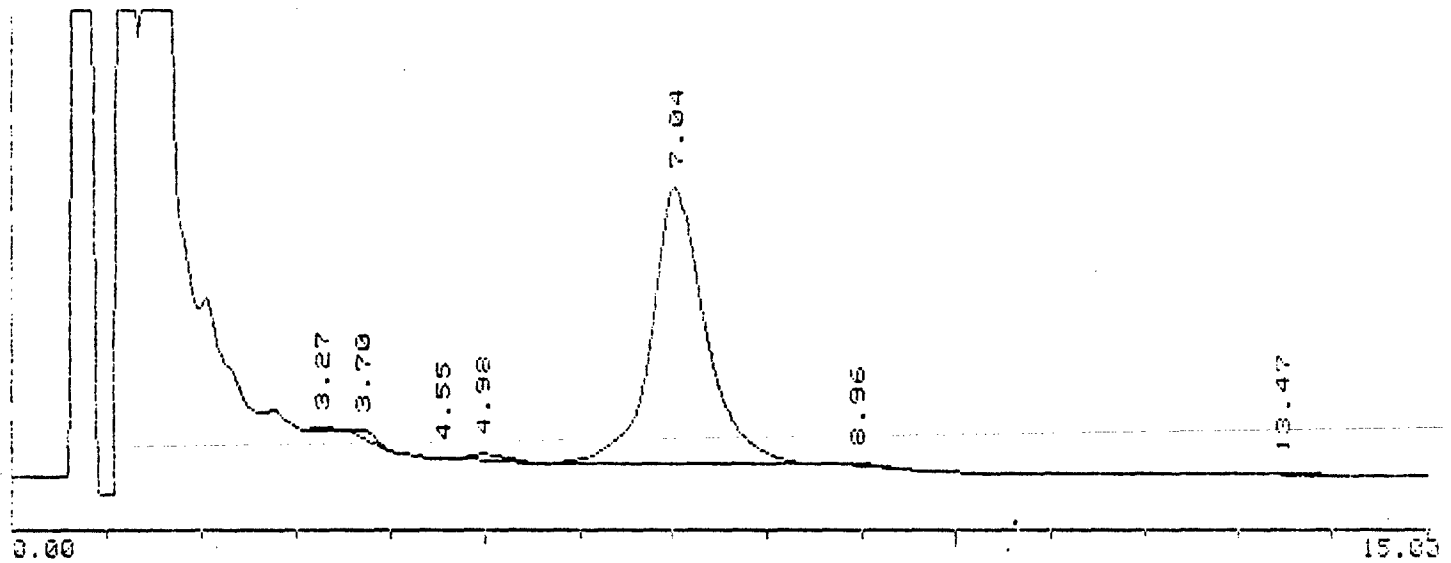
PEAK#	AREA%	RT	AREA BC
1	5.844	3.27	47697 01
2	13.895	3.73	113396 01
3	0.468	4.57	3823 01
4	13.906	5.01	113486 01
5	18.226	6.04	148746 01
6	7.214	7.35	58872 02
7	3.263	7.84	26634 02
8	26.015	9.07	212309 03
9	4.141	12.	33792 02
10	7.028	13.63	57360 03

TOTAL 100. 816115

Section IV

Figure 2. Chromatogram of amended urine.

YY1.RAW URINE.FIL FIGURINE.CFG PW = 6 PT = 70 OF = 10% AT = 256.
SAMPLE: YY1 AT 08/10/87 16:32:54 FILENAME: MATRIX1 FROM /1.A/
DISK FILE: YY1.RAW PEAK WIDTH = 6 ATTENUATION = 256.0



DISK FILE: YY1.RAW FROM / 1.A/ INJECTED AT: 08/10/87 16:32:54

MATRIX CH= A PS= 1
FILE 2 METHOD 0 RUN 2 INDEX 2

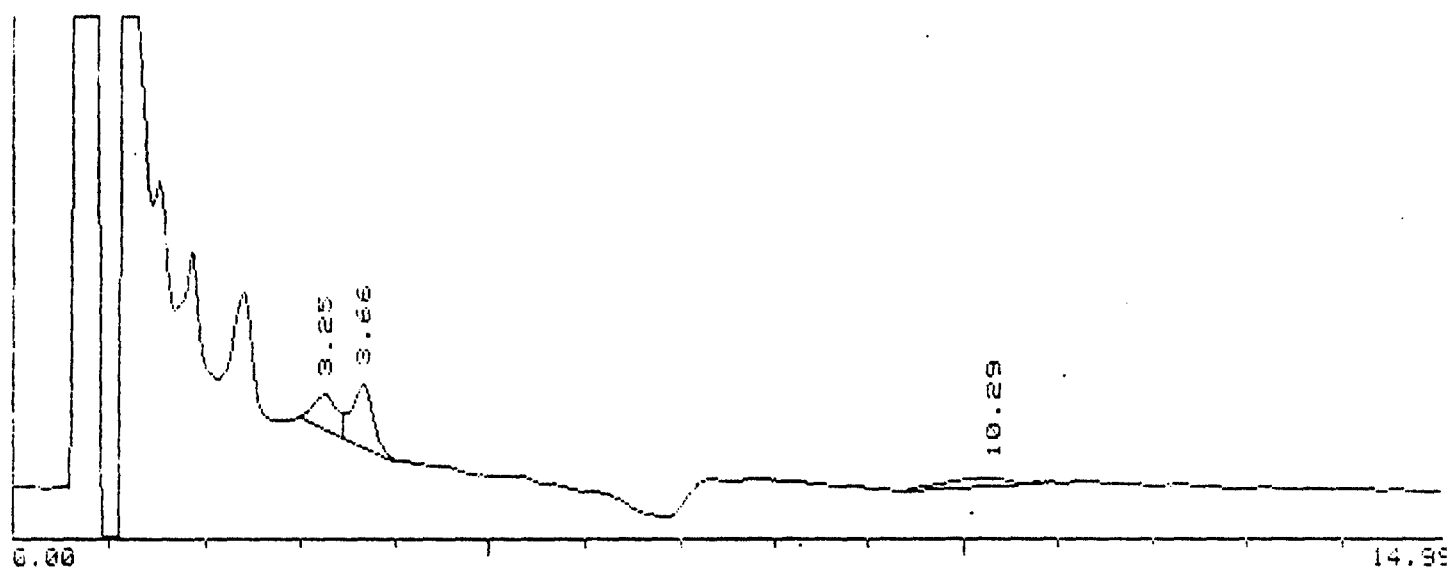
PEAK#	AREA%	RT	AREA	BC
1	0.426	3.27	48999	01
2	1.083	3.7	124739	01
3	0.149	4.55	17094	02
4	1.362	4.98	156801	03
5	96.11	7.04	11064067	01
6	0.559	8.96	64300	01
7	0.311	13.47	35803	01
TOTAL	100.		11511803	

Figure 3. Chromatogram of control plasma.

RY2.RAW PLASMA.FIL PIGPLASM.CFG PW = 6 PT = 70 OF = 10% AT = 8.

SAMPLE: RY2 AT 08/10/87 18:00:09
DISK FILE: RY2.RAW

FILENAME: MATRIX1 FROM /1.A/
PEAK WIDTH = 6 ATTENUATION = 8.0



DISK FILE: RY2.RAW FROM / 1.A/ INJECTED AT: 08/10/87 18:00:09

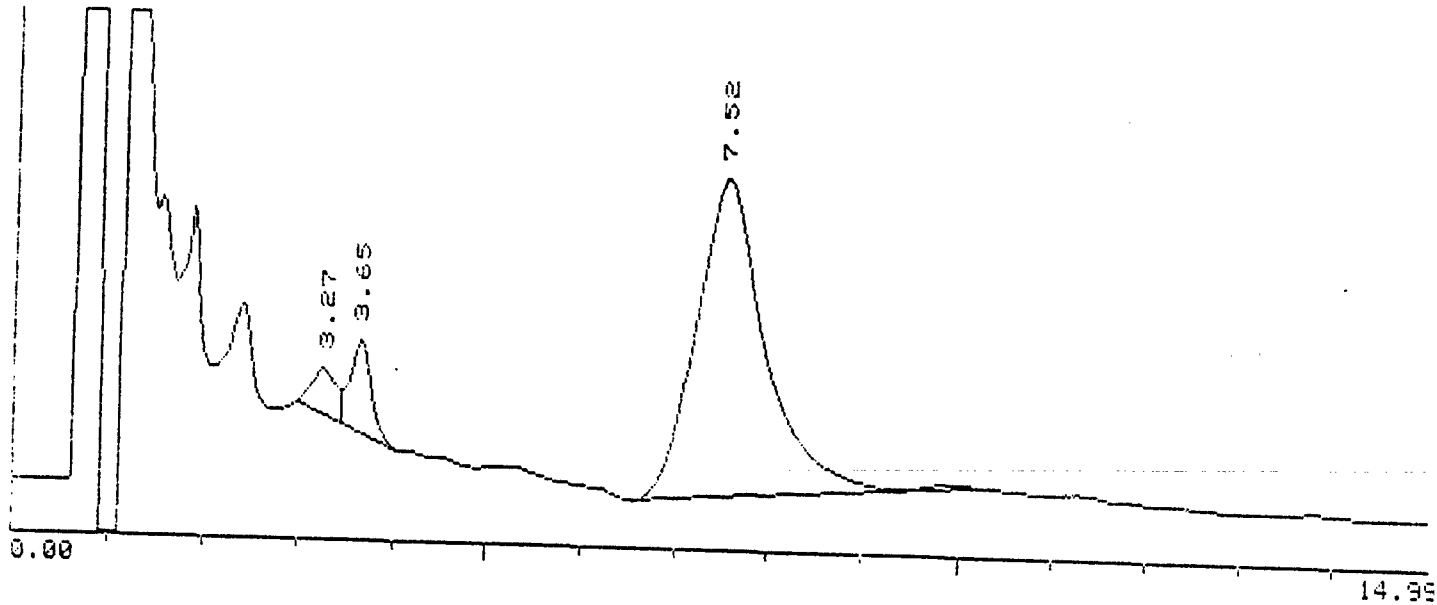
MATRIX CH= A PS= 1
FILE 2 METHOD 0 RUN 2 INDEX 2

PEAK#	AREA%	RT	AREA BC
1	31.587	3.25	19001 02
2	48.753	3.66	29327 03
3	19.66	10.29	11826 01
TOTAL	100.		60154

Section IV

Figure 4. Chromatogram of amended plasma.

SY2.RAW FLASMA.FIL FIGPLASM.CFG PW = 6 PT = 70 OF = 10% AT = 8.
 SAMPLE: SY2 AT 08/10/87 17:43:07 FILENAME: MATRIX1 FROM /1.A/
 DISK FILE: SY2.RAW PEAK WIDTH = 6 ATTENUATION = 8.0



DISK FILE: SY2.RAW FROM / 1.A/ INJECTED AT: 08/10/87 17:43:07

MATRIX
 FILE 2 METHOD 0 RUN 3 INDEX 3 CH= A PS= 1

PEAK#	AREA%	RT	AREA BC
1	4.286	3.27	24545 02
2	7.476	3.65	42810 03
3	88.238	7.52	505297 01
TOTAL	100.		572652

V.. ORAL TOXICITY OF MICROCYSTIN-A

1. Investigation of the oral toxicity of microcystin-A to rats.

A. M. Dahlem, A. S. Hassan, S. P. wanson

EXPERIMENT

Four grams of lyophilized cell material from the Monroe, Wisconsin, Microcystis aeruginosa bloom were combined with 26.6 ml of deionized water and continuously stirred overnight on a stir plate. A slurry of the cell suspension was gavaged into each of four laboratory rats which had been anesthetized with diethyl ether.

Rats

All rats were male and had been previously administered a subtoxic dose of T-2 toxin 2 weeks prior to this study. They were fasted overnight so that a maximum dose of cell material could be administered.

Rat #	Weight	Amount of Material	mg/kg
589	273 g	2 mL	1,102
590	280 g	3 mL	1,611
591	310 g	4 mL	1,940
592*	280 g	3 mL	1,611

*Rat 592 was administered 100 mg of cholestyramine two hours after cell suspension administration.

RESULTS

All animals survived 72 hours after toxin administration and were killed by chloroform inhalation. Gross examination of liver tissue showed no lesions.

CONCLUSIONS

Quantities of lyophilized cell material which are much higher than those which could be consumed in nature do not produce toxic effects in orally dosed rats.

The oral administration to rats of microcystin-A in lyophilized cell material is not a suitable model for the study of orally induced toxicosis.

2. Investigation of the oral toxicity of microcystin-A to mice.

A. Dahlem, A. Hassan, S. Swanson

EXPERIMENT

Purified microcystin-A (1.4 mg) from Wright State University (batch M of toxin) was added to a 3.0 ml disposable test tube with 10 μ l of absolute ethanol to dissolve the toxin. Deionized water (740 μ l) was also pipetted into the test tube, and the tube was vortexed and placed under warm tap water to aid in solubilizing the toxin. Individual aliquots of toxin were then pipetted into individual test tubes and QS to 320 μ l total volume for gavaging. The toxin was then administered via gavage to unanesthetized male Swiss inbred mice weighing from 20 to 22 grams.

RESULTS

Mouse #	Dose	Effect Observed
1	250 μ g/kg	None
2	500 μ g/kg	None
3	1,000 μ g/kg	None
4	2,000 μ g/kg	None
5	4,000 μ g/kg	None
6	8,000 μ g/kg	None
7	16,000 μ g/kg	None
8	32,000 μ g/kg	None

CONCLUSIONS

Acute doses of toxin which are much higher than those which could be consumed as a result of natural exposure produced no effect in mice when given by gavage. The bioavailability of this toxin must be low after oral exposure in mice since, as indicated previously, 1 μ g to 2 μ g of toxin injected IP will kill a mouse in two to three hours.

3. Investigation on the oral toxicity of microcystin-A to chickens.

A. Dahlem, A. Hassan, S. Swanson

EXPERIMENT

Ten grams of lyophilized cell material from the Monroe, Wisconsin, Microcystis aeruginosa bloom were combined with 120.0 ml of deionized water and continuously stirred overnight. All chickens were young roosters which were reared at the University of Illinois and acclimated for two weeks prior to toxin administration. Animals weighed between 350 to 480 grams and were gaining weight throughout the acclimation period. Chickens were not anesthetized prior to gavage and a single use feeding tube was passed into the crop for toxin administration. A slurry of the cell suspension was gavaged into each of four chickens which had been fasted overnight. In addition, four were dosed intravenously (IV) with the toxin and two were not dosed and served as negative controls.

Chicken #	Weight	Treatment	Gross Lesions
Purified Toxin:			
1	.457 kg	25 µg/kg IV	None
2	.460 kg	50 µg/kg IV	+Liver
3	.434 kg	88 µg/kg IV	+Liver
4	.386 kg	200 µg/kg IV	+Liver
Cell Extract:			
5	.415 kg	.25 g/kg Oral	None
6	.446 kg	.42 g/kg Oral	None
7	.401 kg	.83 g/kg Oral	None
8	.478 kg	1.0 g/kg Oral	None
Purified Toxin:			
9	.430 kg	4.6 mg/kg Oral	None
Controls:			
10	.332 kg		None
11	.425 kg		None

RESULTS

All birds survived six hours after toxin administration. Chickens given toxin intravenously at doses of 50, 88, and 200 µg/kg were visibly affected and one animal was in sternal recumbency prior to euthanasia. All animals given toxin by gavage appeared normal at the time of euthanasia. Gross lesions, seen in affected IV dosed birds at necropsy, did not resemble the mammalian lesions seen so far. The chicken livers were not blood engorged but appeared tan and mottled. No liver lesions were seen in orally dosed chickens.

CONCLUSIONS

Chickens are easily dosed orally with toxin or lyophilized cell material but do not appear susceptible to high doses of toxin or cell material. The gross liver lesions observed in chickens from acutely toxic doses of purified peptide differ from those in the mammalian species studied to date.

VI. THE EFFECT OF GLUTATHIONE DEPLETION ON THE IP TOXICITY
OF MICROCYSTIN-A

A. Dahlem, A. Hassan, S. Swanson

EXPERIMENT

Mice were treated with a sublethal dose of microcystin-A (20 µg/kg), an LD₅₀ dose of microcystin-A (37 µg/kg) by IP injection and/or either the glutathione depletor diethyl maleate (DEM) or the inhibitor of glutathione synthesis buthionine sulfoximine (BSO) IP.

BSO was purchased from Chemical Dynamics Laboratories. The BSO dose was always 30 mg per 0.25 kg animal in .75 mL 0.9% saline and was given four hours prior to toxin, in an attempt to maximally deplete glutathione. The DEM animals were administered 0.1 mL of DEM per 100 gram body weight in sesame oil vehicle.

RESULTS

Survival was measured at 24 hours after toxin administration. Animals given DEM followed by toxin appeared sick but did not die. Animals given BSO and toxin were not distinguishable from low toxin controls at either dosage.

Group	Toxin Dose	Survival
Low Toxin Control	20 µg/kg	6/6 (100%)
DEM + Toxin	20 µg/kg	6/6 (100%)
BSO + Toxin	20 µg/kg	6/6 (100%)
BSO + Toxin	37 µg/kg	6/6 (100%)
Medium Toxin Control	60 µg/kg	1/3 (33.3%)
High Toxin Control	90 µg/kg	0/3 (0.0%)

CONCLUSION

These results indicate that glutathione probably does not play a major role in the acute detoxification of this compound. A subtle effect may still

be exerted, however, since DEM animals appeared affected but did not die. It is also possible that glutathione reserves would afford protection in animals in which inhibition of glutathione synthesis was induced prior to microcystin exposure.

VII. VISUALIZATION OF RAT HEPATOCYTES
WITHIN THE PULMONARY VASCULATURE VIA MICROSCOPIC AUTORADIOGRAPHY

S. Hooser, W. Haschek-Hock, M. Kuhlenschmidt

EXPERIMENT

Three hours following IP administration of microcystin-A at 200 µg/kg bw, 5 µg of I¹²⁵ gal-BSA was injected IV in one adult male rat. A separate rat was given the same IP dose of microcystin-A and 5 µg of I¹²⁵ gal-BSA combined with 45 µg of I¹²⁷ gal-BSA IV at 30 and 60 minutes following dosing. Thirty minutes following the injection of gal-BSA, the rats were killed, and liver, lungs, heart, kidneys, spleen, and adrenals were removed and weighed. Radioactivity in these organs was measured via gamma emission counting, and sections of each were fixed by immersion in 10% neutral-buffered formalin.

The sections were dehydrated, embedded in glycomethacrylate, and sectioned at 2 µm or 6 µm. Tissues from a rat not given I¹²⁵ gal-BSA were used as controls. After sectioning, the tissues were placed on precleaned glass slides and were then dipped in Kodak NTB-2 photographic emulsion. The slides were put in light-tight boxes at 0°C to 4°C. At 2, 3, and 4 weeks, one set of the slides (each set contained all tissues) was developed, rinsed, and fixed. Each slide was stained with carbol fuchsin and new methylene blue and coverslipped for microscopic examination.

RESULTS

A rise of radioactivity in the liver and concomitant fall of radioactivity in the blood was measured. No corresponding changes were measured in other organs which were distinguishable from that accounted for by blood radioactivity.

On microscopic examination, numerous grains were seen over the cytoplasm of hepatocytes of rats given I¹²⁵ gal-BSA. Only a few, random grains were seen over the hepatocytes of the control rat. In the liver sections from rats given I¹²⁵ and microcystin-A, numerous degenerated hepatocytes with overlying grains were seen within central veins. In the pulmonary vasculature of rats given I¹²⁵ gal-BSA and microcystin-A, grains were seen overlying the vessels and were more numerous over large cells which resembled degenerate or necrotic hepatocytes. Only randomly scattered grains (background radioactivity) were seen in other organs. No grains were seen over the vasculature or blood cells of the control.

CONCLUSION

These autoradiographic studies further suggest that the large cells appearing within the pulmonary vasculature after toxin administration are hepatocytes. However, background radioactivity was too high for positive confirmation.

VIII. BIOSYNTHETIC RADIOLABELING OF MICROCYSTIN-A

A. Dahlem

INTRODUCTION

In these experiments we tested the hypothesis that addition of radiolabelled glutamic acid to a growing culture of Microcystis aeruginosa strain 7820 would result in labelled microcystin-A. In the normal procedures for growing M. aeruginosa in the laboratory, no amino acids are added to the culture; the algae biosynthesize all necessary amino acids. In order to test the hypothesis in the most general sense we first added a small quantity of C-14 glutamic acid as a racemic mixture. The configuration of glutamic acid in the toxin structure is the D configuration, but it was not known whether only the D-isomer would be incorporated or if the algae would bioconvert the L form to the D for use in the toxin structure.

In the next experiment, higher concentrations of C-14 labelled glutamic acid were added to the growing algae to see if the label incorporation would be proportional to the amount of C-14 glutamic acid present. It is known that cyanobacteria are extremely opportunistic regarding incorporation of preformed nutrients including amino acids and we wanted to determine if the biosynthetic pathway which governs toxin biosynthesis could be saturated.

Finally we tested the hypothesis that 1 isomer of glutamic acid is selected preferentially for incorporation into the toxin structure. Since the cost of tritium labeled D-glutamic acid is 10 times that of tritium labeled L-glutamic acid, we first tested the addition of tritiated L-glutamic acid to the growing algae. Despite the higher cost of the D-labelled amino acid, since the configuration in the toxin is the D-configuration and this form of

glutamic acid occurs infrequently in other Microcystis peptides, we hoped that the D form would be selectively taken up. This could be proven if toxin produced in the presence of added C-14 L-glutamic acid would have low specific activity.

MATERIALS AND METHODS

In the first experiment 10 μCi of glutamic acid, D,L [$1\text{-}^{14}\text{C}$] of specific activity 40 to 60 $\mu\text{Ci}/\text{mmole}$ was added to an actively growing culture of M. aeruginosa strain 7820 in our laboratory as a one-time addition of radiolabel.

In the second experiment 100 μCi of the D,L ^{14}C labelled glutamic acid was added to a growing culture of Microcystis in 10 μCi aliquots every other day for 20 days (total of 10 additions).

In the third experiment 100 μCi of glutamic acid, L-[$3,4\text{-}^3\text{H}$] of specific activity of 40 to 60 $\mu\text{Ci}/\text{mmol}$ was added to a growing culture of M. aeruginosa strain 7820 also in 10 μCi aliquots every other day for 20 days.

RESULTS AND DISCUSSION

Experiment 1 above yielded 1.3 mg of greater than 95% pure microcystin-A (MCYST-A) with a specific activity of 50 to 60 cpm/ μg of toxin.

Experiment 2 above yielded 2.1 mg of greater than 95% pure MCYST-A with a specific activity of 420 to 450 cpm/ μg of toxin.

Experiment 3 above yielded 1.7 mg of greater than 95% pure MCYST-A with a specific activity of 40 to 60 cpm/ μg of toxin.

These results show that toxin of rather low specific activity can be produced by biosynthesis using the relatively low levels of radioactivity described above. They nevertheless indicate that the addition of radiolabelled glutamic acid is likely to serve as a viable alternative for production of labelled MCYST-A.

The third experiment yielded inconclusive results which were difficult to interpret. It was felt that tritiated glutamic acid would provide material of higher specific activity than could be easily and economically obtained with C-14 labelled material, however, we found that a large percentage (42%) of the tritium label had disassociated into the algae growth medium and become tritiated water. Since a relatively large fraction of the label was lost through exchange, interpretation of the specific isomer addition is unclear. This experiment is currently under investigation using C-14 labelled L-glutamic acid.

Taken together these experiments demonstrate that: 1) amended glutamic acid can be taken up by the growing algae and incorporated into the toxin structure, 2) a proportional relationship exists between the amount of labelled glutamic acid added and the resultant specific activity of the toxin produced, and 3) that tritiated L-glutamic acid did not produce toxin with as high a specific activity as produced with D-L mixtures of C-14 labelled glutamic acid.

IX. EVALUATION OF ENZYME RELEASE BY PRIMARY CULTURES
OF HEPATOCYTES FOLLOWING EXPOSURE TO MICROCYSTIN-A

S. B. Hooser

PURPOSE

To evaluate enzyme release from primary cultures of hepatocytes following addition of microcystin-A to the culture media.

PROCEDURE

Forty-eight-hour, primary cultures of rat hepatocytes were exposed to physiologic buffered salines PBS (negative control), carbon tetrachloride (CCl₄) at 0.1 ml/ml of medium, or microcystin-a at 1 µg/ml of medium. At 1, 2, 3, and 6 hours (microcystin-A) or 1 and 6 hours (saline and CCl₄ controls), the medium was aspirated from each of four culture wells, and individually frozen and subsequently analyzed for enzyme activity.

RESULTS

A significant increase in ALP release following exposure to microcystin-A was seen at 3- and 6-hour postadministration; however, no significant increases (as compared to controls) of ALT, AST, or LDH release were seen at any time point examined. Significant increases in release of ALP and AST at 1 and 6 hours and of ALT and LDH at 6 hours were seen in the cultures exposed to CCl₄ (see Table 1).

DISCUSSION

In previous in vivo studies, we observed a measurable increase in serum ALT at 40 to 60 minutes following administration of microcystin-A to rats and an increase in serum ALP beginning at 3 hours. Our in vitro results indicate no increase in release of ALT and an increase in ALP at 3- to 6-hours

postexposure. This in vitro difference is probably not due to a time-related decrease in P₄₅₀ which can occur in cultured hepatocytes because administration of CCl₄ caused large to massive increases of all hepatic enzymes. This would indicate that P₄₅₀ was present in the cultured hepatocytes and was responsible for converting CCl₄ to its active, hepatotoxic form. When compared to previous effects in whole animals, the decreased response of cultured cells to microcystin-A must be due to a lack and/or modification of: (1) the plasma membrane receptor and/or transport system, (2) intracellular enzymes or intracellular organelles that normally activate or are harmed by the toxin, (3) interaction with other hepatic cell types, (4) inadequate concentration of toxin in the cells, or (5) the absence of hypoxic stress associated with in vivo impairment of blood through the liver.

Table 1. Enzyme Release from Cultured Hepatocytes Exposed to Microcystin-A, CCl₄, or Physiologic Buffered Saline (PBS).

Group	Time (hr)	ALP	ALT	AST	LDH
Microcystin-A 1 mg/ml	1	15.3 ± 0.63	5.5 ± 1.2	72.6 ± 2.3	143.5 ± 12.7
	2	21.5 ± 0.29	8.5 ± 0.5	53.3 ± 2.3	123.8 ± 9.6
	3	25.0 ± 0.41*	5.2 ± 0.9	55.3 ± 4.3	87.8 ± 5
	6	32.5 ± 1.55*	6.2 ± 0.6	77.6 ± 4.9	105.3 ± 10
CCl ₄ 0.1 ml/ml media	1	32.5 ± 0.65*	5.7 ± 1.1	755.3 ± 88*	145.5 ± 21
	6	38.5 ± 1.55*	16.2 ± 3.1*	1325.3 ± 53*	245.0 ± 63*
PBS (control)	1	13.8 ± 0.75	8.2 ± 0.96	94.1 ± 12.3	109.8 ± 17.2
	6	17.5 ± 0.65	8.0 ± 1.2	89.6 ± 5.2	129.0 ± 15.5

Mean ± SE, n = 4 for all groups except for media when n = 3.

ALP = Alkaline phosphate (U/L).

ALT = SGPT = Alanine amino transferase (U/L).

AST = SGOI = Aspartate amino transferase (U/L).

LDH = Lactate dehydrogenase (U/L).

* = Treated groups which are significantly different (P < 0.05) from the saline controls.

X. SEQUENTIAL HEPATIC, PULMONARY, AND RENAL ULTRASTRUCTURAL CHANGES
INDUCED BY MICROCYSTIN-A (CYANOGINOSIN LR) IN RATS


S. B. Hooser and W. M. Haschek

Microcystin-A (cyanoginosin LR) is a cyclic heptapeptide hepatotoxin produced by the cyanobacterium, Microcystis aeruginosa. Deaths in livestock and wildlife, as well as human illness, have resulted from ingestion of water containing this species of blue-green algae.¹⁻⁹

As previously shown in our laboratory, when lethal doses (LD₅₀ = approximately 120 µg/kg) of purified hepatotoxin is injected intraperitoneally into rats, light microscopic lesions which correlate with increases in serum alanine amino transferase are seen in the liver beginning 20 to 30 minutes postadministration. Lesions begin centrilobularly and progress to the periportal regions of the lobules over time. Initially, there is mild disassociation and rounding of centrilobular hepatocytes followed rapidly by severe hepatocyte disassociation, rounding, degeneration, and necrosis. By 60 minutes, these changes have progressed to midzonal and periportal regions. In addition, by 60 to 180 minutes there is a breakdown of the sinusoidal endothelium and loss of central veins with severe centrilobular hemorrhage.

Death in rats occurs 20 to 30 hours postadministration. Beginning 50 to 60 minutes postadministration, intact hepatocytes appear in the pulmonary vasculature. Over a 24-hour period, these intact cells are gradually replaced by necrotic cellular debris as increasing severity of necrosis occurs in the liver.

Late in the course of the toxicosis, beginning at 12 hours, the capillaries of the renal cortex contain large amounts of eosinophilic, finely



fibrillar to granular material which does not stain for fibrin. In addition, many renal tubular epithelial cells contain one to several large, clear, intracytoplasmic vacuoles.

A limited number of previous studies have involved characterization of the effects of this hepatotoxin using transmission electron microscopy (TEM) or scanning electron microscopy (SEM). Scanning electron microscopy of freshly prepared, isolated rat hepatocyte suspensions has shown dose-dependent deformation and blebbing within 5 minutes of toxin exposure.^{11,12} Sequential SEM and TEM of mouse livers following intraperitoneal administration of an aqueous M. aeruginosa extract from Australia showed a progressive breakdown of sinusoidal endothelium, disappearance of the space of Dissé, damage to hepatocyte membranes, and "necrotic changes" in hepatocyte cytoplasm. However, these changes initially occurred periportally and progressed centrilobularly. Localization of initial changes in the periportal region has not been reported subsequently.² In sheep given aqueous M. aeruginosa extracts from Australia, TEM from tissues taken approximately 20 hours postadministration showed centrilobular hepatic necrosis with aggregation of the endoplasmic reticulum (ER), displacement of cellular organelles to the periphery, and vacuolation of severely affected cells.⁵ Most recently, a report of a sequential TEM study utilizing purified microcystin-A in mice, at doses of 10 and 100 µg/kg ip, described hepatocyte changes consisting of rough endoplasmic reticulum (RER) vesiculation, mitochondrial swelling, RER degranulation and, at 100 µg/kg, an increase in intracytoplasmic membrane whorls.¹⁰

There are marked differences in the responses of mice and rats to microcystin-A. Among the most prominent of these is the time course of the

toxicosis and lesion development. In mice there is massive, centrilobular to midzonal hemorrhage and death which occur rapidly, 60 to 90 minutes postdosing. In rats, while hepatic necrosis and hemorrhage occur within 60 minutes, the hemorrhage does not appear to be as severe as in mice, and rats survive 24 to 32 hours following administration of a lethal dose of the hepatotoxin.

The purpose of this study was to characterize the sequential ultrastructural hepatic, pulmonary, and renal changes in rats following administration of microcystin-A utilizing perfusion fixation to minimize artifactual changes. Herein, ultrastructural changes are correlated with previously observed light microscopic changes in an attempt to delineate the sequence of lesion development in rats. The discussion contrasts ultrastructural changes in rats with those previously reported for mice.

MATERIALS AND METHODS

Male, Harlan Sprague Dawley rats weighing 200 to 250 g were given food and water ad libitum and kept on a 12-hour light-dark cycle. The rats were injected intraperitoneally (ip) with purified microcystin-A at a lethal dose of 160 µg/kg or with saline (control). At 5, 10, 20, 30, and 60 minutes postdosing, 2 rats were anesthetized with ether (control rats were anesthetized at 60 minutes following saline administration), the thorax was opened and a cannula was placed in the left ventricle. Whole body perfusion and fixation, using Tyrode's solution at 37°C, followed by cool 2.5% glutaraldehyde in 0.1 M isotonic cacodylate buffer and 3% sucrose (pH = 7.2), was performed. Tyrode's solution and fixative were kept at a constant perfusion pressure of 110 mmHg by use of a Cole-Palmer master flex pump. Samples of liver, lung, and kidney were minced into 1 mm cubes and placed in

2.5% glutaraldehyde with 0.1 M isotonic cacodylate buffer (pH = 7.2). Tissue samples were washed in 0.1 M cacodylate buffer with 0.2 M sucrose, postfixed in 1% osmium tetroxide, rinsed, and dehydrated in a graded ethanol series of 10% to 100%. Final dehydration with 100% propylene oxide was followed by infiltration and embedding with epoxy. Thin sections of the specimens were made, mounted on copper grids, stained with uranyl acetate and lead citrate, and viewed with a JEOL 100-CX transmission electron microscope.

RESULTS

In the liver, no ultrastructural changes were seen in the controls or in microcystin-treated rats 5 minutes postdosing (Figure 1). Beginning 10 minutes after microcystin-A administration, in centrilobular areas there was mild widening of intercellular spaces between hepatocytes and occasional invaginations of the plasma membrane. These changes progressed in extent and severity over time.

At 20 minutes, alterations in the hepatocyte plasma membranes were more pronounced, consisting of invaginations with formation of variably sized and shaped cytoplasmic vacuoles. Blebbing, invaginations, and loss of microvilli were seen along the sinusoidal face. In addition, hepatocyte separation was more pronounced and widespread. In areas with severe hepatocyte lesions, widening of sinusoidal endothelial fenestrae was present. Alterations in other hepatic cell types (Kupffer, Ito, bile ducts) were not observed at this time (Figures 2, 3, and 4).

Thirty minutes following administration, there was a marked widening of the space of Disse and a marked loss of hepatocyte sinusoidal microvilli. Blebbing and invagination of the hepatocyte plasma membranes was frequently noted at the sinusoidal surfaces. The widening of the intercellular spaces

between many hepatocytes was more pronounced and widespread. In addition, bile canaliculi in affected areas were frequently dilated with blunting or loss of microvilli.

At 60 minutes, centrilobular areas contained necrotic cells as well as free floating, but intact, organelles (normal appearing nuclei, mitochondria, and RER), together with erythrocytes and platelets. Leukocytes were not observed. Several disassociated hepatocytes which appeared relatively normal, but lacked all or part of their plasma membranes were seen. Endothelium was not recognizable in these areas. In less severely affected regions at 60 minutes, there was prominent hepatocyte rounding, and erythrocytes were frequently seen in the space of Disse, in addition to the increased severity of the 30-minute lesions. There was moderate, focal loss of the sinusoidal endothelium and occasional hepatocyte cell necrosis. Moderate whorling of the RER around normal appearing mitochondria was sometimes noted. Mild mitochondrial swelling in degenerating endothelial cells was occasionally seen (Figures 5-13).

In the lung at 60 minutes, the pulmonary vasculature contained hepatic cellular debris, including relatively intact hepatocytes with recognizable mitochondria, RER, and nuclei. Occasionally, granulocytes containing large amounts of amorphous, phagocytized material were seen in the vasculature. In the kidney at 60 minutes, the capillaries of the renal cortex contained small amounts of necrotic cellular debris, including cytoplasmic fragments and mitochondria, but no intact cells as were found in the lung.

DISCUSSION

The primary ultrastructural changes seen initially in rats after microcystin-A administration are limited to alterations in the plasma membrane

of hepatocytes. The changes seen in this study correlate well with the hepatocyte disassociation and rounding observed previously via light microscopy (LM), although ultrastructural hepatocyte changes are seen as early as 10 minutes postdosing.

Loss of hepatocyte cell-to-cell contact, loss of sinusoidal microvilli, plasma membrane blebbing and invagination, and rounding of hepatocytes could be due to primary effects on the plasma membrane and/or some component of the cellular cytoskeleton. At the present time, it is not clear whether the changes seen in the sinusoidal endothelium and the space of Disse are secondary to hepatocyte changes or if there is also a direct effect on the sinusoidal endothelial cells. However, in the rat, hepatocyte changes do precede all other cellular alterations observed by TEM, which supports the theory that microcystin-A produces primary changes in hepatocytes with sinusoidal endothelial damage occurring secondarily. In addition, cholate, deoxycholate, bromsulphthalein (BSP), and rifampicin have been shown to provide protection to isolated rat hepatocytes exposed to microcystin-A⁴ suggesting that microcystin-A binds to a hepatocyte specific, nonspecific bile-acid receptor as do other low molecular weight cyclic peptides such as phalloidin and somatostatin.

The apparent lack of effect on the majority of hepatic cytoplasmic organelles was unexpected. Even following the loss of the plasma membrane, major organelles still appear largely intact. Most mitochondria do not appear swollen, the majority of RER had not undergone degranulation and hepatic nuclei were not pyknotic, nor was chromatin clumping or margination evident. This is in sharp contrast to the studies reported with mice in which intracytoplasmic organelle changes were among the primary lesions described.

The presence of hepatocytes in the pulmonary vasculature seen via LM at 60 minutes is confirmed with TEM. However, the presence at 60 minutes of hepatic debris in renal cortical capillaries observed with TEM was not recognized via LM until 9 hours postdosing. This suggests that when hepatic debris is released into the circulation from the liver, it is not all trapped by the pulmonary capillaries and that some debris passes into the systemic circulation. Similar accumulations of hepatic debris are undoubtedly lodged in capillary beds of other organs as well.

The prolonged survival times of rats compared to mice might be explained by the differences in sequential hepatic ultrastructural changes in the 2 species. In mice, rapid sinusoidal endothelial breakdown, with subsequent massive intrahepatic hemorrhage and resultant shock, could account for the short survival times observed. In rats, sinusoidal endothelial disruption occurs later, and is associated with extensive hepatocyte disruption and necrosis. Hemorrhage occurs but to a lesser degree and over a longer time period than in mice. Physiological differences in the regulation of hepatic blood flow between rats and mice may also contribute. Death in rats may be due to a combination of loss of hepatic function, associated hypoglycemia, and eventual circulatory collapse.

REFERENCES

1. Elleman, T. C., Falconer, I. R., Jackson, A. R. B., and Runnegar, M. T.: Isolation, characterization, and pathology of the toxin from a Microcystis aeruginosa (= Anacystis cyanea) bloom. Aust. J. Biol. Sci. 31:209-218, 1978.
2. Falconer, I. R., Jackson, A. R. B., Langley, J., and Runnegar, M. T.: Liver pathology in mice in poisoning by the blue-green alga, Microcystis aeruginosa. Aust. J. Biol. Sci. 34:175-187, 1981.
3. Falconer, I. R., Beresford, A., and Runnegar, M. T.: Evidence of liver damage by toxin from a bloom of the blue-green alga, Microcystis aeruginosa. Med. J. Aust. 1:511-514, 1983.
4. Jackson, A. R. B., McInnes, A., Falconer, I. R., and Runnegar, M. T.: Toxicity for sheep of the blue-green alga, Microcystis aeruginosa. Toxicol. Suppl. 3:191-194, 1983.
5. Jackson, A. R. B., McInnes, A., Falconer, I. R., and Runnegar, M. T.: Clinical and pathological changes in sheep experimentally poisoned by the blue-green alga, Microcystis aeruginosa. Vet. Pathol. 21:102-113, 1984.
6. Galey, F. G., Beasley, V. R., Carmichael, W. W., Kleppe, G., Hooser, S. B., and Haschek, W.M.: Blue-green algae (Microcystis aeruginosa) hepatotoxicosis in a herd of dairy cows. Am. J. Vet. Res. 48:1415-1420, 1987.
7. Konst, H., McKercher, P. D., Gorham, P. R., Robertson, A., and Howell, J.: Symptoms and pathology produced by toxic Microcystis aeruginosa NRC-1 in laboratory and domestic animals. Can. J. Comp. Med. Vet. Sci. 29:221-228, 1965.
8. Zin, L. L., and Edwards, W. C.: Toxicity of blue-green algae in livestock. Bov. Pract. 14:151-153, 1979.

9. Slatkin, D. N., Stoner, R. D., and Adams, W. H.: Atypical pulmonary thrombosis caused by a toxic cyanobacterial peptide. *Science* 220:1383-1385, 1983.
10. Dabholkar, A. S., and Carmichael, W. W.: Ultrastructural changes in the mouse liver induced by hepatotoxin from the freshwater cyanobacterium Microcystis aeruginosa strain 7820. *Toxicon*. 25:285-292, 1987.
11. Runnegar, M. T., Falconer, I. R., and Silver, J.: Deformation of isolated rat hepatocytes by a peptide hepatotoxin from the blue-green alga, Microcystis aeruginosa. *Naunyn-Schmiedeberg's Arch. Pharmacol.* 317:268-272, 1981.
12. Runnegar, M. T. C., and Falconer, I. R.: The in vivo and in vitro biological effects of the peptide hepatotoxin from the blue-green alga, Microcystis aeruginosa. *S. African J. Sci.* 78:363-366, 1982.

- Figure 1. Control liver. 13,500 X. N = nucleus; E = endothelial cell; M = mitochondria; S = sinusoid; B = bile canaliculus; SD = space of Dissē.
- Figure 2. Twenty minutes postdosing. Note the loss of cell-to-cell contact, loss of sinusoidal microvilli, membrane invagination, hepatocyte vacuolization, and necrosis. There is widening of sinusoidal endothelial fenestra adjacent to necrotic hepatocytes (arrows). R = erythrocyte, P = platelet, V = hepatocyte vacuole.
- Figure 3. Twenty minutes postdosing. Hepatocytes are losing cell-to-cell contact and there is associated membrane invagination (arrows). The nucleus, mitochondria, and RER appear normal.
- Figure 4. Twenty minutes postdosing. There is loss of hepatocyte sinusoidal microvilli in the space of Dissē and widening of cell-to-cell contact with cytoplasmic invaginations.
- Figure 5. Sixty minutes postdosing. There is rounding of hepatocytes, loss of cell-to-cell contact, loss of sinusoidal microvilli, membrane blebbing, and dilatation of bile canaliculi. Hepatocyte organelles appear normal. There is marked widening of the space of Dissē with erythrocytes (R) present.
- Figure 6. Sixty minutes postdosing. Same as Figure 5.
- Figure 7. Sixty minutes postdosing. In addition to lesions mentioned previously, there is hepatocyte single cell necrosis. Mitochondria and RER in both the necrotic cell and in the hepatic debris seen within the sinusoid appear normal.
- Figure 8. Sixty minutes postdosing. Higher magnification of Figure 7 showing necrotic hepatocytes with RER and mitochondria.

Figure 9. Sixty minutes postdosing. There is loss of hepatic sinusoidal microvilli, severe hepatocyte membrane blebbing (arrow), and erythrocytes present in a greatly widened space of Dissē. Note the integrity of hepatocyte organelles.

Figure 10. Higher magnification of an area similar to Figure 9. Arrow illustrates bleb in hepatocyte cell membrane.

Figure 11. Sixty minutes postdosing. Necrotic hepatic debris intermixed with erythrocytes. A hepatocyte with cytoplasm containing a normal appearing nucleus, mitochondria, and granulated RER, but lacking a plasma membrane is present in the center of the photo.

Figure 12. Sixty minutes postdosing. Higher magnification of Figure 11.

Figure 13. Sixty minutes postdosing. Erythrocytes intermixed with relatively intact appearing mitochondria and RER.



Figure 1 Section VII

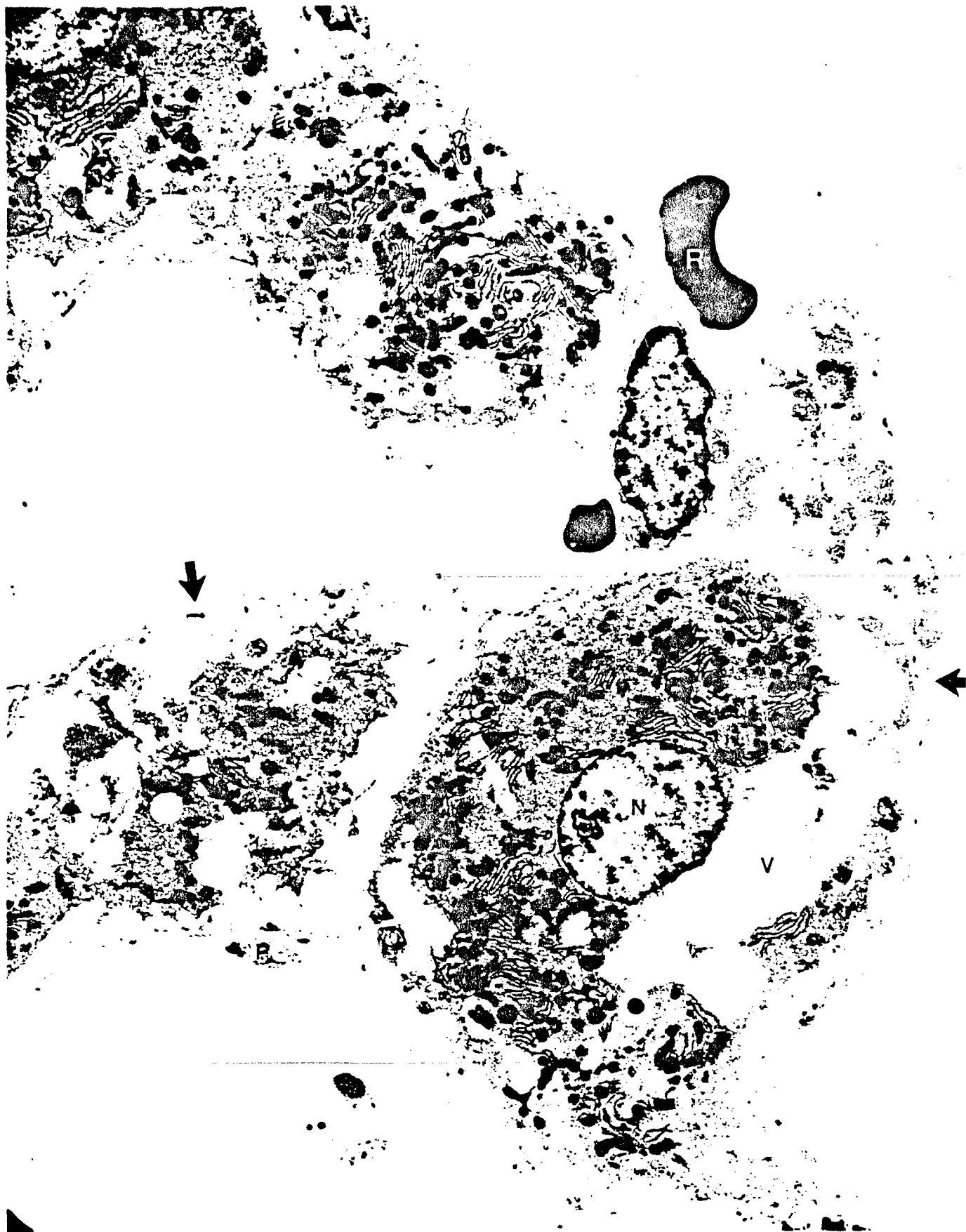


Figure 2 Section VII

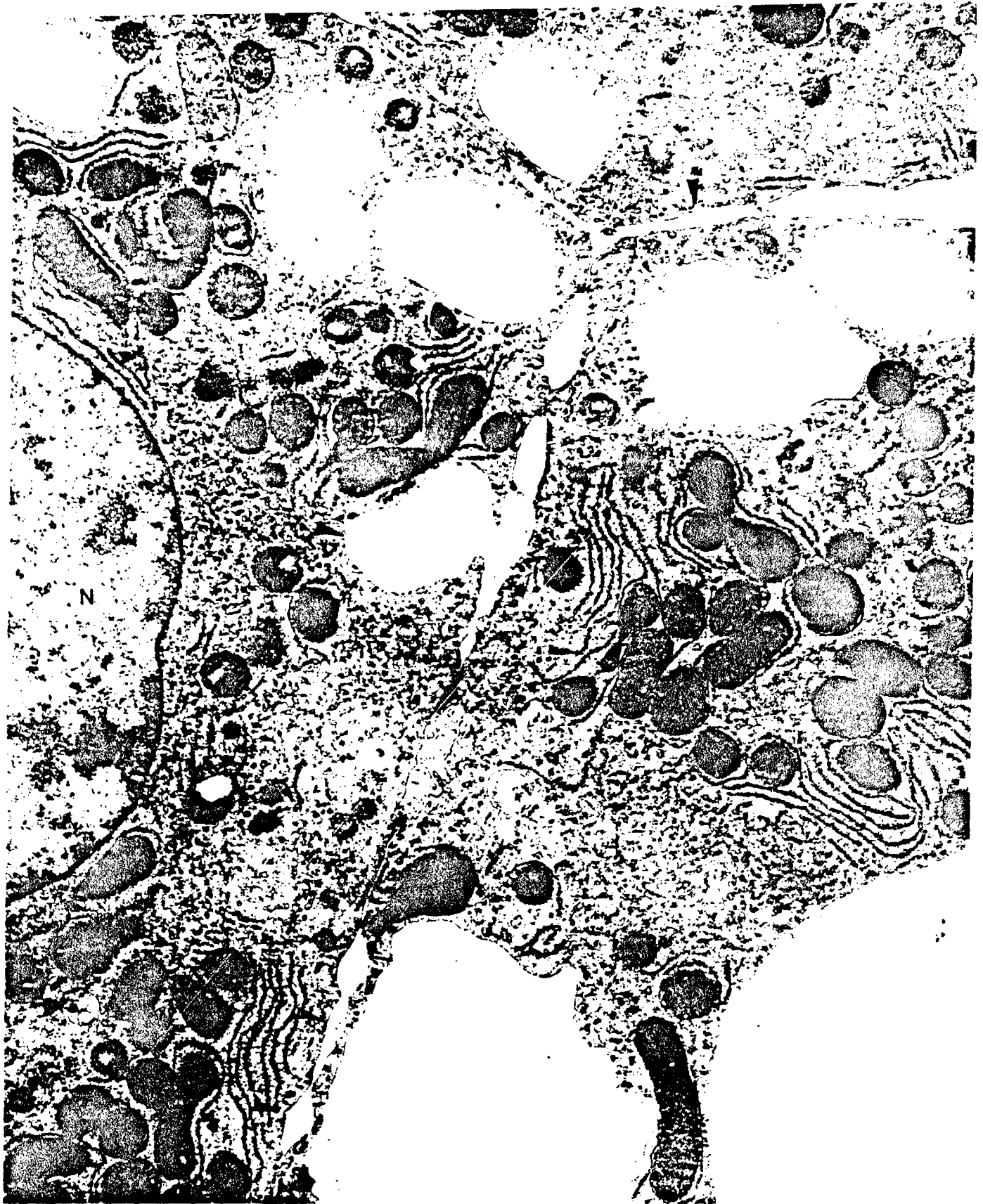


Figure 3 Section VII



Figure 4 Section VII

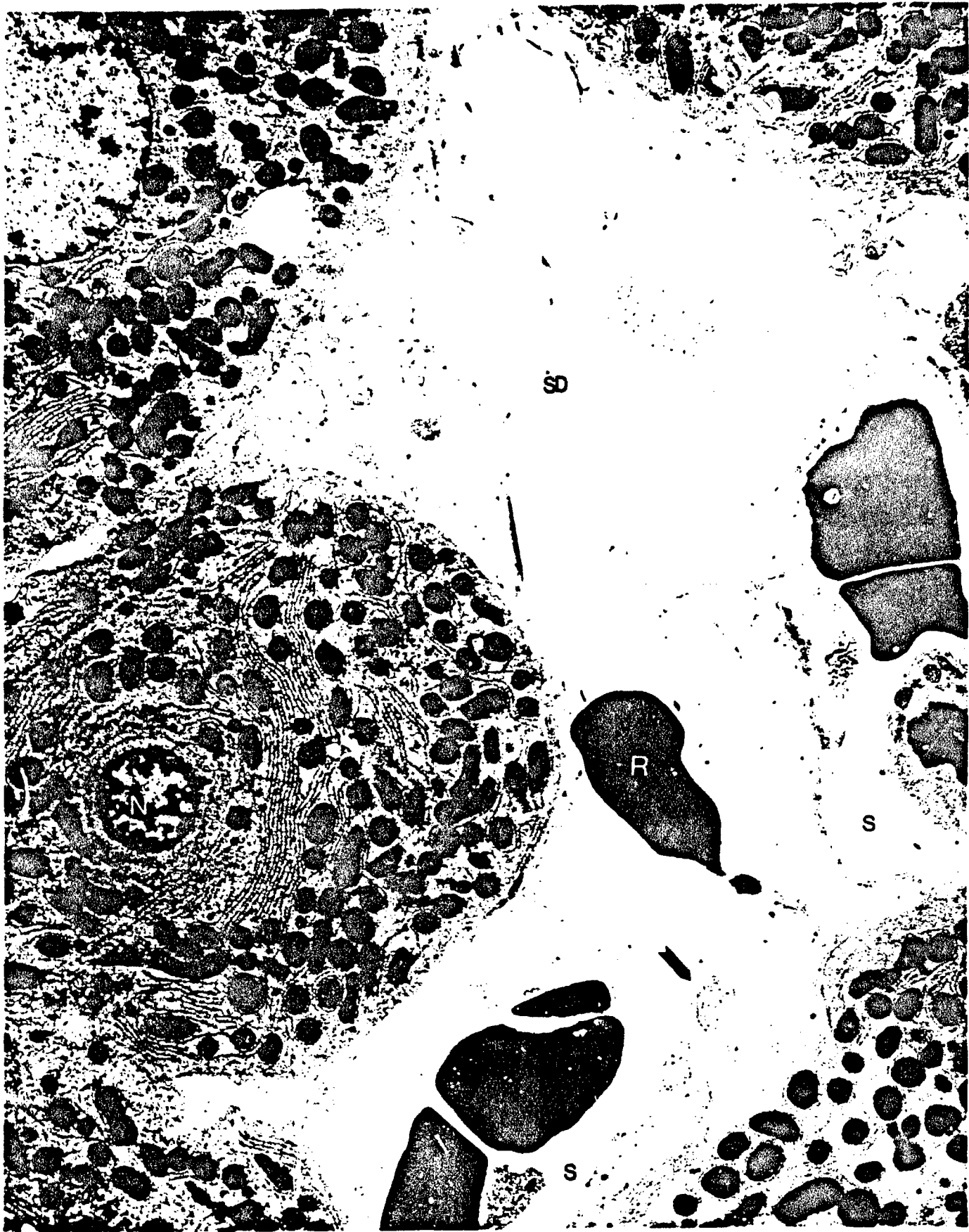


Figure 5 Section VII



Figure 6 Section VII



Figure 7 Section VII



Figure 8 Section VII

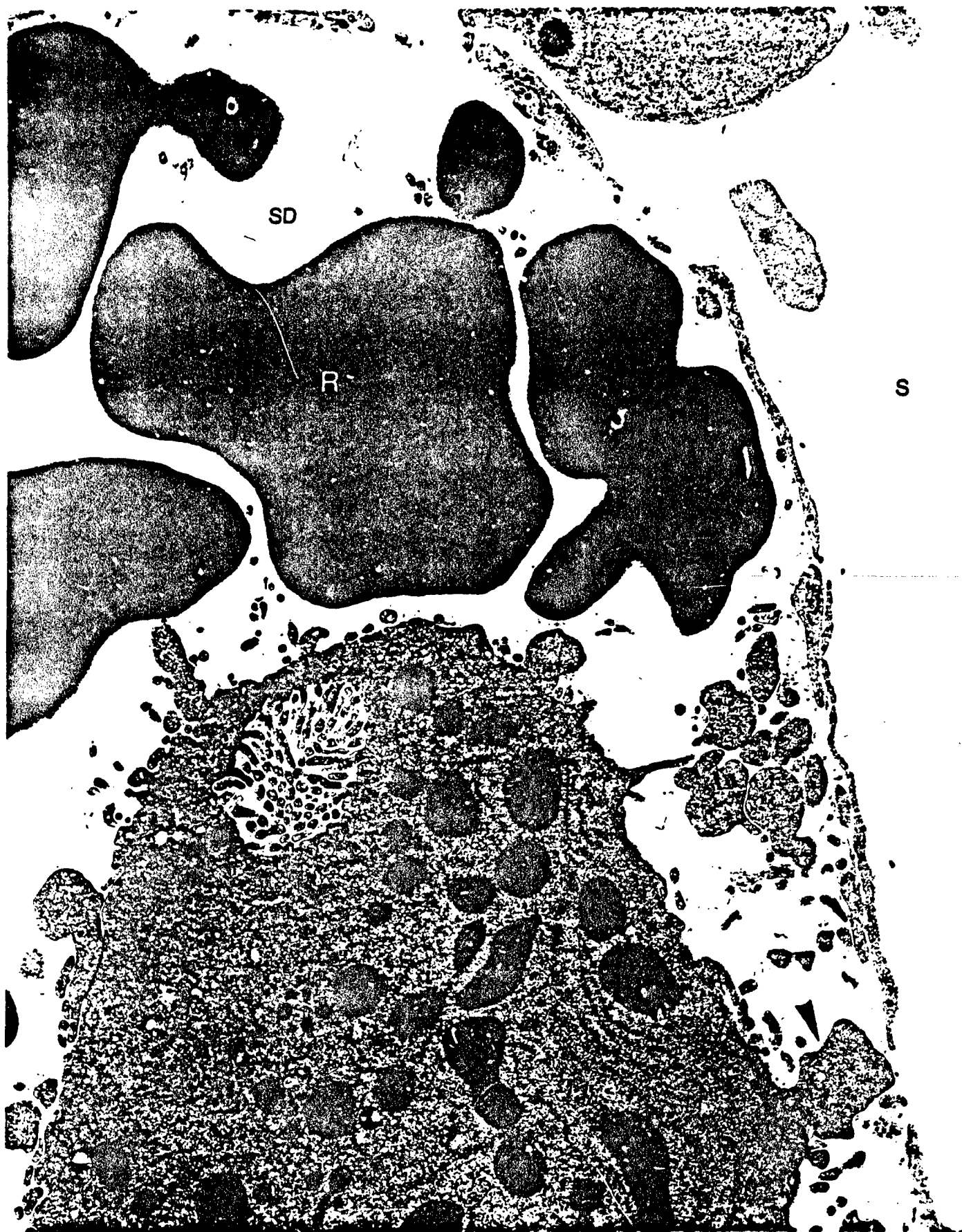


Figure 9 Section VII



Figure 10 Section VII



Figure 11 Section VII



Figure 12 Section VII



Figure 13 Section VII

XI. EFFECTS OF MICROCYSTIN-A ON HEPATIC AND RENAL BLOOD FLOW
AND MEAN AORTIC PRESSURE IN INTRAVENOUSLY DOSED SWINE

K. R. Holmes and R. A. Lovell

INTRODUCTION

The hepatotoxicity of a family of cyclic heptapeptides (microcystins) produced by at least 2 species of blue-green algae is well documented. Currently there are 11 known members in this family (microcystins A-H). The biochemical mechanism of action of these extremely potent (swine iv LD_{min} \leq 30 μ g/kg) hepatotoxins is unknown. Microcystin apparently utilizes bile acid carriers for entry into the hepatocytes and may cause destabilization of the hepatic cytoskeleton.^{1,2} Mice administered a lethal IP dose of microcystin usually die in 1 to 5 hours with an extremely pale carcass and a liver that weighs 1.5 to 2 times that of controls. The actual cause of death is likely a result of shock and acute hepatic failure due to centrilobular and midzonal hepatic necrosis with intrahepatic hemorrhage.

Hepatic hemodynamics have major impacts on cardiovascular, intermediary metabolic, and endocrine functions.³ Altered hepatic circulation appears to play an important role in the liver lesions produced by halothane.⁴ To our knowledge, hepatic blood flow in microcystin toxicosis has not been characterized. In this paper we present liver and kidney blood flow data obtained using the temperature pulse decay (TPD) method^{5,6} in anesthetized gilts intravenously administered a lethal (72 μ g/kg) or toxic-sublethal (25 μ g/kg) dose of > 95% pure microcystin-A (MCYST-A) for up to 5 hours postdosing. The study is partially complete at this time. In order to convey the overall scope of the study, certain methods are described which are not

reflected in the results or discussion. These will be described when the study is complete.

MATERIALS AND METHODS

Gilts (16 to 25 kg) raised under specific pathogen-free (SPF) conditions were purchased from the University of Illinois, College of Veterinary Medicine Research Farm. Upon arrival each animal was bled from the anterior vena cava to determine presurgical CBC and serum chemistry values. Each gilt was administered vitamin E (1.5 IU/L), sodium selenite (55 µg of Se/kg), and vitamin K1 (1.5 mg/kg) intramuscularly. These gilts were housed in the College of Veterinary Medicine Laboratory Animal Care Facilities and provided with water and feed (16% protein corn-soybean ration) ad libitum. Twenty-four hours prior to dosing, all feed was removed from the stall.

Each gilt was subjected to endotracheal intubation after: 1) an 18- to 20-gauge catheter was implanted in the lateral ear vein; 2) 50 mg/kg of alpha-chloralose (1% solution) was administered iv; 3) 20 mg/kg of ketamine HCl (10% solution) was administered iv; and 4) 3/4 ml of 2% lidocaine was sprayed on and around the larynx. Following a 7 to 8 cm incision in the right jugular furrow region caudal to the base of the right ear, 18-gauge Tygon catheters were implanted in the jugular vein and carotid artery so that central venous and aortic pressures could be measured. Using a right paracostal-paralumbar incision through the abdominal wall, a 20-gauge Tygon catheter was placed in the portal vein located in the last 65 cm of the small intestine (ileum). Five to eight TPD probes were implanted into the liver and 4 to 5 TPD probes were implanted into the right kidney. One ml of heparin (1,000 IU) was sprayed around the TPD probe wires to aid in their removal at the conclusion of the study. The abdominal and cervical incision sites were apposed using towel clamps.

During the surgical portion of the experiment, ketamine and alpha-chloralose were supplemented (iv) as needed to maintain a surgical plane of anesthesia. After TPD probe implantation, anesthesia (plane 2) was maintained using iv supplements of alpha-chloralose as needed. Ketamine (< 15 mg slowly iv) was supplemented as needed after TPD probe implantation to calm excessive muscular activity. Gilts were required to breathe on their own during the pre- and postdosing data collection periods. Ten minutes of assisted ventilation was provided 1 time to any high dose (72 µg/kg) gilt which became apneic during a period of hypotension (mean aortic blood pressure between 40 and 65 mmHg).

Systolic, diastolic, mean and pulse pressures, as well as heart rate, were measured from the aortic catheter. Mean pressure was measured from the portal vein catheter. Mean central venous pressure was measured from the jugular catheter. Gould-Statham pressure transducers were connected to the catheters to measure the pressure wave. The pressure wave signal was conditioned by a Gilson Model 5/6H Physiograph and recorded using Buxco Hemodynamic Analyzer. Three ECG leads, placed in the right forelimb, left forelimb, and left hindlimb, were used to measure the following electrocardiographic parameters: Q, R, S, T, P, and ST height; Q, R, S, and P width; RR, QRS, ST, QT, QTC, PRQ, and PR intervals. The ECG wave signal was conditioned by the Gilson Physiograph and recorded with a Buxco ECG Analyzer. These ECG and hemodynamic parameters were measured every 20 seconds throughout the experiment.

The appropriate dose (0 µg/kg = control, n = 4; 25 µg/kg = toxic-sublethal, n = 6; 72 µg/kg = lethal, n = 6) of > 95% pure MCYST-A was placed in a 40 C water bath to warm it to body temperature. The hepatotoxin dosing solution was then delivered over a 90-second period into the jugular vein

catheter which was then flushed with 10 ml of a warmed, heparinized Ringer's solution.

The 6 most consistent TPD probes (2 to 3 in kidney and 3 to 4 in liver) were established prior to the commencement of the 30 to 45 minute predosing period. During the predosing period and for 2 hours postdosing, liver and kidney blood flow were measured every 3 minutes from each established TPD probe site. From 2 hours postdosing until 5 hours postdosing, liver and kidney blood flow were measured every 6 minutes.

Arterial blood samples were collected 5 to 15 minutes prior to MCYST-A dosing and 45, 90, 150, 210, and 300 minutes postdosing and/or immediately prior to death. Parameters included complete blood count (3 ml), serum chemistry profile (10 ml), blood gases and electrolytes (3 ml), and lactate concentration (1.0 ml). Six minutes postdosing, a 10 ml arterial blood sample was collected for determination of MCYST-A concentration. The aortic catheter was flushed with 10 ml of a warmed heparinized Ringer's solution after each collection period.

Gilts still alive 5 hours postdosing were killed by exsanguination after iv ketamine supplementation was given to produce a surgical plane of anesthesia. The following tissues were placed in 10% neutral-buffered formalin within 2 hours of death/euthanasia; liver (including gallbladder and bile duct), kidneys, adrenals, spleen, pancreas, stomach, duodenum, jejunum, ileum, cecum, ascending spiral colon, descending spiral colon, rectum, mesenteric lymph node, ovary and uterus, urinary bladder, quadriceps muscle, bone marrow (femur), skin, tongue, thyroid, parotid salivary gland, esophagus, trachea, eye, brain (whole), thymus, submandibular lymph node, lung, left and right atria, and left and right ventricles with interventricular septum.

RESULTS

The hepatic and renal blood flow and mean aortic pressure vs time from the first 10 gilts are presented in Figures 1 to 20 and the Appendix to Section XI (page 203). In the high dose gilts, an increase in portal venous pressure preceded the precipitous fall in mean aortic pressure. Results with regard to analytical, pathologic, clinical pathologic, electrocardiographic, and hemodynamic (other than mean aortic pressure) end points will be presented in subsequent reports.

DISCUSSION

Liver blood flow markedly declines approximately 10 to 20 minutes before the precipitous fall in arterial blood pressure in the high dose (72 $\mu\text{g/kg}$) gilt surviving more than 1 hour. Renal blood flow closely parallels aortic blood pressure in these gilts. In the high dose gilts, the portal venous pressure has increased while the central venous pressure has decreased during the postdosing period. In contrast, in the low dose group (25 $\mu\text{g/kg}$) there is marked variation between animals in liver and kidney blood flow and little change in portal and central venous pressures over time. The differences in renal and hepatic perfusion are probably due to greater individual variation in the lower portion of the extremely steep lethal dose response curve of MCYST-A. In the control gilts, mean aortic blood pressure never declined below 88 mmHg and liver and kidney blood flow changed little from predosing values.

CONCLUSION

From this study, it appears that markedly reduced hepatic perfusion occurs early in the toxicosis produced by MCYST-A in swine. The reduction in blood flow is such that intrahepatic hypoxia may make a major contribution to the

destructive process observed in this organ in lethally dosed animals. In contrast, reduction in renal blood flow is apparently a response to the decline in aortic pressure. Future plans call for correlation between blood flow changes and sequential pathologic changes in livers of microcystin-dosed swine.

REFERENCES

1. Runnegar, M. T. C. and Falconer, I. R. The in vivo and in vitro biological effects of the peptide hepatotoxin from the blue-green alga Microcystis aeruginosa. S. Afr. J. Sci. 78:363-366, 1982.
2. Runnegar, M. T. C. and Falconer, I. R. Effect of toxin from the cyanobacterium Microcystis aeruginosa on ultrastructural morphology and actin polymerization in isolated hepatocytes. Toxicon 24(2):109-115, 1986.
3. Andreen, M., Irestedt, L., and Zetterstrom, B. The different responses of the hepatic arterial bed to hypovolemia and to halothane anesthesia. Acta. Anesth. Scand. 21:457-469, 1977.
4. Lutt, W. W. and Greenway, C. V. Conceptual review of the hepatic vascular bed. Hepatology 7(5):952-963, 1987.
5. Adams, T., Spielman, W. S., Holmes, K. R., Heisey, S. R., and Chen, M. M. Proposed methods for the measurement of regional renal blood flow using heat transfer analysis. Annals. Biomed. Engr. 13:237-258, 1985.
6. Arkin, H., Chen, M. M., and Holmes, K. R. Precision of the thermal pulse-decay method and optimal measurement time interval. Adv. Bioengr. ASME 7-8, 1984.

FIGURE LEGENDS

Figures 1-16. Mean hepatic and renal blood flow and mean aortic pressure vs. time in gilts dosed intravenously with microcystin-A (MCYST-A) at 0 $\mu\text{g/kg}$ (N = 4), 25 $\mu\text{g/kg}$ (N = 6), and 75 $\mu\text{g/kg}$ (N = 6). The details on individual measurements are given in the Appendix to Section XI on page 203.

Figure 17. Hepatic perfusion of control group (●) (n = 4), toxic sublethal group (○) (n = 6), lethal group (▽) (n = 6). Hepatic perfusion values represent the 6-minute group mean (\pm SEM) and were obtained from 2 to 4 temperature-pulse decay probes in each gilt. After an animal died, hepatic perfusion was 0 for the remainder of the experiment.

Figure 18. Renal perfusion of control group (●) (n = 4), toxic sublethal group (○) (n = 6), lethal group (▽) (n = 6). Renal perfusion values represent the 6-minute group mean (\pm SEM) and were obtained from 1 to 3 temperature-pulse decay probes in each gilt. After an animal died, renal perfusion was 0 for the remainder of the experiment.

Figure 19. Aortic mean (AOM) pressure of control group (●) (n = 4), toxic sublethal group (○) (n = 6), lethal group (▽) (n = 6). AOM values represent the 6-minute group mean (\pm SEM) for each group. AOM values in the lethal group were derived only from live animals (n decreased with time).

Gilt #3045

MCLR iv 00 ug/kg

○—○ Mean Renal Perfusion

▲—▲ Mean Hepatic Perfusion

■—■ Arterial

Mean pressure

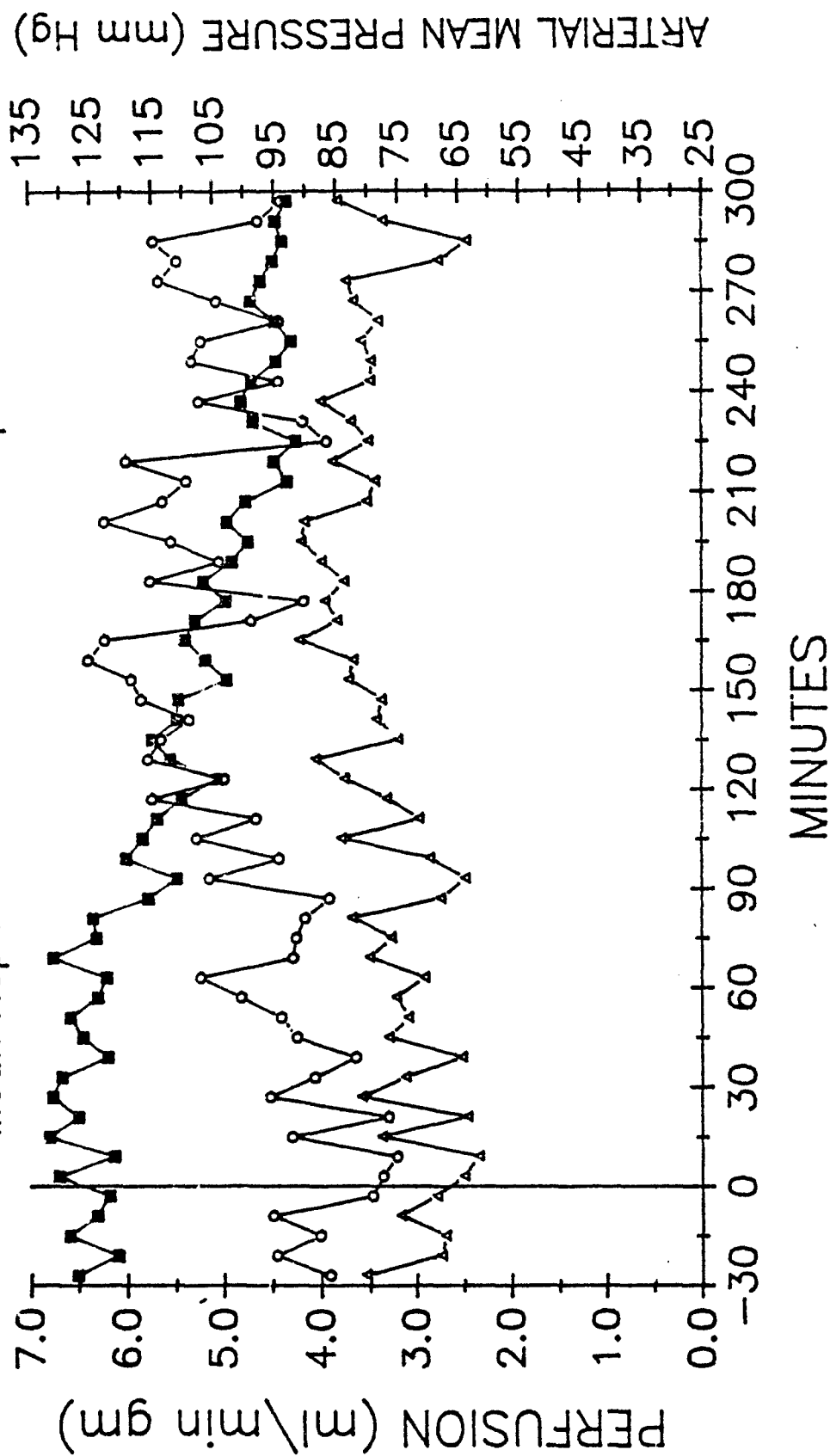


Figure 1

Section XI

Gilt #3230 MCLR iv 00 ug/kg

○ — Mean Renal Perfusion

△ — Mean Hepatic Perfusion

■ — Arterial

Mean pressure

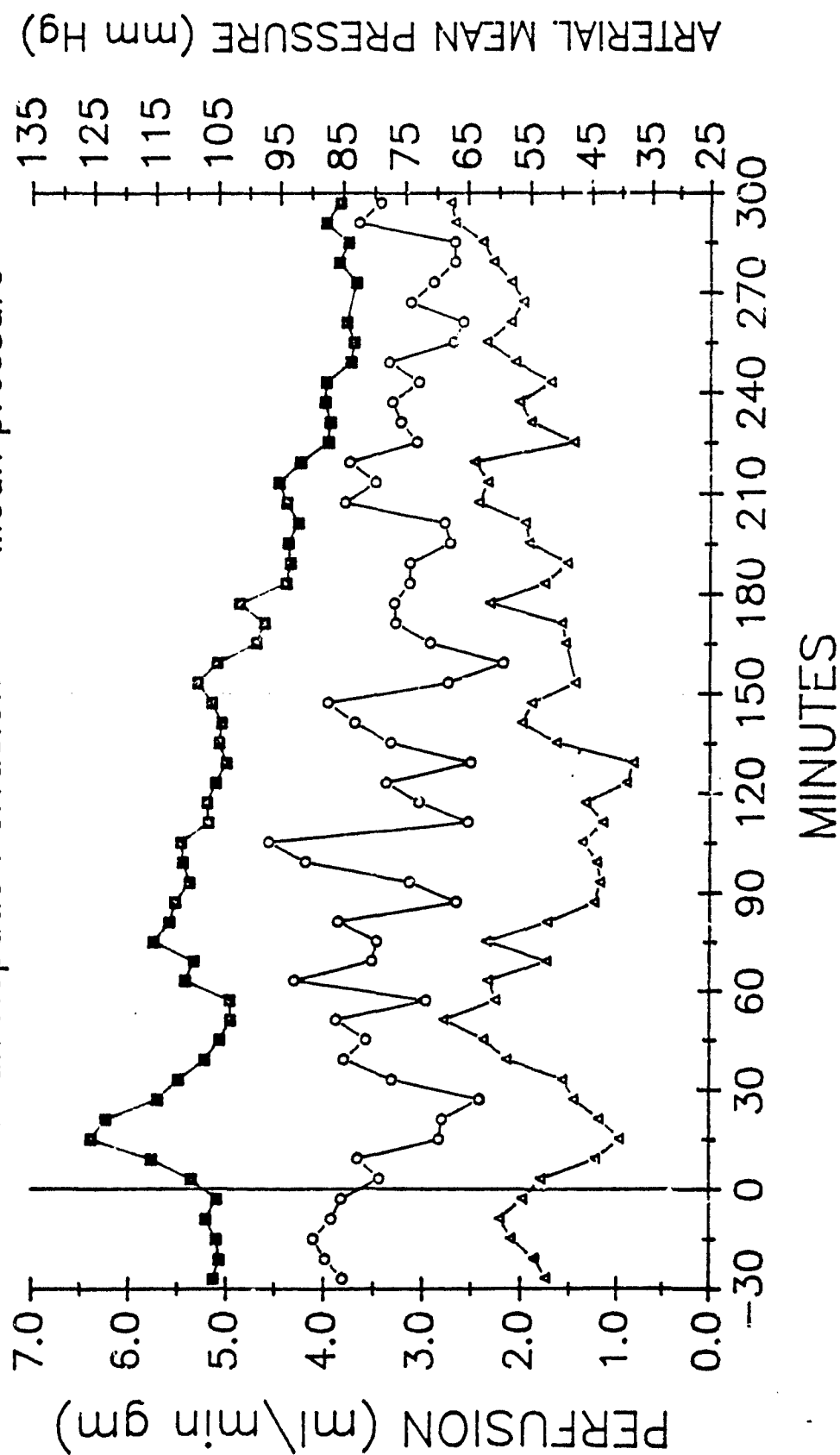


Figure 2

Section XI

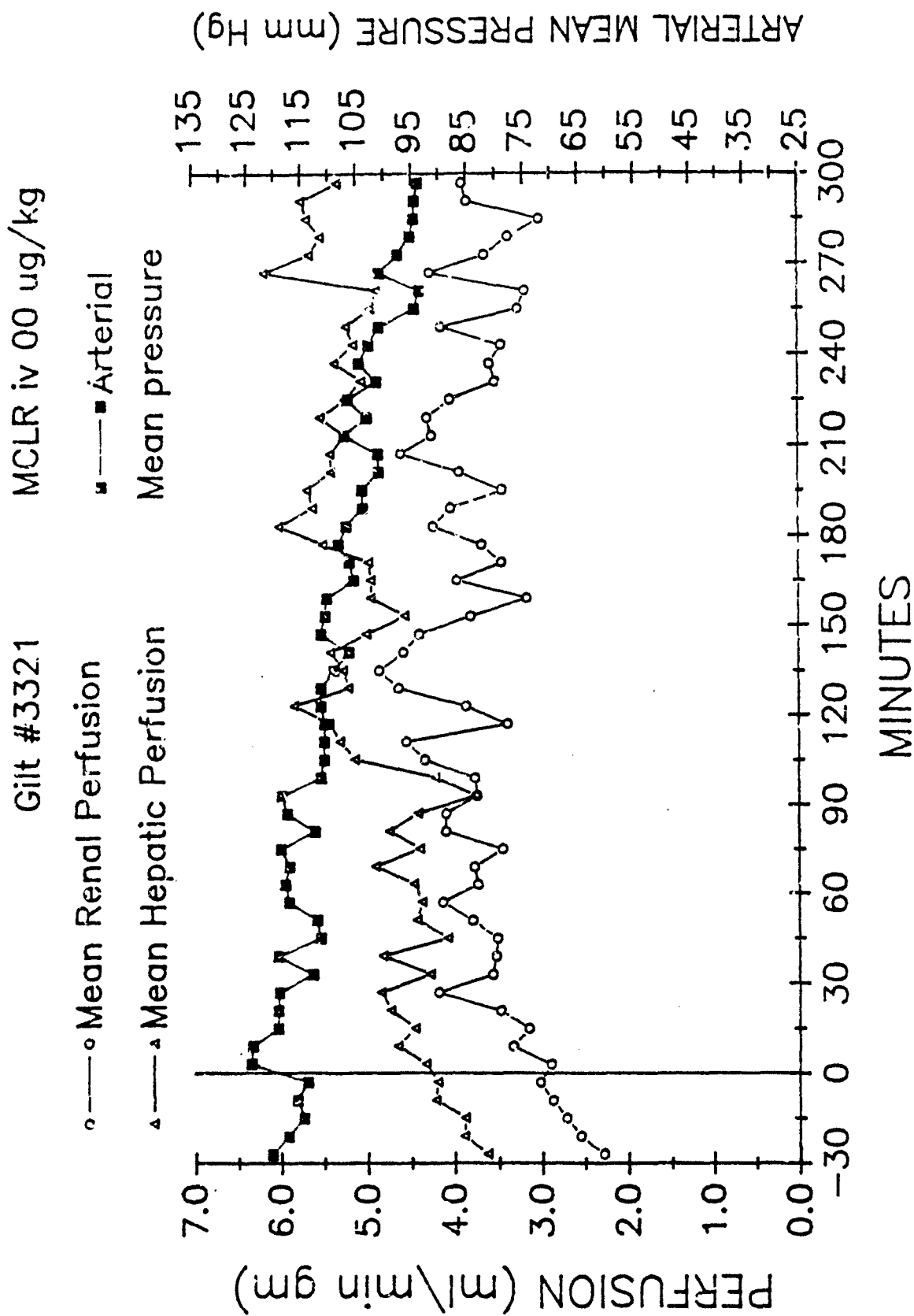


Figure 3

Section XI

Gilt #2895

MCLR iv 25 ug/kg

○—○ Mean Renal Perfusion
▲—▲ Mean Hepatic Perfusion

■—■ Arterial
Mean pressure

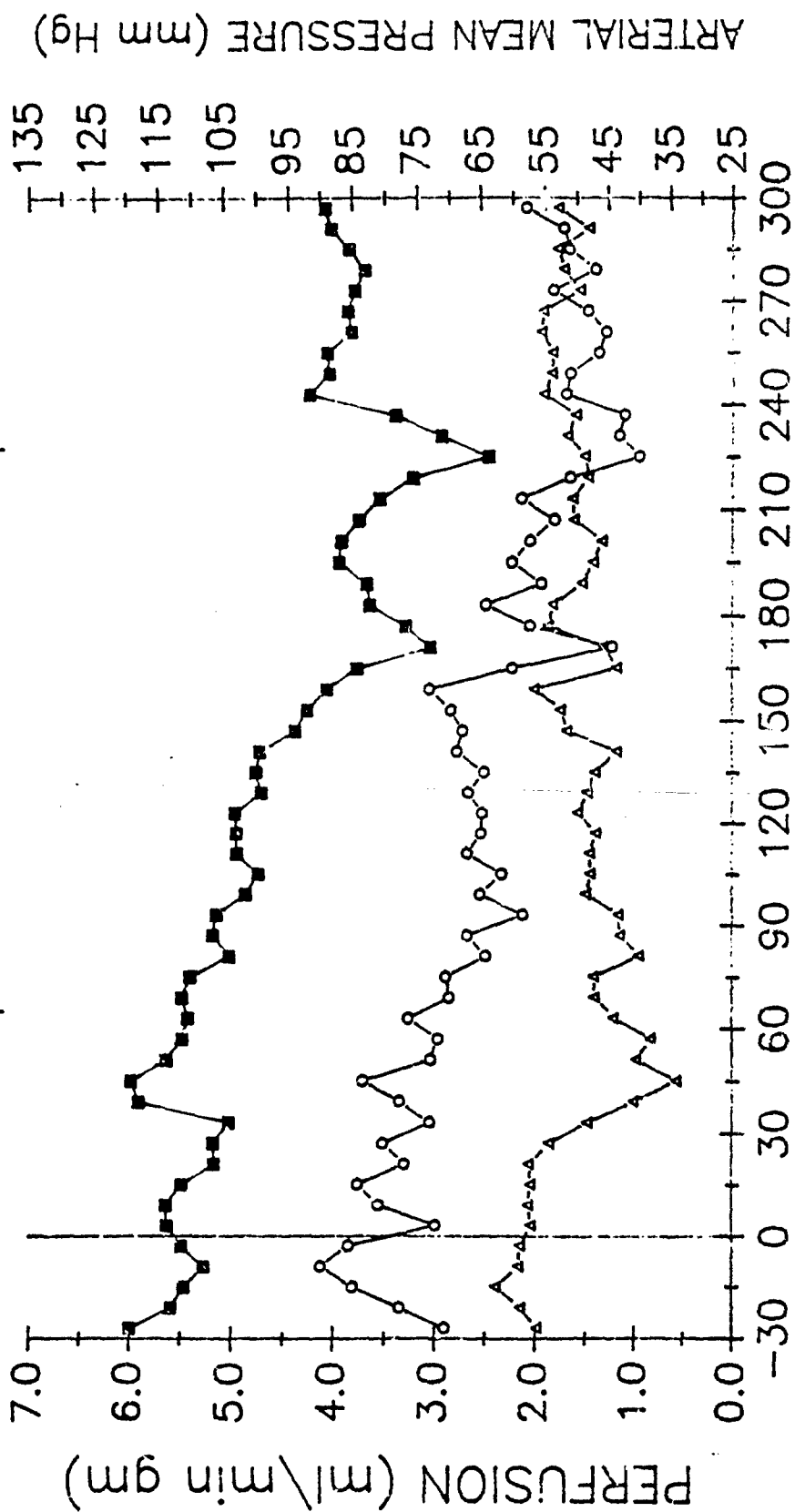


Figure 4

Section XI

Gilt #2987

MCLR iv 25 ug/kg

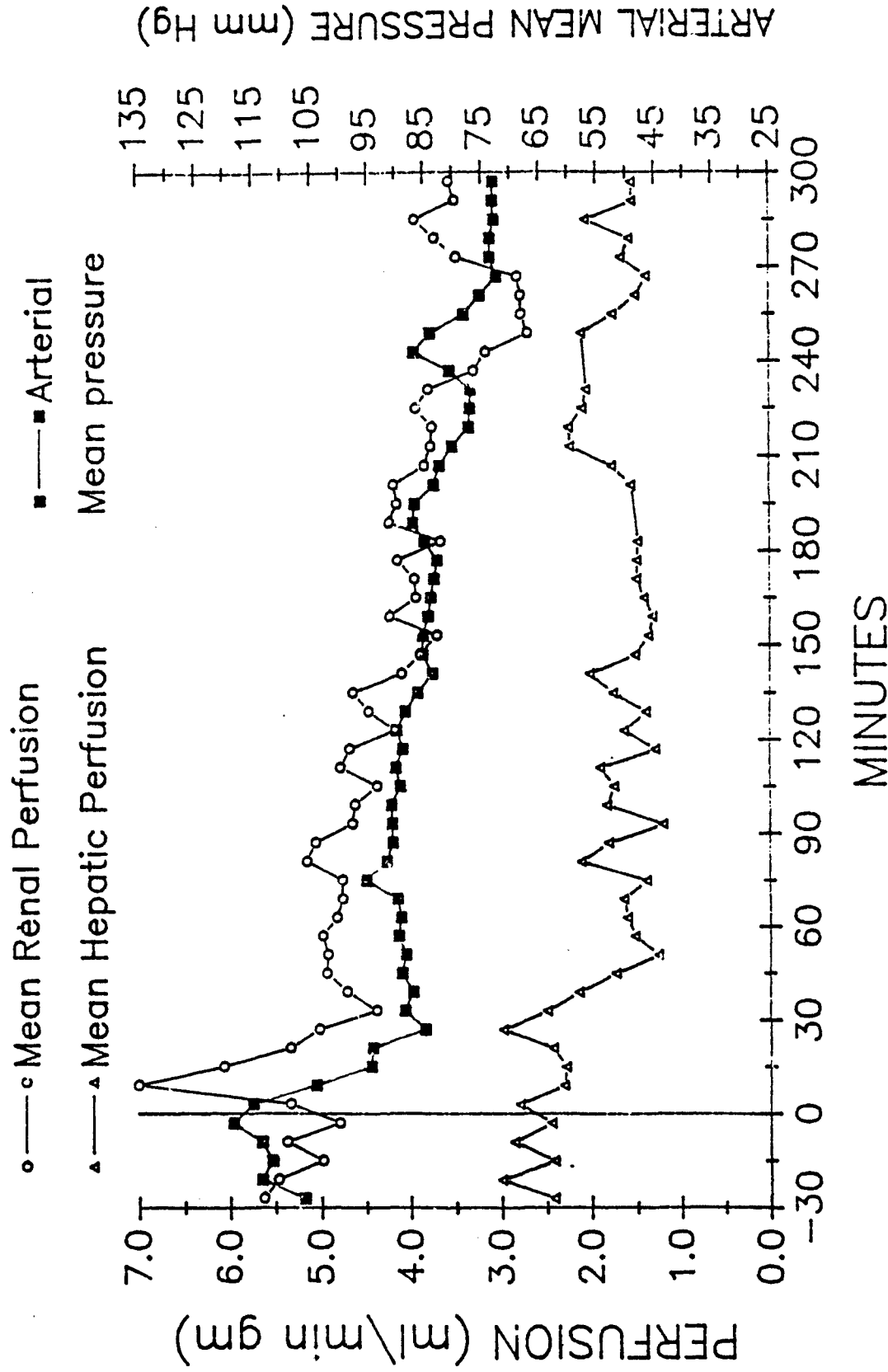


Figure 5

Section XI

Gilt #2964

MCLR iv 25 ug/kg

○—○ Mean Renal Perfusion

■—■ Arterial

▲—▲ Mean Hepatic Perfusion

Mean pressure

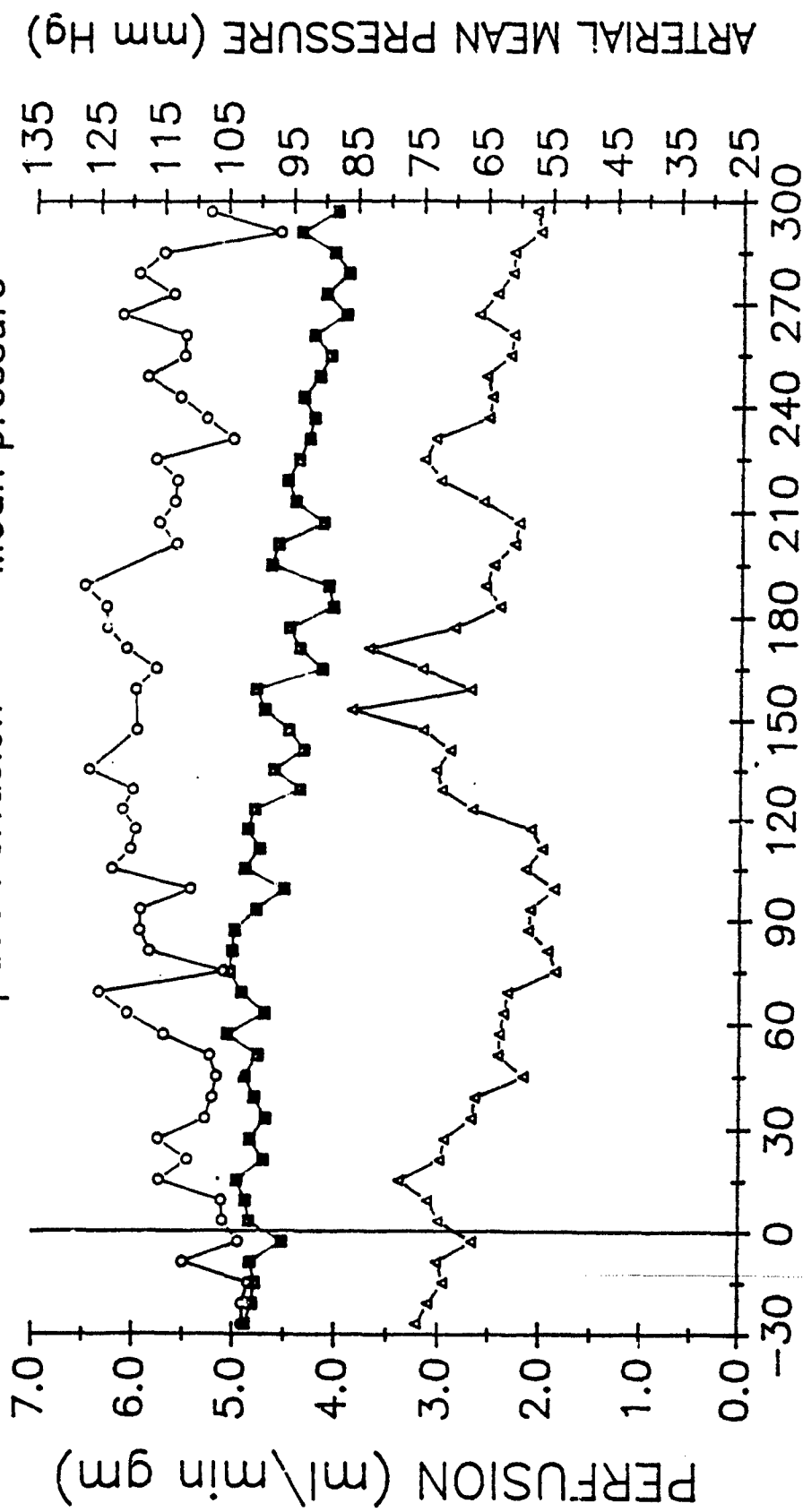


Figure 6

Section XI

Gilt #2957

MCLR iv 25 ug/kg

○—○ Mean Renal Perfusion
▲—▲ Mean Hepatic Perfusion

■—■ Arterial
Mean pressure

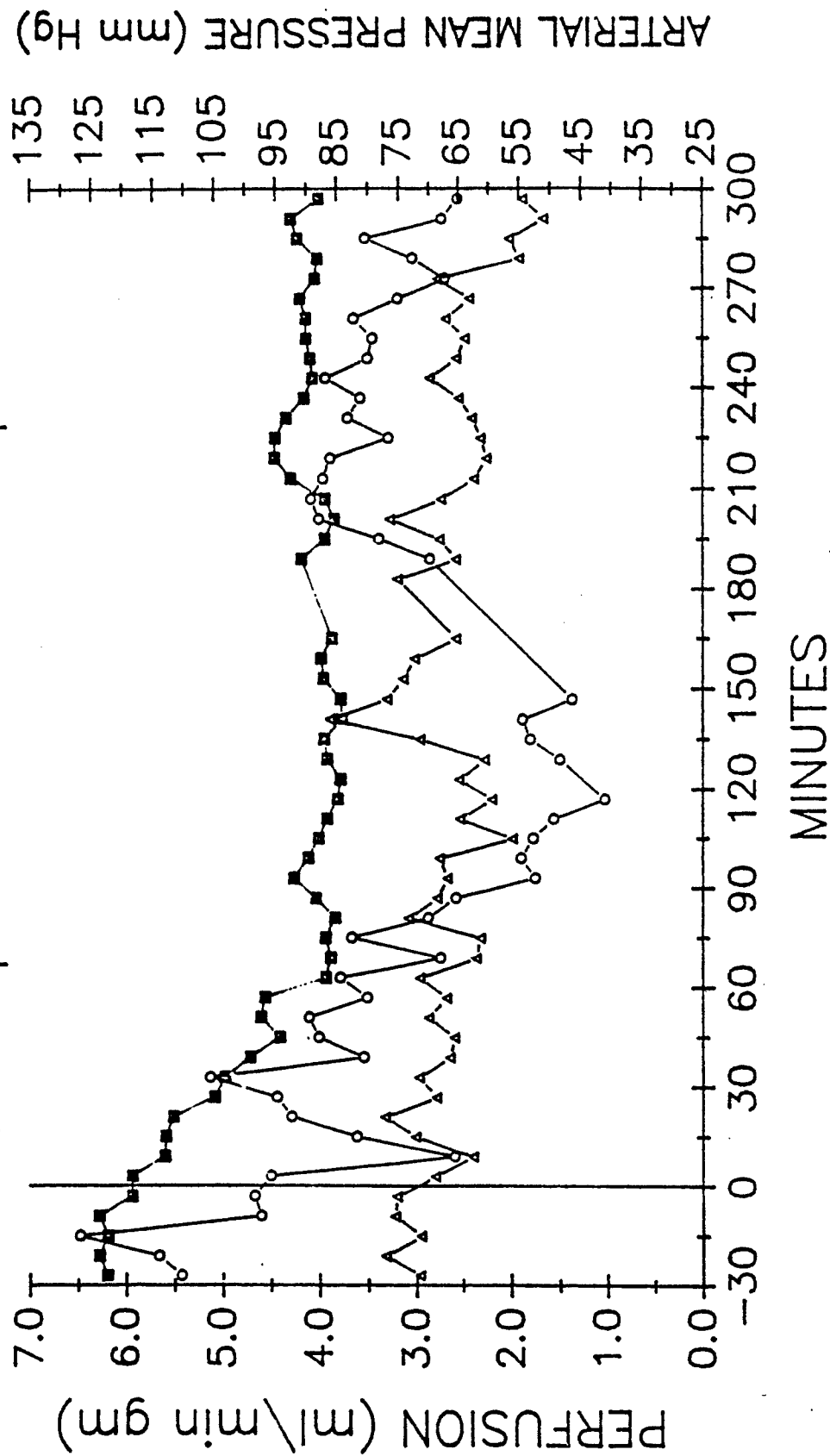


Figure 7

Section XI

Gilt #3080

MCLR iv 25 ug/kg

○—○ Mean Renal Perfusion

■—■ Arterial

△—△ Mean Hepatic Perfusion

Mean pressure

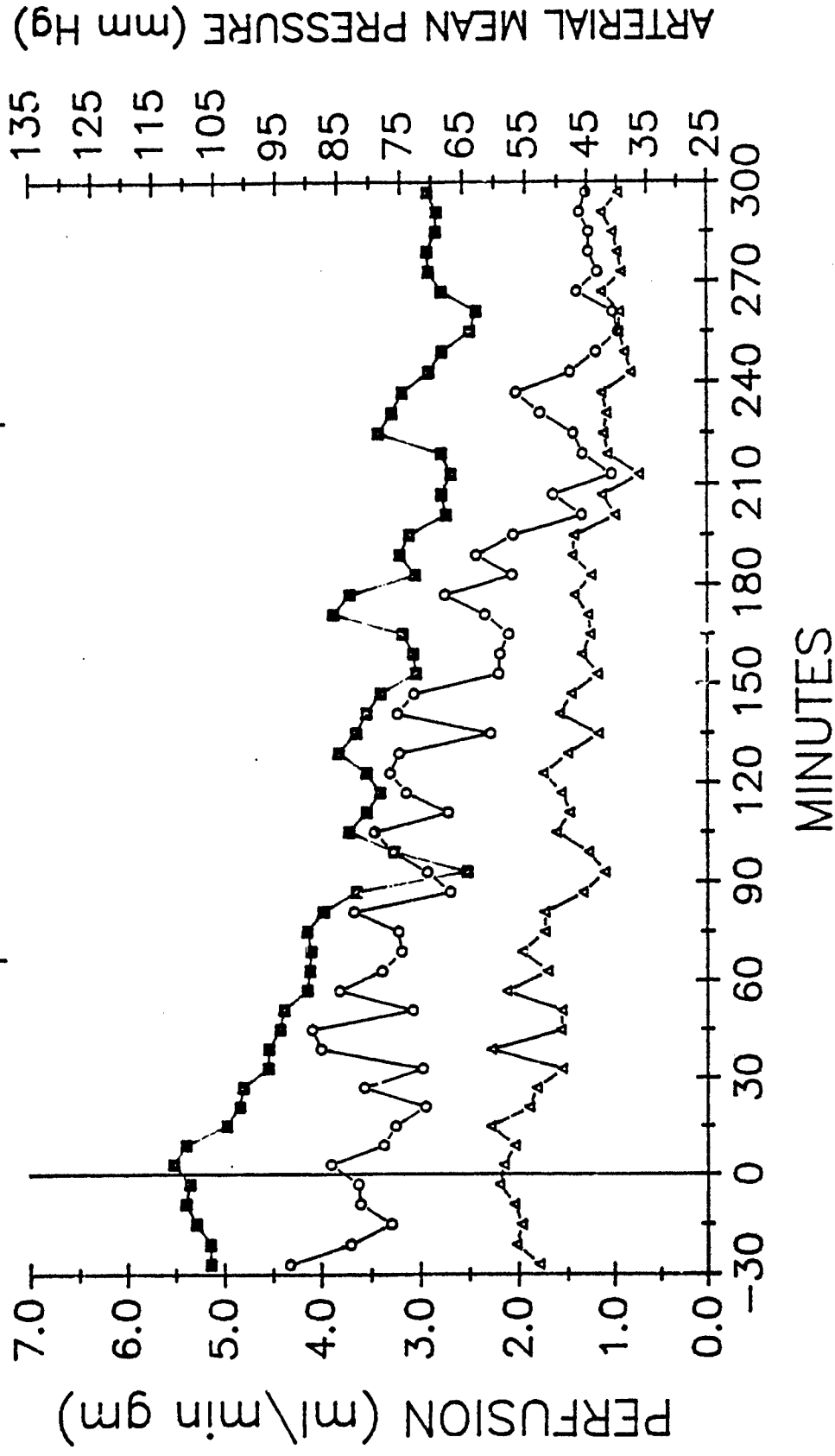


Figure 8

Section XI

Gilt #3312

MCLR iv 25 ug/kg

○—○ Mean Renal Perfusion

▲—▲ Mean Hepatic Perfusion

■—■ Arterial

Mean pressure

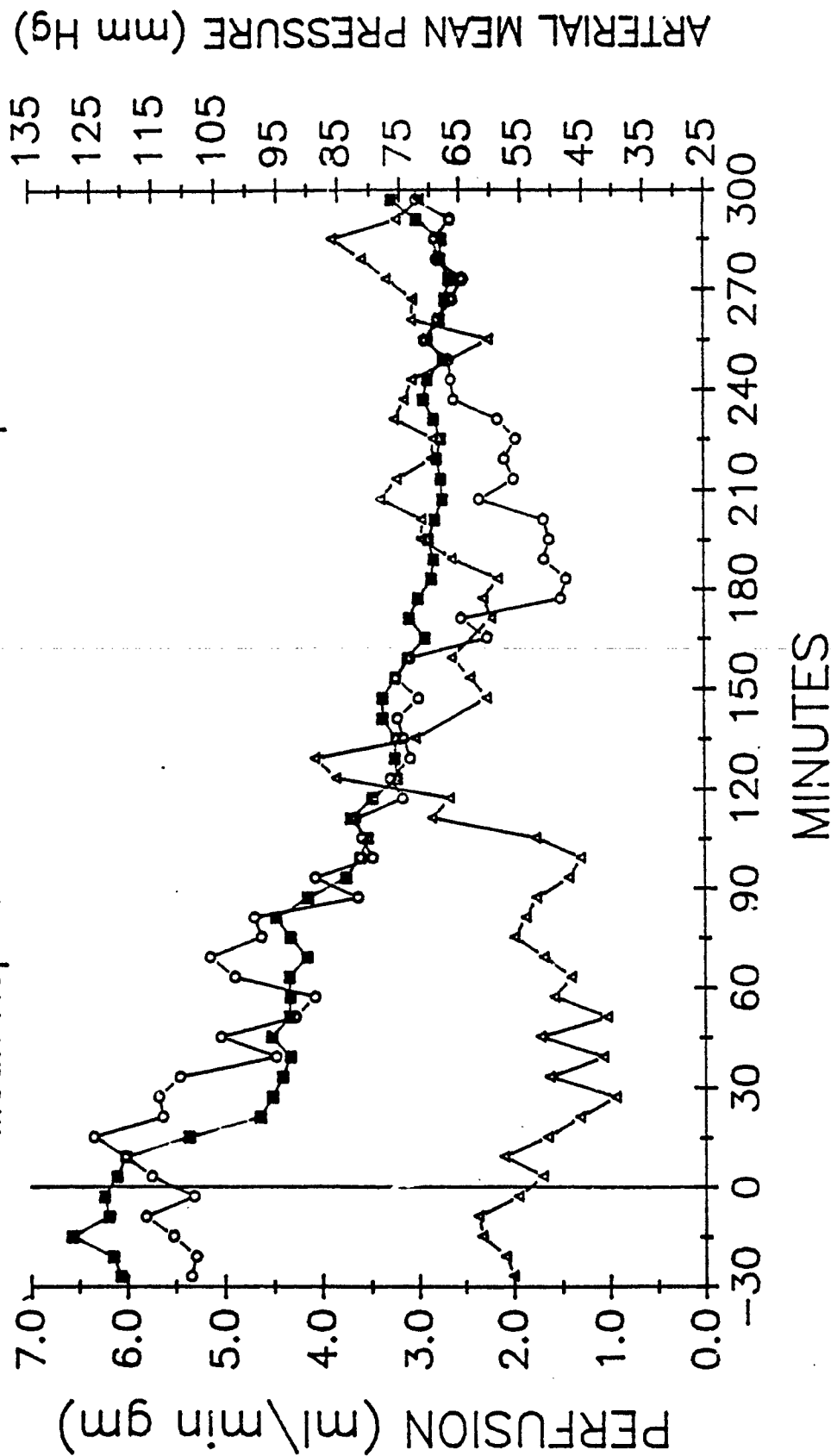


Figure 9

Section XI

Gilt #2896

MCLR iv 72 ug/kg

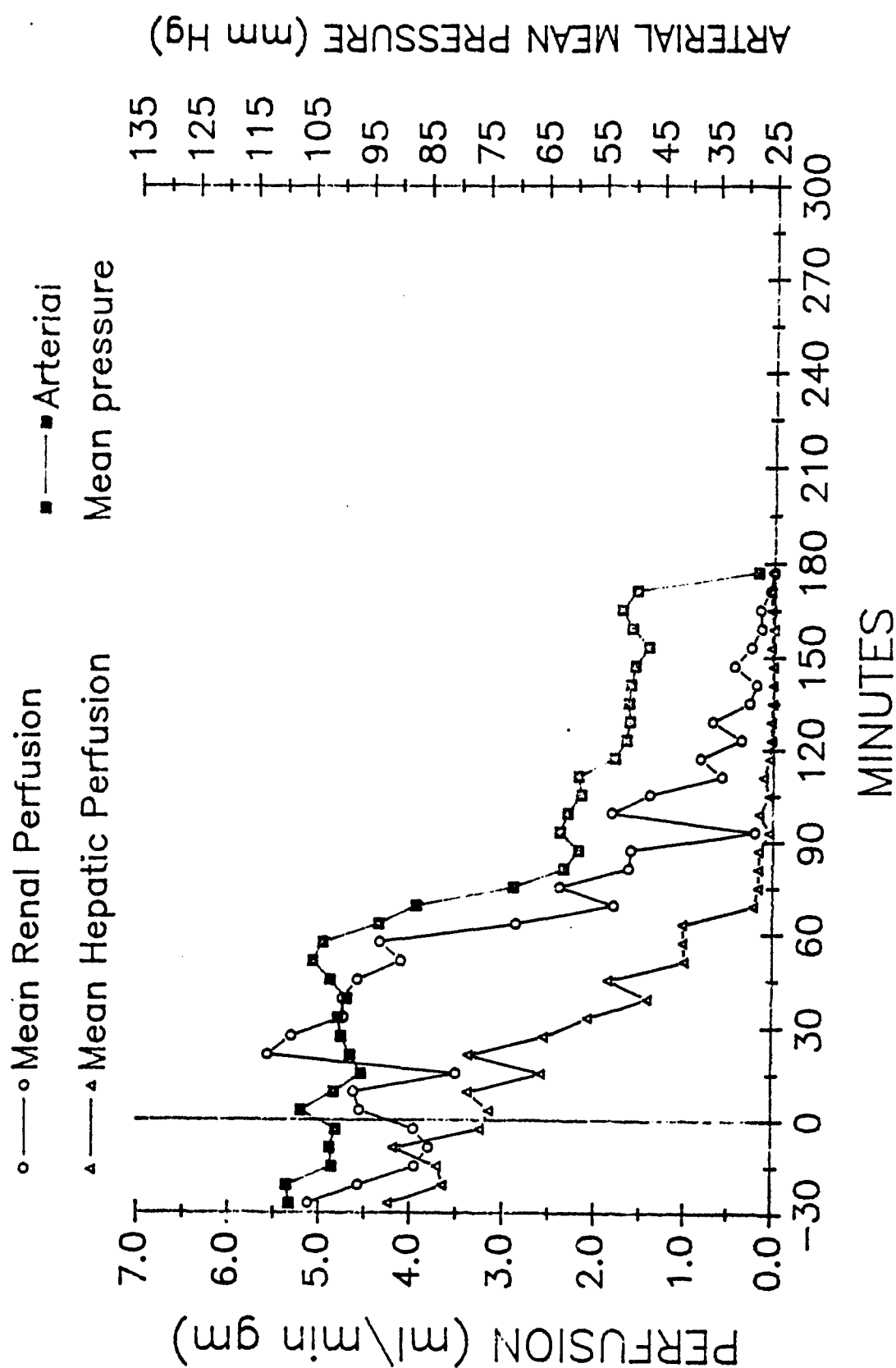


Figure 10

Section XI

Gilt #3015 MCLR iv 72 ug/kg

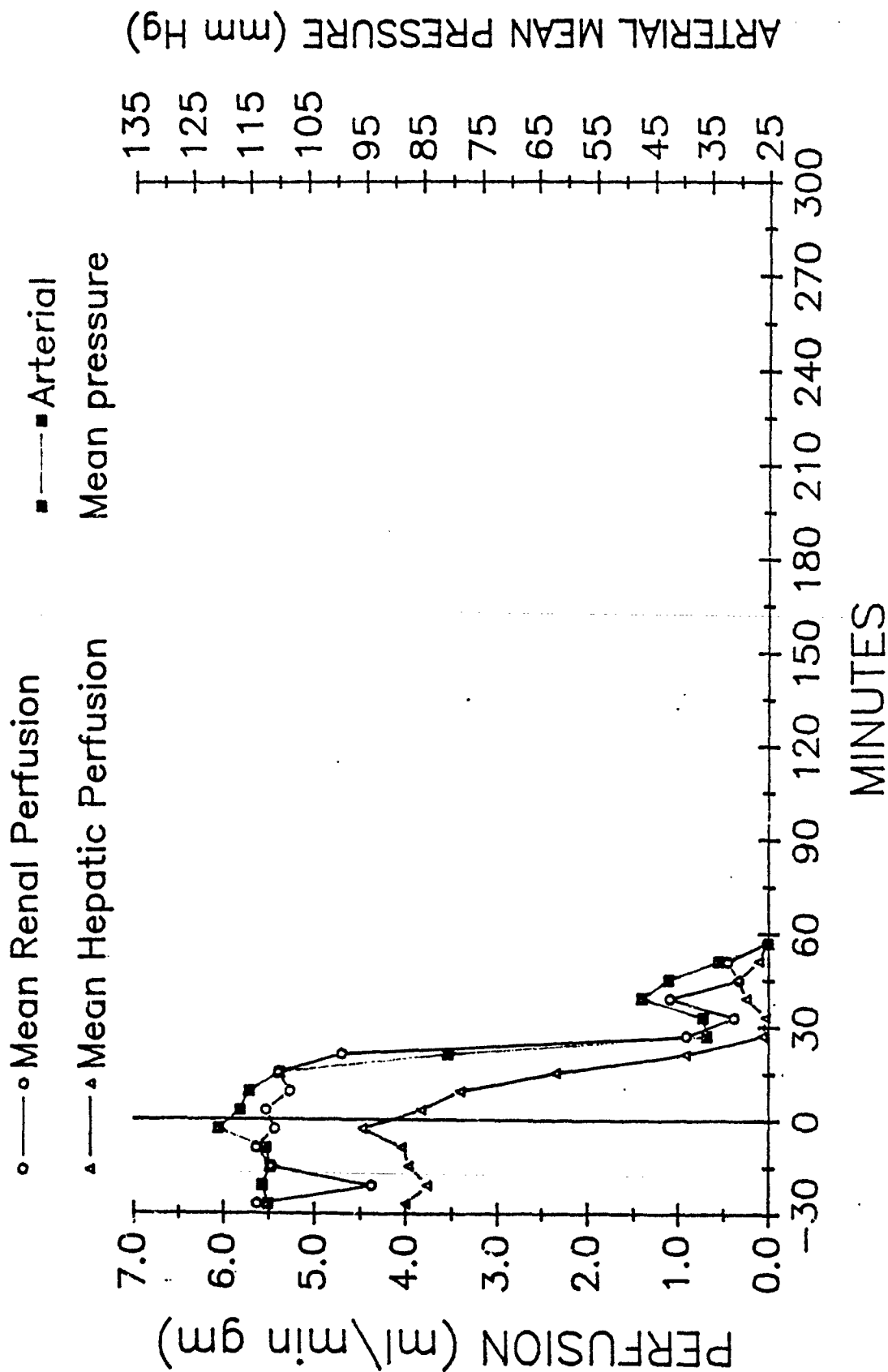


Figure 11
Section XI

Gilt #3044 MCLR iv 72 ug/kg

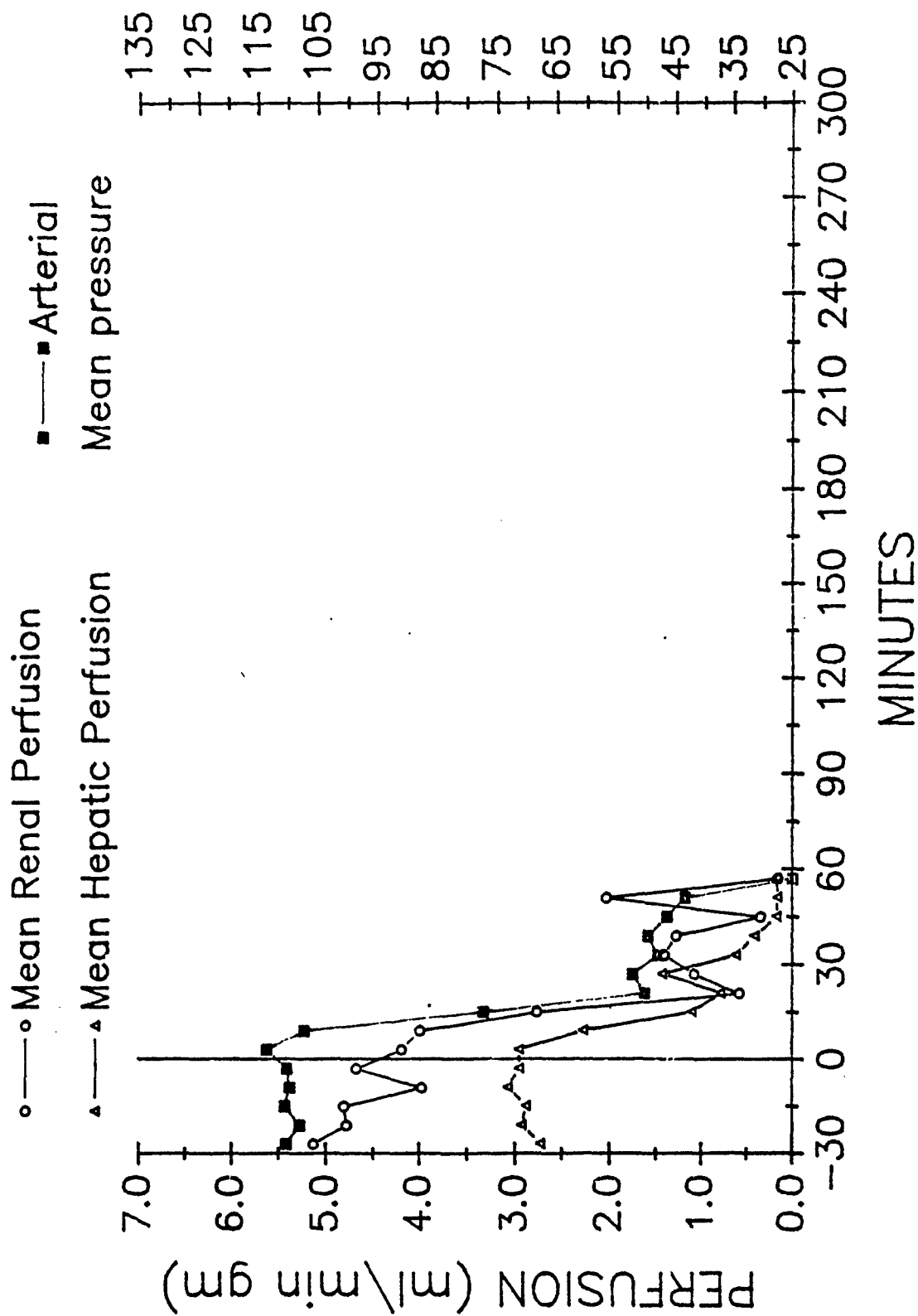


Figure 12

Section XI

Gilt #3132 MCLR iv 72 ug/kg

○ — Mean Renal Perfusion
 ▲ — Mean Hepatic Perfusion

■ — Arterial
 — Mean pressure

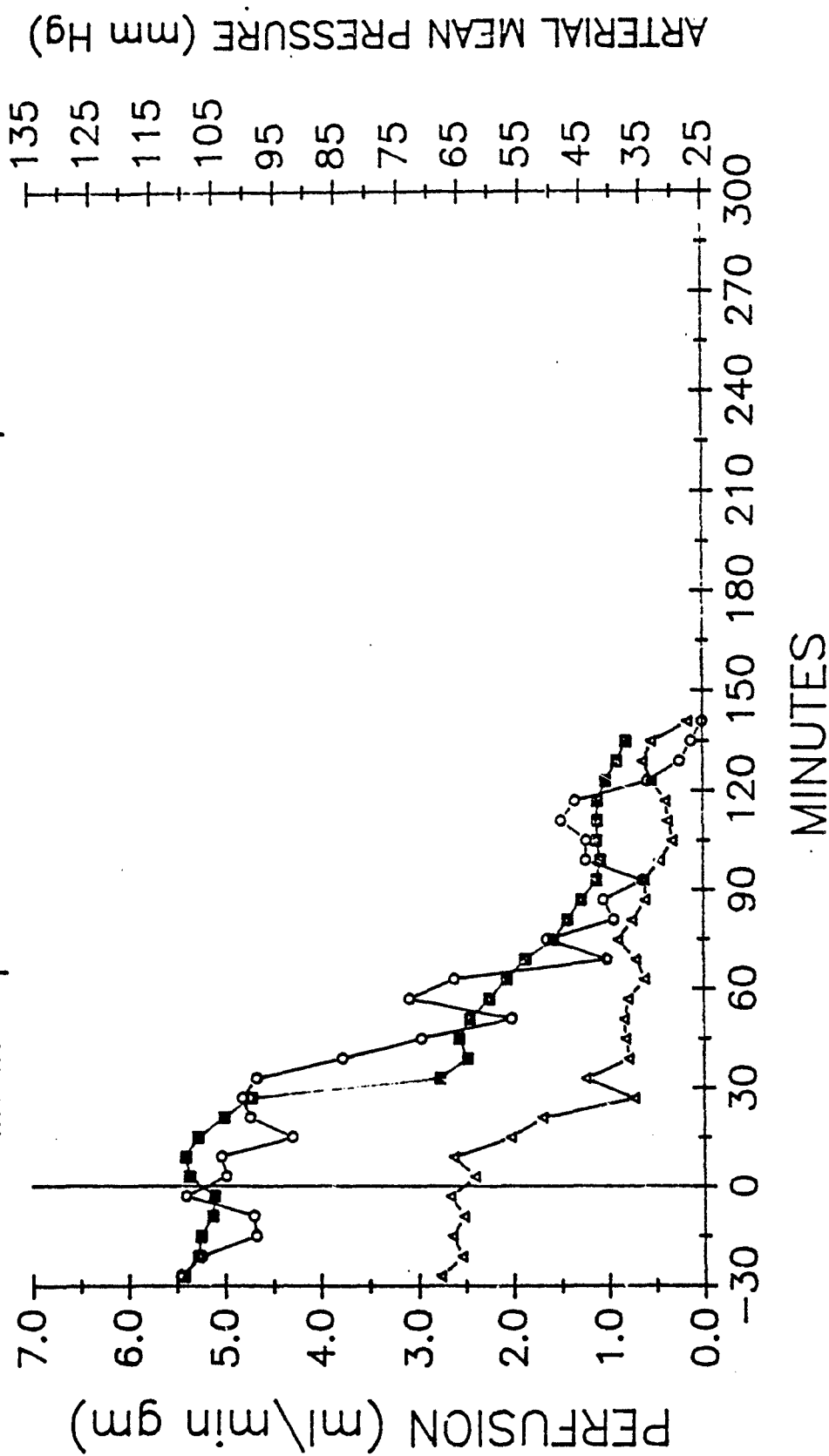


Figure 13

Section XI

Gilt #3183

MCLR iv 72 ug/kg

○—○ Mean Renal Perfusion
 ▲—▲ Mean Hepatic Perfusion

■—■ Arterial
 Mean pressure

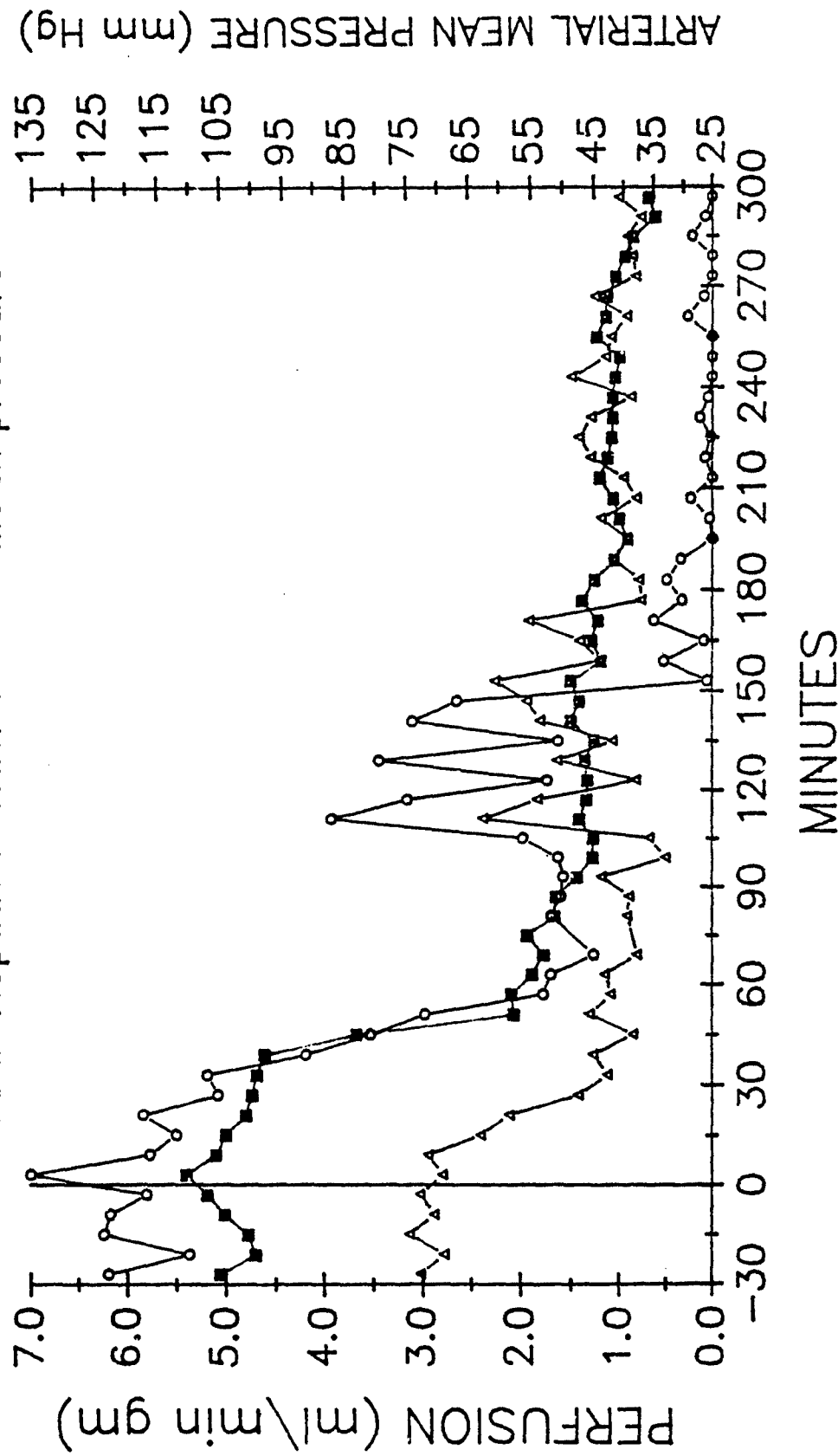


Figure 14

Section XI

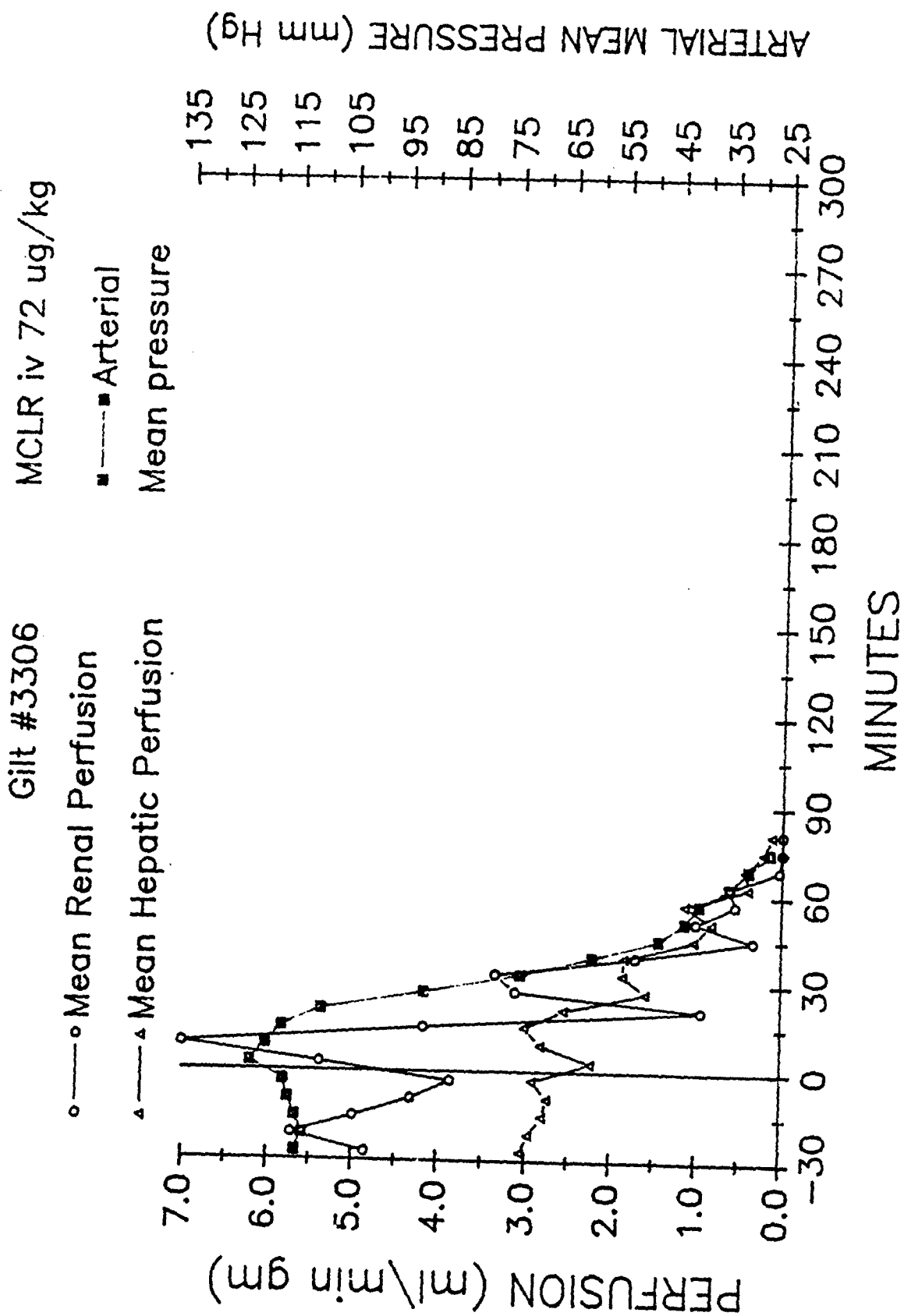


Figure 15
Section XI

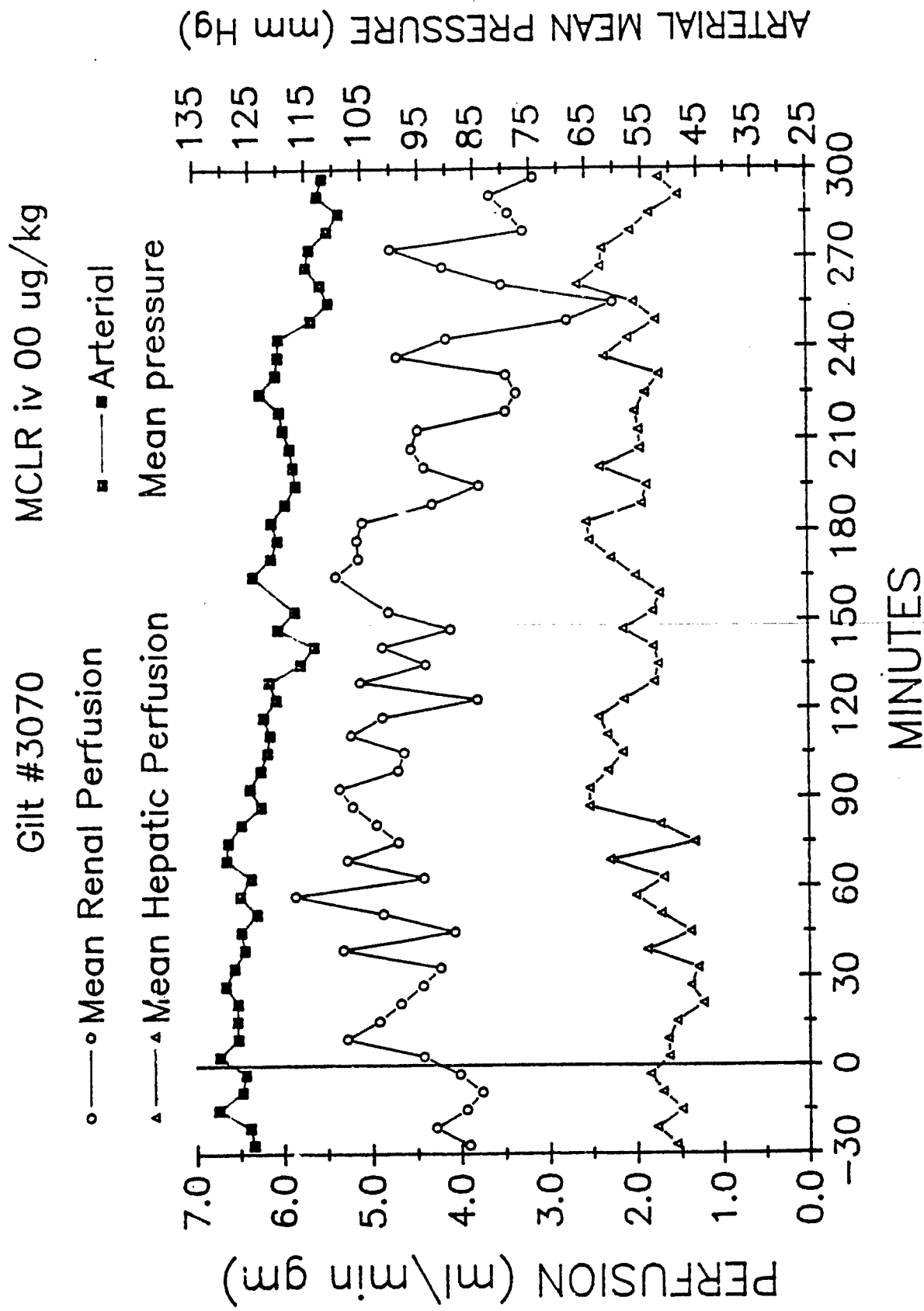


Figure 16

Section XI

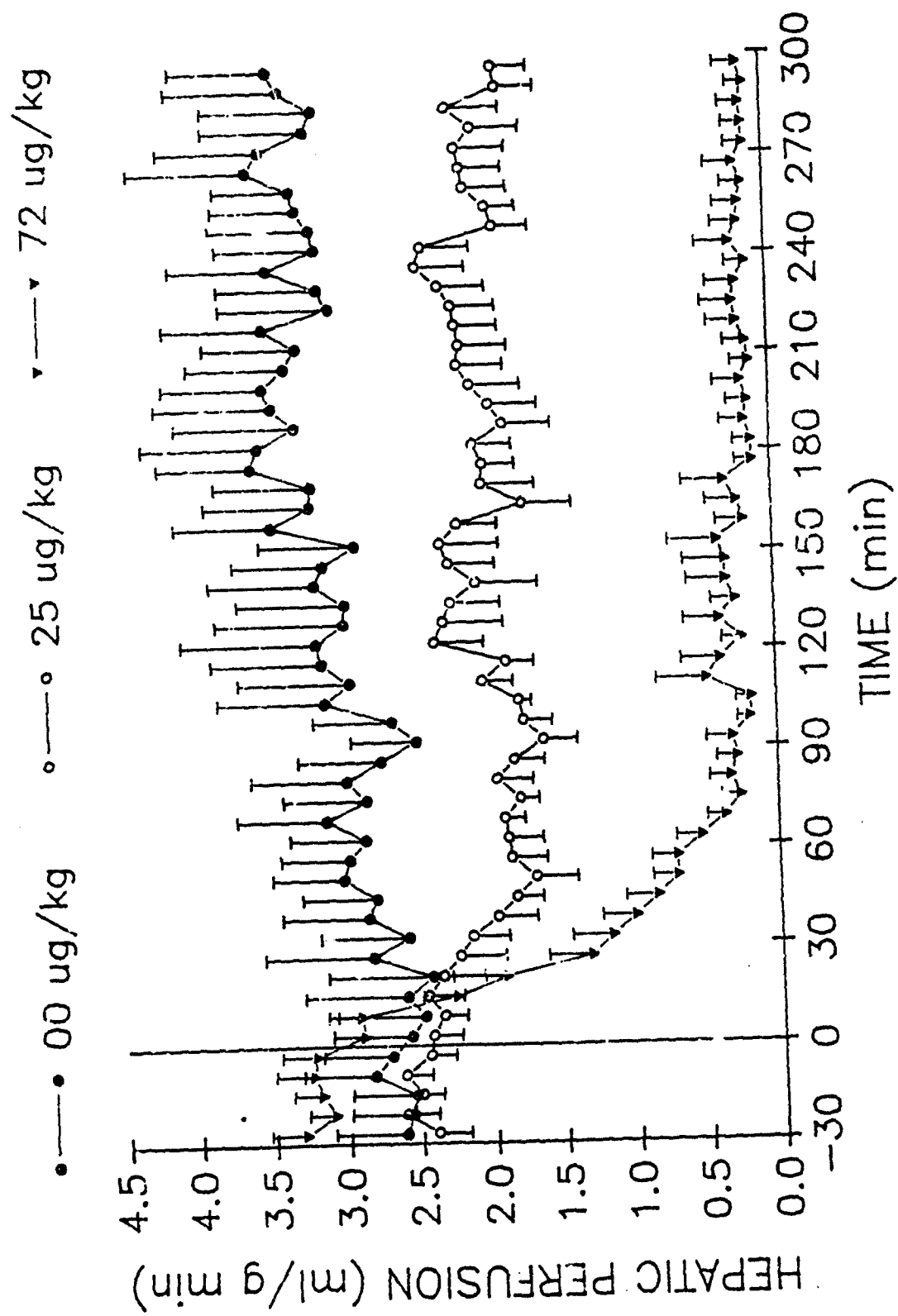


Figure 17

Section XI

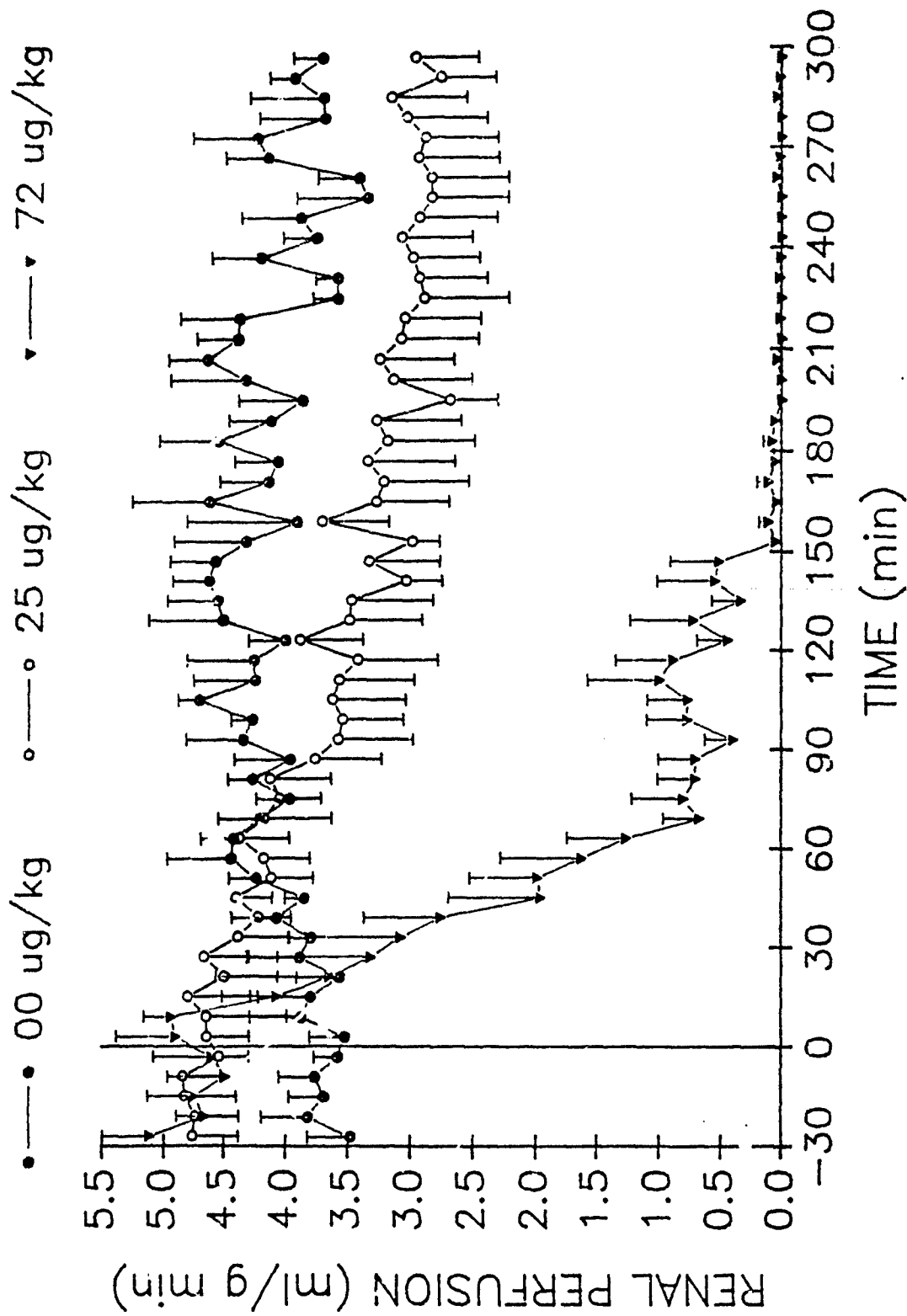


Figure 18

Section XI

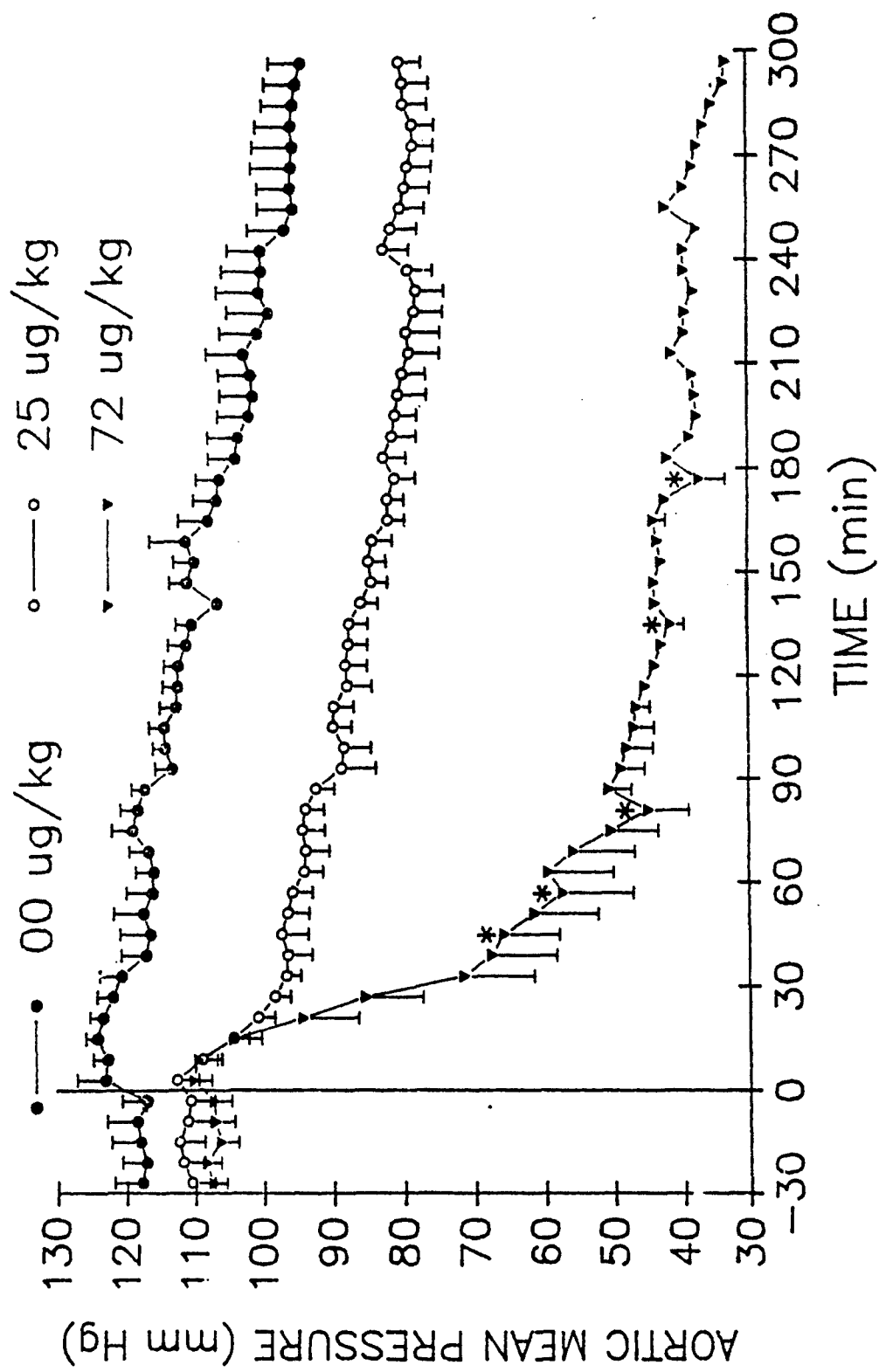


Figure 19

Section XI

XII. ARGINASE ACTIVITY IN TWELVE TISSUES AND SERUM, SERUM ARGINASE HALF-LIFE, AND CHANGES IN SERUM ARGINASE ACTIVITY FOLLOWING ADMINISTRATION OF MICROCYSTIN-A (CYANOGINOSIN-LR) IN SWINE.

Randall A. Lovell, DVM, Walter E. Hoffmann, DVM, PhD,
William M. Valentine, DVM, PhD, Lisa A. Lund, DVM, Andrew M. Dahlem
Stephen B. Hooser, DVM, MS, and Wanda M. Haschek-Hock, DVM, PhD

ABSTRACT

The mean serum arginase activity in these 6 swine was 2.29 IU/L. Following an IV injection of 2.0 ml/kg of a porcine liver extract containing 145 IU/ml arginase activity, the serum arginase half-life was 128.5 minutes in a gilt and 85.8 minutes in a barrow. Microcystin-A, a potent heptapeptide-hepatotoxin produced by at least 2 species of cyanobacteria (blue-green algae), induced marked increases in serum arginase activity which were dose dependent with respect to latency and magnitude. The serum arginase activity exceeded 240 IU/L 14 hours after a sublethal IV dose (16 µg/kg) of microcystin-A, and returned to near baseline values by 26 hours postdosing. The lethal IV dose (24 µg/kg) of microcystin-A produced a serum arginase activity of approximately 1,450 IU/L, and death within 5.5 hours of administration. Serum arginase activity never exceeded 22 IU/L during the 24-hour postdosing period in a gilt administered the ethanol/saline vehicle.

INTRODUCTION

Serum activities of liver specific enzymes are considered to be among the most sensitive and reliable tests for detecting mild to severe hepatocellular damage and biliary obstruction. Once certain fundamental characteristics of an enzyme are determined, serum enzyme activity can provide insight into the

location, duration, severity, and mechanism involved in a particular hepatopathy.

Arginase is emerging as an important addition to the commonly used serum enzymes employed to monitor liver integrity. Arginase catalyzes the conversion of arginine to urea and ornithine. Formerly, arginase determinations have been based upon quantifying the amount of urea produced from the substrate arginine. Due to the presence of considerable amounts of urea in the serum normally, it was necessary to perform repeated salt precipitations of proteins or gel filtration to separate urea from arginase. These separations proved time consuming and required multiple technical manipulations, rendering the procedure impractical for routine use. Development of a direct colorimetric method for determination of the ornithine produced from arginine¹ has facilitated the application of arginase determination on a routine basis. Additionally, the reagents and standards necessary for this determination method can be prepared from commercially available chemicals and have a reported stability of at least 1 year when stored at 0 to 5°C in amber glass bottles.¹

The development of practical analytical techniques and determination of arginase activity in specific tissues²⁻⁴ has increased its use as a diagnostic aid in numerous species. In accordance with its liver specificity in ureotelic animals^{5,6} and its cytoplasmic location in liver parenchymal cells^{7,8} arginase has been shown to be a good indicator of hepatic necrosis induced by carbon tetrachloride.^{1,2,9,10}

Considering the prominent role that swine fulfill in research today, the availability of serum arginase as a clinical assay for this species would appear to be an important development. This study was therefore undertaken to establish the basic criteria necessary to interpret serum arginase activities

as a diagnostic and prognostic indicator of hepatic damage in swine. The arginase activity in 12 tissues of 6 swine, the serum arginase half-life in 2 swine, and serum arginase activity changes following IV administration of a sublethal and lethal dose of microcystin-A (cyanoginosin-LR), a potent cyanobacterial heptapeptide hepatotoxin, are presented.

MATERIALS AND METHODS

Animal Specimens for Tissue Arginase Activity

See Annual Report 1986, page 146.

Tissue Processing and Arginase Activity Analysis

See Annual Report 1986, pages 146-147.

Liver Extract Solution Preparation for Arginase Half-life Determination

A liver extract solution was derived from a healthy gilt purchased from the University of Illinois Veterinary Medicine Research Farm (UIVMRF). This gilt was killed by electrocution and the liver was placed on ice within 10 minutes of death. The liver was frozen (0 to -5°C) for 1 week until the day prior to dosing. The liver was homogenized in physiologic saline after thawing at room temperature, and the homogenate centrifuged at 500 x g and 4°C for 30 minutes. The supernatant was further diluted with physiologic saline until it was comprised of 1 g liver/120 ml physiologic saline. This extract solution provided 145 IU arginase activity/ml prior to administration.

Animal and Specimen Handling for Serum Arginase Half-life Determination

Two crossbred, 12-week-old littermate pigs (a gilt and a barrow) were purchased from the UIVMRF. Following a 24-hour fast, ketamine^a (20 mg/kg, IM) followed by thiamylal^b (to effect, IV) were administered to induce and maintain anesthesia. A 16-gauge catheter^c was placed into the anterior vena cava after an external jugular vein cutdown. The catheter was capped, filled with heparin,^d and buried subcutaneously caudal to the base of the right ear.

2.0 ml/kg IV dose of liver extract. Serum arginase activity reached 578 IU/L in the gilt and 854 IU/L in the barrow following liver extract administration. Both pigs had a predosing serum arginase activity of 1 IU/L and both pigs vomited twice between 3 and 5 minutes after liver extract administration. No further adverse effects were observed and both pigs ate normally later that morning and afternoon. The serum arginase half-lives for the gilt and the barrow were 128.5 and 85.8 minutes, respectively.

Liver Histopathology of Swine Administered Microcystin-A

No significant histologic changes were seen in the gilt administered the ethanol/saline vehicle. The liver of the pig, dosed at 16 µg/kg, had moderate, acute, centrilobular hepatocyte degeneration, and necrosis with mild to moderate hemorrhage in these areas. The liver of the pig, dosed at 24 µg/kg, was severely affected with massive hepatocyte degeneration, and necrosis with severe hemorrhage in all lobular regions except for a rim of periportal hepatocytes a few cells wide.

Serum Arginase Activity of the Microcystin-A Dosed Swine

Figure 2 displays the serum arginase activities of the 2 gilts administered microcystin-A and the gilt administered ethanol and normal saline only. Serum arginase activity of the swine given an IV injection of vehicle remained between 0 and 22 IU/L over the entire 24-hour period. Increases in serum arginase activity occurred between 8 to 14 hours after IV injection of a sublethal dose (16 µg/kg) of microcystin-A, with a maximal value of approximately 250 IU/L at 14 hours. Serum arginase values returned to baseline values within 26 hours following the sublethal dose of microcystin-A. The lethal dose of microcystin-A of 24 µg/kg produced a marked increase in serum arginase from 2 hours after IV administration until immediately prior to death when a maximum value of approximately 1,450 IU/L was reached.

DISCUSSION

A comparison of tissue arginase activities in Table 1 demonstrates that liver, pancreas, and kidney contain the greatest amount of activity/g organ weight. Liver arginase activities are approximately 1 order of magnitude greater than that of pancreas or kidney, 2 orders of magnitude greater than salivary glands and jejunal mucosa, 3 orders of magnitude greater than the quadriceps muscles, and 4 orders of magnitude greater than the other tissues examined. These relative arginase activities suggest that large increases in serum arginase activities would primarily be the result of hepatocellular damage. This contention is strengthened when the relative mass of the liver is compared to that of the pancreas and kidney.

Species variation in tissue and serum arginase activity have been reviewed.⁴ In general, tissue arginase activities in other species have presented a similar relative distribution as that observed here for swine. In a paper comparing isoenzymes in liver and kidney tissue of 10 species, arginase activity of porcine liver and kidney was determined to be 44 IU/g and 1.55 IU/g, respectively;³ similar to the values reported here of 34 IU/g for liver and 3.24 IU/g in kidney. In other domestic species, the highest liver arginase activity reported has been in the dog (445 IU/g) and the lowest in sheep (100 IU/g),² thus the values of 34 and 44 IU/g in swine are the lowest determined to date. The serum arginase activity in the swine measured here of 2.29 IU/L falls between the activity of 0.50 IU/L reported for the dog and 21.30 IU/L for the rat,² and close to that of 1 IU/L previously reported for swine.¹ The serum arginase half-lives of 85.8 and 128.5 minutes were similar to that reported in a calf (80 minutes).² This is in contrast to the 19-hour half-life of another urea cycle enzyme, ornithine carbamyl transferase, in swine.¹¹

The hepatotoxicity of microcystin-A has been well documented.¹²⁻¹⁵ Hepatic lesions attributable to microcystin-A observed in mice and rats are numerous and include loss of sinusoidal epithelium, vesiculation of the rough endoplasmic reticulum (mice), swollen mitochondria (mice), cell lysis, and centrilobular necrosis. Figure 2 suggests that the latency and magnitude of serum arginase activity increases following microcystin-A administration are dose-dependent. Prior investigations have evaluated serum arginase elevations in various species resulting from hepatic damage induced by carbon tetrachloride and metabolic changes associated with starvation and corticosteroids.^{1,2,9,10} Serum arginase activity reached 316 IU/L at 24 to 48 hours subsequent to oral administration of 0.2 to 3.0 ml/kg body weight of carbon tetrachloride in swine.¹ This can be compared to the maximum values of 250 and 1,450 IU/L following IV administration of a sublethal and lethal dose of microcystin-A.

The differences in behavior of arginase and the transaminase levels in the serum of the dog, horse, sheep, and calf have afforded a technique for distinguishing the duration of a hepatic insult and evaluating the repair processes.² Subsequent to acute hepatic necrosis induced by orally administered CCl₄ in these 4 species, arginase values rose significantly within hours and returned to normal or below normal values within 3 to 4 days. Transaminases in these species evidenced the same rapid rise but remained elevated over a week. The more rapid return to normal levels of arginase in nonprogressive liver necrosis enables a determination of the nature of the injury: a progressive hepatic lesion would be necessary to maintain an increase in serum arginase. Serum arginase activities in swine given microcystin-A appear to follow a shorter time course, with values

returning to normal within 26 hours of the sublethal dose. The liver specificity and rapid rate of clearance of arginase from serum suggest that it will be a meaningful parameter for detecting acute hepatic injury and assessing progressive vs nonprogressive hepatotoxic processes in swine.

REFERENCES

1. Mia, K. S. and Koger, H. D. Direct colorimetric determination of serum arginase in various domestic animals. *Am. J. Vet. Res.* 39:1381-1381, 1978.
2. Cornelius, C. E., Douglas, G. M., Gronwall, R. R., et al. Comparative studies on plasma arginase and transaminases in hepatic necrosis. *Cornell. Vet.* 53:181-191, 1963.
3. Parembaska, Z., Baranczyk, A., and Jachimowicz, J. Arginase isoenzymes in liver and kidney of some mammals. *Acta. Biochim. Pol.* 18:79-85, 1971.
4. Boyd, J. W. The mechanisms relating to increases in plasma enzymes and isoenzymes in diseases of animals. *Vet. Clin. Pathol.* 2:9-24, 1981.
5. Greenberg, D. M. Arginase. In: Boyer, P. D., Lardy, H., and Myrback, K. eds. *The Enzymes*. New York: Academic Press 259-267, 1960.
6. Cornelius, C. E. Liver function. In: Kaneko, J. J. ed. *Clinical Biochemistry of Domestic Animals*. New York: Academic Press 230-236, 1970.
7. Shrzypek-Oslecka, I., Rahden-Staron, I., and Porembaska, Z. Subcellular localization of arginase in rat liver. *Acta. Biochem. Pol.* 27:203-208, 1980.
8. Sumitani, A. Immunological studies of liver arginase in man and various kinds of vertebrates. *Hiroshima J. Med. Sci.* 26:59-80, 1977.
9. Cacciatore, L. and Antonietello, S. Arginase activity of mouse serum and liver tissue in some conditions of experimental liver damage. *Enzymologia* 41:112-120, 1971.
10. Cargill, C. F. and Shields, R. P. Plasma arginase as a liver function test. *J. Comp. Pathol.* 81:447-454, 1971.

11. Massarrat, S. Enzyme kinetics, half-life, and immunological properties of I-131-labelled transaminases in pig blood. *Nature* 206:508-509, 1965.
12. Foxall, T. L. and Sasner, J. J., Jr. Effects of a hepatic toxin from the cyanophyte Microcystis aeruginosa. *Environ. Sci. Res.* 20:365-387, 1980.
13. Falconer, I. R., Jackson, A. R. B., Langley, J., and Runnegar, M. T. C. Liver pathology in mice in poisoning by blue-green alga Microcystis aeruginosa. *Aust. J. Biol. Sci.* 34:179-187, 1981.
14. Runnegar, M. T. C. and Falconer, I. R. The in vivo and in vitro biological effects of the peptide hepatotoxin from the blue-green alga Microcystis aeruginosa. *S. Afr. J. Sci.* 78:363-366, 1982.
15. Dabholkar, A. S. and Carmichael, W. W. Ultrastructural changes in the mouse liver induced by hepatotoxin from the freshwater cyanobacterium Microcystis aeruginosa strain 7820. *Toxicon* 25:285-292, 1987.

Footnotes

^aKetaset, Bristol Laboratories, Syracuse, NY.

^bBio-tal, Bio-Ceutic Division, Boehringer Ingleheim Animal Health Inc.,
St. Joseph, MO.

^cTygon Microbore Tubing, A. Daigger and Co., Chicago, IL.

^dHeparin, Elkins-Sinn Inc., Cherry Hill, NJ.

^eLidocaine, The Butler Co., Columbus, OH.

^fHalothane, Halocarbon Laboratories Inc., Hackensack, NJ.

^gPreparation described in Harada K, Suzuki M, Dahlem A, et al. Improvement of
purification method for toxic peptides produced by cyanobacteria. Toxicon in
press.

Table 1. Mean, standard deviation (SD), and range of arginase activity in tissues and serums of swine.

Tissue	Mean (IU/g)	SD (IU/g)	Range (IU/g)	No. of Animals
Liver	34.01	25.48	13.68 to 74.89	6
Pancreas	5.43	2.22	2.60 to 9.25	6
Kidney	3.24	1.57	1.12 to 5.79	6
Salivary gland	0.52	0.27	0.27 to 0.97	6
Jejunal mucosa	0.47	0.16	0.23 to 0.63	6
Quadriceps	0.10	0.07	0.00 to 0.18	5
Lung	0.03	0.04	0.00 to 0.08	6
Adrenal	0.03	0.04	0.00 to 0.11	6
Spleen	0.03	0.04	0.00 to 0.06	2
Brain	0.01	0.01	0.00 to 0.03	6
Heart	0.01	0.01	0.00 to 0.03	6
Diaphragm	0.03	--	--	1
Serum	2.29*	2.58*	0.00 to 5.24*	6

* = IU/L

Figure 1. Natural log of serum arginase activity as a function of time in a gilt (■) and a barrow (○) following IV administration of 2.0 ml/kg of a swine liver extract having 145 IU/ml arginase activity.

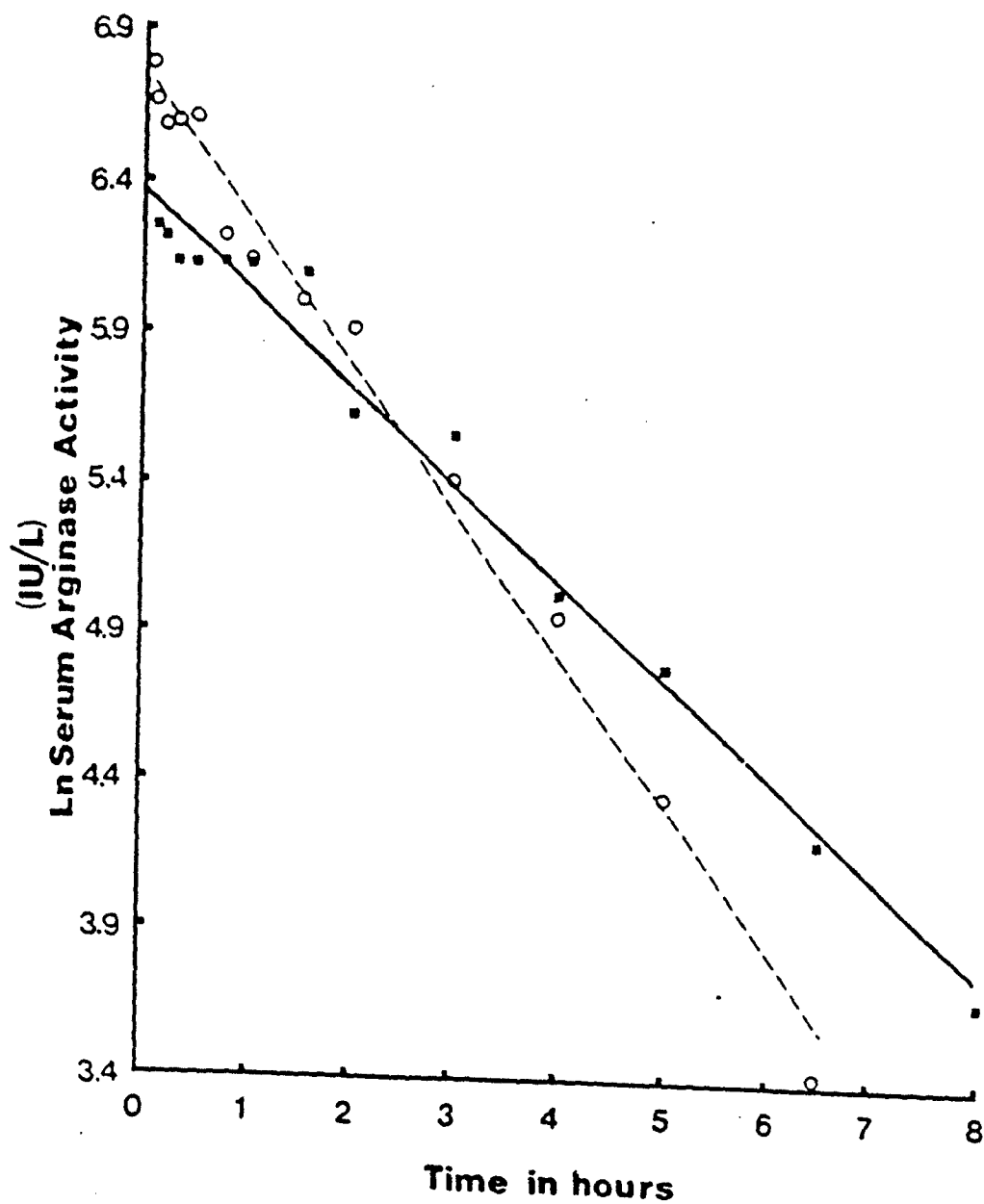
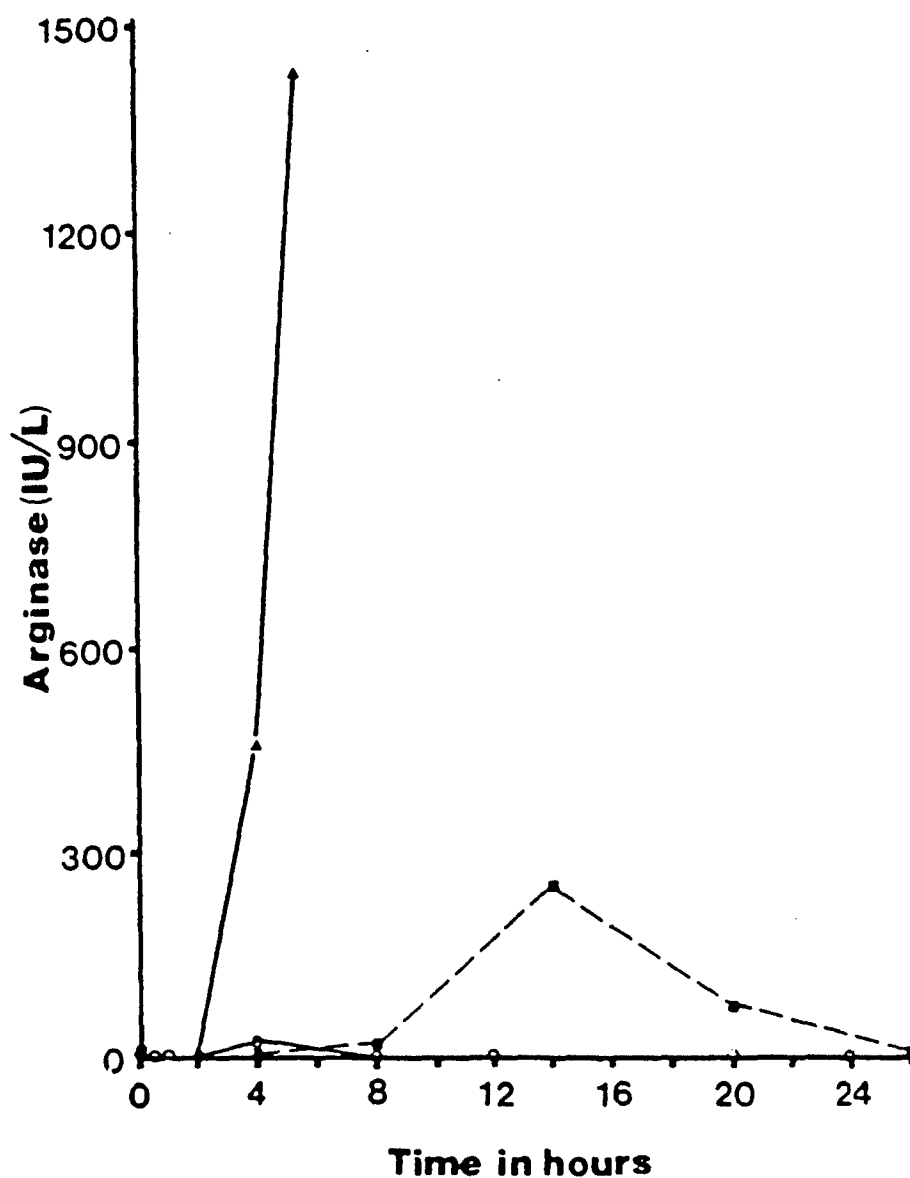


Figure 2. Serum arginase activity as a function of time in a gilt administered an IV injection of the ethanol and normal saline vehicle (○), a sublethal dose of 16 $\mu\text{g/kg}$ (■), or a lethal dose of 24 $\mu\text{g/kg}$ (▲) microcystin-A.



XIII. TOXICITY OF ONE OR TWO INTRAPERITONEAL DOSES OF
MICROCYSTIN-A IN MALE SWISS WEBSTER MICE

Randall A. Lovell, DVM

ABSTRACT

Male Swiss Webster (SW) mice were administered various i.p. dosages of microcystin-A (MCYST-A) to establish dose-response curves and to determine if a sublethal dose of MCYST-A provides protection against a LD₁₀₀ min given 3 days later. Microcystin-A has a steep dose-lethal response curve in SW mice: LD₅₀ = 60 µg/kg, LD₀ max = 50 µg/kg, and LD₁₀₀ min = 70 to 75 µg/kg. Liver weights increased 51% and kidney weights increased 20% within 200 min following i.p. administration of a LD₁₀₀ min of MCYST-A in naive mice. Grossly and histologically, the marked increase in liver weight appeared to be caused primarily from intrahepatic hemorrhage and death is probably a result of hemorrhagic shock. Administration of a LD₂₃ resulted in significantly increased survivability and survival time when a subsequent LD₁₀₀ min was given 3 days later. Survivors of the LD₂₃/LD₁₀₀ min regimen had 96-hour postdosing liver weights which were not significantly different from those of mice which died acutely after the same hepatotoxin treatments. These survivors showed weakness, recumbency, anorexia, and jaundice and had marked gross liver lesions. Histologically these lesions were undergoing rapid reparative processes.

INTRODUCTION

This paper reports the results of a study designed to determine whether administration of MCYST-A would protect against a second consistently lethal dose of MCYST-A. Clinical signs, survival times, liver and combined kidney

weights, and lesions in male Swiss Webster mice are also reported following 1 or 2 i.p. doses of purified MCYST-A. The study was conducted in part to confirm presumptive evidence suggestive of a protective effect of MCYST-A from a second dose of the toxin in Balb-C mice, as reported on pages 131-144 of the 1986 Annual Report.

MATERIALS AND METHODS

One hundred forty-four male, 6-week-old, Swiss-Webster mice weighing 22 to 28 grams were obtained from the Charles River Company. The mice were fed a commercial rodent chow and provided water ad libitum. They were placed on a 12-hour light/12-hour dark photoperiod and given a 2-week acclimation period.

All doses were given by i.p. administration. The MCYST-A solution consisted of > 95% pure MCYST-A, in a vehicle of 0.9% saline containing 0.1% ethanol. Preliminary trials with 30 mice established 55 $\mu\text{g/kg}$ as an approximate LD_{30} dose and 75 $\mu\text{g/kg}$ as an approximate LD_{100} min.

On Day 0, 48 mice were administered 55 $\mu\text{g/kg}$ of a freshly prepared solution (3.0 $\mu\text{g/ml}$) of MCYST-A. Thirty-six mice were administered an equivalent volume of vehicle. Three days later, the 37 MCYST-A dosed mice that survived the Day 0 hepatotoxin dosing, 24 of the Day 0 vehicle-dosed mice, and 24 additional mice given no Day 0 treatment were administered MCYST-A i.p. at 75 $\mu\text{g/kg}$. Also on Day 3, 12 of the mice given the vehicle on Day 0 and 6 mice given no Day 0 treatment were administered the vehicle.

Half of the mice administered the vehicle on Day 0 and Day 3 and the mice given the vehicle only on Day 3 were killed on Day 4. All preliminary and formal study mice surviving a dose of hepatotoxin and the remaining mice given the vehicle on Day 0 and Day 3 were killed on Day 7. Improper dosing or a left microkidney caused 2 mice to be disqualified from this study. Monitoring of clinical signs was conducted for 10 hours after the Day 0 and Day 3 dosings

and every 4 hours thereafter. Necropsies were performed within 4 hours of death. Mice were killed by cervical dislocation and liver (including gallbladder) and combined kidney weights (capsule removed) weights were obtained. All organ weight data was transformed to percentage live body weight (% bw). Sections of kidneys, liver, heart, lung, and spleen were fixed in 10% neutral buffered formalin, routinely processed, embedded in paraffin, cut at 5 to 6 μ , and stained with hematoxylin and eosin.

STATISTICAL ANALYSIS

Covariate analysis was performed on the natural logarithms of the liver weight (LLIVWT) and kidney weight (LKIDWT) data from the 95 mice administered MCYST-A during the formal study (raw data without transformation to natural logarithms is presented in the Appendix for Section XIII which begins on page 245). In these analyses, mice were grouped (TRT) according to their Day 0 and Day 3 treatments (Table 1). The following models were used in the covariate analysis of this data:

- a. $LLIVWT = \text{CONSTANT} + \text{TRT} + \text{LST}$
- b. $LLIVWT = \text{CONSTANT} + \text{TRT} + \text{RES}$
- c. $LKIDWT = \text{CONSTANT} + \text{TRT} + \text{LST}$
- d. $LKIDWT = \text{CONSTANT} + \text{TRT} + \text{RES}$

In these models, LST and RES serve as the covariate; LST = natural log of survival time in minutes; and RES = a response variable chosen on the basis of clinical signs and gross lesions present in mice which survived for similar periods of time. If survival time < 5.5 hours, the RES = peracute death; if survival time \geq 5.5 hours and < 48 hours, then RES = acute death; if survival time \geq 48 hours and < 96 hours, then RES = subacute death; if survival time \geq 96 hours, then RES = survivor; if mice were administered vehicle on Day 3, then RES = control.

The Student Newman Keuls' (SNK) test of means with unequal sample sizes and the Bartlett Test for homogeneity of group variances were also used to check for differences ($\alpha = 0.05$) in:

- a. LLIVWT and LKIDWT among the 3 vehicle control groups.
- b. LLIVWT among the 11 TRT x RES groups (Table 2).
- c. LKIDWT among the 5 RES groups (Table 3).
- d. Rank of survival time among the 4 TRT groups (Table 4); only mice which died were used in this comparison.

The cumulative probability for the binomial (CPB) (Fleiss, 1981) was used to test for significant differences (outside the 95% confidence interval) in survival between TRT groups 55/75, Veh/75, and no trt/75 following the 75 ug/kg ip dose of MCYST-A on Day 3 (Table 5). Student's t-test was used to compare the LLIVWT and LKIDWT of the 17 formal vehicle control mice with those of the 18 preliminary mice that survived 10 to 12 days after single doses of MCYST-A (Table 6).

RESULTS

Analyses of survival time and survival data are presented in Tables 4 and 5. In mice that died peracutely, decreased responsiveness/movement was the first observed adverse effect occurring 35 to 50 min postdosing. Piloerection, limited movement, increased respiratory rate, and mild pallor of the extremities followed. A peculiar "hopping movement" was observed in the majority of these mice within 45 min of death. Mice would be recumbent and still, away from the other mice, with eyes closed when a whole body tremor, opening of the eyes, and a "hop" of up to several cm in height was observed. This reaction, which lasted less than 3 seconds and occurred more than once in many mice, was quickly followed by a return to the eyes closed, recumbent

position. Severe pallor of the extremities, weakness (inability to stand), and marked increases in rate and depth of respiration preceded death.

In mice that died acutely, decreased responsiveness-movement, first occurred at 50 to 75 min postdosing. The mice were capable of walking around the cage for several hours after onset of ill effects. The stage of piloerection, limited movement, increased respiratory rate and pallor of the extremities progressed much slower in mice that died acutely vs those that died peracutely. None of the mice which died acutely were observed attempting to eat or drink after the onset of clinical signs. The "hopping movement," was observed sporadically in this group, but it was not as severe as in mice that died peracutely and was not always associated with impending death.

In the mice that died subacutely, decreased responsiveness-movement was evident within 90 min postdosing. These mice would slowly walk when gently urged for 40 hours postdosing but were often observed lying still. Some of the mice drank and attempted to eat between 48 hours postdosing and death. After these activities, the mice were recumbent for several minutes with prominent increases in rate and depth of respiration. Jaundice and an enlarged abdomen developed between 48 hours postdosing and death in several mice of this group. The "hopping movement" was observed sporadically beginning at 36 hours postdosing in 2 mice of this group.

Of 9 mice that survived the second dose of MCYST-A, 3 showed no ill effects for the entire 96-hour postdosing observation period. Two of these mice were given the vehicle on Day 0. The 6 mice that survived and exhibited clinical signs had been given MCYST-A at 55 µg/kg on Day 0. In these 6 mice, decreased responsiveness-movement was evident within 2 hours postdosing (Day 3), but they never lost the ability to walk slowly when gently urged. No

"hopping movements" were observed in these 6 mice. For 48 hours postdosing, these mice lay still with other cage members. From 60 hours postdosing until these mice were killed by cervical dislocation (96 hours postdosing), a slow but steady improvement in appetite, strength, and responsiveness was observed. These 6 mice developed mild-severe jaundice and 1 developed a severely enlarged abdomen between 48 and 96 hours postdosing. Mice were classified as survivors and the experiment was terminated at approximately 96 hours postdosing because all mice still alive following MCYST-A administration on Day 3 had been observed: (a) eating, (b) drinking, and (c) rearing (which was not observed postdosing in any mouse that died).

No clinical signs were observed in any mouse administered the vehicle alone. At 24 hours after the Day 0 treatment, no clinical signs were observed in any of the surviving mice.

Organ Weights

In both LLIVWT models, there was a significant difference ($p < .001$) in mean liver weight among the 4 treatment (TRT) groups. The covariate, either RES or LST, had a significant influence ($p < .001$) on liver weight. The comparison of LLIVWT between groups sorted by the 2 variables (RES and TRT) which significantly influenced liver weights in the covariate analysis is presented in Table 3.

In both LKIDWT models, there were no significant differences ($p = .62$ or $.70$) in mean kidney weight among the 4 treatment (TRT) groups. In contrast, the covariate, either RES or LST, had a significant influence ($p < .001$) on kidney weight. The comparison of LKIDWT by response (RES) is presented in Table 3.

Gross Lesions

Mice that died peracutely had markedly swollen, hemorrhagic dark red livers and severe pallor of the carcass. Mice that died acutely had severely swollen hemorrhagic mottled reddish-brown livers with moderate-severe pallor of the carcass. Mice that died subacutely had moderately swollen extremely mottled red-white livers with mild-severe jaundice, and moderate pallor of the carcass. The 6 survivors that displayed clinical signs had moderately to severely enlarged, firm, solid white to mottled pink-white livers and mild-moderate pallor of the carcass. Gross lesions were not found in the kidneys of any mice in this study. No gross lesions were present in the 3 survivors that displayed no adverse effects and in the 17 vehicle control mice.

Histologic Lesions

Treatment associated lesions were restricted to the liver. All mice that died peracutely had similar lesions, characterized by severe centrilobular hepatocyte disassociation, rounding, degeneration, and necrosis, which frequently extended into the midzonal hepatocytes. Marked hepatocyte loss was evident in these regions. In severely affected areas, there was breakdown and loss of sinusoidal endothelium, disruption of normal architecture, and severe hemorrhage. Hepatocytes in less severely affected midzonal and periportal areas often had one to several large, clear, intracytoplasmic vacuoles. In most lobules, all hepatocytes were affected except for a rim of periportal hepatocytes from 1 to 6 cell layers deep. These liver lesions were identical to those observed in Balb-C mice which died peracutely in a previous study.

The livers of mice surviving 5.5 to 24 hours were similar to those described above except that hepatocyte disassociation and necrosis in the most severely affected centrilobular regions were more marked with prominent

cellular shrinkage, nuclear pyknosis, and karyorrhexis. In addition, small numbers of neutrophils and a few lymphocytes were seen infiltrating these areas. Moderate cellular swelling was present in periportal and remaining midzonal hepatocytes resulting in a reduction of sinusoidal lumina.

The livers of mice surviving 24 to 48 hours were characterized by severe centrilobular and variable midzonal hemorrhage with an infiltration of moderate numbers of neutrophils and smaller numbers of lymphocytes and macrophages. The remaining hepatocytes in these areas had undergone coagulative necrosis and were frequently replaced by cellular debris. Intact, midzonal, and periportal hepatocytes were moderately swollen causing obliteration of numerous sinusoids. In scattered areas, these hepatocytes often contained one to several large, clear, intracytoplasmic vacuoles.

The livers of mice surviving 48 to 72 hours appeared similar to those at 48 hours or were characterized by severe infiltration of macrophages with a few neutrophils, lymphocytes, and fibroblasts into the centrilobular areas. There was a marked reduction in erythrocytes and cellular debris. Hepatocytes adjacent to centrilobular areas were haphazardly packed together with no normal architecture. The hepatocytes had abundant, streaming, slightly basophilic cytoplasm and large, pale nuclei often containing several prominent nucleoli. Remaining midzonal and periportal hepatocytes were severely swollen, forming almost continuous sheets of cells which obscured almost all sinusoids in these areas. The cytoplasm of these cells was often pale and contained numerous very small cytoplasmic vacuoles.

The livers of mice surviving 72 to 96 hours were similar to mice at 48 and 72 hours. In centrilobular areas, 1 to 3 mitotic figures were seen per high power field, in addition to numerous small capillaries (neovascularization).

Small to moderate numbers of macrophages and a few lymphocytes had infiltrated these areas. Cellular swelling obliterating most of the sinusoidal lumina was prominent in midzonal and periportal regions.

DISCUSSION

A steep dose lethal response curve was evident in the preliminary mice of this study and the LD₀ max (50 µg/kg) was approximately 83% of the LD₅₀ (60 µg/kg). This was in agreement with intraruminal administration of algal cells in sheep in which the consistently sublethal dose was greater than 90% of the LD₅₀ (Jackson *et al.*, 1984).

During 2 trials preceding this study, a "protective effect" was suggested when: a) 2 Balb-C mice survived a MCYST-A dose of 30 µg/kg and 3 days later survived a 35 or 40 µg/kg i.p. dose, and b) 3 of 5 male Balb-C mice survived a 30 µg/kg (LD₃₀) dose and 2 days later survived a 40 µg/kg (LD₁₀₀ min) dose. Due to the small number of animals, however, the protective effect results in these studies were considered inconclusive. The LD₂₃ dose of MCYST-A in this study did provide a "protective effect" from an LD₁₀₀ min administered 3 days later. The "protective effect" was manifested in both increased survival time and survival (Table 4 and 5). Even though we selected for "resistant" individuals in the 55/75 group, there was a highly significant increase in rank of survival time in the 55/75 group when compared to the survival time of the most "resistant" 77% of mice in the other 3 treatment groups. Thus, the sublethal effects of the 55 µg/kg dose appear to be responsible for the increased survival time. Dose also significantly influenced rank of survival time since the 24 naive mice given no trt/75 died at an earlier time than the 11 naive mice after being given 55 µg/kg. Increased survival in the 55/75 group cannot be attributed to prevention of massive increases in liver weight

(Table 2) or solely to the primary effects of the MCYST-A administered on Day 0 since mice given veh/75 also had survivors. Since pharmacologic doses of hydrocortisone prevented deaths in mice given "lethal" doses of MCYST-A (Adams et al., 1985), then the stress of handling, the administration of vehicle (ethanol and physiologic saline), and the sublethal effects of MCYST-A may all play a role in increased survival.

Unlike CCl₄, mixed function oxidase inhibitors do not seem to effect the toxicity of MCYST-A (Adams et al., 1985). Bile acid carriers are likely to be involved in entry of the microcystin into hepatocytes (Runnegar et al., 1981), in its absorption from the intestinal tract, and in its selective accumulation in the liver (Falconer et al., 1986). Bile acid uptake by the perinatal rat liver is limited by immaturity of bile acid carriers (Suchy et al., 1986), and this may explain why young (1 to 3 weeks) mice were unaffected by "lethal" doses of MCYST-A (Adams et al., 1985).

The "protective effect" of the LD23 of MCYST-A in this study is similar to the "protective effect" of a sublethal dose of carbon tetrachloride (Adams et al., 1985). With CCl₄, an increase in survival time was observed after mice were subsequently challenged with a "lethal" dose of MCYST-A although > 80% of the mice died within 4 days. The protective effect induced by the 2 agents could be a result of less efficient uptake by the bile acid carriers of the damaged hepatocytes or lesser acute hemorrhage into the already disrupted and distended liver, among other possibilities.

In mice which died peracutely, those given 55/75 had significantly higher liver weights than mice given veh/75 and no trt/75. This suggests that the sublethal (55 µg/kg) dose of MCYST-A had caused a slight increase in liver weight prior to the lethal dose, similar to the findings in a previous study

with Balb-C mice. There was a definite inverse relationship between survival time and liver weight in the mice that died (Table 2). As predicted by the preliminary study, the 24 no trt/75 mice that died peracutely had significantly greater liver weights than the 9 that died peracutely after one 55 µg/kg dose (Table 3). Although dose appeared to affect liver weight in this study, the possibility that more susceptible mice died with lower liver weights was not ruled out. In the 3 survivors that showed no clinical signs and had livers that appeared grossly and histologically normal, liver weights were higher than the highest vehicle control value, indicating that some liver damage had occurred due to MCYST-A administration.

The marked increase in liver weight of mice that die following MCYST-A administration grossly and histologically appears to be caused primarily by hemorrhage. These findings and the extreme pallor of the carcass were compatible with death from hemorrhagic shock. Although the exact mechanism of action of MCYST-A is unknown, it has been suggested that it may cause destabilization of the liver cytoskeleton (Runnegar and Falconer, 1982; Runnegar and Falconer, 1986). Whether significant destabilization actually occurs and whether this causes sufficient disruption of liver architecture to result in hemorrhage remains to be demonstrated.

The time course and degree of changes in organ weights and gross/histologic findings suggests that the liver is the primary target organ and that the kidneys are secondarily affected following administration of MCYST-A. The significant increase in kidney weight may be related to hypoxia, edema, decreased glomerular filtration rate (increased solute retention), and/or embolic hepatic debris that has passed through the lungs.

The liver and kidney weight data of the 18 preliminary mice (Table 6), when compared to the 17 control mice, suggest that recovery from a single

sublethal dose of MCYST-A is accompanied by a significant dose dependent decline in liver weight and gain in kidney weight 10 to 12 days postdosing.

There were marked gross differences between the dark red, enlarged, hemorrhagic livers of mice which died peracutely and the livers of most 55/75 survivors which were swollen, firm, and nearly solid white. Prior to this study, we had observed no significant variation in lesions and no subacute or chronic lesions in the livers of animals that died spontaneously following MCYST-A administration. Mice and rats either survived with no visible lesions or they died with extensive hepatic damage. Following a sublethal dose of MCYST-A, hepatocyte necrosis and hemorrhage in mice that survive a subsequent LD₁₀₀ min are of reduced severity, involving only the centrilobular and portions of the midzonal regions of most lobules. More importantly, within 48 to 96 hours, degenerative changes cease, and active reparative processes, including hepatocyte mitosis, neovascularization, and phagocytosis of necrotic debris rapidly proceeds. This is in contrast to some hepatotoxic agents such as carbon tetrachloride which causes the development of degenerative hepatic changes and fibrosis over long periods of time after the initial exposure (Schiff and Schiff, 1982). The present study indicates that subacute hepatic lesions following MCYST-A administration can occur, and repair of the hepatic lesions begins rapidly thereafter. The subacute and chronic effects of sublethal exposure to MCYST-A deserve closer scrutiny.

REFERENCES

- Adams WH, Stoner RD, Adams DG, Slatkin DN, Seigelman HW. Pathophysiologic effects of a toxic peptide from Microcystis aeruginosa. Toxicon 1985; 23(2):441-447
- Falconer IR, Buckley T, Runnegar MTC. Biological half-life, organ distribution and excretion of ¹²⁵I-labelled toxic peptide from the blue-green alga Microcystis aeruginosa. Aust J Biol Sci 1985; 39:17-22
- Fleiss JL. Statistical Methods for Rates and Proportions. New York: John Wiley, 2nd edition, 1981, pp. 100-109
- Jackson ARB, McInnes A, Falconer IR, Runnegar MTC. Clinical and pathologic changes in sheep experimentally poisoned by the blue-green alga (Microcystis aeruginosa). Vet Pathol 1984; 21:102-113
- Runnegar MTC, Falconer IR. The in vivo and in vitro biological effects of the peptide hepatotoxin from the blue-green alga Microcystis aeruginosa. S Afr J Sci 1982; 78:363-366
- Runnegar MTC, Falconer IR. Effect of toxin from the cyanobacterium Microcystis aeruginosa on ultrastructural morphology and actin polymerization in isolated hepatocytes. Toxicon 1986; 24(2):109-115
- Runnegar MTC, Falconer IR, Silver J. Deformation of isolated rat hepatocytes by a peptide hepatotoxin from the blue-green alga Microcystis aeruginosa. Naunyn-Schmiedeberg's Arch Pharmacol 1981; 317:268-272
- Schiff L, Schiff ER. Diseases of the Liver. Philadelphia, PA: JB Lippincott Co., 1982, pp. 622-624, 650-652, 868-869
- Suchy FJ, Bucuvalas JC, Goodrich AL, Moyer SM, Blitzer BL. Taurocholate transport and Na⁺-K⁺-ATPase activity in fetal and neonatal rat liver plasma membrane vesicles. Am J Physiol: GI Liver Physio 1986; 14(5):665-673

Table 1. Day 0 and Day 3 treatment (TRT) groups of microcystin-A (MCYST-A) in 6-week-old male Swiss Webster mice.

Day 0 TRT--i.p. Dose of MCYST-A	Day 3 TRT--i.p. Dose of MCYST-A	N	Representation of TRT in the Test
55 µg/kg	--	11	55/--
55 µg/kg	75 µg/kg	37	55/75
Vehicle	75 µg/kg	23	Veh/75
No treatment	75 µg/kg	24	no trt/75

-- Mice died following Day 0 treatment.

N = number of mice.

Table 2. Means and standard deviations of the natural logs of liver weight (percent bw) of 6-week-old male Swiss Webster mice. They are grouped according to treatment (TRT) and response (RES).

Day 0 TRT	Day 3 TRT	Response	N	Natural Log Liver Weight \pm SD	SNK *
no trt/veh	vehicle	vehicle control	17	1.674 \pm 0.068	A
vehicle	75 μ g/kg	survivor	2	1.799 \pm 0.048	B
55 μ g/kg	--	acute death	2	1.871 \pm 0.023	B,C
55 μ g/kg	75 μ g/kg	subacute death	8	1.893 \pm 0.088	B,C
vehicle	75 μ g/kg	acute death	2	1.901 \pm 0.059	B,C
55 μ g/kg	75 μ g/kg	survivor	7	1.984 \pm 0.115	C,D
55 μ g/kg	75 μ g/kg	acute death	7	2.017 \pm 0.021	D,E
55 μ g/kg	--	peracute death	9	2.023 \pm 0.057	D,E
vehicle	75 μ g/kg	peracute death	19	2.056 \pm 0.054	E,F
no trt	75 μ g/kg	peracute death	24	2.085 \pm 0.057	F
55 μ g/kg	75 μ g/kg	peracute death	15	2.151 \pm 0.054	G

*Means with different letters are significantly different ($p \leq .05$) from each other.

The Bartlett Test for homogeneity of group variances did not detect significant differences ($p = .054$).

--Mice died following Day 0 treatment.

Table 3. Means and standard deviations of the natural logs of kidney weight (percent bw) in 6-week-old male Swiss Webster mice. They are grouped according to response (RES).

Response	N	Natural Log Kidney Weight Mean \pm SD	SNK *
Survivors	9	0.178 \pm 0.101	A
Vehicle control	17	0.187 \pm 0.081	A
Subacute death	8	0.248 \pm 0.102	A
Acute death	11	0.339 \pm 0.080	B
Peracute death	67	0.372 \pm 0.084	B

*Means with different letters are significantly different ($p \leq .05$) from each other by the SNK test.

The Bartlett Test for homogeneity of group variances did not detect significant differences.

Table 4. Means and standard deviations of the natural logs of survival time in minutes and the rank of survival time for the 86 mice which died following MCVST-A administration in 6-week-old male Swiss Webster mice. They are grouped according to treatment (TRT).

Day 0 TRT	Day 3 TRT	N	Rank of Survival Time Mean \pm SD	SNK *	Natural Log of Survival Time Mean \pm SD
no trt	75 μ g/kg	24	21.9 \pm 16.2	A	4.919 \pm 0.185
vehicle	75 μ g/kg	21	31.8 \pm 19.2	A	5.198 \pm 0.655
55 μ g/kg	--	11	48.5 \pm 21.2	B	5.415 \pm 0.702
55 μ g/kg	75 μ g/kg	30	71.5 \pm 17.3	C	6.501 \pm 1.293

*Rank of survival time means with different letters are significantly different ($p \leq .05$) from each other by the SNK test.

The Bartlett Test for homogeneity of group variances of rank of survival time did not detect significant differences. No comparison between groups based on natural log of survival time in minutes was performed since the Bartlett Test for homogeneity of group variances was significant ($p < .001$).

--Mice died following Day 0 treatment.

Table 5. Number and percentage of 6-week-old male Swiss Webster mice surviving a LD₁₀₀ min of MCYST-A. These mice are grouped according to treatment (TRT).

Day 0 TRT	Day 3 TRT	N	# Surv	% Surv	*	95% Confidence Interval (CPB)
55 µg/kg	75 µg/kg	37	7	18.9	A	7.96 to 35.16%
vehicle	75 µg/kg	23	2	8.7	A,B	1.07 to 28.04%
no trt	75 µg/kg	24	0	0.0	B	0.00 to 14.25%

*Percent survivors with different letters are significantly different (outside the 95% confidence interval of the CPB) from each other.

Table 6. Means and standard deviations for the LLIVWT and LKIDWT for the 18 preliminary study mice surviving various i.p. doses of MCYST-A for 10 to 12 days.

Dose	Survival Time	N	LLIVWT Mean \pm SD	LKIDWT Mean \pm SD
35 μ g/kg	12 days	1	1.452	0.392
50 μ g/kg	10 to 12 days	8	1.542 \pm .030	0.299 \pm .065
55 μ g/kg	10 to 11 days	3	1.568 \pm .056	0.276 \pm .064
60 μ g/kg	10 days	4	1.586 \pm .054	0.260 \pm .017
65 μ g/kg	10 days	2	1.637 \pm .080	0.255 \pm .000
35 to 65 μ g/kg	10 to 12 days	18	1.562 \pm .057	0.287 \pm .058

XIV. INHIBITION OF BRAIN CHOLINESTERASE AND REVERSIBILITY
OF PLASMA, RED BLOOD CELL, AND DIAPHRAGM CHOLINESTERASE
IN MICE AFTER INJECTION OF ANATOXIN-A(S) COMPARED
TO CARBAMATE AND ORGANOPHOSPHORUS AGENTS

W. O. Cook

INTRODUCTION

Physiologically distinct neurotoxins isolated from strains of the freshwater cyanobacterium Anabaena flos-aquae from Canada have been termed "anatoxins (antx)-a, -b, -d, -a(s), and -b(s)" (1). These toxins were distinguished from one another based on opisthotonus, salivation, and survival time in exposed mice, rats, and chickens. Antx-a(s) and -b(s) caused clinical signs similar to antx-a and antx-b, but also stimulated excessive salivation as indicated by the "s". Production is somewhat strain specific; Anabaena flos-aquae NRC 44-1 produces antx-a, whereas Anabaena flos-aquae NRC 525-17 produces antx-a(s) (2).

In mice and rats antx-a(s) produced signs of excessive nicotinic and muscarinic cholinergic stimulation (2). Mice pretreated with atropine sulfate and injected intraperitoneally (ip) with high doses of antx-a(s) survived longer and had no parasympathomimetic signs, but still died of respiratory arrest and convulsions suggesting that toxicity was due to more than just the muscarinic action of antx-a(s). Mahmood and Carmichael postulated that the mechanism of toxicity of antx-a(s) was cholinesterase (ChE) inhibition after demonstrating that antx-a(s) in vitro was an irreversible inhibitor of human red blood cell and electric eel (EC 3.1.1.7) ChE, and in vivo inhibited rat serum ChE activity (2,4). Because of its extremely polar character, as

evidenced by minimal migration even with very polar solvents on normal phase thin-layer silica chromatography plates (Dahlem and Beasley, personal communication, 1987), antx-a(s) would be expected to cross the blood-brain barrier poorly.

The purpose of this study was to examine the in vivo reversibility of plasma, red blood cell (RBC), and diaphragm ChE-induced inhibition due to antx-a(s) in mice. To aid in interpretation, antx-a(s) was compared to the reversible, peripheral-acting carbamate, pyridostigmine bromide, and to the central and peripheral-acting, irreversible organophosphorus compound, paraoxon. The preliminary study which helped to enable this work is presented on pages 34-35 of the 1986 Annual Report.

MATERIALS AND METHODS

Male, 25g to 35g, Balb/c mice (Sprague Dawley, Indianapolis, IN) were housed in air-conditioned quarters on a 10/14 hour dark/light cycle and were provided food (Rodent Blox, Wayne Research Animal Diet, Bemis Co., Inc., Peoria, IL) and water ad libitum.

Mice were injected ip with semipurified antx-a(s), pyridostigmine bromide (Regonol, Organon Inc., West Orange, NJ), paraoxon (Sigma Chemical Co., St. Louis, MO), or a control solution of distilled deionized water containing 1% ethanol. Distilled deionized water was used in diluting all toxicants for dosing. Antx-a(s) was produced by the method of Mahmood and Carmichael (5); stored at -20°C prior to use; and brought into solution for dosing with ethanol such that the final dosing solution contained less than 1% ethanol. Antx-a(s) produced by this method was only semipure. Paraoxon, stored at a concentration of less than 10 mM in dry acetone at -20°C prior to use, contained less than 1% acetone in the final dosing solution. The control

solution was administered at a volume/body weight equal to that used for antx-a(s), which was the maximum volume utilized for the toxicants.

To evaluate in vivo reversibility, mice were injected ip with a control solution or predetermined LD₄₀ doses of: antx-a(s), pyridostigmine bromide, and paraoxon. Mice were killed by decapitation at 0, 5, 15, 30, 60, or 240 minutes, or 1, 2, or 8 days postdosing, and whole blood was collected in polypropylene centrifuge tubes containing 20 µl of sodium heparin. Diaphragms of mice that were killed or died were excised, blotted, and frozen at -80°C.

Mice were observed for clinical signs at 0, 5, 10, 15, 30, 60, 120, 180, 240, 480, 1,440 (1 day) minutes and daily thereafter for 7 days. Salivation, diarrhea, and lacrimation were scored on a scale of 1 to 4 (1 = normal, 4 = severely increased), and dyspnea, tremors, and fasciculations were recorded as present or absent. The duration of a clinical sign of toxicosis was recorded as the mean of the times of the final observation of the abnormality and the subsequent observation. Time of death was recorded to the nearest minute. Brain, diaphragm, spleen, gastrointestinal tract, pancreas, heart, sciatic nerve, liver, lung, and kidney tissue were fixed in 10% neutral-buffered formalin, sectioned at 6 microns, and stained with hematoxylin and eosin for histologic examination.

Tissue was ground in Broeck Tissue Grinders (Fisher Co., Itasca, IL) with 20 ml of pH 8 phosphate buffer containing 1% octyl phenoxy polyethoxyethanol (Triton X-100, Sigma Chemical Co., St. Louis, MO); the product centrifuged at 347.6 relative centrifugal force (RCF) for 10 minutes; and 200 µl of the supernatant added to cuvettes containing 2.5 ml of pH 8 phosphate buffer.

Plasma and RBC were separated from whole blood by centrifugation at 547.4 RCF for 5 minutes and assayed for ChE by the Ellman method (6). Ten µl plasma

samples were diluted to 10 ml with pH 8 phosphate buffer and 3 ml aliquots added to cuvettes for assay. Fifty μ l of 0.01 M dithionitrobenzoic acid (DTNB) and 20 μ l of 0.075 M acetylthiocholine iodide (ACTI) were added to the cuvettes and absorption was measured for 4 minutes at 412 nm on a Perkin Elmer Lambda 3 UV/VIS Spectrophotometer (Perkin Elmer, Norwalk, CT). Fifty μ l of RBC were lysed with 0.95 ml of 5% octyl phenoxy polyethoxyethanol (Triton X-100, Sigma Chemical Co., St. Louis, MO); 100 μ l of the lysate was diluted to 10 ml with pH 8 phosphate buffer; and 3 ml was analyzed with DTNB and ACTI as above. Diaphragm tissue was homogenized with 0.05 ml of pH 8 phosphate buffer per mg of tissue in a Broeck Tissue Grinder (Fisher Co., Itasca, IL); the homogenate was centrifuged at 67 RCF for 10 minutes; and 100 μ l of supernatant was added to 2.5 ml of pH 8 phosphate buffer for analysis with DTNB and ACTI as above.

The LD₄₀ doses of toxicants were calculated using SAS probit analysis (SAS Institute, Inc., Cary, NC). Comparisons of plasma, RBC, brain, and diaphragm ChE activities between the various toxicant-treated groups and control group of mice were performed using the SAS (SAS Institute Inc., Cary, NC) General Linear Model combined with Tukey's Test. A level of $\alpha = 0.05$ was used to identify significant effects.

To compare the overall persistence of functional abnormalities caused by the various toxicants, the clinical sign data, examined at each time point, was transformed to + (at least 1 abnormality present) or - (no observed abnormalities) before analysis. For survival data and duration of clinical signs, comparisons among the various groups were performed using the SAS Lifetest method and Wilcoxon Test.

RESULTS

The results of plasma, RBC, and diaphragm ChE assays in control and toxicant-dosed (at the LD₄₀) mice are presented in Figure 1. In mice that died from antx-a(s) toxicosis, diaphragm ChE activity was significantly inhibited compared to controls; but the degree of inhibition induced by a lethal dose of antx-a(s) was less than in mice that died after administration of paraoxon or pyridostigmine (Table 1). At the LD₄₀, the survival time of mice injected with antx-a(s) was significantly longer than with mice injected with pyridostigmine or paraoxon ($p = 0.0001$ and 0.0004 , respectively). Mean survival time (first 24 hours) for antx-a(s), paraoxon, and pyridostigmine were 93, 11, and 15 minutes, respectively. In this study, the muscarinic effects (lacrimation, diarrhea, and salivation caused by antx-a(s) appeared at least as severe as those caused by paraoxon and pyridostigmine (Figure 3). The nicotinic effects (fasciculations and tremors) of antx-a(s) appeared less severe. Results of the comparisons of duration of clinical signs between mice injected ip with antx-a(s), paraoxon, and pyridostigmine are presented in Table 2. In general, maximum clinical effects in mice injected with antx-a(s) occurred at least 60 minutes after dosing, which was later than observed with other toxicants. Mice that died from antx-a(s) toxicosis became dyspneic, cyanotic, and had clonic, rolling seizures at death. Dilated small and large intestines were occasionally observed at necropsy in mice that died after injection of toxicants. Histologic examination of tissues from control and toxicant-dosed mice did not reveal any lesions.

DISCUSSION

ChE enzymes in various sites differ in structure and susceptibility to different inhibitors. Due to differences in chemical structure, various

Inhibitors can have widely different intrinsic activities on isolated enzymes. Other factors such as tissue (blood-brain, membrane, dermal, etc.) barriers, limit the access of inhibitors to sites of action to varying degrees. The rate and extent of absorption, metabolism, distribution, susceptibility of various enzymes to inhibition and the intrinsic activity of the inhibitor govern both the toxicity and the spectrum of toxic effects. It is necessary to determine the nature of toxin-induced inhibition at various sites in order to understand the physiologic alterations causing significant dysfunction and death.

Cyanosis, dyspnea, and the clonic nature of seizures in mice injected with antx-a(s) were consistent with ChE inhibition and associated acetylcholine stimulation at peripheral-muscarinic and nicotinic cholinergic receptors that resulted in terminal hypoxia and respiratory failure.

Mice that died from antx-a(s) toxicosis did so later than mice dosed with the other toxicants. The later onset of death in mice from antx-a(s), as compared to the much more lipophilic toxicant paraoxon, may be a result of the comparatively slow absorption or distribution of this polar algal toxin, such that it could not reach critical sites of action as readily; but it probably does not reflect a delay needed for bioactivation in view of previous studies indicating a direct effect of antx-a(s) on ChE in vitro (3).

In these studies, effects on mice injected with antx-a(s) lasted longer than those in mice given the long-acting reversible carbamate, pyridostigmine, and persisted for a time similar to those induced by the irreversible ChE inhibitor, paraoxon. The in vivo persistence of clinical signs with antx-a(s) is consistent with the irreversible inhibition of ChE activity observed in vitro. Similarly, antx-a(s) inhibited ChE in plasma, RBC, and diaphragm

tissue for a longer period of time than pyridostigmine bromide, with a duration of action similar to that of paraoxon. The red blood cell ChE enzyme appeared the most susceptible of those analyzed to persistent in vivo inhibition by antx-a(s). Despite the fact that paraoxon behaves as an irreversible inhibitor of ChE in vitro, the in vivo, mean persistence of inhibition of erythrocyte ChE induced by this organophosphorus compound was less than with antx-a(s), although the difference was not statistically significant. Similarly, Mahmood et al. (3) found that in vitro antx-a(s) bound to red blood cell ChE more tightly than another organophosphorus agent, diisopropylfluorophosphate (DFP).

Animals that die from toxicosis induced by ChE inhibitors may succumb to muscarinic, nicotinic, central nervous system, or combined effects. The prolongation of survival in antx-a(s)-dosed mice as a result of treatment with atropine (2) suggested that nicotinic effects may have become more important in the lethal syndrome when the muscarinic receptors were blocked. In the present study, muscarinic signs were more severe in antx-a(s)-dosed animals than in those given the other anticholinesterase compounds, while inhibition of diaphragm ChE and nicotinic signs were less severe. Also, diaphragm ChE activities were similar in mice that survived antx-a(s) administration (up to 1 day postdosing) and those that died after being given the toxin. Thus, the present study indicates that the peripheral nicotinic effect due to ChE inhibition in antx-a(s) toxicosis may be less important than the associated muscarinic effects at the time of death, as compared to the results with either pyridostigmine or paraoxon.

REFERENCES

1. Carmichael, W. W., and Gorham, P. R.: Anatoxins from clones of Anabaena flos-aquae isolated from lakes of western Canada. Mit. Internat. Verein. Limnol. 21:285-295, 1978.
2. Mahmood, N. A., and Carmichael W. W.: The pharmacology of anatoxin-a(s), a neurotoxin produced by the freshwater cyanobacteria Anabaena flos-aquae NRC 525-17. Toxicon 24(5):434-454, 1986.
3. Mahmood, N. A., Carmichael, W. W., and Hyde, E. G.: Kinetic analysis of the inhibition of acetylcholinesterase (E.C. 3.1.17) by anatoxin-a(s). Part 1. Conference on Natural Toxins from Aquatic and Marine Environments, Woods Hole, Massachusetts, August 27-30, 1987. (Abstract)
4. Mahmood, N. A., and Carmichael, W. W.: Anatoxin-a(s), an irreversible anticholinesterase from blue-green Anabaena flos-aquae NRC 525-17. Toxicon, in press, 1987.
5. Carmichael, W. W., and Mahmood, N. A.: Toxins from freshwater cyanobacteria. In Ragelis, E. (Ed.), Seafood Toxins. ACS Symposium Series 262, ACS Publications, Washington, D.C., 377-389, 1984.
6. Ellman, G. L., Courtney, K. D., Andres, V., and Featherstone, R. M.: A new and rapid colorimetric determination of acetylcholinesterase activity. Biochem. Pharmacol. 7:88-95, 1961.

Table 1. Comparison of diaphragm cholinesterase activities of control mice and mice that died after ip injection of LD₄₀ doses of anatoxin-a(s), paraoxon, and pyridostigmine.

Diaphragm Acetylcholinesterase Activity*		
Toxicant	(μ M/g/Min)	Tukey's Grouping ⁺
Control	1.12 \pm 0.28	A
Anatoxin-a(s)	0.73 \pm 0.14	B
Pyridostigmine	0.29 \pm 0.26	C
Paraoxon	0.03 \pm 0.08	C

*Values are expressed as mean \pm SD.

⁺Cholinesterase means with the same letter are not significantly different (p < 0.05).

Table 2. Comparison of duration of clinical signs between mice injected ip with an LD₄₀ dose of anatoxin-a(s) (A), paraoxon (P), or pyridostigmine (Y).

	A vs P	A vs Y	P vs Y
Salivation	0.0033 (A)*	0.0001 (A)	0.6990
Diarrhea	0.1854	0.0005 (A)	0.0003 (P)
Lacrimation	0.0093 (P)	0.0001 (A)	0.0001 (P)
Respiratory Difficulty	0.0734	0.0001 (A)	0.0001 (P)
Tremors	0.0094 (P)	0.3715	0.0001 (P)
Fasciculations	0.0001 (P)	0.0812	0.0001 (P)
All Signs	0.0295 (P)	0.0001 (A)	0.0001 (P)

*Letters in parentheses indicate the toxicant that caused the greater duration of the clinical sign.

Figure 1A. Plasma cholinesterase activities of control mice (●) and mice given an LD₄₀ dose of anatoxin-a(s) (○), paraoxon (▲), or pyridostigmine (△), by ip administration. Letters indicate results of Tukey's tests between toxicants at individual time points with different letters indicating significant differences ($p < 0.05$) between means of toxicants.

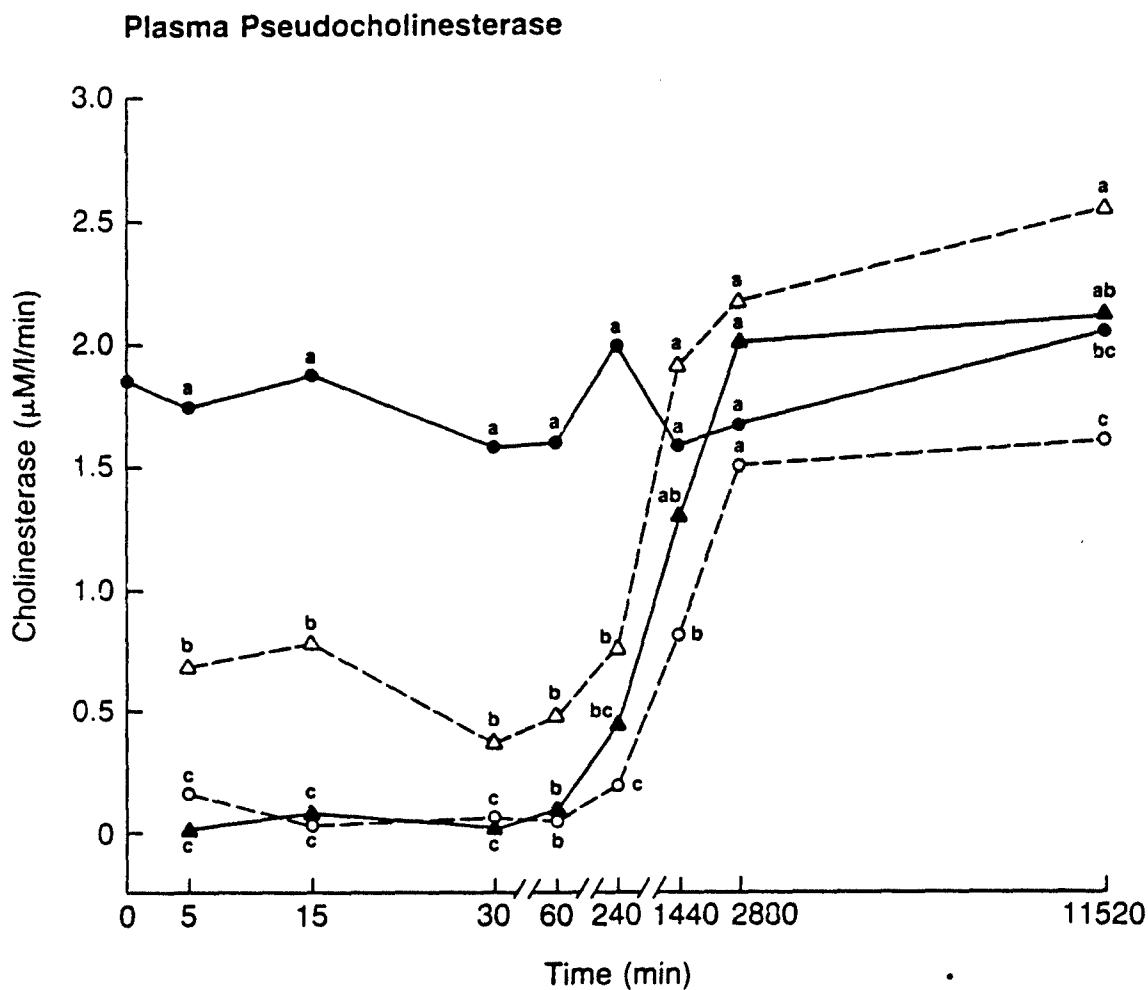


Figure 1B. Red blood cell cholinesterase activities of control mice (●) and mice give an LD₄₀ dose of anatoxin-a(s) (○), paraoxon (▲), or pyridostigmine (△), by ip administration. Letters indicate results of Tukey's tests between toxicants at individual time points with different letters indicating significant differences ($p < 0.05$) between means of toxicants.

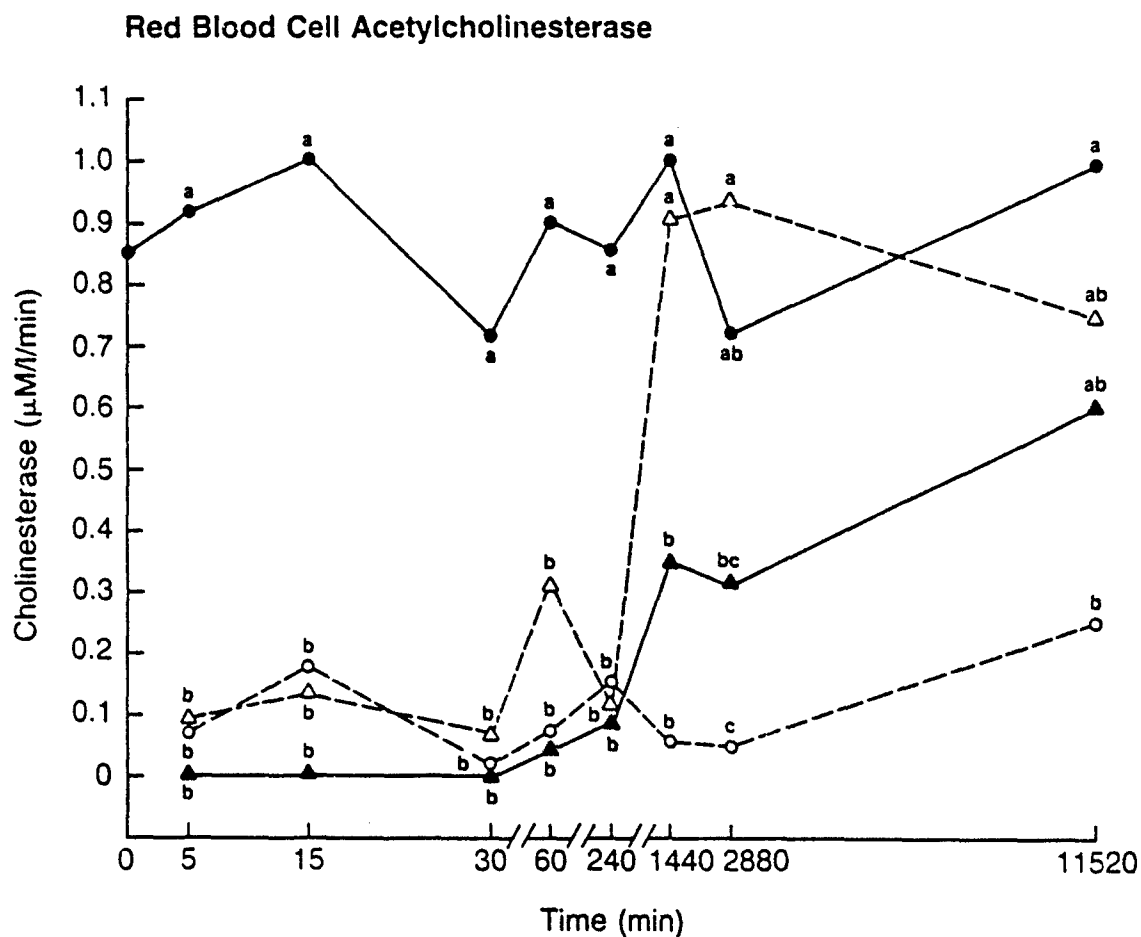


Figure 1C. Diaphragm cholinesterase activities of control mice (●) and mice given an LD₄₀ dose of anatoxin-a(s) (○), paraoxon (▲), or pyridostigmine (△), by ip administration. Letters indicate results of Tukey's tests between toxicants at individual time points with different letters indicating significant differences ($p < 0.05$) between means of toxicants.

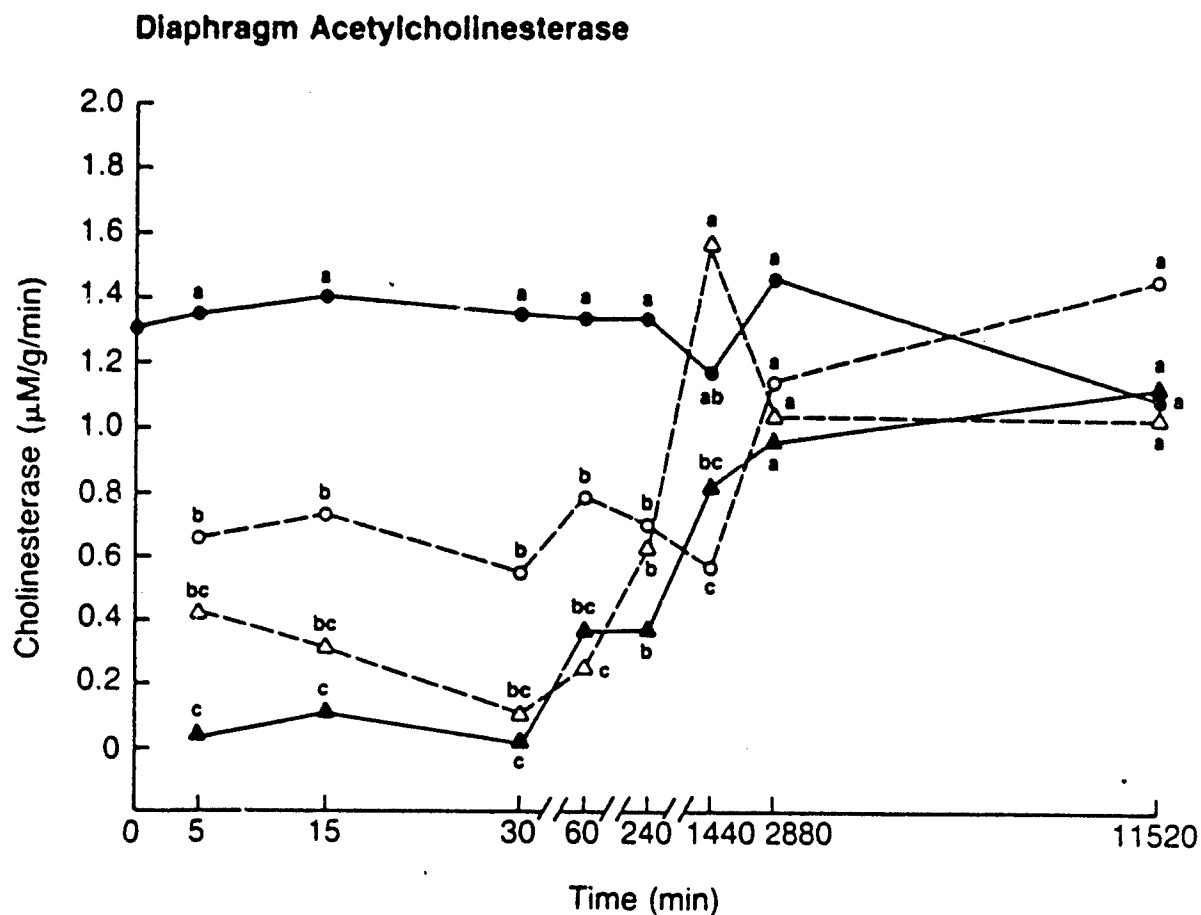
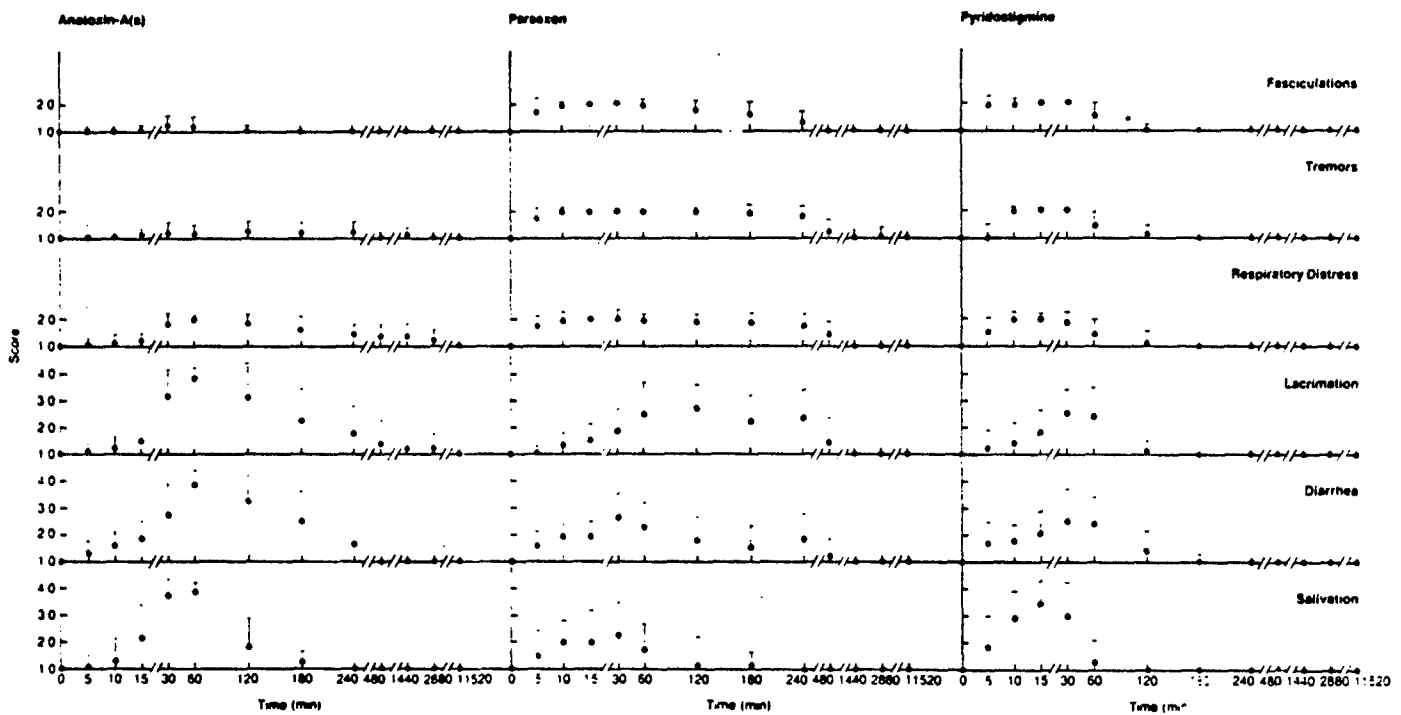


Figure 2. Means (\pm SD) for clinical signs (salivation, diarrhea, and lacrimation) graded 1 to 4; tremors and fasciculations graded 1 to 2 (absent or present) of mice given an LD₄₀ dose of anatoxin-a(s), paraoxon, or pyridostigmine by ip administration.



XV. NEUROBEHAVIORAL EFFECTS OF NICOTINE, ATROPINE,
PARAOXON, AND PHYSOSTIGMINE ON LONG-EVANS RATS

W. O. Cook, J. A. Dellinger, S. S. Singh

INTRODUCTION

Calibration of neurobehavioral equipment was performed this year. In this calibration, 24 Long-Evans Sprague-Dawley rats were tested for behavioral effects resulting from intraperitoneal (ip) injections of atropine sulfate, nicotine, paraoxon, or physostigmine salicylate. Neurobehavior was assessed using figure 8 maze activity (F8) (Photobeam Activity System, San Diego Instrument, San Diego, CA) (counts/5 min), accelerating rotarod performance (AR) (Omni Rotor RR, Omnitech Electronics, Inc., Columbus, OH) (sec on rod), grip strength (GS) (kg), and startle response (SR) (San Diego Instruments, San Diego, CA) (amplitude voltages and latency in msec).

MATERIALS AND METHODS

In the first experiment to determine the dose response relationships from ip injections of atropine sulfate (Med-Tech, Inc., Elwood, KS), nicotine free base (Sigma Chemical, St., Louis, MO), and physostigmine salicylate (Forest Pharmaceutical, St. Louis, MO) on F8, AR, GS, and SR, 48 male, 400 to 600 g, Sprague-Dawley Long Evans rats were housed on a 12/12 hour light/dark cycle and provided food (Lab-Blox, Wayne Research Animal Diet, Bemis Co., Peoria, IL) and water ad libitum. Forty-eight rats were randomly divided into 2 groups. Group 1 was used for Figure 8 Maze. Group 2 was trained to run on the AR and then used for GS, AR, and SR testing. The rats were used in a 4 x 4 Latin square design with 4 animals each being given 1 of 3 treatment levels of 1 drug or the vehicle (control). The Latin square for each drug was then

repeated after a period of 3 weeks with each animal receiving a different drug than in the first 4 x 4 session. The results were then averaged over the 8 rats that received each drug. One week was allowed between injections and 1 month between drugs. The treatment levels were: 0, 25, 50, and 100 mg of atropine sulfate; 0, 75, 150, and 300 µg of nicotine; and 0, 75, 150, and 300 µg of physostigmine salicylate per kg of body weight. Sterile 0.9% saline was used in diluting all toxicants for dosing. Atropine sulfate was administered 10 to 15 minutes prior to testing, physostigmine 5 to 10 minutes prior to testing, and nicotine 0 to 5 minutes prior to testing. SR, AR, and GS were tested twice over a 2-hour period, at 5 and 60, 10 and 65, and 25 and 80 minutes, respectively, after dosing and F8 activity was recorded for 1 hour postinjection for the other 24 rats.

Whole body startle was evaluated in terms of maximum amplitude (Vm), average amplitude (Vx), and response time (Rt). The animals were placed in the startle chambers and allowed to acclimate to the chambers and background noise for a period of 5 minutes before the start of the test. Then 6 of each type of stimulus were presented to each rat in a semi-random order with variable interstimulus interval (ISI) (between 5 to 10 seconds). The first trial for each stimulus type was disregarded. Four types of startle responses were evaluated: (1) acoustic startle response, the rats were subjected to a noise of 120 dB for a period of 20 msec; (2) tactile startle response, the rats were subjected to a puff of air (15 psi) for 20 msec; (3) prepulse inhibition 1, the rats were subjected to a brief low intensity acoustic stimuli (prepulse) of 100 dB for 5 msec shortly before (95 msec) a tactile stimulus for 20 msec; and (4) prepulse inhibition 2, similar to prepulse inhibition 1 with the exception that the ISI was decreased to 5 msec.

In a second experiment to determine the dose response relationship of paraoxon on F8, AR, GS, and SR, 24 male, 400 to 600 g, Sprague-Dawley Long-Evans rats were housed on a 12/12 hour light/dark cycle and provided food (Lab-Blox, Wayne Research Animal Diet, Bemis Co., Peoria, IL) and water ad libitum. Rats were dosed ip with either 200 or 400 µg of paraoxon (Sigma Chemical Co., St. Louis, MO)/kg body weight (BW), or a control solution with 8 animals per treatment group. Sterile saline (0.9%) was used in diluting paraoxon for dosing. Paraoxon was stored at a concentration of less than 10 mM in dry acetone at -20°C prior to use, and contained 1% or less acetone in the final dosing solution. Four rats were dosed each day at 11:00 am with each treatment represented at least once. Rats were pretested for AR performance, ranked by performance, and randomly assigned to 1 of the 3 treatment groups in a counter balance design. At 15 minutes postdosing, rats were placed in the F8 system and monitored for 60 minutes. Forelimb GS was measured on each rat postdosing at 80 minutes. AR performance for every rat was determined at 85 minutes postdosing. The AR challenge consisted of accelerating the rod to a speed of 80 revolutions per minute over 8 seconds and recording the length of time rats ran on the rod to the nearest 0.1 second. Startle response evaluation was performed for 20 minutes at 100 minutes postdosing.

At 120 minutes postdosing, under carbon dioxide gas anesthesia, the peritoneal cavity of each rat was surgically opened, 3 ml of blood was collected in a heparinized syringe from the caudal vena cava, and the rat killed by exsanguination. Each sample was centrifuged at 600 x g for 10 minutes, then plasma and erythrocytes (RBC) were separated for modified Ellman cholinesterase (ChE) assays (1). Brain aChE assays were performed by the

modified Ellman method with further modifications by Harlin and Ness (2). The RBC were resuspended in an equal volume of cold 0.9% isotonic sodium chloride and centrifuged at $600 \times g$ for 10 minutes. The supernatant was discarded and the wash repeated twice. To lyse fresh RBC, 0.1 ml of washed RBC were diluted in 1.9 ml of 5% octyl phenoxy polyethoxyethanol (Triton X-100, Sigma Chemical Co., St. Louis, MO) solution and a 0.1 ml aliquot of the lysed solution was diluted to 10 ml with 0.1 M phosphate buffer (pH 8.0). For plasma ChE, a 10 μ l sample was diluted to 10 ml with 0.1 M phosphate buffer (pH 8.0). The ChE assay used 3.0 ml of the phosphate buffer sample and 50 μ l of 0.01 M dithiobisnitrobenzoic acid to which 20 μ l of the substrate, 0.075 M acetylthiocholine iodide was added.

Each rat brain was hand macerated and 0.5 g homogenized (Biohomogenizer Model M 133/1281-0, Biospec Products, Inc., Bartlesville, OK) in 25 ml of 1% Triton X. Two hundred μ l of the homogenate was added to cuvettes containing 2.5 ml of pH 8 phosphate buffer containing 1% Triton X and analyzed for ChE activity as above. Absorbance on a Shimadzu 160 UV/VIS Spectrophotometer was read at 412 nm for 6 minutes and the results recorded as μ M/g/min for brain ChE activity. For RBC and plasma ChE activity, results were recorded as μ M/L/min. On every fourth sample a duplicate was run. Control samples were used as references for calculating the percentage of ChE inhibition in groups of treated rats.

STATISTICAL ANALYSIS

In the 2 experiments, comparisons of SR, F8, GS, AR, and ChE activity between groups of toxicant-treated rats and the control group were performed using the SAS (SAS Institute, Cary, NC) General Linear Model (GLM) with Tukey's Test at $\alpha = 0.05$ to determine significant differences. General linear models

were designed to include, where appropriate, animal, weight, treatment, trial type, and time.

RESULTS

AR performance was decreased by atropine, physostigmine, and nicotine with a recovery after 1 hour (Figure 1). GS was decreased by nicotine and atropine with a recovery after 1 hour (Figure 1).

Atropine reduced all SR response maximum amplitudes for all doses (Figure 2). The 150 µg dose of nicotine increased the prepulse 1 and tactile SR amplitudes. Similar to nicotine, the 150 µg dose of physostigmine increased the tactile SR amplitude. Similar to atropine and nicotine, the 300 µg dose of physostigmine reduced the audio SR amplitude.

Atropine reduced all average audio, prepulse 1, and tactile SR amplitudes. The 150 µg dose of nicotine increased the average audio, prepulse 1, and tactile SR amplitudes (Figure 3). The 150 µg dose of physostigmine increased the average prepulse 1 and tactile SR amplitudes similar to nicotine. The 300 µg dose of physostigmine decreased the average audio SR amplitude similar to atropine.

Atropine reduced both audio and tactile response time (RT) (Figure 4). Nicotine did not affect audio RT but increased tactile RT. Physostigmine resulted in decreased audio RT (similar to atropine) and increased tactile RT (similar to nicotine).

The 150 µg dose of nicotine and the 50 µg dose of atropine increased F8 activity (Figure 5). All doses of physostigmine decreased F8 activity.

ChE results of paraoxon-treated and control rats are presented in Figure 6. Brain ChE was inhibited 57% and 19% with 400 µg/kg and 200 µg/kg paraoxon, respectively. No significant differences were detected in GS or AR

performance between the 2 paraoxon-dosed and control groups of rats (Figure 6). Audio and tactile SR amplitudes were increased with 200 µg/kg of paraoxon and decreased with 400 µg/kg of paraoxon with a statistical difference ($p < 0.05$) detected between the doses of paraoxon, but not between the paraoxon doses and the control. Initial F8 exploratory activity and activity during the remainder of the 60 minute F8 session were decreased in paraoxon treated rats in a dose-related fashion (Figure 6).

DISCUSSION

With atropine, nicotine, and physostigmine, the neurobehavioral screen detected decrements in dosed animals that were reversible in nature. Physostigmine and nicotine caused decrements in exploratory activity in the Figure 8 Maze that were indicative of centrally acting toxicants. This finding may be attributable to the fact that both have direct and/or indirect effects at nicotinic sites. Overall, paraoxon affected the sensory and exploratory behavior paradigms, but did not affect neuromuscular or balancing performance at these treatment levels.

To enable future assessment of learning and memory associated with visual and tactile stimuli after exposure to neurotoxins, the neurobehavioral startle equipment has been equipped with potentiated startle. Toxicants with known central and/or peripheral sites of action and known effects on the nervous system can be used in evaluating neurobehavioral decrements and mechanisms of action of algal neurotoxins. Subsequent studies will help to identify the nature of threshold effects and define the relationship between doses that cause clinical signs and those that cause neurobehavioral decrements that may not be detectable by simple observation.

The blue-green algae neurotoxin anatoxin-a(s) will be tested to ascertain if neurobehavioral decrements are produced that are similar to those observed with paraoxon. In addition, studies will be conducted to characterize central versus peripheral and rapidly versus slowly reversible effects on neurobehavioral criteria.

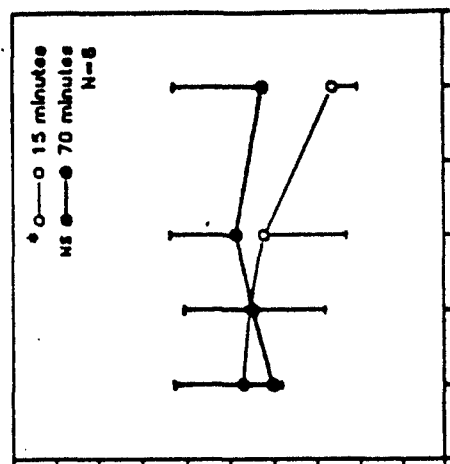
REFERENCES

1. Ellman, G. E., Courtney, K. D., Andres, V., and Featherston, R. M.: A new and rapid colorimetric determination of acetylcholinesterase activity. *Biochem. Pharmacol.* 7:88-95, 1961.
2. Harlin, K. S., and Ness, D.: Brain cholinesterase-normal enzyme activity levels in several large and small animal species. *Am. Assn. Vet. Lab. Diag.*, 29th Annual Proceedings, 457-469, 1986.

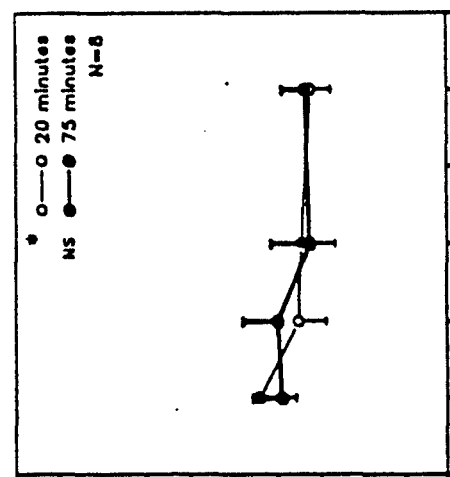
FIGURE LEGENDS

- Figure 1. Accelerod and hindlimb grip strength following nicotine, atropine, and physostigmine. (* = significant dose effects. ($F(3,14)$, $p < .05$; NS = not significant dose effects.) The numbers in parenthesis, that is 3 and 14, stand for the degrees of freedom for the dose and the error term used to calculate the F value in the statistical model.
- Figure 2. Maximum startle response amplitude following nicotine, atropine, and physostigmine. (* = significant dose effect. ($F(3,142)$, $p < .05$; NS = not significant dose effects.)
- Figure 3. Average startle amplitude following nicotine, atropine, and physostigmine. (* = significant dose effects. ($F(3,142)$, $p < .05$; NS = not significant dose effects.)
- Figure 4. Startle response time (RT) following nicotine, atropine, and physostigmine. (* = significant dose effects. ($F(3,142)$, $p < .05$; NS = not significant dose effects.)
- Figure 5. Figure 8 Maze activity following nicotine, atropine, and physostigmine. (* = significant dose effects. ($F(3,308)$, $p < .05$; NS = not significant dose effects.)
- Figure 6. Plasma, red blood cells (RBC), and brain cholinesterase activities, grip strength, accelerating rotarod performance, and figure 8 activity in Long-Evans rats dosed ip with a control solution, or 200 or 400 μ g of paraoxon/kg body weight and killed at 24 hours postdosing.

PHYSOSTIGMINE



ATROPINE



NICOTINE

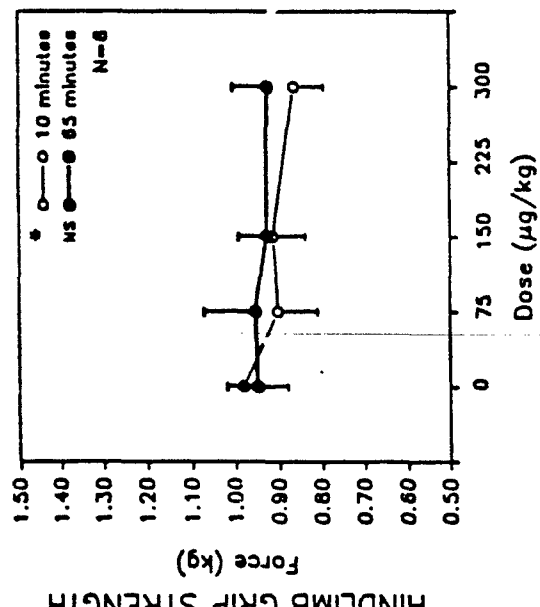
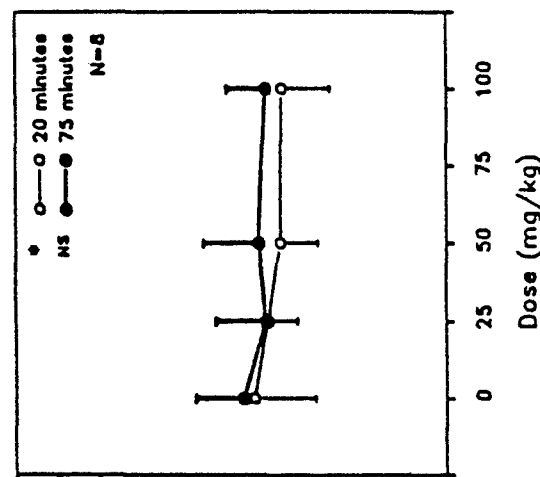
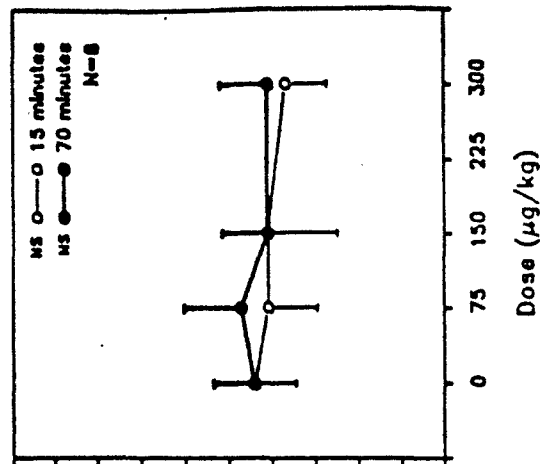
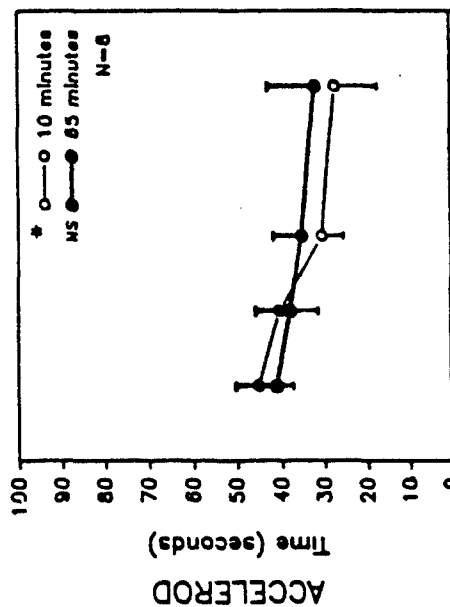


Figure 1
Section XV

GRAPH 2

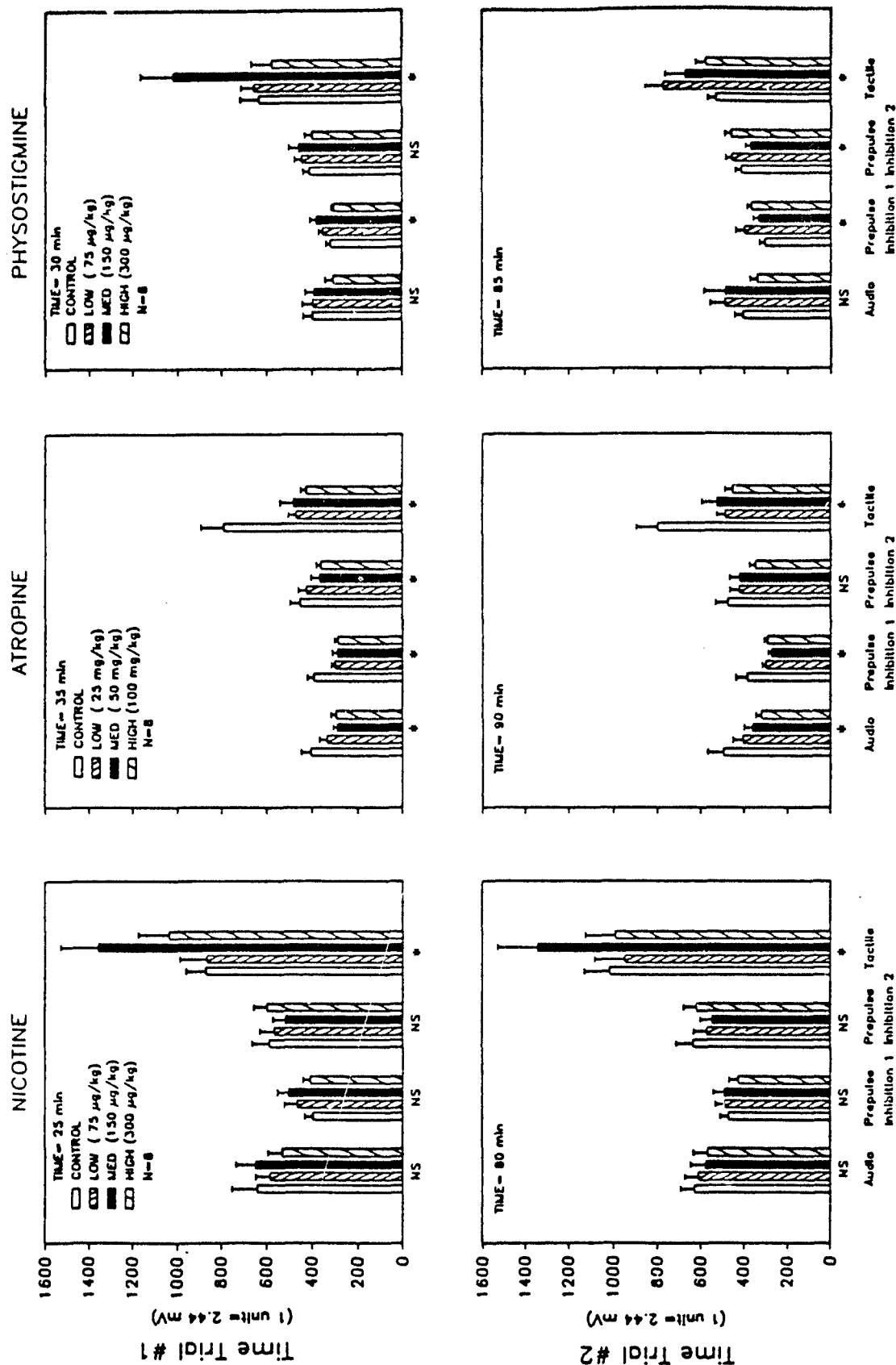


Figure 2

GRAPH 3

AVERAGE STARTLE AMPLITUDE

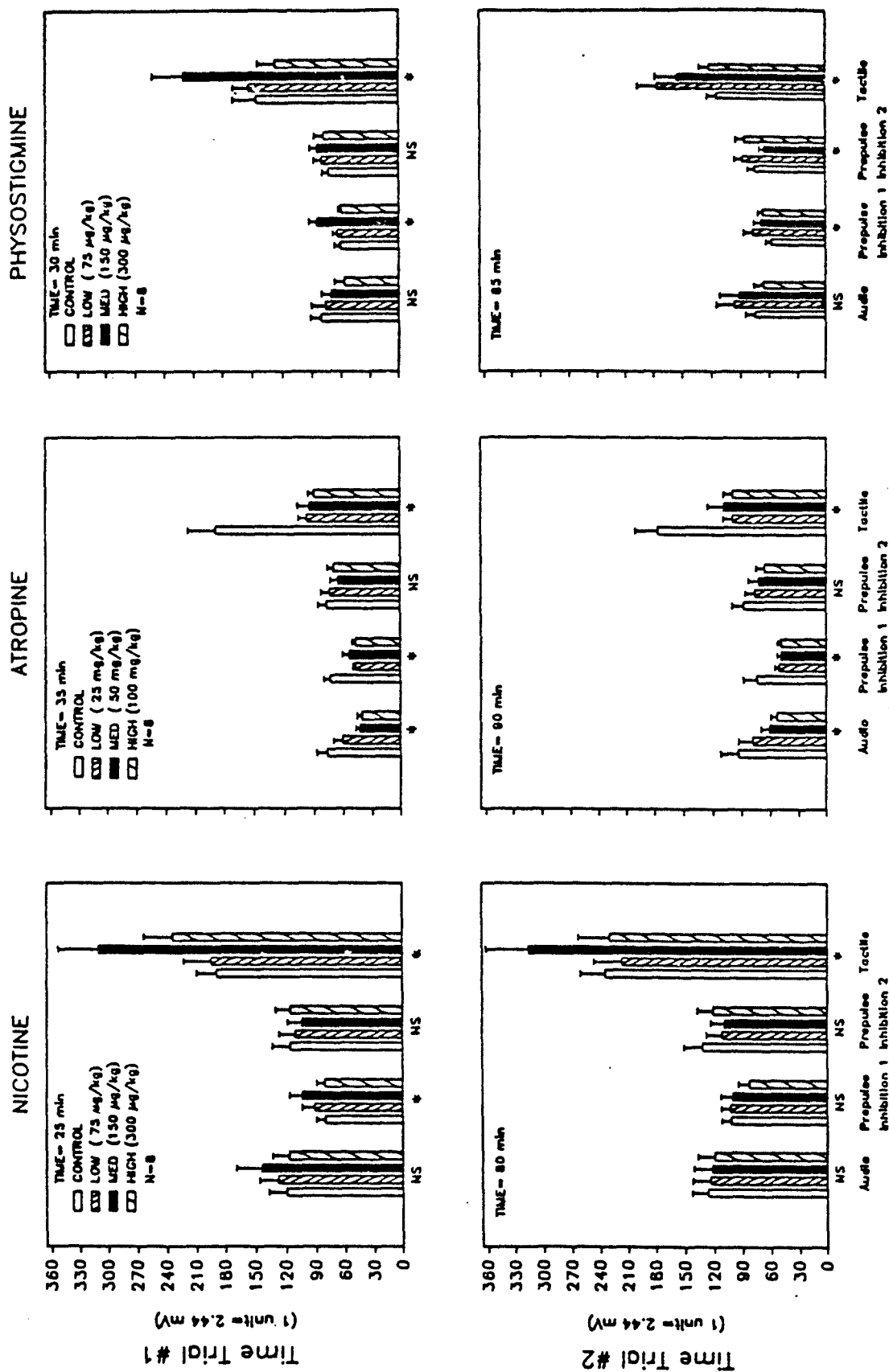


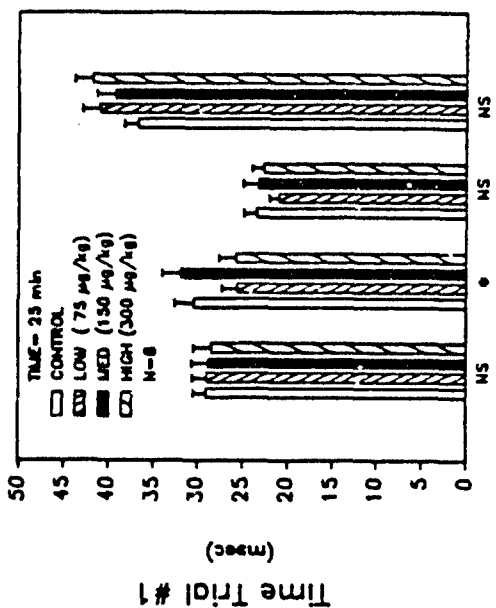
Figure 3

Section XV

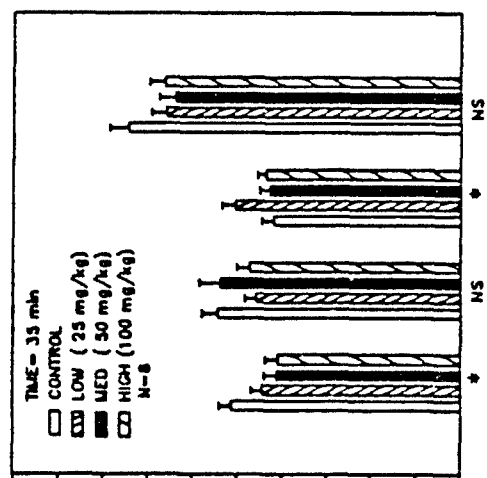
STARTLE RESPONSE TIME (RT)

GRAPH 4

NICOTINE



ATROPINE



PHYSOSTIGMINE

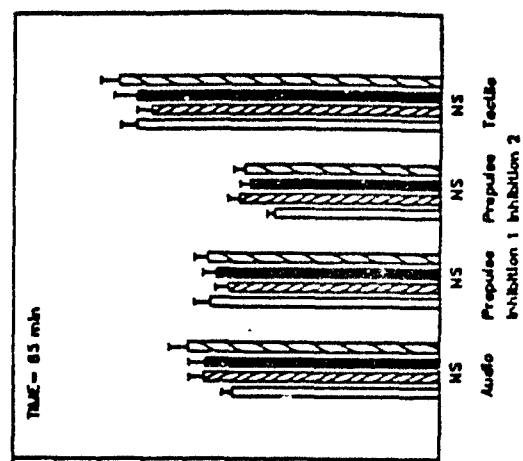
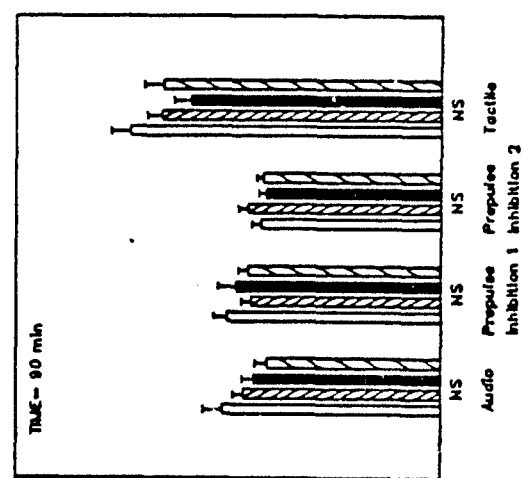
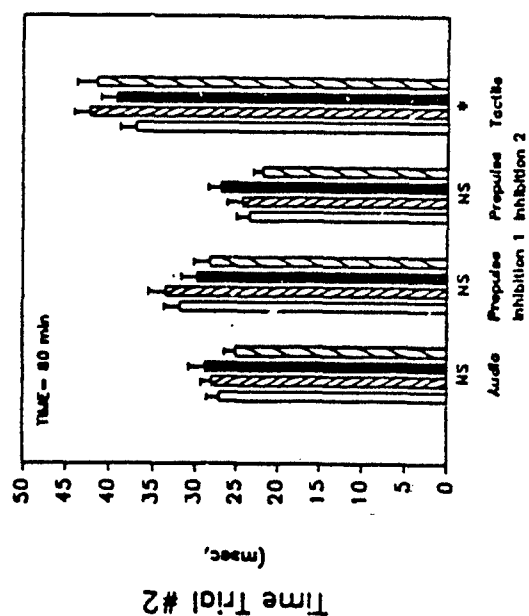
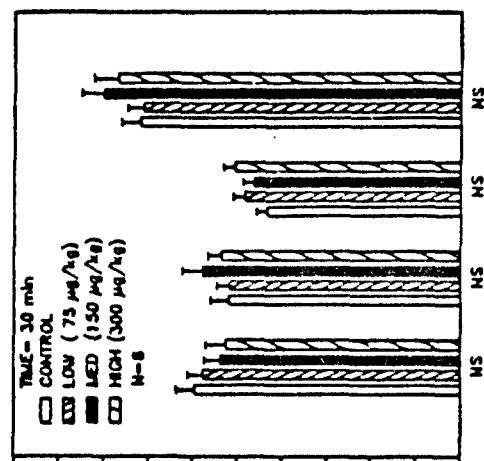


Figure 4

GRAPH 5

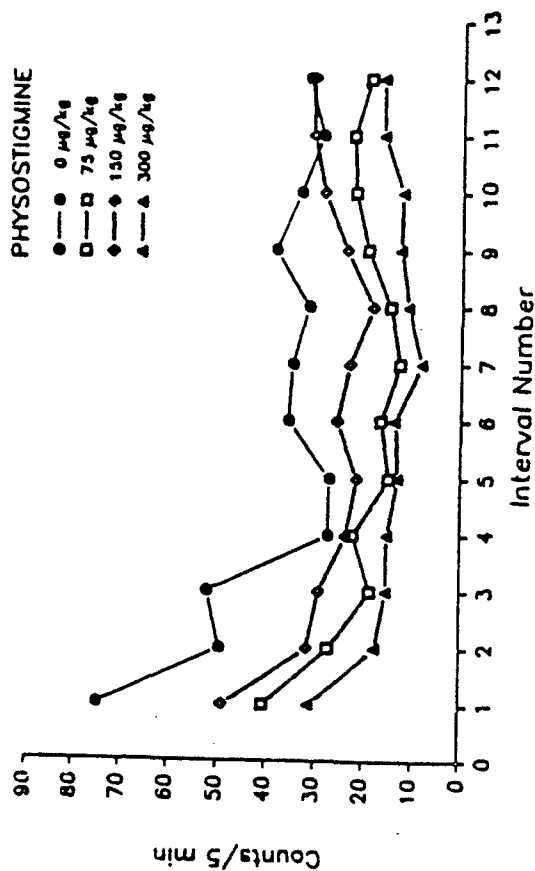
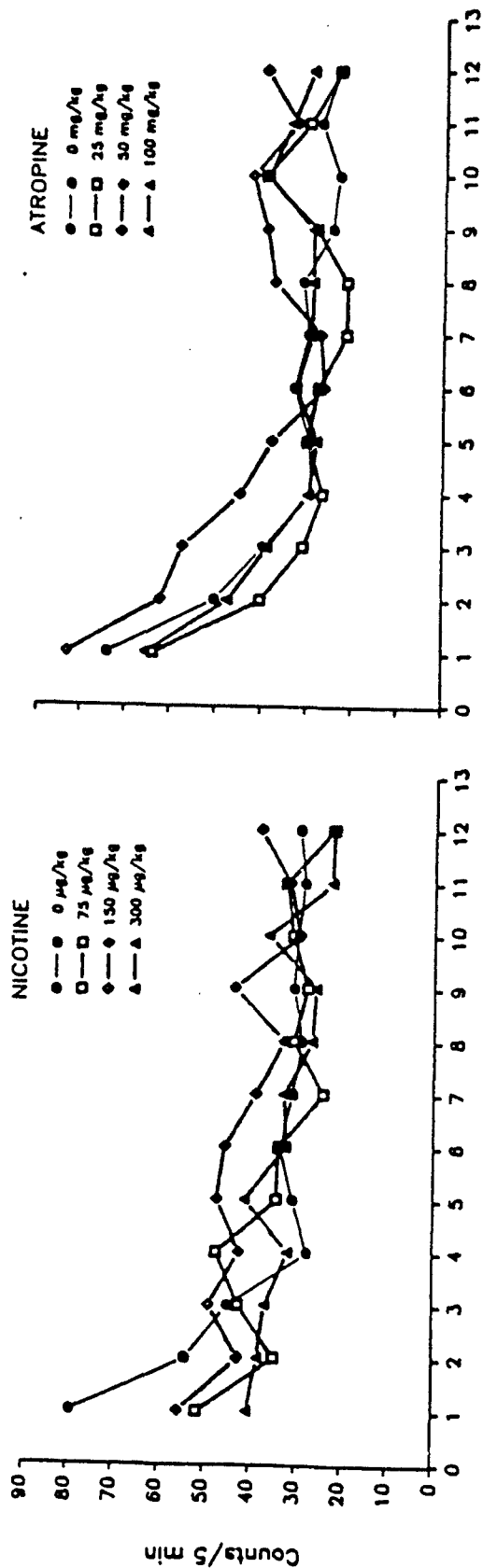


Figure 5
Section XV

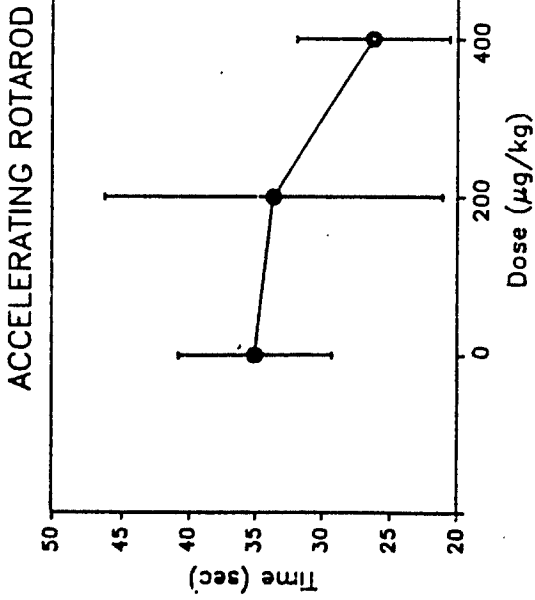
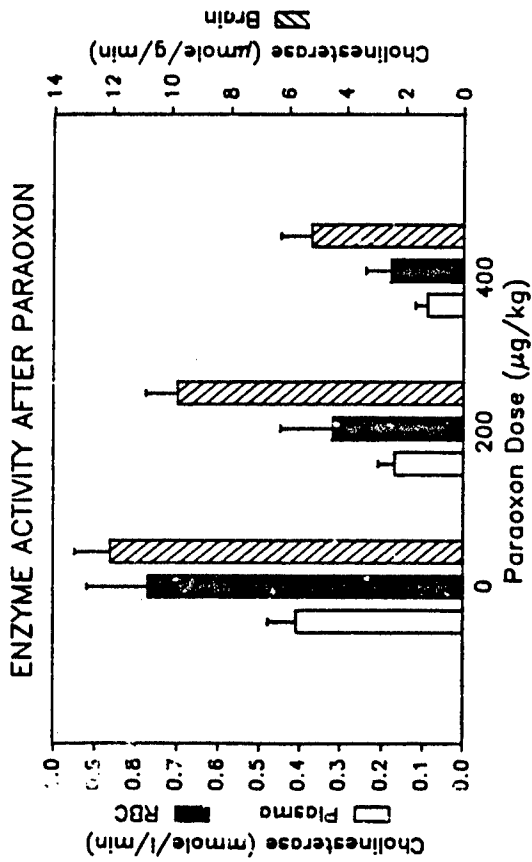
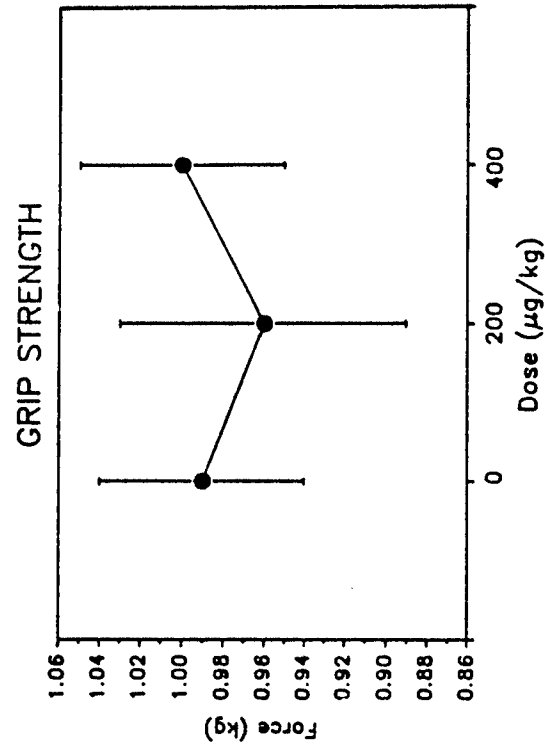


FIGURE 8 ACTIVITY

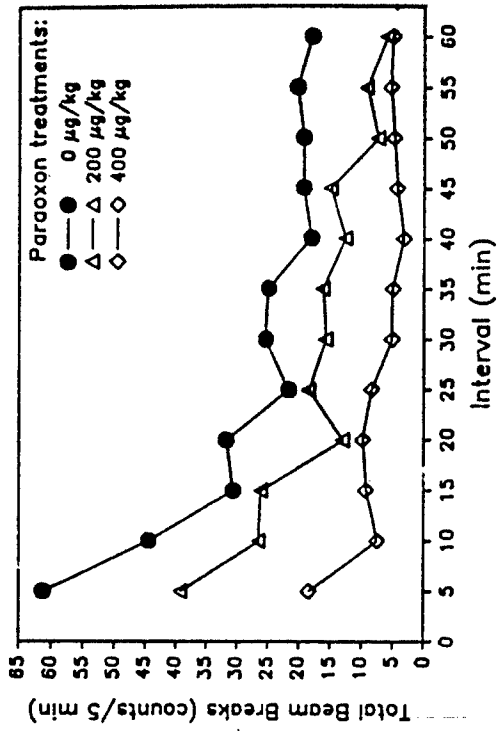


Figure 6

Section XV

XVI. ANATOXIN-A(S) PURIFICATION AND INHIBITION OF ELECTRIC EEL
AND HUMAN ERYTHROCYTE ACETYLCHOLINESTERASE

N. A. Mahmood and W. Carmichael

INTRODUCTION

The major effort spent since the last annual report involved the production of purified and semi-purified antx-a(s) for structural elucidation. The remaining portion of the time was spent on developing newer extraction techniques, modifying current purification procedures, and analyzing the kinetics of acetylcholinesterase inhibition. The development of a workable procedure is critical not only for ease of operation, but also for the production of antx-a(s) with a higher degree of purity. The previous method (see first annual report) was found to be time-consuming and did not result in adequate purification. Since then several extraction procedures have been assessed and these will be discussed together with the modified purification procedure.

In addition to toxin purification, the kinetics of inhibition of acetylcholinesterase from different sources was analyzed. The kinetic constants obtained were compared with the known irreversible anticholinesterase agent, diisopropyl-fluorophosphate (DFP).

PURIFICATION

Experiment

Before extraction, all lyophilized cells were tested for toxicity and found to have an LD₅₀ of 50 mg/kg or less (ip mouse).

A. Extraction Procedures:

Ethanol acidified with concentrated acetic acid (pH 4) was used for extraction in replacement of acidified water. The main advantage of using

acidified ethanol over water is that the extract is devoid of thick purplish pigments. Even though acidified ethanol extracted antx-a(s) efficiently from the lyophilized cells, it is not the solvent of choice for extracting large quantities of lyophilized cells (> 20 g). Since the main objective is to obtain milligram quantities of antx-a(s) from these cells, additional extraction solvents and purification procedures were tried. These included trifluoroacetic acid as an alternate extracting solvent and ion-exchangers for the preliminary purification step.

Trifluoroacetic acid (TFA) at 2 different concentrations, 0.05% and 1.0% were used to extract 20 g of lyophilized cells of Anabaena flos-aquae. Ten g of cells were stirred in each solvent (500 ml) for 24 hours; the extracts were then centrifuged at 10,000 rpm for 1.5 hours at 4°C. The supernatant was air dried. These fractions were not subjected to solid phase extraction on C 18 disposable columns as performed in the previous procedure. This was done to improve toxin recovery by eliminating an extra step in the purification method. Another deviation from the previous procedure was to use a strong cationic exchanger resin (Dowex AG 50 W-X8) instead of gel filtration (Sephadex G-15) as the first purification step.

For comparison, two 10 g batches of lyophilized cells were extracted using acidified ethanol. The extract was stirred for 24 hours, centrifuged at 10,000 rpm for 1.5 hours at 4°C, and air dried. These fractions were loaded on a disposable solid phase C 18 extraction column. These columns were prepared as described previously (see first annual report). Gel filtration was not used, instead the fractions were divided equally and purified on 2 different ion exchangers, Amberlite IRP 64, and the benzene sulfonic acid (SCX).

B. Chromatographic Separations:

The 3 cationic exchangers used were:

1. Strong cation exchanger Dowex AG 50 W-X8.
2. Weak cationic exchanger Amberlite IRP 64.
3. Strong cationic exchanger benzene sulfonic acid (SCX).

The Dowex AG 50 resin (hydrogen form) was first washed with 500 ml of 1 N hydrochloric acid and then loaded on a Pharmacia column (Bioprocess, 40 * 113 mm). The column was then rinsed with another 250 ml of 1 N hydrochloric acid and allowed to equilibrate overnight. The sample to be loaded on this column came from the TFA extractions which were loaded in a volume of approximately 50 ml. The column was first washed with 500 ml of 0.5 N ammonium hydroxide and the toxin was eluted with 500 ml of 1 N ammonium hydroxide. In order to stabilize the toxin, an equal volume of 1 N acetic acid was added to the eluant. The eluant was air dried and the toxicity determined using mouse bioassay.

The preparation of Amberlite IRP 64 was as follows: first the gel (10 g, hydrogen form) was rinsed with 0.5 N NaOH and decanted. This procedure was repeated several times. Then the gel was rinsed with 0.5 N HCl several times. Twenty ml of the gel was poured into a column (1.5 * 18 cm) and equilibrated with 150 ml of 0.5 N HCl. The sample loaded on the column was from the acidified ethanol extraction. After loading the sample, the column was first rinsed with 20 ml water followed by a linear gradient elution (0 to 0.5 M acetic acid). Seven ml fractions were collected using a fraction collector (Gilson 201). The toxic fractions were determined using mouse bioassay.

The last cationic exchanger that was tested was a prepacked solid phase benzene sulfonic acid extraction column (3 ml). The column was

first rinsed with 5 ml of acetonitrile followed with 15 ml of 1 M acetic acid. The sample from the acidified ethanol extraction was loaded, rinsed with 10 ml of water followed with 10 ml of 1 N NaOH. The eluant was collected directly in 15 ml of 1 M acetic acid solution. The eluant was air dried and the toxicity checked using mouse bioassay.

C. Analytical HPLC of Antx-a(s):

Once the toxicity of the above fractions had been determined, these fractions were separated on the HPLC using semi-preparative and/or analytical columns (cyanopropyl 1 * 250 mm and 4.6 * 150 mm). This time the elution was carried out isocratically (10 mM ammonium acetate/1 mM acetic acid [80/20], 1.5 ml/min) and the toxin detected at 230 nm. The peaks collected were checked for toxicity using mouse bioassay. The pooled toxic peak was rerun on a second analytical cyanopropyl column.

Ultraviolet wavelength scan was done on the isolated peak using a Cray 219 spectrophotometer. The estimated LD₅₀ (ip mouse) was also determined for 1 of the isolated single peaks.

RESULTS AND DISCUSSION

A comparison of the activities of the primary extracts from TFA and acidified ethanol (determined by mouse bioassay) indicated that the TFA extracts exhibited 50% less activity than the acidified ethanol extracts. The only advantage observed with the TFA extracts was the reduction in the extracted pigments compared to the acidified ethanol extracts.

The purifications on Dowex 50 and SCX resulted in higher salt content in the final samples. Since the next step in the purification involves HPLC, these samples were found to be unsuitable for further purification. It was also observed that the activities of these samples were less than the original samples before the ion exchange chromatography step.

On Amberlite IRP 64, antx-a(s) was eluted from the column when the acetic acid concentration approached 0.3 M. The toxin was completely eluted before the gradient reached 0.5 M acetic acid. The pooled fractions when purified further by analytical HPLC gave a clean separation (Figure 1). On the second run the collected toxic peak was found to be 80% pure (Figure 2). The single peak HPLC profile (Figure 3) of antx-a(s) indicates that repeated runs are necessary in order to achieve a pure toxin. It was also observed that the toxin retention time varies not only between different types of columns but also with the same column after repeated runs. This variation is more pronounced as the column ages.

To summarize, the modified procedure for antx-a(s) extraction and purification (Figure 4) differs from the original procedure slightly. Instead of gel filtration, ion-exchange chromatography was used in the separation step of the modified procedure. This procedure provides cleaner (less pigments) samples for HPLC runs. It was observed that it took 2 weeks to process 10 g of lyophilized cells and the average yield is 0.1 mg/10 g lyophilized cells.

The LD₅₀ of the isolated toxin was determined in mice intraperitoneally was found to be around 31 µg/kg (Table 1). An interesting observation was that, at doses of 25, 27.5, and 30 µg/kg which resulted in only muscarinic effects as clinical symptoms, all of these mice survived. At higher doses of 32.5 to 200 µg/kg, nicotinic signs, including fasciculations and respiratory distress, were observed and these animals died. This is in agreement with the studies reported previously (1) that atropine sulfate (muscarinic antagonist) did not prevent deaths in mice acutely dosed with antx-a(s). It appears that both muscarinic and nicotinic effects are present in lethally doses animals.

CHOLINESTERASE INHIBITION

Experiment

A. Secondary Plots

Antx-a(s) inhibition of electric eel and human erythrocyte acetylcholinesterase (EC 3.1.1.7) has been reported in the last annual. The "primary plots" showed first-order inhibition indicating an irreversible effect. Further analysis of the inhibitions was carried out using "secondary plots" to compare the equilibrium (K_d), phosphorylation (k_2), and inhibition constants (k_i).

The "secondary plots" were derived from the "primary plots." The slopes (reciprocal values) of the inhibited enzyme at different antx-a(s) concentrations obtained from "primary plots" were plotted against antx-a(s) concentrations (reciprocal values). The y-intercept gave $1/k_2$ and x-intercept gave $1/K_d$. A typical "secondary plot" for the inhibition of eel acetylcholinesterase is shown in Figure 6.

B. Kinetic Studies

All assays were carried out at room temperature, utilizing the method of Ellman et al. (2). The enzyme activity was measured using an LKB spectrophotometer (Ultraspec 4050). The assay medium for the enzyme activity contained pH 8 KH_2PO_4 buffer (3 ml), dithiobisnitrobenzoic acid (0.1 ml), 50 μl of enzyme (0.25 U), 20 μl of 0.075 M acetylthiocholine and antx-a(s) at various concentrations (0.2 to 2 μl). The activity was determined by measuring the increase in absorbance at 412 nm at 10 s intervals for 1 minute. In the inhibition studies, the substrate was added to the assay medium containing enzyme, antx-a(s) or diisopropyl-fluorophosphate (DFP), and dithiobisnitrobenzoic acid after a given time

of inhibition. Concentrations of DFP in the range of 0.32×10^{-3} to 0.32×10^{-5} M were used.

The kinetic analysis of the inhibition was done based on the inhibition scheme:



The inhibition is characterized by the dissociation constant K_d (k_{-1}/k_1) and phosphorylation constant (k_2). Further kinetic analysis was carried out using the equation of Main and Iverson (3):

$$1/p = \frac{K_d}{[I]} k_2 + \frac{1}{k_2}$$

where $[I]$ is the inhibitor concentration and p is the first order rate constant at constant $[I]$.

RESULTS AND DISCUSSION

The mechanism of the inhibition of acetylcholinesterase was found to be similar to known irreversible organophosphorus anticholinesterase agents (4). The inhibition is characterized by the initial formation of reversible Michaelis complex followed by an irreversible complex. Whether phosphorylation or some other process is responsible for the irreversible character of antx-a(s)-induced inhibition is presently unknown.

The results show that antx-a(s) has a higher affinity for human erythrocyte acetylcholinesterase ($K_d = 0.253 \mu\text{M}$) than electric eel ($K_d = 3.67 \mu\text{M}$) (Table 2). Also, the affinity of antx-a(s) for electric eel acetylcholinesterase is greater than that of DFP ($K_d = 300 \mu\text{M}$).

The overall rate of reaction measured by k_1 (k_2/K_d) indicates that human erythrocyte acetylcholinesterase ($k_1 = 84 \mu\text{M min}$) is more sensitive to

inhibition by antx-a(s) than electric eel acetylcholinesterase ($k_i = 1.36 \mu\text{M min}$). Also, eel acetylcholinesterase is less sensitive to inhibition by DFP ($k_i = 0.033 \mu\text{M min}$) than to inhibition by antx-a(s).

The kinetic studies suggest that the affinity and "phosphorylation rates" vary between eel and human erythrocytes. It is not known whether the membrane-bound character of acetylcholinesterase of erythrocytes might have contributed to the differences. The greater potency of antx-a(s) compared to DFP might be due to antx-a(s) binding at more than the esteratic site of the enzyme.

TOXIN PRODUCTION

A total of 210 g of A. flos-aquae NRC-525-17 cells were extracted since the last annual report. The majority of these cells were low in toxicity, with an average LD_{50} (ip mouse) of 100 mg/kg. All of the toxin, either in the purified or semi-purified form, was used for structural studies.

REFERENCES

1. Mahmood, N. A. and Carmichael, W. W. Toxicon 24:425, 1986.
2. Ellman, G. L., et al. Biochem, Pharmac. 7:88, 1961.
3. Main, A. R. and Iverson, F. Biochem. J. 100:525, 1966.
4. Mahmood, N. A. and Carmichael, W. W. Toxicon 25:1221, 1987.

Table 1. LD₅₀ determination of HPLC purified antx-a(s) in mice.

Dose μ g/kg (ip)	Number Treated	Number Deaths	Presence of Cholinergic* Symptoms:		Survival Time (min.) (mean \pm SEM)
			Muscarinic ^a	Nicotinic ^b	
12.5	6	none**	-	-	
25.0	6	none**	+	-	
27.5	6	none**	+	-	
30.0	6	none**	+	-	
32.5	6	5	+	+	44.8 \pm 14.0
40.0	6	6	+	+	40.0 \pm 6.0
50.0	6	6	+	+	27.2 \pm 8.7
100.0	6	6	+	+	8.0 \pm 1.7
200.0	6	6	+	+	6.5 \pm 1.1

*It was observed that the muscarinic effects disappeared in the survived mice. It is postulated that muscarinic effects alone were insufficient to kill the mice.

**All survived > 24 hours.

^aSalivation, lacrimation, diarrhea.

^bFasciculation, respiratory distress.

Table 2. Affinity equilibrium (K_d), "phosphorylation rate" (k_2), and biomolecular rate (k_1) constants for the inhibition of aChE by antx-a(s) and DFP.

Toxin	aChE					
	Electric Eel			Human Erythrocytes		
	K_{dx}^+ (μM)	k_2^* (\min^{-1})	k_1 ($\mu M^{-1} \min^{-1}$)	K_{dx}^+ (μM)	k_2^* (\min^{-1})	k_1 ($\mu M^{-1} \min^{-1}$)
Antx-a(s)	3.67	5	1.36	0.25	21.40	84
DFP	300	10	0.03			

* K_d and k_2 were determined from the "secondary plots." K_d is the reciprocal of the abscissa intercept and k_2 is the reciprocal of the ordinate intercept.

+The proposed M.W. of 267 for antx-a(s) was used to calculate K_d .

VRB:11b/37
12/12/88

Figures 1-3. Typical analytical HPLC profiles of antx-a(s). Sample from ion-exchange chromatography (Amberlite IRP 64) gave a toxic peak at approximately 10 minutes (Figure 1). The pooled toxic peak was rerun (Figure 2) and showed purity of approximately 80%. The column used was an Altech cyanopropyl (4.6 * 150 mm). Mobile phase: 10 mM ammonium acetate/1 mM acetic acid (80/20, v/v). The toxic peak was detected at 230 nm at 0.1 AUFS. The purity of the toxin is shown in Figure 3. An Altex (Beckman) cyanopropyl column (4.6 * 150 mm) was used. The running conditions were the same as that of Figures 1 and 2.

FIG 1

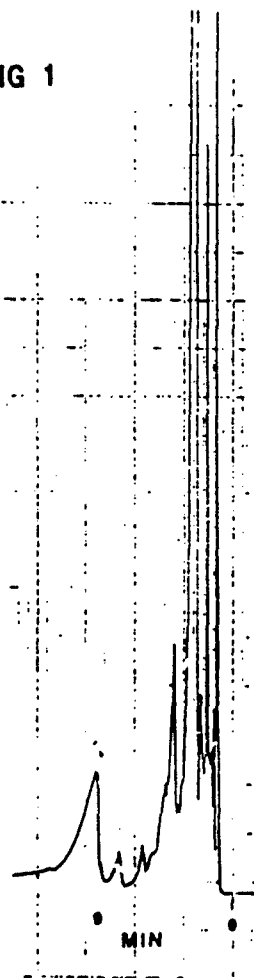


FIG 2

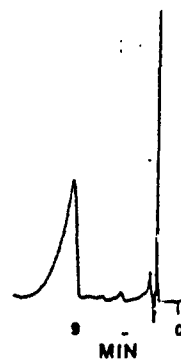


FIG 3



Figure 4. Extraction procedure used for antx-a(s).

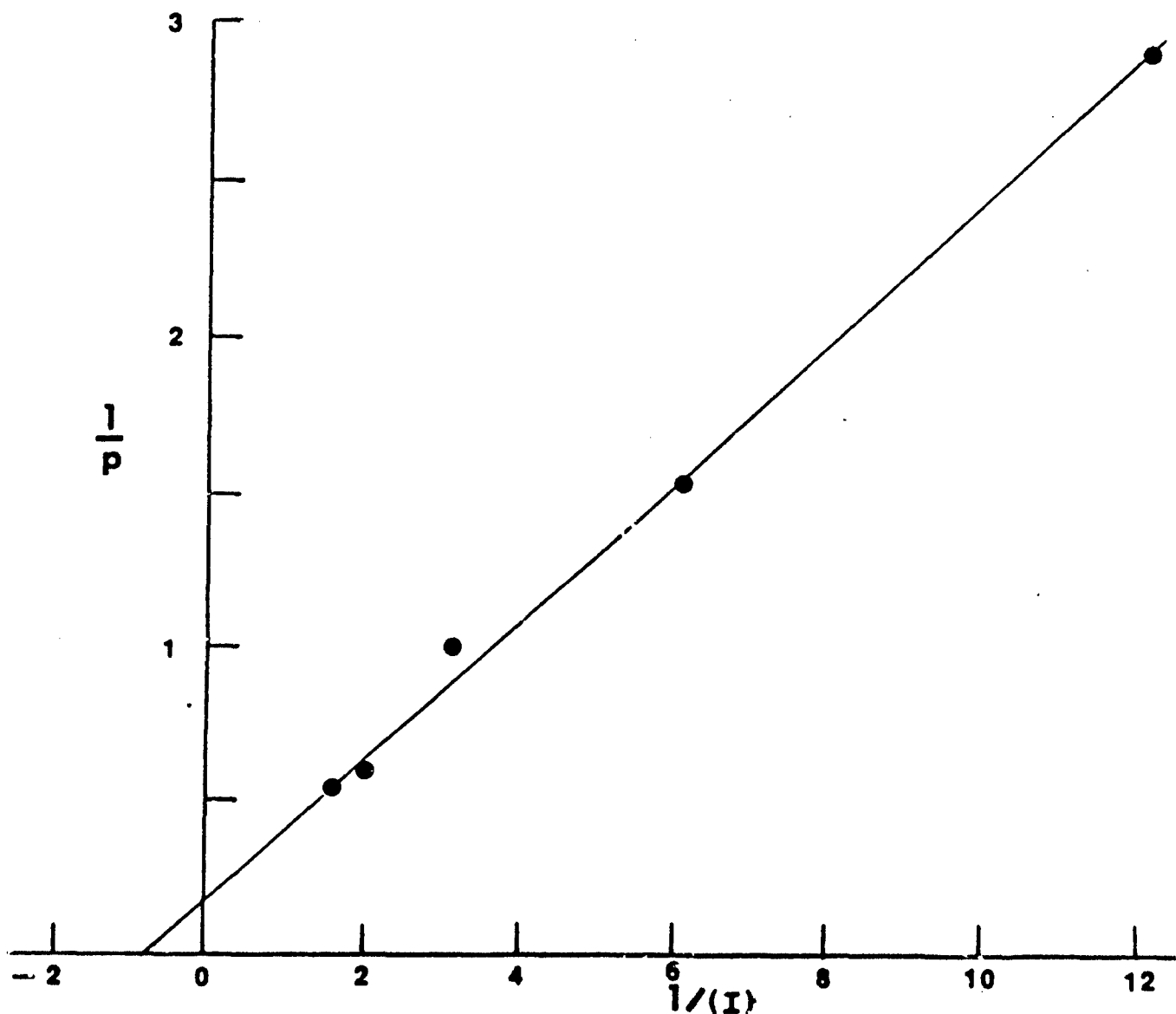
EXTRACTION PROCEDURE USED FOR ANATOXIN-a(s)

lyophilized cells (10 g)
in acidified ethanol (pH 4.0)--150 mL
(acidified with concentrated acetic acid)
↓
stir 24 hours
↓
centrifuge 10,000 rpm 1 hour 30 minutes
↓
supernatant
(re-extract pellet if still toxic)
↓
air drying
↓
reconstitute in 0.1 M acetic acid
(20 mL)
↓
solid phase extraction
C₁₈ (Bondelut)
↓
ion-exchange chromatography
(Amberlite IRP 64) (toxin elutes at 0.3 to 0.5 M acetic acid)
(linear gradient 0 to 1 M acetic acid)
↓
*semi-preparative HPLC (CN) if
sample heavily pigmented
↓
analytical HPLC CN
10 mm Amm. acetate/a mm acetic acid (80:20)
↓
Analytical HPLC CN

*Omit if not pigmented

Section XVI

Figure 5. Inhibition of electric eel acetylcholinesterase by antx-a(s)-- the "secondary plot." Note that p is the first-order rate constant which was the rate of inhibition at that antx-a(s) concentration was derived from the "primary plot;" $[I]$ is the antx-a(s) concentration. The intercept on the $1/p$ axis is $1/k_2$ and the intercept on the $1/[I]$ axis is $-1/K_d$.



Section XVI

APPENDIX TO SECTION XI

Numerical data for individual pulse decay probes used to measure renal and hepatic perfusion in swine.

GILT #3070

00 µg/kg MCYST-A iv

Time = minutes in relation to the dose of MCYST-A.

Kid1 and Kid2 = kidney perfusion measured from 2 TPD (temperature pulse decay) probes in ml/min gm.

Liv1, Liv2, and Liv3 = liver perfusion measured from 3 TPD probes in ml/min gm.

AoM = aortic mean pressure in mmHg.

-- = data not available.

Note: The organ perfusion and blood pressure parameters were measured every 6 minutes from 120 to 300 minutes postdosing. Half of the 3-minute averages presented in this raw data from 120 to 300 minutes are means of the 2 closest 6-minute values. Example: The 132-minute organ perfusion and blood pressure values were derived by taking the mean of the data collected at 129 and 135 minutes. Six-minute means for hepatic and renal perfusion and arterial mean pressure were calculated from this raw data.

Time	Kid1	Kid2	Liv1	Liv2	Liv3	AoM
-27	3.8	4.42	1.96	1.04	1.39	124.1
-24	3.1	4.32	2.96	0.72	1.24	125.3
-21	4.49	4.57	3.2	0.94	1.12	125
-18	3.71	4.38	2.72	1.17	1.49	125.8
-15	3.61	4.42	1.79	0.7	1.24	127.7
-12	3.35	4.38	2.54	1.25	1.39	134.6
-9	3.08	4.35	3.07	1.15	1.11	128.3
-6	3.33	4.29	2.88	0.82	1.22	125.3
-3	3.48	4.07	3.53	1.21	1.29	123.7
0	4	4.52	2.61	1.47	0.99	128.7
3	3.5	4.74	2.53	1.11	1.41	131.2
6	4.31	5.17	2.54	1.18	1.03	130.7
9	5.08	5.32	2.92	1.3	1.28	128.3
12	--	5.46	2.51	0.62	1.24	126.8
15	4.97	4.94	2.93	0.94	0.93	128.7
18	4.88	4.91	2.53	0.71	1.19	126.7
21	4.12	4.82	1.9	0.56	0.75	127
24	4.76	5.05	2.45	0.8	0.92	128.2
27	3.68	4.54	2.17	0.4	1.23	129
30	4.63	4.89	2.38	0.87	1.22	130.6
33	4.06	4.49	2.36	0.78	1.21	128.6
36	3.83	4.55	1.66	0.59	1.14	127.8
39	4.52	5.28	1.62	1.24	0.94	125.6
42	6.05	5.47	3.43	2.08	1.94	127
45	--	4.35	1.86	1.05	0.8	127.2
48	3.18	4.67	1.71	1.87	0.95	126.6
51	4.41	5.6	1.77	2.08	0.61	125.6

Time	Kid1	Kid2	Liv1	Liv2	Liv3	AOM
54	4.35	5.17	2.33	2.52	1	122.5
57	5.27	6.14	2.72	2.05	1.17	129.9
60	5.45	6.61	3.15	1.5	1.4	124.3
63	2.96	3.95	1.63	2.42	1.63	124.8
66	4.8	5.96	1.95	1.48	1.01	125.4
69	4.97	6.19	2.94	2.61	1.38	130.3
72	4.85	5.11	2.04	3.4	1.38	128.9
75	3.27	3.91	0.74	1.35	0.97	127.6
78	5.68	5.98	2.96	1.1	0.81	130.9
81	4.56	4.57	2.36	2.16	1.49	125.2
84	5.38	5.29	1.3	2.1	0.93	128.4
87	6.1	5.8	4.05	2.09	1.61	123
90	4.57	4.39	3.94	2.29	1.17	123.4
93	4.88	4.32	3.75	2.62	1.81	126.2
96	5.7	6.56	3.09	3.24	0.6	124.3
99	--	5.9	3.14	2.64	1.16	124.1
102	3.99	4.24	3.77	1.97	1.16	122.4
105	4.89	4.42	3.08	2.13	1.39	122.4
108	4.61	4.64	3.15	2.01	1.06	121.7
111	6.42	6.32	3.37	2.71	1.12	121.6
114	3.65	4.54	2.94	2.48	1.27	121.6
117	--	6.32	3.72	3.02	0.93	122.7
120	3.68	4.64	3.22	2.56	1.02	122.8
123	2.94	3.55	3.35	2.06	1.27	119.6
126	3.95	4.76	2.85	2.07	1.11	121.3
129	4.95	5.97	2.34	2.08	0.94	123
132	4.34	5.25	2.33	2.04	0.96	120.4
135	3.73	4.52	2.32	2	0.97	117.8
138	4.1	5.21	2.2	2.11	0.82	114.4
141	4.47	5.9	2.08	2.21	0.66	111.1
144	4.22	4.93	2.35	2.5	0.96	116.1
147	3.97	3.95	2.62	2.79	1.26	121.1
150	--	4.38	2.19	2.6	1.32	119.1
153	--	4.81	1.76	2.4	1.37	117.1
156	--	--	1.47	2.27	1.51	--
159	--	--	1.17	2.14	1.64	--
162	--	--	1.93	2.06	1.36	--
165	--	5.42	2.68	1.93	1.07	125.5
168	--	5.37	2.48	2.63	1.07	123.7
171	4.97	5.32	2.28	3.27	1.06	121.9
174	4.98	5.28	2.45	3.28	1.24	120.7
177	4.98	5.24	2.61	3.28	1.42	119.5
180	5.04	5.35	2.69	3.51	1.54	120.6
183	5.09	5.45	2.77	3.73	1.65	121.8
186	4.81	5.01	2.31	3.15	1.63	120.6
189	4.53	4.56	1.84	2.57	1.61	119.4
192	3.78	4.34	2.33	2.1	1.03	118
195	3.02	4.11	2.82	1.62	0.45	116.7
198	3.48	4.47	2.75	2.4	1.11	117

Time	Kid1	Kid2	Liv1	Liv2	Liv3	AOM
201	3.93	4.83	2.67	3.17	1.76	117.3
204	3.89	4.95	2.48	2.72	1.5	117.3
207	3.85	5.06	2.29	2.26	1.23	117.4
210	4.14	5.12	2.37	2.44	0.98	118.3
213	4.43	5.17	2.44	2.62	0.73	119.3
216	3.86	4.41	1.94	2.69	1.25	118.8
219	3.28	3.65	1.43	2.75	1.76	118.3
222	3.28	3.64	1.38	2.77	1.82	121.1
225	3.28	3.62	1.32	2.78	1.88	124
228	3.19	3.28	1.11	2.6	1.52	122.3
231	3.1	2.93	0.89	2.41	1.16	120.6
234	3.79	4	1.79	2.52	1.5	120
237	4.47	5.07	2.68	2.63	1.84	119.4
240	4.33	4.93	2.85	2.57	1.4	120.3
243	4.19	4.78	3.02	2.51	0.95	121.3
246	3.25	4.3	2.84	2.14	0.88	118.2
249	2.3	3.81	2.65	1.77	0.8	115.1
252	1.61	3.29	2.35	2.03	0.86	112.8
255	0.91	2.77	2.04	2.28	0.92	110.6
258	1.65	3.6	2.81	2.63	1.27	111
261	2.38	4.42	3.57	2.98	1.62	111.4
264	2.97	4.24	3.28	2.8	1.53	113.1
267	3.56	4.05	2.99	2.61	1.43	114.8
270	4.2	4.88	2.88	2.8	1.51	114.8
273	4.84	5.71	2.76	2.98	1.59	114.9
276	3.86	4.66	2.55	2.63	1.56	113.5
279	2.88	3.6	2.34	2.28	1.52	112.1
282	2.8	3.74	2.32	2.34	1.36	109.8
285	2.71	3.87	2.3	2.39	1.19	107.6
288	2.83	4.28	1.95	2.13	0.93	110.2
291	2.95	4.69	1.59	1.87	0.67	112.9
294	2.63	4.25	2.01	1.89	0.87	112.5
297	2.3	3.81	2.43	1.91	1.07	112.2
300	2.52	3.91	1.96	2.06	0.81	111.4

GILT #3045

00 µg/kg MCYST-A iv

Time = minutes in relation to the dose of MCYST-A.

Kid1 and Kid2 = kidney perfusion measured from 2 TPD (temperature pulse decay) probes in ml/min gm.

Liv1, Liv2, Liv3, and Liv4 = liver perfusion measured from 4 TPD probes in ml/min gm.

AoM = aortic mean pressure in mmHg.

-- = data not available.

Note: The organ perfusion and blood pressure parameters were measured every 6 minutes from 120 to 300 minutes postdosing. Half of the 3-minute averages presented in this raw data from 120 to 300 minutes are means of the 2 closest 6-minute values. Example: The 135-minute organ perfusion and blood pressure values were derived by taking the mean of the data collected at 132 and 138 minutes. Six-minute means for hepatic and renal perfusion and arterial mean pressure were calculated from this raw data.

Time	Kid1	Kid2	Liv1	Liv2	Liv3	Liv4	AoM
-27	3.4	4.92	2.72	3	2.63	5.6	130.9
-24	3.27	4.05	2.31	2.85	2.27	6.87	123.9
-21	4.76	4.39	2.45	3.2	2.35	5.59	123.4
-18	4.07	4.6	1.98	1.39	2.14	--	118.2
-15	3.55	4.08	2.05	1.91	2.36	--	125
-12	3.46	4.94	2.64	2.4	2.84	4.62	132.5
-9	3.86	4.08	1.94	1.95	2.27	4.29	123.2
-6	5.96	4.08	2.79	--	4.07	4.84	125.3
-3	4.41	3.51	2.35	2.64	1.89	4.67	122.2
0	2.43	3.52	2.52	2.73	2.65	--	122.3
3	3.35	3.78	2.27	2.31	2.42	4.33	127.9
6	2.33	3.97	2.21	1.48	2.41	--	133
9	3.26	3.15	1.99	1.47	2.1	3.18	121.4
12	--	--	2.61	2.06	2.46	2.83	--
15	3.74	5.1	2.83	3.23	3.19	4.97	128.8
18	3.88	4.47	2.74	3.21	3.25	3.5	135.4
21	3.5	2.82	2.29	1.15	1.82	2.4	123.3
24	--	3.57	2.97	2.6	2.93	3.47	131.2
27	4.99	4.32	3.04	3.35	2.95	5.26	132.8
30	--	4.24	2.8	3.14	2.88	5.16	130.1
33	3.51	4.38	2.93	3.61	3.21	4.4	126.1
36	3.54	4.83	2.92	2.66	2.83	2.3	133.9
39	2.81	4.47	2.29	1.45	2.22	--	122.5
42	--	--	2.48	2.31	2.7	4.11	--
45	3.64	5.76	3.44	--	3.68	2.13	127.6
48	3.73	3.85	3.1	3.41	2.71	4.53	125.4

Time	K1d1	K1d2	L1v1	L1v2	L1v3	L1v4	AOM
51	4.12	4.55	3.02	3.02	3.34	2.22	130.3
54	4.37	4.6	3.2	3.81	2.92	--	127
57	--	--	2.89	2.77	2.9	4.54	--
60	4.03	5.61	2.93	2.96	2.76	3.92	124.1
63	--	5.24	3.06	2.51	2.69	2.85	122.6
66	--	--	3.06	3.06	2.84	3.11	--
69	--	--	3.19	3.07	3.16	--	--
72	4.23	4.34	3.17	3.29	3.09	5.48	131.4
75	4.36	4.34	3.5	2.98	3.14	5.1	122.3
78	3.75	4.35	3.24	2.59	3.2	2.29	126.3
81	4.27	4.43	3.43	--	4.22	--	128.8
84	3.85	4.08	2.82	3.42	3.08	5.03	120.8
87	3.87	3.68	3.12	--	2.96	--	115.2
90	3.78	4.31	2.75	3.04	1.77	--	116.7
93	4.24	7.13	3.16	0.78	1.38	1.78	113.8
96	4.73	4.5	3.25	3.13	2.57	3.71	108.7
99	3.45	5.02	4.12	1.88	2.29	3.29	116.2
102	4.13	5.1	3.66	2.54	3.01	1.92	122.7
105	4.55	4.21	3.57	4.93	2.91	--	112.5
108	6.26	6.1	3.89	--	3.56	--	121
111	3.64	4.88	3.89	2.45	2.27	3.05	115.4
114	4.18	5.94	4.26	2.09	2.8	2.82	113.5
117	6.11	6.51	3.39	2.93	2.42	--	113
120	4.93	5.41	4.21	2.82	2.61	4.72	107.8
123	4.84	5.26	4.44	3.2	3.06	--	105.6
126	4.74	5.1	4.66	3.58	3.5	--	103.4
129	5.05	5.94	4.58	3.71	3.25	--	109.3
132	5.36	6.78	4.5	3.83	3	5.43	115.3
135	5.19	6.39	--	3.56	2.95	--	115.2
138	5.01	5.99	--	3.28	2.9	--	115.1
141	4.99	5.82	--	3.34	2.8	--	112.5
144	4.97	5.64	3.98	3.4	2.69	4.25	110
147	5.19	6.15	4.19	3.07	2.8	--	110.6
150	5.41	6.65	4.4	2.74	2.9	--	111.2
153	5.8	6.16	4.53	3.22	3.22	--	105.7
156	6.18	5.66	4.65	3.7	3.54	2.99	100.2
159	6.07	6.4	4.73	3.3	3.49	3.18	104.4
162	5.96	7.14	4.8	2.89	3.43	3.37	108.6
165	5.91	6.75	5.07	3.66	3.74	3.57	109.4
168	5.86	6.36	5.34	4.43	4.04	3.76	110.2
171	4.92	5.43	5.23	3.75	3.68	3.35	108.8
174	3.97	4.5	5.12	3.07	3.32	2.93	107.5
177	4.09	4.29	4.91	3.54	--	3.13	104.5
180	4.2	4.07	4.7	4.01	--	3.33	101.6
183	5.46	4.97	4.65	--	--	3.01	105.1
186	6.72	5.87	4.6	--	--	2.69	108.6
189	5.76	5.15	--	--	--	--	104.2
192	4.8	4.43	--	3.97	--	--	99.8
195	5.13	5.34	--	--	--	--	99.6

Time	Kid1	Kid2	Liv1	Liv2	Liv3	Liv4	AoM
198	5.45	6.24	5.09	--	--	3.28	99.4
201	6.1	6.1	4.83	--	--	3.12	101.7
204	6.74	5.95	4.57	5.26	--	2.96	104.1
207	6.17	5.56	4.04	4.52	--	2.71	101.2
210	5.6	5.16	3.51	3.77	--	2.45	98.4
213	5.45	5.3	3.52	3.73	--	2.82	94.8
216	5.29	5.44	3.52	3.69	--	3.19	91.3
219	5.72	5.86	4.29	3.37	--	3.52	93.9
222	6.14	6.27	5.06	3.05	--	3.84	96.5
225	4.44	4.93	4.63	2.72	--	--	93.3
228	2.73	3.58	4.19	2.39	--	--	90
231	3.84	3.82	4.52	2.5	--	--	95.7
234	4.94	4.06	4.85	2.6	--	3.82	101.3
237	5.31	4.68	5.12	2.83	--	3.76	100.8
240	5.68	5.3	5.38	3.05	--	3.7	100.3
243	4.82	4.73	4.85	2.71	--	3.41	99.3
246	3.95	4.16	4.31	2.37	--	3.11	98.2
249	4.8	4.99	3.85	2.26	--	4.06	95.9
252	5.64	5.82	3.38	2.14	--	5	93.6
255	5.6	5.18	3.23	2.36	--	5.03	92.8
258	5.55	4.54	3.08	2.57	--	5.06	91.9
261	4.72	4.52	--	2.86	--	4.19	93.9
264	3.89	4.5	--	3.14	--	3.31	96
267	4.51	5.03	--	3.27	--	3.73	97.9
270	5.12	5.56	--	3.4	--	4.14	99.9
273	5.7	5.41	--	3.22	--	4.34	98.2
276	6.27	5.25	3.41	3.03	--	4.53	96.4
279	5.86	5.27	3.38	2.42	--	--	95.7
282	5.44	5.29	3.34	1.8	--	--	94.9
285	5.73	5.46	3.06	1.91	--	--	94.1
288	6.01	5.63	2.78	2.02	--	--	93.3
291	5.07	4.98	3.93	2.11	--	--	94.3
294	4.12	4.32	5.07	2.2	--	--	95.4
297	4.28	4.39	5.24	2.24	--	--	93.8
300	4.43	4.45	5.4	2.27	--	--	92.2

Time = minutes in relation to the dose of MCYST-A.

Kid1 and Kid2 = kidney perfusion measured from 2 TPD (temperature pulse decay) probes in ml/min gm.

Liv1, Liv2, and Liv3 = liver perfusion measured from 3 TPD probes in ml/min gm.

AoM = aortic mean pressure in mmHg.

-- = data not available.

Note: The organ perfusion and blood pressure parameters were measured every 6 minutes from 120 to 300 minutes postdosing. Half of the 3-minute averages presented in this raw data from 120 to 300 minutes are means of the 2 closest 6-minute values. Example: The 135-minute organ perfusion and blood pressure values were derived by taking the mean of the data collected at 132 and 138 minutes. Six-minute means for hepatic and renal perfusion and arterial mean pressure were calculated from this raw data.

Time	Kid1	Kid2	Liv1	Liv2	Liv3	AoM
-27	3.32	4.49	1.39	1.66	2.26	107.1
-24	3	4.43	1.21	1.4	2.49	103.9
-21	3.32	4.67	1.29	1.78	2.31	104.5
-18	3.27	4.66	1.4	1.91	2.45	104.6
-15	3.27	4.81	1.54	1.82	2.73	104.3
-12	3.41	4.91	1.83	1.89	2.74	105.8
-9	2.72	4.1	2.03	1.7	2.95	106.2
-6	3.58	5.28	1.73	1.93	2.88	107.3
-3	3.38	4.81	1.6	1.96	2.98	105.2
0	2.86	4.23	1.26	1.6	2.44	104.8
3	2.96	4.4	1.54	1.55	2.68	107.9
6	2.61	3.76	1.31	1.28	2.35	110.4
9	3.01	4.55	0.77	1.15	1.61	113.3
12	2.77	4.3	0.48	1.83	1.44	117.7
15	2.36	3.45	0.22	1.73	1.15	123.7
18	2.23	3.26	0.26	1.38	1.02	126.9
21	2.09	3	0.46	1.67	1.21	124.5
24	2.33	3.76	0.63	1.65	1.46	121.3
27	1.55	2.28	0.76	1.68	1.65	114.1
30	2.38	3.44	1.01	1.71	1.86	114.9
33	2.87	3.89	0.96	1.77	1.91	112.2
36	2.75	3.74	1.01	1.69	2.07	110.4
39	3	4.57	1.7	2.44	2.09	108.9
42	3.05	4.59	2.06	2.36	2.17	105.3
45	2.74	4.11	2.54	2.52	2.55	104.7
48	2.94	4.52	1.81	2.32	2.5	104.6
51	2.77	4.22	2.05	2.36	2.92	103.5

Time	Kid1	Kid2	Liv1	Liv2	Liv3	AoM
54	3.46	5.07	2.42	3.17	3.75	102.3
57	3.06	4.18	2.07	3.18	3.59	104.8
60	1.95	2.66	--	1.06	1.34	101.2
63	3.19	5.03	1.79	2.49	2.64	107.9
66	3.76	5.23	--	2.03	2.67	112.6
69	2.93	4.31	1.02	2.29	2.08	108.4
72	2.52	4.3	1.07	2.09	1.83	109.2
75	--	--	1.59	3.57	3.44	119.3
78	3.1	3.84	0.82	2.15	2.49	111.3
81	3.97	5.43	1.02	2.56	2.27	114.3
84	2.59	3.46	0.82	1.38	2.29	111.2
87	2.34	3.08	0.51	1.67	1.69	111.3
90	2.2	3	0.81	0.74	1.97	112.4
93	2.14	3.26	0.51	0.7	2.09	108.1
96	2.96	4.18	0.27	0.63	2.82	111
99	2.58	3.77	0.39	1.12	2.12	108.8
102	4.31	6.1	0.6	0.53	2.46	112.4
105	3.45	4.83	0.64	1.19	2.15	111.1
108	4.2	5.8	0.46	1.24	2.47	110.9
111	2.49	3.47	0.41	1.17	1.85	108.9
114	1.68	2.51	0.23	1.39	1.81	104.3
117	2.9	4.37	0.95	1.73	2.22	108.3
120	1.82	3.07	0.51	1.19	1.35	105.2
123	2.38	3.75	0.41	0.99	1.41	105.3
126	2.94	4.43	0.3	0.78	1.46	105.4
129	2.29	3.51	0.16	0.66	1.68	104.2
132	1.64	2.59	0	0.54	1.89	103
135	2.35	3.5	0.79	0.92	2.37	104.2
138	3.05	4.41	1.56	1.3	2.85	105.4
141	3.01	4.41	1.5	1.61	2.77	104.7
144	2.96	4.4	1.43	1.92	2.68	104
147	2.99	4.75	1.25	1.91	2.62	105.3
150	3.01	5.1	1.07	1.89	2.56	106.6
153	2.45	3.91	1.15	1.24	2.32	107.7
156	1.88	2.71	1.22	0.58	2.08	108.8
159	1.77	2.67	--	--	--	106.3
162	1.65	2.62	--	--	--	103.8
165	2.16	3.17	--	--	--	100.4
168	2.66	3.72	0.69	1.95	1.98	97.1
171	2.72	3.78	0.79	1.77	2.14	97.3
174	2.78	3.84	0.89	1.59	2.3	97.6
177	2.77	3.82	1.31	2.21	2.71	100.2
180	2.75	3.82	1.72	2.82	3.11	102.8
183	2.63	3.74	1.24	2.15	2.68	96.9
186	2.51	3.65	0.75	1.47	2.24	91
189	2.56	3.67	0.62	1.62	2.29	92.5
192	2.61	3.68	0.48	1.76	2.34	94
195	2.29	3.44	0.86	1.94	2.57	93.8
198	1.97	3.2	1.24	2.12	2.79	93.6

Time	Kid1	Kid2	Liv1	Liv2	Liv3	AoM
201	2.16	3.28	1.2	1.95	2.82	92.6
204	2.34	3.35	1.16	1.78	2.85	91.5
207	2.83	4.13	1.63	2.1	3.07	93.1
210	3.32	4.91	2.09	2.42	3.28	94.7
213	2.99	4.4	1.7	2.36	3.22	95
216	2.66	3.89	1.3	2.3	3.15	93.3
219	2.89	4.3	1.57	2.56	3.07	92.9
222	3.11	4.7	1.83	2.81	2.98	90.5
225	2.64	4.05	1.11	1.93	2.41	88.3
228	2.16	3.4	0.38	1.04	1.84	86.2
231	2.45	3.71	0.8	1.7	2.39	86.7
234	2.73	4.02	1.22	2.36	2.93	87.2
237	2.79	3.88	--	1.94	2.52	87.6
240	2.84	3.74	--	1.52	2.1	87.9
243	2.63	3.62	--	1.67	2.1	87.7
246	2.41	3.5	0.78	1.82	2.09	87.4
249	2.7	3.73	1.07	2.26	2.35	84.9
252	2.99	3.96	1.35	2.69	2.61	82.4
255	2.49	3.42	1.6	2.36	2.96	82.9
258	1.98	2.88	1.85	2.02	3.31	83.5
261	2.07	3.01	1.22	2.48	2.9	84.1
264	2.15	3.14	0.59	2.94	2.49	84.6
267	2.4	3.41	0.93	--	2.74	--
270	2.85	3.85	1.27	--	2.98	--
273	2.4	3.63	1.37	--	2.87	--
276	2.14	3.41	1.46	2.03	2.76	82.8
279	2.15	3.27	--	2.25	2.39	84.7
282	2.16	3.12	--	2.46	2.02	86.5
285	2.18	3.15	--	2.3	2.5	84.9
288	2.2	3.18	2.04	2.14	2.97	83.3
291	2.68	3.99	2.34	2.16	3.23	86.2
294	3.16	4.79	2.63	2.17	3.48	89
297	2.87	4.36	1.96	2.74	3.51	86.6
300	2.58	3.93	1.29	3.3	3.53	84.2

GILT #3321

00 µg/kg MCYST-A iv

Time = minutes in relation to the dose of MCYST-A.

Kid1 and Kid2 = kidney perfusion measured from 2 TPD (temperature pulse decay) probes in ml/min gm.

Liv1, Liv2, and Liv3 = liver perfusion measured from 3 TPD probes in ml/min gm.

AoM = aortic mean pressure in mmHg.

-- = data not available.

Note: The organ perfusion and blood pressure parameters were measured every 6 minutes from 120 to 300 minutes postdosing. Half of the 3-minute averages presented in this raw data from 120 to 300 minutes are means of the 2 closest 6-minute values. Example: The 132-minute organ perfusion and blood pressure values were derived by taking the mean of the data collected at 129 and 135 minutes. Six-minute means for hepatic and renal perfusion and arterial mean pressure were calculated from this raw data.

Time	Kid1	Kid2	Liv1	Liv2	Liv3	AoM
-27	2.32	2.18	4.16	2.77	4.86	120.8
-24	2.36	2.28	3.61	2.26	4.14	121.2
-21	2.53	2.79	4.26	2.47	4.7	118.4
-18	2.44	2.43	4.29	2.72	4.91	117.6
-15	2.61	2.56	3.95	2.56	4.46	114.4
-12	2.75	2.93	4.53	2.76	5.05	116
-9	2.52	2.77	4.78	3.27	5.26	116
-6	3.07	3.14	4.22	2.72	5.09	116.8
-3	3.18	3.2	4.33	2.54	4.73	116.8
0	2.7	2.98	3.91	3.88	5.79	112
3	3.72	3.85	4.55	2.76	5.09	--
6	1.98	2	3.88	4.16	5.58	124.8
9	3.16	3.67	5.44	2.3	5.19	130.8
12	3.37	3.14	4.25	4.89	5.89	118.4
15	3.28	3.18	4.59	4.91	5.74	114.8
18	2.69	3.43	3.89	2.8	4.8	124.8
21	--	4.38	5.07	4.67	6.49	115.2
24	2.61	3.43	4.43	2.61	5.16	124.4
27	3.5	4.1	5.08	2.78	5.21	124.8
30	4.48	4.65	4.72	4.41	6.89	114.4
33	3.11	3.46	3.28	3.58	4.07	112.8
36	3.91	3.75	4.53	4.49	5.7	114
39	3.79	3.75	4.31	4.13	5.7	115.6
42	3.13	3.4	5.29	3.16	6.37	124
45	4.09	4.17	4.04	4	4.98	113.2
48	2.96	2.8	3.81	3.19	4.41	110.8
51	3.89	3.8	4.57	4.43	4.9	109.6

Time	Kid1	Kid2	Liv1	Liv2	Liv3	AoM
54	3.5	3.92	3.95	3.66	5.06	115.6
57	3.92	5.21	4.19	3.74	5.19	120
60	3.34	4.04	3.28	3.8	5.02	115.6
63	2.94	3.96	3.91	3.43	4.84	123.2
66	4.22	3.75	5.65	3.42	5.52	113.6
69	3.19	4.34	4.74	3.47	5.74	122.4
72	3.57	3.92	4.4	3.85	7.22	112.8
75	2.8	3.61	4.54	2.8	4.98	124
78	3.65	3.69	4.73	3.24	6.07	114.4
81	4.07	4.41	5.12	4.77	7.29	110.8
84	3.52	4.36	3.53	3.83	3.94	115.2
87	3.75	4.32	4.33	3.35	4.72	120
90	3.6	4.66	4.53	4.13	5.35	116
93	3.14	4.19	3.83	3.15	3.93	116.8
96	3.27	4.31	3.5	3.76	4.3	121.2
99	3.01	4.05	3.79	3.47	3.39	113.6
102	3.35	4.58	4.59	4.56	5.45	110
105	3.94	4.96	5.04	4.7	5.01	111.2
108	4.14	4.27	5.08	3.69	7.27	111.2
111	4.09	5.33	6.16	5.66	6.51	110.4
114	4.05	4.71	4.17	4.66	4.66	112
117	3.54	3.89	5.46	4.63	7.16	108.4
120	3.06	3	5.04	3.45	6.8	113.6
123	3.48	3.67	5.29	4.82	6.65	112.4
126	3.89	4.34	5.53	6.19	6.5	111.2
129	4.29	4.63	5.18	4.78	6.52	111.6
132	4.69	4.92	4.83	3.36	6.54	112
135	4.76	4.91	4.73	3.62	7.08	110.2
138	4.83	4.89	4.63	3.88	7.61	108.4
141	4.53	4.81	4.66	4.05	7.48	107.2
144	4.22	4.72	4.59	4.21	7.35	106
147	4.33	4.5	4.76	3.94	6.7	109.8
150	4.43	4.27	4.82	3.67	6.05	113.6
153	3.79	4.16	4.15	3.96	5.84	111.8
156	3.14	4.05	3.48	4.25	5.63	110
159	2.91	3.68	4.15	3.91	6.28	110.4
162	2.68	3.31	4.82	3.56	6.92	110.8
165	3.26	4	4.43	4.18	6.38	107.4
168	3.84	4.69	4.03	4.8	5.84	104
171	3.46	3.97	4.42	4.24	6.17	105.6
174	3.07	3.24	4.8	3.67	6.49	107.2
177	3.4	3.59	4.99	3.68	7.3	108
180	3.72	3.93	5.18	3.68	8.11	108.8
183	3.93	4.25	5.48	4.06	8.12	107.6
186	4.13	4.57	5.78	4.43	8.13	106.4
189	3.89	4.36	5.36	4.72	7.24	104.8
192	3.65	4.15	4.94	5	6.34	103.2
195	3.23	3.94	5.05	4.76	6.95	103.8
198	2.81	3.73	5.16	4.52	7.56	104.4

Time	Kid1	Kid2	Liv1	Liv2	Liv3	AoM
201	3.35	4.04	4.73	4.38	7.41	102.2
204	3.89	4.35	4.29	4.24	7.25	100
207	4.25	4.52	4.68	4.21	7.16	100.8
210	4.8	4.68	5.07	4.18	7.07	101.6
213	4.48	4.32	5.31	4	6.59	105.4
216	4.16	3.96	5.54	3.81	6.11	109.2
219	4.09	4.33	5.4	4.11	6.66	105.2
222	4.01	4.69	5.26	4.41	7.21	101.2
225	3.89	4.36	5.13	3.84	7.1	104.8
228	3.76	4.03	4.99	3.27	6.99	108.4
231	3.39	3.88	5	3.75	6.4	103.8
234	3.01	3.73	5.01	4.23	5.81	99.2
237	3.26	3.74	5.24	4.31	6.16	102.8
240	3.51	3.75	5.47	4.38	6.51	106.4
243	3.45	3.55	5.34	3.89	6.47	104
246	3.38	3.34	5.21	3.4	6.42	101.6
249	3.84	3.89	5.38	3.52	6.54	101.2
252	4.29	4.44	5.54	3.63	6.65	100.8
255	3.55	3.68	4.75	3.71	6.67	96.6
258	2.8	2.92	3.95	3.79	6.68	92.4
261	2.9	3.22	4.79	3.62	6.12	93.2
264	2.99	3.52	5.63	3.45	5.56	94
267	3.81	4.02	6.55	4.01	6.65	98.6
270	4.62	4.52	7.46	4.57	7.74	103.2
273	3.83	4.04	6.1	4.38	7.37	99.4
276	3.03	3.55	4.73	4.18	6.99	95.6
279	3.09	3.57	4.66	4.41	7.23	95.4
282	3.15	3.59	4.59	4.64	7.47	95.2
285	2.88	3.35	4.85	4.6	7.44	94.8
288	2.61	3.11	5.11	4.55	7.41	94.4
291	3.2	3.79	5.16	4.52	7.46	94.4
294	3.78	4.47	5.21	4.49	7.5	94.4
297	3.67	4.24	4.89	4.41	7.04	94
300	3.55	4	4.57	4.32	6.57	93.6

GILT #2895

25 µg/kg MCYST-A iv

Time = minutes in relation to the dose of MCYST-A.

Kid1 and Kid2 = kidney perfusion measured from 2 TPD (temperature pulse decay) probes in ml/min gm.

Liv1 and Liv2 = liver perfusion measured from 2 TPD probes in ml/min gm.

AoM = aortic mean pressure in mmHg.

-- = data not available.

Note: The organ perfusion and blood pressure parameters were measured every 6 minutes from 120 to 300 minutes postdosing. Half of the 3-minute averages presented in this raw data from 120 to 300 minutes are means of the 2 closest 6-minute values. Example: The 132-minute organ perfusion and blood pressure values were derived by taking the mean of the data collected at 129 and 135 minutes. Six-minute means for hepatic and renal perfusion and arterial mean pressure were calculated from this raw data.

Time	Kid1	Kid2	Liv1	Liv2	AoM
-27	3.16	2.75	1.62	2.68	121
-24	2.75	2.95	1.3	2.31	117.5
-21	3.05	3.25	1.7	2.5	112.2
-18	3.33	3.78	1.86	2.52	113.5
-15	3.21	4.45	1.85	2.65	112.1
-12	3.21	4.35	2.34	2.69	109.6
-9	3.53	4.84	1.78	2.5	107.2
-6	3.48	4.64	1.84	2.51	108.5
-3	3.4	4.22	1.91	2.54	108.1
0	3.37	4.4	1.54	2.59	114.5
3	2.64	2.23	1.55	2.29	109.7
6	3.32	3.78	1.69	2.6	117.2
9	3.42	3.78	1.55	2.52	114.5
12	3.19	3.84	1.45	2.73	112.8
15	3.31	3.88	1.4	2.63	112.9
18	3.37	4.48	1.35	2.78	109.7
21	3.24	3.84	1.39	2.78	107.6
24	2.93	3.18	1.16	2.89	104.9
27	3.17	3.7	1.1	2.9	105.7
30	3.35	3.83	0.92	2.48	107.1
33	3.18	2.99	0.69	2.42	103.8
36	2.64	3.38	1.01	1.76	104.2
39	2.91	4.2	0.51	1.72	117.1
42	2.72	3.58	0.21	1.57	118.7
45	2.54	3.45	0.6	1.64	121.2
48	2.37	--	--	--	116.9
51	2.63	3.35	0.47	1.48	113.5

Time	Kid1	Kid2	Liv1	Liv2	AOM
54	2.65	3.53	0.55	1.4	113.7
57	2.65	3.34	0.37	1.26	111.2
60	2.58	3.3	0.61	1.07	111.1
63	2.54	3.56	0.45	0.85	111
66	2.64	4.31	1.97	1.57	109.5
69	2.27	3.04	1.65	1.54	111.2
72	2.95	3.16	1.06	1.36	111.2
75	2.62	3.33	1.25	1.36	111
78	2.49	3.08	1.66	1.36	108.9
81	2.37	2.98	0.51	1.06	106
84	2.19	2.42	1.03	1.19	101.8
87	2.45	3.19	1.38	1.23	105.7
90	2.11	2.96	1.13	0.84	107.3
93	2.39	2.87	1.53	1	106.1
96	1.44	1.8	1.06	1.06	105.7
99	2.37	3	1.3	1.4	102.2
102	2.23	2.59	1.68	1.07	100.6
105	2.29	2.32	1.42	1.36	98.9
108	2.1	2.61	1.54	1.46	100
111	2.25	2.96	1.1	1.01	102.6
114	2.23	3.28	1.83	1.87	103
117	2.2	3.13	1.56	1.5	100.7
120	2.19	2.64	1.28	1.22	105
123	2.175	2.805	1.61	1.32	103.7
126	2.16	2.97	1.94	1.42	102.4
129	2.36	3.15	1.26	1.65	98.9
132	2.31	2.855	1.41	1.58	99.2
135	2.26	2.56	1.56	1.51	99.5
138	2.47	2.74	1.255	1.275	100.2
141	2.68	2.92	0.35	1.04	100.9
144	2.505	3.02	1.405	1.31	97.5
147	2.33	3.12	1.86	1.58	94.1
150	2.315	3.13	1.815	1.47	93.5
153	2.3	3.14	1.77	1.36	92.9
156	2.23	3.685	2.24	1.605	90.95
159	2.16	4.23	2.71	1.85	89
162	2.16	3.665	1.83	1.64	88.55
165	2.16	3.1	0.95	1.43	88.1
168	1.605	2.06	0.925	1.41	80.2
171	1.05	1.02	0.9	1.39	72.3
174	1.345	1.53	1.18	1.82	73.55
177	1.64	2.04	1.46	2.25	74.8
180	1.985	2.565	1.675	2.095	78.7
183	2.33	3.09	1.80	1.94	82.6
186	1.885	2.66	1.66	1.805	81.95
189	1.44	2.23	1.43	1.67	81.3
192	1.655	2.435	1.345	1.68	84.1
195	1.87	2.64	1.26	1.59	86.9
198	1.79	2.645	1.26	1.46	87.05

Time	Kid1	Kid2	Liv1	Liv2	AOM
201	1.71	2.65	1.26	1.23	87.2
204	1.615	2.24	1.495	1.34	86
207	1.52	1.83	1.73	1.45	84.8
210	1.76	2.13	1.745	1.52	82.85
213	2	2.43	1.76	1.59	80.9
216	1.855	2.275	1.61	1.545	80.55
219	1.71	2.12	1.46	1.5	80.2
222	1.37	1.405	1.39	1.515	70.85
225	1.03	0.69	1.32	1.53	61.5
228	1.23	0.875	1.5	1.67	65.95
231	1.43	1.06	1.68	1.81	70.4
234	1.27	0.895	1.695	1.53	71.95
237	1.11	0.73	1.71	1.25	73.5
240	1.29	1.31	1.955	1.46	83.15
243	1.47	1.89	2.2	1.67	92.8
246	1.485	1.935	1.99	1.785	90.35
249	1.5	1.98	1.78	1.9	87.9
252	1.405	1.735	1.865	1.78	89.05
255	1.31	1.49	1.95	1.66	90.2
258	1.365	1.325	1.98	1.72	87.5
261	1.42	1.16	2.01	1.78	84.8
264	1.27	1.325	2.2	1.75	85.25
267	1.12	1.49	2.39	1.72	85.7
270	1.415	1.895	1.84	1.74	85.5
273	1.71	2.3	1.29	1.76	85.3
276	1.425	1.875	1.53	1.645	83.85
279	1.14	1.45	1.77	1.53	82.4
282	1.375	1.635	1.905	1.645	83.55
285	1.61	1.82	2.04	1.76	84.7
288	1.545	1.69	1.695	1.6	86.15
291	1.48	1.56	1.35	1.44	87.6
294	1.785	2.065	1.625	1.44	88.95
297	2.09	2.57	1.9	1.44	90.3
300	1.62	2.11	2.09	1.65	88.1

GILT #2987

25 µg/kg MCYST-A iv

Time = minutes in relation to the dose of MCYST-A.

Kid1 and Kid2 = kidney perfusion measured from 2 TPD (temperature pulse decay) probes in ml/min gm.

Liv1 and Liv2 = liver perfusion measured from 2 TPD probes in ml/min gm.

AoM = aortic mean pressure in mmHg.

-- = data not available.

Note: The organ perfusion and blood pressure parameters were measured every 6 minutes from 120 to 300 minutes postdosing. Half of the 3-minute averages presented in this raw data from 120 to 300 minutes are means of the 2 closest 6-minute values. Example: The 153-minute organ perfusion and blood pressure values were derived by taking the mean of the data collected at 150 and 156 minutes. Six-minute means for hepatic and renal perfusion and arterial mean pressure were calculated from this raw data.

Time	Kid1	Kid2	Liv1	Liv2	AoM
-27	5.06	6.4	3.27	1.02	105.4
-24	5.01	6.03	4.15	1.19	107.4
-21	5.32	6.14	4.6	1.2	106.6
-18	4.81	5.59	4.54	1.61	120.9
-15	5.07	5.6	3.97	1.06	115.2
-12	4.27	4.98	3.17	1.41	108.7
-9	4.63	5.92	3.72	1.8	108.3
-6	5.22	5.7	3.86	1.99	119.1
-3	4.45	5.48	4.38	2	116.9
0	4.48	4.75	2.42	0.92	120.4
3	4.35	5.43	4.27	1.56	118.5
6	5.31	6.23	3.77	1.54	111.9
9	6.25	8.11	4.04	1.68	110.3
12	--	--	--	1.15	98.4
15	5.79	7	3.22	1.73	95.2
18	5.36	6.1	2.78	1.35	94.2
21	4.83	5.36	2.81	2.13	97.7
24	5.2	5.92	3.26	1.45	91.3
27	4.65	4.83	3.66	1.98	84.3
30	5.1	5.48	4.19	2.03	86.1
33	3.6	4.36	3.37	1.1	88.3
36	4.41	5.11	3.31	1.6	89.1
39	4.35	4.73	2.45	1.51	84.5
42	4.51	5.22	3.3	1.21	90
45	4.81	5.44	3.14	1.11	88.3
48	4.26	5.2	1.6	1	90.1
51	4.71	5.64	2.16	0.81	87

Time	Kid1	Kid2	Liv1	Liv2	AcM
54	4.14	5.18	1.23	0.76	90
57	4.66	5.33	2.43	0.83	89.8
60	4.29	5.61	2.1	0.66	89.8
63	4.76	5.67	2.42	1.03	89.3
66	4.01	--	1.78	1.12	89.4
69	4.15	4.21	2.22	1.41	87.4
72	4.94	5.71	2.16	0.71	92.5
75	4.53	5.19	2.34	0.77	93.2
78	4.36	4.92	1.7	0.66	97.7
81	4.92	5.96	2.42	2.11	91.3
84	4.39	5.31	2.37	1.44	92.3
87	4.24	5.38	3.24	1.28	90.3
90	4.72	5.85	1.3	1.32	91.2
93	4.65	5.13	2.47	0.46	91.4
96	4.04	4.73	--	0.62	90.3
99	4.02	4.47	1.27	1.31	89.2
102	4.66	5.29	2.51	2.14	92.8
105	4.35	4.09	2.9	0.69	88.6
108	4.38	4.56	2.62	0.69	90.2
111	4.48	4.85	2.09	2.11	90.1
114	4.55	5.2	2.48	0.82	90.2
117	4.79	5.17	1.64	1.04	89.1
120	4.32	4.39	1.85	0.53	88.7
123	4.08	4.36	2.24	0.71	89.6
126	3.84	4.33	2.62	0.89	90.4
129	4.21	4.45	1.79	--	89.1
132	4.58	4.57	0.95	--	87.8
135	4.55	4.68	1.64	--	86.8
138	4.52	4.78	2.33	1.23	85.7
141	4.21	4.33	2.45	1.39	84.3
144	3.89	3.87	2.56	1.55	83
147	3.85	3.89	2.44	0.92	84.6
150	3.81	3.91	2.32	0.28	86.2
153	3.77	3.71	2.33	0.33	85.6
156	3.72	3.51	2.33	0.38	85
159	4.02	4.01	1.98	0.65	84.6
162	4.31	4.51	1.63	0.92	84.2
165	4.05	4.11	2.08	0.63	84
168	3.79	3.7	2.53	0.33	83.8
171	3.95	3.78	2.53	0.39	83.4
174	4.1	3.86	2.52	0.44	83.1
177	4.11	4.04	2.54	0.41	82.8
180	4.11	4.21	2.55	0.37	82.6
183	3.94	3.68	2.48	0.44	84.2
186	3.77	3.14	2.41	0.5	85.7
189	4.17	3.75	--	0.38	86.6
192	4.57	4.36	--	0.25	87.4
195	4.34	4.14	--	0.22	86.9
198	4.11	3.91	1.37	0.18	86.5

Time	K1d1	K1d2	L1v1	L1v2	AoM
201	4.15	4.07	2.1	0.46	84.3
204	4.19	4.22	2.83	0.73	82.2
207	4	3.88	2.78	0.73	82.2
210	3.81	3.54	2.72	0.73	82.2
213	3.82	3.61	2.37	--	80.8
216	3.83	3.68	2.02	--	79.3
219	3.91	3.56	2.53	--	77.9
222	3.98	3.44	3.03	1.08	76.5
225	4.04	3.64	3.18	0.94	76.8
228	4.1	3.84	3.32	0.8	77.1
231	4	3.67	3.24	0.83	76.9
234	3.89	3.5	3.15	0.85	76.8
237	3.5	3.32	3.34	--	79.3
240	3.11	3.13	3.52	--	81.7
243	3.05	3.21	3.16	--	86.8
246	--	--	2.8	--	--
249	2.83	2.82	2.82	--	86.6
252	2.66	2.35	2.83	0.56	81.2
255	2.79	2.53	2.69	0.74	79.1
258	2.92	2.7	2.54	0.92	76.9
261	2.92	2.61	2.31	0.81	75.8
264	2.92	2.52	2.08	0.69	74.6
267	2.89	2.63	2.17	0.56	73.1
270	2.86	2.73	2.26	0.43	71.5
273	3.27	3.2	2.53	0.55	72.8
276	3.68	3.67	2.79	0.67	74.1
279	3.72	3.66	2.65	0.57	73.7
282	3.75	3.64	2.5	0.47	73.2
285	3.83	3.85	2.8	0.89	72.9
288	3.91	4.06	3.1	1.3	72.6
291	3.59	3.7	2.69	0.79	72.8
294	3.26	3.33	2.28	0.27	73.1
297	3.37	3.54	2.45	0.43	72.9
300	3.48	3.74	2.61	0.58	72.8

GILT #2964

25 µg/kg MCVST-A iv

Time = minutes in relation to the dose of MCVST-A.

Kid1 and Kid2 = kidney perfusion measured from 2 TPD (temperature pulse decay) probes in ml/min gm.

Liv1, Liv2, and Liv3 = liver perfusion measured from 3 TPD probes in ml/min gm.

AoM = aortic mean pressure in mmHg.

-- = data not available.

Note: The organ perfusion and blood pressure parameters were measured every 6 minutes from 120 to 300 minutes postdosing. Half of the 3-minute averages presented in this raw data from 120 to 300 minutes are means of the 2 closest 6-minute values. Example: The 129-minute organ perfusion and blood pressure values were derived by taking the mean of the data collected at 126 and 132 minutes. Six-minute means for hepatic and renal perfusion and arterial mean pressure were calculated from this raw data.

Time	Kid1	Kid2	Liv1	Liv2	Liv3	AoM
-27	6.23	3.15	1.8	5.32	2.1	103.6
-24	6.71	3.54	2.05	5.62	2.41	99.7
-21	6.63	3.38	1.78	5.13	3.5	100.7
-18	6.14	3.5	1.83	3.91	2.46	100.5
-15	6.3	3.31	2.14	4.39	2.43	101.8
-12	6.5	3.28	2.1	3.84	2.82	98.6
-9	7.6	4.11	2.05	4.23	2.71	101.3
-6	6.72	3.6	2.1	4.47	2.55	100.5
-3	6.8	3.73	1.98	3.62	2.27	93.9
0	6.11	3.18	1.83	4.17	2.17	98.4
3	6.56	3.8	2.02	4.02	2.46	101.6
6	6.58	3.5	2.11	4.48	2.95	100.8
9	6.46	3.6	2.23	4.05	2.87	101.9
12	6.67	3.76	2.27	4.16	3.1	101.5
15	6.85	3.9	2.07	4.38	3.16	102.2
18	7.68	4.56	2.18	4.27	4.29	104
21	6.81	3.68	1.92	3.78	2.88	98.1
24	7.28	4.1	2.04	3.6	3.73	100
27	7.13	4.1	1.73	4.04	2.93	101.3
30	7.5	4.29	1.73	3.89	3.35	100.9
33	6.09	3.38	1.39	4.18	2.18	96.6
36	7.53	4.15	1.71	3.45	3.15	100.8
39	7.6	4.23	1.56	3.41	3.82	100.6
42	5.73	3.32	1.53	3.27	2.27	100.3
45	6.71	3.94	1.19	3.19	2.27	104.2
48	6.36	3.7	1.26	3.18	1.89	99.7
51	6.46	3.58	1.49	3.36	2.22	95

Time	Kid1	Kid2	Liv1	Liv2	Liv3	AoM
54	6.96	4	1.35	3.21	2.88	104.9
57	6.46	3.61	1.3	3.28	2.27	109.4
60	8.1	4.67	1.39	3.26	2.94	100.1
63	7.79	4.35	1.21	3.25	2.58	99.9
66	--	3.64	1.2	3.47	2.47	98
69	--	4.72	1.01	2.93	2.42	100.4
72	8.22	4.48	1.52	3.62	2.44	104.6
75	7.19	4	0.94	3.03	1.97	106
78	6.08	3.19	1.06	3.13	1	102.9
81	7.79	4.17	1.01	2.82	2.4	100.8
84	7.36	4.09	0.88	2.84	1.64	107.2
87	7.22	3.94	1.15	2.95	1.99	102.2
90	8.05	4.58	1.08	3.06	2.5	105
93	8.41	4.6	1.14	3.12	3.48	97.8
96	6.81	3.93	0.59	2.7	1.58	102.6
99	6.82	3.55	0.74	2.77	1.46	97.1
102	7.3	4.12	1.15	2.83	2.27	95
105	8.06	4.36	0.98	3.36	2.84	102.1
108	8.14	4.34	1.11	2.99	1.61	102
111	7.2	3.69	0.94	2.68	1.74	95.3
114	8.44	4.82	1.16	3.03	2.36	104.3
117	6.89	3.91	0.97	3.15	1.82	101
120	8.45	4.72	1	3.13	2.56	102.3
123	8.24	4.31	1.08	3.01	3.51	101.1
126	8.03	3.9	1.16	2.88	4.46	100
129	7.9	4.1	1.41	3.02	4.38	95.8
132	7.77	4.29	1.65	3.16	4.29	91.5
135	8.17	4.46	1.6	3.08	4.44	95.6
138	8.57	4.62	1.55	2.99	4.59	99.7
141	--	4.05	1.44	3.22	4.19	95.3
144	--	3.47	1.33	3.45	3.79	90.8
147	--	3.83	1.67	3.69	3.86	93.9
150	7.78	4.18	2	3.93	3.93	97
153	--	4.45	2.03	4.15	4.84	98.4
156	--	4.71	2.05	4.37	5.74	99.9
159	--	4.33	1.97	3.77	--	100.2
162	8.03	3.95	1.88	3.17	--	100.6
165	7.82	3.9	1.98	3.57	--	93.7
168	7.6	3.85	2.08	3.97	4.33	86.8
171	7.85	4.09	2.28	4.4	4.19	91.4
174	8.09	4.33	2.48	4.82	4.04	96.1
177	8.16	4.37	2.01	4	3.51	95.7
180	8.22	4.4	1.53	3.18	2.98	95.2
183	8.14	4.46	1.41	3.34	2.65	90.8
186	8.06	4.52	1.29	3.49	2.32	86.4
189	8.34	4.54	1.43	3.64	2.43	88.3
192	8.61	4.56	1.57	3.78	2.53	90.3
195	--	4.64	1.53	3.44	2.63	95.6
198	--	4.72	1.48	3.1	2.72	100.9

Time	Kid1	Kid2	Liv1	Liv2	Liv3	AoM
201	--	4.35	1.59	3.21	2.2	98.4
204	7.23	3.98	1.69	3.31	1.67	96
207	7.41	4.03	1.46	3.33	1.91	92.1
210	7.58	4.08	1.23	3.34	2.14	88.2
213	7.33	4.06	1.71	3.34	2.37	92.4
216	7.07	4.03	2.18	3.34	2.6	96.7
219	7.11	4.06	2.06	3.75	2.92	96.1
222	7.14	4.08	1.94	4.16	3.23	95.5
225	7.36	4.13	1.89	4.37	3.21	94.6
228	7.58	4.17	1.83	4.58	3.19	93.6
231	6.75	3.89	1.89	4.66	2.78	92.8
234	5.91	3.61	1.95	4.74	2.36	92
237	6.32	3.94	1.81	3.78	2.52	91.8
240	6.73	4.26	1.66	2.81	2.67	91.6
243	6.78	4.32	1.83	2.82	2.76	92.8
246	6.82	4.38	1.99	2.82	2.84	94
249	7.12	4.48	1.64	2.9	3.15	91.9
252	7.41	4.57	1.28	2.98	3.45	89.8
255	7.07	4.31	1.47	2.89	2.87	89.4
258	6.73	4.04	1.66	2.8	2.28	89
261	6.8	4.16	1.56	2.85	2.44	90.8
264	6.87	4.27	1.46	2.89	2.6	92.7
267	7.37	4.54	1.44	3.02	3.15	88.8
270	7.87	4.8	1.41	3.14	3.69	84.8
273	7.32	4.43	1.38	3.08	3.21	88.2
276	6.77	4.05	1.35	3.01	2.72	91.5
279	7.28	4.31	1.23	3.1	2.64	88.1
282	7.78	4.56	1.11	3.19	2.56	84.7
285	7.42	4.35	1.34	3.3	2.25	87.3
288	7.05	4.13	1.56	3.4	1.93	89.9
291	6.19	3.66	1.36	3.24	1.77	92.5
294	5.32	3.18	1.15	3.08	1.6	95.1
297	6.16	3.71	1.26	3.1	1.73	90.4
300	7	4.23	1.37	3.11	1.85	85.8

GILT #2957

25 µg/kg MCYST-A iv

Time = minutes in relation to the dose of MCYST-A.

Kid1 = kidney perfusion measured from 1 TPD (temperature pulse decay) probe in ml/min gm.

Liv1, Liv2, Liv3, and Liv4 = liver perfusion measured from 4 TPD probes in ml/min gm.

AoM = aortic mean pressure in mmHg.

-- = data not available.

Note: The organ perfusion and blood pressure parameters were measured every 6 minutes from 120 to 300 minutes postdosing. Half of the 3-minute averages presented in this raw data from 120 to 300 minutes are means of the 2 closest 6-minute values. Example: The 129-minute organ perfusion and blood pressure values were derived by taking the mean of the data collected at 126 and 132 minutes. Six-minute means for hepatic and renal perfusion and arterial mean pressure were calculated from this raw data.

Time	Kid1	Liv1	Liv2	Liv3	Liv4	AoM
-27	5.03	2.23	1.82	2.39	5.26	122.3
-24	5.83	1.67	2.55	1.39	6.39	122.4
-21	5.8	2.7	2.54	1.75	6.37	123.9
-18	5.53	2.31	2.52	1.91	6.48	123.4
-15	7.22	1.76	1.51	1.24	4.07	120.6
-12	5.75	2.33	2.54	3.48	6.67	123.9
-9	5.02	2.27	2.18	3.86	5.25	126.1
-6	4.19	2.24	2.29	2.53	5.17	121.3
-3	5	2.39	2.42	1.65	5.47	118.3
0	4.35	2.32	2.64	2.36	6.39	118.4
3	4.82	2.2	2.22	2.67	5.37	121.3
6	4.19	1.64	1.06	3.52	3.7	115.3
9	2.53	2.03	1.24	3.31	3.94	113.4
12	2.65	1.88	1.96	0.62	4.16	112.6
15	4.1	2.58	2.47	3.09	5.37	112.6
18	3.14	1.84	1.99	2.02	4.73	113.1
21	4.45	2.08	1.78	4.29	5.07	111.8
24	4.14	2.57	2.54	2.81	5.47	111.5
27	4.01	1.81	1.56	3.23	3.83	106.7
30	4.88	2.24	2.34	2.02	5.22	103.1
33	5.77	2.35	2.29	3.29	5.37	101.6
36	4.5	2.15	2.16	2.23	3.94	104.9
39	3.84	2.07	2.19	3.06	4.65	101.1
42	3.25	1.88	1.8	1.43	4.01	97.2
45	4.36	1.91	1.94	3.2	4.27	95.5
48	3.66	1.43	1.83	2.07	4.06	93.2

Time	Kid1	Liv1	Liv2	Liv3	Liv4	AoM
51	3.61	2.62	2.89	2.12	4.86	95.8
54	4.61	1.87	1.84	2.33	4.41	99.1
57	3.03	2.32	1.73	2.11	4.05	97.4
60	3.99	1.86	2.08	2.68	4.55	96.1
63	2.55	1.7	2.32	2.84	4.95	89.6
66	4.02	1.66	1.96	3.85	4.43	84
69	3	1.38	1.76	1.99	4.08	85.2
72	2.48	1.57	1.91	2.03	4.14	86.8
75	3.81	1.68	1.56	2.43	4.32	86.2
78	3.53	1.18	1.75	1.69	3.91	87.5
81	2.88	2.02	2.2	2.73	4.9	85.3
84	2.87	2.31	1.8	4.69	4.02	85.3
87	2.25	2.14	2.07	3.04	4.6	87.9
90	2.9	1.77	1.83	2.79	3.94	89
93	--	1.97	2.72	2.27	4.94	92.3
96	1.75	1.38	2.41	1.52	4.11	91.8
99	2.4	2.19	2.92	1.82	5	90.2
102	1.39	1.61	2.27	2.25	3.93	89.2
105	1.94	1.59	1.62	2.55	3.38	89.5
108	1.6	1.35	1.25	1.43	2.68	86.5
111	1.94	1.62	1.94	2.23	4.05	86.6
114	1.18	1.79	2.26	2.3	4.05	86.5
117	1.23	1.5	1.68	1.35	3.66	83.2
120	0.82	1.63	2.33	1.34	4.05	86.5
123	--	1.78	2.26	1.81	4.04	85.1
126	--	1.93	2.18	2.27	4.02	83.7
129	--	1.75	1.97	1.84	3.96	85.6
132	1.5	1.56	1.75	1.4	3.9	87.5
135	1.7	1.66	2.39	2.41	4.3	87.2
138	1.9	1.76	3.02	3.42	4.69	86.9
141	1.89	2.09	3.36	3.84	5.37	85.05
144	1.87	2.42	3.7	4.25	6.05	83.2
147	1.54	2.16	3.04	4.03	5.05	83.95
150	1.2	1.89	2.37	3.81	4.04	84.7
153	--	1.84	2.49	3.54	4.52	86.35
156	--	1.79	2.61	3.26	4.99	88
159	--	2.23	2.51	--	4.42	87.7
162	--	2.66	2.41	--	3.85	87.4
165	--	2.08	2.23	--	3.78	86.3
168	--	1.5	2.05	2.63	3.71	85.2
171	--	--	--	--	--	--
174	--	--	--	--	--	--
177	--	--	--	--	--	--
180	--	--	--	--	--	--
183	--	--	--	--	--	--
186	--	1.37	3.03	--	4.57	--
189	3.21	1.89	1.89	--	3.07	93.1
192	2.49	1.9	2.43	2.21	4.59	88.5
195	3.09	1.95	2.38	2.25	4.44	87.45

Time	Kid1	Liv1	Liv2	Liv3	Liv4	AoM
198	3.68	1.99	2.32	2.31	4.29	86.4
201	3.9	2.15	2.43	3.72	4.06	85.7
204	4.11	2.31	2.54	5.13	3.83	85
207	4.1	2.09	1.76	4.16	3.87	86.25
210	4.08	1.87	0.97	3.18	3.9	87.5
213	4	1.9	1.07	3.03	3.65	90.95
216	3.92	1.93	1.16	2.87	3.4	94.2
219	3.9	1.95	0.99	2.43	3.75	94.85
222	3.87	1.96	0.82	1.98	4.09	95.5
225	3.48	2	0.73	2.48	3.9	95.2
228	3.09	2.04	0.63	2.98	3.7	94.9
231	3.5	2.14	0.8	2.84	3.74	93.8
234	3.91	2.23	0.97	2.69	3.78	92.7
237	3.69	2.16	1.47	2.63	3.73	91.1
240	3.46	2.09	1.97	2.57	3.68	89.5
243	3.78	2.07	2.14	2.77	4.05	89.1
246	4.09	2.05	2.31	2.97	4.42	88.7
249	3.7	1.84	2.12	2.91	3.89	89.1
252	3.3	1.63	1.92	2.85	3.35	89.5
255	3.4	1.79	2.23	2.34	3.49	89.8
258	3.5	1.94	2.54	1.82	3.63	90.1
261	3.6	2.02	2.42	2.11	3.9	90.05
264	3.69	2.1	2.29	2.4	4.16	90
267	3.36	1.92	2.14	2.04	4.02	90.65
270	3.02	1.73	1.98	1.68	3.88	91.3
273	2.8	1.81	2.55	2.18	3.94	99.45
276	2.58	1.88	3.12	2.68	4	87.6
279	2.89	1.79	1.62	2.33	3.24	87.95
282	3.19	1.69	0.12	1.97	2.48	88.3
285	3.42	1.95	0.29	2.1	3.11	90.4
288	3.64	2.21	0.46	2.22	3.73	92.5
291	3.03	1.83	0.42	1.61	3.44	92.5
294	2.42	1.44	0.37	0.99	3.14	92.5
297	2.51	1.69	0.62	1.22	3.44	89.45
300	2.6	1.94	0.87	1.45	3.74	86.4

Time = minutes in relation to the dose of MCYST-A.

Kid1 and Kid2 = kidney perfusion measured from 2 TPD (temperature pulse decay) probes in ml/min gm.

Liv1, Liv2, Liv3, and Liv4 = liver perfusion measured from 4 TPD probes in ml/min gm.

AoM = aortic mean pressure in mmHg.

-- = data not available.

Note: The organ perfusion and blood pressure parameters were measured every 6 minutes from 120 to 300 minutes postdosing. Half of the 3-minute averages presented in this raw data from 120 to 300 minutes are means of the 2 closest 6-minute values. Example: The 132-minute organ perfusion and blood pressure values were derived by taking the mean of the data collected at 129 and 135 minutes. Six-minute means for hepatic and renal perfusion and arterial mean pressure were calculated from this raw data.

Time	Kid1	Kid2	Liv1	Liv2	Liv3	Liv4	AoM
-27	3.72	4.52	--	2.69	1.55	1.24	104.2
-24	4.27	4.79	--	1.88	1.38	1.98	107.3
-21	3.49	4.09	--	2.66	1.48	1.97	104.8
-18	3.13	4.1	4.13	1.36	1.06	1.46	106.9
-15	2.79	3.6	3.94	1.43	0.47	0.93	110.9
-12	3.16	3.63	4.11	1.95	1.18	1.7	105.4
-9	3.68	4.07	4.72	1.71	0.84	1.69	110.6
-6	2.85	3.83	3.27	1.28	0.89	1.92	109.1
-3	3.27	3.56	3.91	0.82	0.91	1.09	109.1
0	3.65	4.03	4.7	2.76	1.55	1.81	109.3
3	3.63	4.22	4.77	1.73	1.03	1.65	113.2
6	3.59	4.17	4.26	1.09	1.29	1.34	110.4
9	3.26	3.53	4.32	1.62	0.86	1.77	111.7
12	3.01	3.68	3.35	--	0.84	1.46	107.9
15	3.57	4.01	4.12	1.79	1.62	1.62	105.2
18	2.46	2.96	2.75	2.81	2.15	1.36	101.2
21	3.12	3.95	3.55	2.1	1.32	1.07	100.6
24	2.01	2.69	2.15	2.02	1.76	1.08	101.5
27	3.17	4.13	3.37	2.78	1.55	0.52	101.5
30	3.24	3.72	3.68	1.51	0.42	0.63	99.5
33	1.85	4.43	5.34	2.2	0.84	0.69	96
36	1.54	2.07	1.99	0.11	0.36	0.87	97
39	3.87	4.57	4.7	2.91	1.57	1.2	97.9
42	3.4	4.16	4.26	1.58	0.97	0.97	94.9
45	3.02	3.61	3.66	2.29	0.97	0.92	94.6
48	4.78	4.96	--	0.65	--	0.89	94.5

Time	K1d1	K1d2	L1v1	L1v2	L1v3	L1v4	AoM
51	3.54	3.98	4.45	1.12	0.75	1.09	95.1
54	2.14	2.63	2.49	1.09	0.43	0.99	92.7
57	3.56	3.9	4.76	1.52	0.91	1.55	89.6
60	3.53	4.21	4.6	1.86	0.84	0.84	90.6
63	2.46	3.4	3.18	0.95	0.49	0.63	89
66	3.54	4.14	3.55	2.53	1.47	0.77	90.3
69	3.71	4.08	4.71	2.49	1.02	0.67	89
72	2.84	2.11	4.02	1.29	0.56	0.87	89.9
75	2.98	3.35	3.35	1.74	1.23	0.71	90
78	3.07	3.47	3.97	1.46	0.57	0.77	90.2
81	3.75	3.74	4.63	1.36	0.6	0.63	89.1
84	3.38	3.8	4.14	0.98	0.83	0.64	85.8
87	2.85	3.46	3.34	1.1	0.36	0.25	83.5
90	1.86	2.58	1.78	1.87	1.38	0.47	80.9
93	2.61	3.66	4.2	0.34	0.1	0.42	63.2
96	1.98	3.43	1.86	0.75	0.46	0.57	65.8
99	--	--	--	1.37	0.81	0.43	76.4
102	2.76	3.78	3.55	1.44	0.85	0.38	76
105	2.93	3.63	3.84	1.24	0.5	0.47	81.9
108	3.34	3.94	4.48	1.41	0.67	0.25	84.9
111	3.35	4.2	4.22	1.66	0.95	0.39	88.4
114	1.55	1.73	1.76	1.64	0.83	0.26	72.7
117	3.37	3.42	4.75	1.13	0.4	0.44	78.8
120	2.85	2.91	4.52	0.52	0.05	0.63	78.1
123	2.96	3.37	4.44	1.04	0.52	0.55	79.8
126	3.06	3.82	4.35	1.55	0.99	0.47	91.4
129	3.27	3.97	4.2	1.07	0.67	0.6	85.7
132	2.48	3.11	3.32	0.73	0.58	0.68	84.3
135	1.69	2.25	2.43	0.38	0.48	0.76	82.8
138	2.29	2.87	2.91	1.01	0.8	0.46	81.7
141	2.88	3.49	3.38	1.63	1.12	0.16	80.6
144	3.1	3.43	3.81	1.52	0.79	0.16	80.5
147	3.32	3.36	4.23	1.4	0.45	0.16	80.4
150	2.71	2.82	3.71	0.94	0.32	0.35	76.3
153	2.09	2.27	3.18	0.47	0.19	0.54	72.3
156	2.08	2.32	2.91	1.05	0.58	0.37	73
159	2.06	2.36	2.63	1.63	0.96	0.19	73.7
162	2.09	2.2	2.31	1.69	1.02	0.2	72.5
165	2.12	2.04	1.99	1.74	1.07	0.21	71.3
168	1.86	2.33	2.08	1.38	1.14	0.29	78.3
171	1.59	2.62	2.16	1.01	1.21	0.37	85.4
174	2.16	2.95	2.66	1.17	1.15	0.37	86.2
177	2.73	3.28	3.16	1.32	1.09	0.36	86.9
180	2.34	2.59	3.07	1.12	0.66	0.48	79.4
183	1.95	1.89	2.97	0.91	0.22	0.59	71.9
186	2.15	2.22	3.33	0.98	0.32	0.48	73.5
189	2.34	2.55	3.69	1.04	0.41	0.36	75.1
192	2.28	2.5	3.62	1.34	0.49	0.49	75.4
195	2.21	2.45	3.54	1.64	0.56	0.62	75.7

Time	Kid1	Kid2	Liv1	Liv2	Liv3	Liv4	AOM
198	1.71	1.78	2.9	1.03	0.37	0.62	71.6
201	1.2	1.1	2.26	0.41	0.18	0.62	67.4
204	1.54	1.49	2.66	0.76	0.3	0.58	68.1
207	1.88	1.88	3.06	1.1	0.41	0.54	68.7
210	1.46	1.34	2.1	0.86	0.3	0.51	68.2
213	1.03	0.8	1.14	0.61	0.19	0.48	67.6
216	1.23	1	1.76	0.88	0.2	0.43	66.3
219	1.42	1.2	2.38	1.15	0.21	0.37	64.9
222	1.44	1.24	2.29	1.18	0.44	0.4	72.1
225	1.45	1.27	2.2	1.21	0.66	0.43	79.3
228	1.58	1.41	2.19	1.21	0.51	0.37	77.9
231	1.71	1.55	2.17	1.2	0.36	0.3	76.5
234	1.95	1.86	2.34	1.32	0.47	0.35	76.3
237	2.18	2.16	2.5	1.43	0.57	0.4	76.1
240	1.87	1.83	2.33	1.11	0.29	0.3	73.4
243	1.56	1.49	2.16	0.79	0	0.19	70.7
246	1.5	1.27	2.09	0.8	0.07	0.3	70.1
249	1.43	1.05	2.01	0.8	0.13	0.4	69.5
252	1.25	0.98	1.77	1.06	0.37	0.42	67.1
255	1.06	0.9	1.52	1.32	0.6	0.43	64.7
258	1.15	0.68	1.5	1.09	0.48	0.53	63
261	1.23	0.46	1.48	0.85	0.35	0.63	61.2
264	1.39	0.93	1.83	1.09	0.53	0.61	64.5
267	1.55	1.39	2.17	1.32	0.7	0.56	67.8
270	1.42	1.18	1.88	1.17	0.63	0.48	69
273	1.28	0.97	1.59	1.01	0.56	0.37	70.2
276	1.32	1.08	2.05	0.87	0.38	0.38	70.7
279	1.35	1.19	2.5	0.73	0.19	0.38	71.1
282	1.26	1.23	2.37	0.83	0.17	0.41	70.2
285	1.17	1.27	2.23	0.92	0.14	0.43	69.3
288	1.41	1.17	2.43	0.97	0.3	0.58	69.2
291	1.64	1.07	2.62	1.01	0.45	0.72	69
294	1.52	1.18	2.33	0.82	0.35	0.62	69.2
297	1.39	1.28	2.04	0.62	0.24	0.52	69.3
300	1.37	1.1	2.15	0.78	0.52	0.62	71.9

GILT #3312

25 µg/kg MCYST-A iv

Time = minutes in relation to the dose of MCYST-A.

Kid1, Kid2, and Kid3 = kidney perfusion measured from 3 TPD (temperature pulse decay) probes in ml/min gm.

Liv1 and Liv2 = liver perfusion measured from 2 TPD probes in ml/min gm.

AoM = aortic mean pressure in mmHg.

-- = data not available.

Note: The organ perfusion and blood pressure parameters were measured every 6 minutes from 120 to 300 minutes postdosing. Half of the 3-minute averages presented in this raw data from 120 to 300 minutes are means of the 2 closest 6-minute values. Example: The 129-minute organ perfusion and blood pressure values were derived by taking the mean of the data collected at 126 and 132 minutes. Six-minute means for hepatic and renal perfusion and arterial mean pressure were calculated from this raw data.

Time	Kid1	Kid2	Kid3	Liv1	Liv2	AoM
-27	5	5.5	4.85	2.43	1.37	116.7
-24	5.27	5.89	5.58	2.68	1.54	123.9
-21	4.98	5.68	5.21	2.7	1.26	124.2
-18	4.93	6.05	4.93	2.71	1.68	119
-15	5.08	5.98	5.39	2.84	1.64	124.5
-12	5.31	6.09	5.32	2.86	1.96	132.1
-9	5.48	6.48	5.65	2.77	1.88	118.6
-6	5.5	6.28	5.47	2.89	1.93	125.9
-3	5.16	5.97	5.33	2.65	1.44	126.1
0	4.88	5.78	4.77	2.41	1.29	119.9
3	5.09	5.94	5.35	2.32	0.89	122.3
6	5.34	6.37	6.41	2.45	1.13	119.6
9	6.06	6.58	6.22	2.39	2.37	121.4
12	5.37	6.3	5.56	2.48	1.14	117.4
15	6.6	6.89	7.15	1.3	1.72	110.7
18	5.47	6.39	5.59	1.56	1.99	107.8
21	5.68	6.49	5.76	1.19	1.22	98.2
24	5.01	5.65	5.21	1.06	1.77	97.6
27	6.5	6.56	7.03	0.91	1.7	96.6
30	4.53	5.17	4.25	0.58	0.55	95.2
33	5.57	6	5.98	1.04	2	94.1
36	4.97	5.19	5.03	1.32	2.13	94.4
39	5.04	5.86	5.38	1.17	2.29	93.9
42	3.14	3.9	3.53	0.79	0	92
45	4.44	6.23	4.59	1.43	1.6	98.7
48	4.16	5.77	3.04	1.21	2.62	93.3
51	3.5	4.81	4.66	0.85	1.46	93.4

Time	Kid1	Kid2	Kid3	Liv1	Liv2	AoM
54	3.47	4.6	4.59	0.56	1.21	92.7
57	3.49	5.04	4.49	1.04	0.99	93.1
60	2.85	4.56	3.97	1.39	2.86	92.8
63	3.96	5.49	5.23	1.37	1.8	93.5
66	--	--	--	1.33	1.08	92.7
69	4.45	5.59	5.23	1.3	2.65	90.5
72	4.09	5.61	5.92	1.09	--	89.8
75	3.6	4.88	4.59	1.28	2.97	90.2
78	4.07	5.5	5.1	1.25	2.42	95.6
81	3.9	5.24	4.92	1.38	2.39	96.2
84	4.17	5	4.95	1.26	2.41	94.3
87	2.8	3.56	3.25	1.07	2.09	93.1
90	3.69	4.68	3.74	1.64	2.2	86.9
93	4.5	5.49	3.76	1.95	0.86	87.3
96	3.18	4.22	3.22	1.07	1.79	80.3
99	3.33	4.25	3.56	1.15	1	81.7
102	2.92	3.74	3.04	1.44	1.58	81.3
105	3.04	3.86	3.54	1.48	1.39	80.8
108	3.61	4.08	3.34	1.39	2.77	79.9
111	2.26	--	2.16	1.31	1.89	81.7
114	4.61	5.45	3.74	2.44	5.73	84.2
117	2.26	2.61	2.47	1.12	3.91	79.7
120	3.36	4.12	4.12	1.14	4.44	79.4
123	2.82	3.87	1.76	1.08	5.91	76.8
126	2.27	3.61	3.39	1.01	7.37	74.2
129	2.61	3.47	3.16	1.08	7.13	75.3
132	2.94	3.33	2.93	1.15	6.88	76.4
135	2.95	3.49	2.93	0.97	5.73	75.9
138	2.95	3.64	2.93	0.78	4.58	75.4
141	3.2	3.51	2.89	0.77	--	77.1
144	3.45	3.38	2.84	0.76	--	78.7
147	3.07	3.35	2.78	0.95	--	78.2
150	2.68	3.32	2.72	1.13	4.7	77.6
153	2.93	3.53	2.9	0.91	4.28	76.4
156	3.18	3.74	3.08	0.69	3.85	75.2
159	--	3.3	--	0.72	4.3	74.2
162	--	2.85	--	0.75	4.75	73.2
165	--	2.39	--	0.73	--	71.6
168	2.09	1.92	2.63	0.71	--	70
171	2.33	2.54	2.41	0.74	--	72.3
174	2.56	3.15	2.19	0.76	5.14	74.6
177	1.9	2.17	1.56	0.88	4.15	72.8
180	1.24	1.19	0.93	1	3.16	71.1
183	1.33	1.57	1.11	1.01	3.24	70.2
186	1.41	1.94	1.28	1.01	3.31	69.2
189	1.51	1.91	1.44	1.16	3.78	69.3
192	1.66	1.87	1.59	1.3	4.25	69.3
195	1.42	1.62	1.9	1.22	4.57	69.9
198	1.18	1.36	2.21	1.14	4.88	70.5

Time	Kid1	Kid2	Kid3	Liv1	Liv2	AOM
201	1.27	1.55	2.11	1.14	4.81	69.6
204	1.36	1.74	2.01	1.13	4.73	68.6
207	1.73	2.25	2.4	1.15	5.32	68.1
210	2.1	2.76	2.78	1.16	5.9	67.5
213	1.87	2.51	2.13	1.21	5.43	67.9
216	1.64	2.25	1.47	1.25	4.96	68.3
219	1.84	2.3	1.81	1.21	4.66	68.6
222	2.03	2.34	2.15	1.16	4.35	68.9
225	1.77	2.3	--	1.23	4.38	68.3
228	1.5	2.26	--	1.29	4.41	67.8
231	1.73	2.33	--	1.33	4.89	68.8
234	1.96	2.39	2.32	1.37	5.36	69.7
237	2.36	2.37	2.71	1.3	5.12	70.6
240	2.76	2.35	3.1	1.23	4.88	71.4
243	2.37	2.71	2.93	1.3	4.8	70.7
246	1.98	3.07	2.76	1.37	4.72	69.9
249	2.06	2.97	2.89	1.34	--	68.4
252	2.14	2.87	3.02	1.3	--	66.9
255	2.35	3.1	3.08	1.31	--	69.2
258	2.56	3.33	3.13	1.31	4.1	71.4
261	2.46	3.07	3.04	1.48	4.4	69.3
264	2.36	2.81	2.95	1.65	4.7	67.2
267	2.29	2.84	2.84	1.56	4.62	67.3
270	2.21	2.86	2.73	1.47	4.53	67.3
273	2.19	2.68	2.77	1.53	4.91	66.8
276	2.16	2.49	2.8	1.58	5.28	66.4
279	2.26	2.7	3.11	1.78	5.28	67.6
282	2.36	2.9	3.42	1.97	5.28	68.7
285	2.34	2.93	3.25	1.9	5.69	68.2
288	2.31	2.96	3.07	1.82	6.1	67.7
291	2.28	2.85	2.94	1.84	5.09	70.7
294	2.24	2.73	2.81	1.86	4.07	73.7
297	2.43	3.02	3.18	1.83	4.11	75.5
300	2.61	3.31	3.54	1.8	4.14	77.3

Time = minutes in relation to the dose of MCYST-A.

Kid1, Kid2, and Kid3 = kidney perfusion measured from 3 TPD (temperature pulse decay) probes in ml/min gm.

Liv1, Liv2 and Liv3 = liver perfusion measured from 3 TPD probes in ml/min gm.

AoM = aortic mean pressure in mmHg.

-- = data not available.

Note: Six-minute means for hepatic and renal perfusion and arterial mean pressure were calculated from this raw data.

Time	Kid1	Kid2	Kid3	Liv1	Liv2	Liv3	AoM
-27	--	4.69	5.84	3.81	5.32	4.19	104.5
-24	--	5.02	4.91	--	4.75	3.06	112.9
-21	--	4.18	5.18	2.7	4.37	2.99	113.7
-18	3.79	4.56	5.11	3.91	4.79	3.02	104.6
-15	2.66	4.2	4.1	3	5.5	3.02	101.1
-12	2.6	4.35	5.75	3.72	4.6	2.31	101.4
-9	2.37	4.23	--	2.81	4.8	3.1	100.3
-6	3.37	5.21	--	4.95	5.19	4.2	103.2
-3	1.92	5.12	3.56	2.88	3.05	1.6	99
0	3.44	5.39	6.31	3.15	5.25	3.49	102.4
3	3.18	5.16	5	3.11	4.84	3.02	107.9
6	3.21	5.16	5.62	2.4	3.49	1.96	105.7
9	2.93	4.73	4.2	2.81	3.98	2.4	101.7
12	3.27	5.4	7.19	3.84	3.6	3.6	100.3
15	2.86	4.82	3.71	2.66	3.75	1.8	96.4
18	2.53	3.8	3.3	2.22	3.23	1.77	96.3
21	3.86	6.78	7.94	3.67	3.92	3.64	98.9
24	2.97	4.56	7.35	2.79	3.04	3.16	97.8
27	3.05	5.27	6.43	2.65	2.61	2.24	99.6
30	3.88	6.15	7.09	2.86	3.02	1.9	100.2
33	2.77	4.45	6.41	2.71	1.88	1.27	99
36	2.97	5.02	6.78	2.9	2.07	1.55	101.8
39	2.55	5.05	4.72	1.82	1.37	0.47	98.8
42	3.44	5.74	7.01	1.1	2.52	1.18	99.1
45	3.21	6.01	5.12	2.79	1.47	0.89	100
48	2.77	4.42	6	2.86	1.83	1.24	103.7
51	2.82	3.74	5.89	1.19	1.79	0.53	106.3
54	2.9	4.42	4.87	0.9	1.37	0.16	103.5
57	3.09	4.82	5.27	1.37	1.14	0.39	102.6
60	3.04	5.42	4.41	1.09	1.18	0.88	103.6
63	2.01	2.88	3.7	1.24	1.07	0.72	96.9
66	--	--	--	--	--	--	89.9

Time	Kid1	Kid2	Kid3	Liv1	Liv2	Liv3	AoM
69	1.33	3.13	--	0.17	0.41	0.5	91
72	0.92	--	--	0.03	0.14	0	83
75	--	--	--	0	0.15	0.09	75.1
78	1.6	3.18	--	0.07	0.14	0.47	65.9
81	1.56	2.66	--	0.12	0.14	0.26	65
84	--	--	0.67	--	0.17	0.07	58.7
87	--	--	6.29	0.49	0.1	0.11	62.3
90	0	0	0.16	0	0.16	0.07	56.5
93	0.11	0.06	0.44	0.09	0.04	0	61.5
96	--	--	--	0	0.07	0	63.6
99	0.72	1.2	2.31	0.03	0.2	0.12	59.5
102	1.19	2.04	3.45	0.3	0.16	0.07	62.9
105	0.43	0.58	3.2	0	0.13	0.03	61.1
108	--	--	--	0	0.06	0	56.7
111	0.58	--	--	0	0.03	0	59.3
114	--	--	--	0.5	0.06	0.03	59.5
117	0.28	0	1.89	0	0.09	0	54.3
120	0.62	0.6	1.57	0.12	0	0	51.9
123	0.03	--	0.73	0	0.09	0	51.2
126	0	--	0.68	0	0	0	51.1
129	0.52	0	0.67	0	0	0	50.2
132	0.85	0.65	1.43	0.11	0	0	51
135	--	--	--	0	0	0	50
138	0.04	--	0.5	0	0	0	51.5
141	0.41	0	0.49	0	0	0	50.6
144	0.05	0	0.23	0	0.04	0	50.4
147	0.73	0	1.11	0	0	0	50.8
150	0.06	0.49	0.27	0.03	0	0	48.6
153	0	0.42	0.24	0.09	0	0	48
156	0	0.52	0.34	0.06	0	0	46.7
159	0	0.07	0	0	0	0	48.3
162	0.13	0.5	0.17	0	0	0	52.3
165	0	0.38	0	0.15	0	0	53.2
168	0	0.57	0	0	0	0	50.9
171	0	0	0.02	0	0	0.05	51.8
174	0.27	0	0	0	0.02	0.09	47.1
177	0	0	0	0	0	0	32.6
180	0	0	0	0	0.06	0	23.1

GILT #3015

72 µg/kg MCYST-A iv

Time = minutes in relation to the dose of MCYST-A.

Kid1, Kid2, and Kid3 = kidney perfusion measured from 3 TPD (temperature pulse decay) probes in ml/min gm.

Liv1, Liv2, and Liv3 = liver perfusion measured from 3 TPD probes in ml/min gm.

AoM = aortic mean pressure in mmHg.

-- = data not available.

Note: Six-minute means for hepatic and renal perfusion and arterial mean pressure were calculated from this raw data.

Time	Kid1	Kid2	Kid3	Liv1	Liv2	Liv3	AoM
-27	4.81	4.87	6.94	1.95	5.18	--	111.3
-24	4.98	5.35	6.83	2.07	5.15	5.58	111.9
-21	4.37	4.38	--	2.09	4.77	3.99	112.6
-18	--	--	--	2.41	5.5	--	--
-15	4.13	4.18	6.95	2.11	4.04	4.43	117.3
-12	5.04	5.48	7.05	2.36	5.28	5.49	105.1
-9	4.84	5.27	6.88	2.05	5.34	4.94	110.8
-6	5.08	4.98	6.79	2.14	5.19	4.53	113.2
-3	--	--	--	2.19	5.05	5.04	--
0	4.79	4.37	7.16	2.26	5.72	6.58	120.3
3	4.91	5.31	7	1.87	5.41	4.84	117.1
6	4.92	4.95	6.11	1.79	4.69	4.28	115.9
9	4.8	4.81	6.64	1.86	4.21	4.36	116.3
12	4.55	4.53	6.31	1.85	4.17	3.92	113.5
15	5.04	4.69	7.67	1.45	3.38	3.99	112.5
18	4.27	4.42	6.31	1.21	1.88	2.1	106.8
21	--	--	6.34	2.27	0	1.1	100
24	4.34	3.02	5.12	1.53	0	0.54	61.1
27	1.08	1.12	2.16	0.14	0.03	0.17	37.5
30	0.49	0.25	0.35	0.04	0	0	34
33	0	0	--	0	0	0	32.2
36	0.34	0.52	1.05	0.15	0	0	40.6
39	0.76	1	1.74	0.28	0.09	0.04	45.6
42	0.71	0.67	1.7	0.41	0.41	--	48.9
45	0.44	--	0.55	1.49	0.29	0	44.6
48	--	--	0	0.26	0	0	40.3
51	0.95	--	0.65	0.45	0	--	36
54	0.39	0.3	0	0	0	0.07	31.5
57	0	0	0	0	0	0	27.1
60	0.02	0	0.11	0	0	0.07	22.1

GILT #3044

72 µg/kg MCYST-A iv

Time = minutes in relation to the dose of MCYST-A.

Kid1 and Kid2 = kidney perfusion measured from 2 TPD (temperature pulse decay) probes in ml/min gm.

Liv1, Liv2, Liv3, and Liv4 = liver perfusion measured from 4 TPD probes in ml/min gm.

AoM = aortic mean pressure in mmHg.

-- = data not available.

Note: Six-minute means for hepatic and renal perfusion and arterial mean pressure were calculated from this raw data and are presented in a graph which follows.

Time	Kid1	Kid2	Liv1	Liv2	Liv3	Liv4	AoM
-27	4.39	6.29	2.59	2.39	4.07	2.03	110.9
-24	4.51	5.33	--	2.51	4.23	1.26	109.6
-21	4.37	6.19	2.57	2.76	4.4	2.01	111.2
-18	3.69	4.89	2.06	3.02	4.17	2.46	104.9
-15	4.12	--	1.87	2.63	4.5	1.75	108.4
-12	4.3	6.01	2.62	3.11	4.92	1.66	112.6
-9	3.35	3.59	1.34	3.86	6.05	2.39	109.6
-6	4.28	4.65	1.92	2.9	4.98	1.18	109.7
-3	4.26	6.68	2.87	3.57	4.22	1.05	111.5
0	3.76	4.03	1.65	3.45	5.13	1.71	108.9
3	3.39	4.73	1.89	3.79	5.27	1.78	117.7
6	3.99	4.65	1.72	2.71	5.65	0.86	109.3
9	2.87	4.16	1.38	2.67	5.18	1.46	109.7
12	3.74	5.2	1.62	2.07	2.88	0.94	104.9
15	3.24	4.51	1.47	1.23	2.97	1.01	92.2
18	1.92	1.39	0	0.34	--	0.69	62.7
21	0.72	--	0	0.97	1.01	1.02	52
24	0.43	--	0.1	1.23	0.62	1.3	49
27	0.97	1.58	1.61	2.11	0.64	2	53.3
30	0.55	1.22	1.39	1.62	0.27	1.81	51.9
33	--	2.38	0.71	1.31	0	1.12	48
36	0.43	--	0.44	0.68	0	0.64	48.6
39	0	--	0.58	0.4	0.05	0.9	50.3
42	0.98	2.84	0.09	0.38	0	0.88	49.6
45	0.13	--	0	0.19	0	0.61	47.9
48	0.51	0.41	0	0	0	0.6	45.6
51	0.05	4.01	0	0.53	0	0.23	49.5
54	--	--	0.08	0.41	0	0.05	37.7
57	0.32	--	0	0.14	0.22	0.3	32
60	0	--	--	0	--	0.36	17.3

Time = minutes in relation to the dose of MCYST-A.

Kid1, Kid2, and Kid3 = kidney perfusion measured from 3 TPD (temperature pulse decay) probes in ml/min gm.

Liv1 and Liv2 = liver perfusion measured from 2 TPD probes in ml/min gm.

AoM = aortic mean pressure in mmHg.

-- = data not available.

Note: Six-minute means for hepatic and renal perfusion and arterial mean pressure were calculated from this raw data.

Time	Kid1	Kid2	Kid3	Liv1	Liv2	AoM
-27	6.1	6.29	4.47	2.9	2.86	110.9
-24	6.03	5.87	3.99	2.68	2.62	109.6
-21	5.99	5.83	4.23	2.68	2.22	108
-18	5.25	5.72	3.79	2.62	2.61	107.7
-15	5.55	4.87	3.37	3.12	2.67	90.8
-12	5.44	5.37	3.43	2.65	2.11	107.4
-9	5.63	5.27	3.15	2.76	2.5	106.7
-6	5.39	5.29	3.45	2.7	2.1	104.4
-3	5.86	5.68	4.26	3.06	2.27	104.9
0	6.4	6.08	4.11	2.96	2.34	105.7
3	5.8	5.91	3.93	2.61	1.95	109.2
6	5.6	5.25	3.41	3	2.02	109.5
9	6.21	6.18	4.51	2.82	2.65	111.6
12	5.39	4.94	2.95	2.65	2.36	108.2
15	4.88	4.6	2.63	2.53	1.57	107.1
18	5.43	5.08	3.14	2.07	1.89	108.7
21	5.06	4.48	2.68	2.44	1.96	105.2
24	5.55	5.66	4.97	1.23	1.15	102.2
27	4.91	5.17	4.5	1.02	0.92	101.3
30	4.53	5.33	4.42	0.49	0.44	97
33	4.65	6.03	4.64	1.38	1.47	74.2
36	4.37	4.92	3.38	0.93	1.18	62.7
39	4.09	5.35	3.01	0.75	0.8	61.8
42	3.37	4.21	2.54	0.73	0.82	65.9
45	3.12	4.62	2.53	0.75	0.95	61.8
48	2.46	3.52	1.5	0.7	0.84	68.8
51	2.19	3	0.82	0.66	1.01	61.8
54	--	--	--	0.79	0.82	65
57	2.36	4.17	3.32	0.73	0.81	60
60	1.9	3.84	2.9	0.69	0.89	60.4
63	1.54	2.86	2	0.46	0.52	57.2
66	2.08	4.2	2.95	0.65	0.8	57.5

Time	Kid1	Kid2	Kid3	Liv1	Liv2	AOM
69	0.61	1.54	0.9	0.72	0.6	56.6
72	0.69	1.69	0.62	0.9	0.58	52.1
75	1.33	2.81	1.57	0.96	0.6	51.8
78	0.94	2.15	1.05	1.13	0.85	47.7
81	0.62	1.77	0.79	1.08	0.39	48.4
84	0.5	1.5	0.4	1.04	0.43	46.4
87	0.47	1.94	0.26	1.01	0.45	45
90	0.67	1.96	0.96	0.42	0.51	45.2
93	0.47	1.38	0.11	0.5	1.11	43.6
96	0	1.16	--	0.32	0.48	41.5
99	0.2	1.49	0	0.34	0.37	42
102	1.05	3.08	1.55	0.6	0.47	41.7
105	0.35	2	0.58	0.29	0.41	41.8
108	0.69	2.62	1.11	0.25	0.31	43.2
111	1.1	2.67	2.13	0.5	0.07	41.9
114	0.34	1.71	0.97	0.38	0.49	42.8
117	0.68	2.37	1.75	0.54	0.24	42.6
120	0.28	1.86	1.02	0.56	0.2	42.1
123	0.05	0.87	0.13	0.48	0.64	40.6
126	0.14	1.2	1.02	0.63	0.36	41.3
129	0	0.68	0	0.87	0.35	39.3
132	0	0.6	0.16	0.84	0.42	38.9
135	0	0.47	0	0.77	0.36	34.6
138	0	0.24	0	0.67	0.3	40.4
141	0	0	0	0.62	0	13

GILT #3183

72 µg/kg MCYST-A iv

Time = minutes in relation to the dose of MCYST-A.

Kid1 = kidney perfusion measured from 1 TPD (temperature pulse decay) probe in ml/min gm.

Liv1, Liv2, Liv3, and Liv4 = liver perfusion measured from 4 TPD probes in ml/min gm.

AoM = aortic mean pressure in mmHg.

-- = data not available.

Note: The organ perfusion and blood pressure parameters were measured every 6 minutes from 222 to 300 minutes postdosing. Half of the 3-minute averages presented in this raw data from 222 to 300 minutes are means of the 2 closest 6-minute values. Example: The 261-minute organ perfusion and blood pressure values were derived by taking the mean of the data collected at 258 and 264 minutes. Six-minute means for hepatic and renal perfusion and arterial mean pressure were calculated from this raw data.

Time	Kid1	Liv1	Liv2	Liv3	Liv4	AoM
-27	6.34	3.7	1.79	2.8	3.62	103.7
-24	6.04	3.65	1.36	3.25	3.92	105.1
-21	5.52	--	1.55	2.2	3.94	100.8
-18	5.21	4.14	1.47	2.91	3.17	96.8
-15	6.32	3.31	1.79	3.05	4.15	99
-12	6.15	3.84	1.4	3.67	3.78	100.9
-9	6.27	3.64	1.54	2.91	3.61	104.3
-6	6.07	3.17	1.47	3.2	3.4	103.1
-3	5.57	3.99	1.25	3.42	3.12	105.1
0	6.04	3.05	1.4	3.79	4.13	108
3	7.22	4	1.48	3.92	2.96	110.3
6	6.79	2.41	1.23	3.08	3.22	109.5
9	5.98	2.5	1.28	3.77	3.06	107.1
12	5.57	4.35	1.7	3.61	3.22	103.2
15	5.92	3.66	1.25	3.69	3.45	105
18	5.08	1.73	1.1	0.92	3.34	102.1
21	6.14	2.83	1.21	2.59	3.22	97.6
24	5.55	2.12	1.09	1.18	2.57	103.2
27	5.28	1.85	1.04	1.44	3.09	99
30	4.89	0.87	0.87	0.3	1.86	99.9
33	5.35	1.08	0.65	0	2.15	99.9
36	5.03	1.01	0.96	0.74	2.29	97.4
39	4.29	1.01	0.78	0	1.89	98.2
42	4.09	0.75	0.89	2.22	2.57	96.8
45	3.63	0.87	1.01	0	2	94.4
48	3.43	--	0.91	0.54	0.54	71

Time	Kid1	Liv1	Liv2	Liv3	Liv4	AoM
51	3.74	2.27	0.83	2.44	1.57	59.7
54	2.21	1.14	0.34	--	0.53	55.2
57	2.24	1.89	1.24	1.68	1.25	62
60	1.3	1.05	0.81	0	0.69	53.6
63	3.39	1.94	1.63	1.2	1.71	55
66	0	1.08	0.8	0	0.77	54.2
69	0.5	1.23	1.05	0	1.01	53.3
72	2.03	1.08	1.03	0	1.02	52.3
75	--	--	--	--	--	57
78	--	--	--	--	--	53.7
81	1.5	0.92	0.99	0	0.65	49.1
84	1.88	1.29	1.55	0.51	1.29	53
87	0.77	0.67	0.61	--	0.38	50.6
90	2.43	1.05	1.57	0.58	1.31	51.1
93	--	--	2.96	2	0	46.7
96	1.57	--	1.87	0.22	0	48.3
99	1.78	0.16	1.44	0	0	44.6
102	1.47	0.59	1.75	0	0	45.4
105	1.95	0.65	1.68	0	0	46
108	2.01	0.7	2.07	0	0.24	43.8
111	3.93	1.22	3.45	1.29	1.42	43.8
114	--	2.05	4.35	2.23	2.97	50.6
117	4.07	1.35	3.93	2.62	2.21	46.5
120	2.25	1.19	2.34	0.54	0.44	45.6
123	1.16	0.83	1.84	0	0	41.7
126	2.31	1.15	2.02	0	0.64	50.1
129	5.17	1.64	3.78	2.68	2.3	46.2
132	1.73	0.67	1.75	0	0.23	46.5
135	0.32	0.74	1.62	0	0	47.1
138	2.93	1.11	2.85	0.89	1.24	42.4
141	1.46	0.86	1.29	--	0.14	49.6
144	4.76	1.66	4.04	2.04	2.58	47.5
147	3.91	1.65	4.52	2.74	3.7	44.7
150	1.39	0.86	1.93	0	0.08	49.7
153	0.1	1.17	3.62	1.29	1.25	49.4
156	0	1.11	4.37	2.89	2.31	47.7
159	0.57	0.59	2.14	--	0.66	43.2
162	0.47	0.72	2.24	0.95	1.08	44
165	0	1.11	2.77	0.14	1.09	46
168	0.17	1.15	3.24	0.3	1.44	44.5
171	0.58	0.81	1.74	0	0.45	44.2
174	0.68	1.62	4.21	2.58	3.89	44.2
177	0	0.97	1.72	--	0.5	46
180	0.64	0.52	0.8	--	0	47.5
183	0.49	0.75	1.21	0	0	47.1
186	0.49	0.86	2.38	0	1	42.4
189	0.67	0.9	2.96	0.04	2.05	42.2
192	0	0.52	1.74	0	0.23	40.7
195	0	0.71	1.59	--	0	39.1

Time	K1d1	L1v1	L1v2	L1v3	L1v4	AOM
198	0	0.75	2.09	0.47	0.73	39.3
201	0	0.85	2.98	0	1.3	40.9
204	0.06	0.96	2.25	0.12	1.03	40.4
207	0.37	1.05	2.01	0	0	41.5
210	0.09	1.15	2.06	0	0.16	41.8
213	0	1.15	2.33	0	0.18	42.6
216	0	1.1	2.73	0	0.06	45.2
219	0.07	1.04	1.94	0	0.57	43.1
222	0.08	1.21	2.89	1.69	0.98	42.1
225	0.04	1.11	2.82	1.09	1	42
228	0	1.01	2.75	0.48	1.02	41.8
231	0.09	1.28	2.65	0.32	0.94	41.8
234	0.17	1.55	2.54	0.15	0.85	41.7
237	0.09	1.49	2.01	0.08	0.43	41.8
240	0	1.42	1.47	0	0	41.8
243	0	1.46	2.04	0.63	0.8	41.5
246	0	1.5	2.61	1.25	1.6	41.1
249	0	1.47	2.29	0.63	0.96	40.8
252	0	1.44	1.96	0	0.32	40.4
255	0	1.34	2.13	0.04	0.61	43.1
258	0	1.23	2.3	0.08	0.89	45.8
261	0.18	1.25	2.06	0.04	0.58	43.9
264	0.35	1.27	1.82	0	0.27	42
267	0.18	1.26	2.12	0.12	0.97	42.5
270	0	1.24	2.42	0.23	1.67	43
273	0	1.23	1.81	0.12	0.86	41.8
276	0	1.21	1.19	0	0.05	40.7
279	0	1.06	1.65	0	0.37	40
282	0	0.91	2.1	0	0.69	39.4
285	0.15	1.11	1.96	0	0.59	38.7
288	0.29	1.31	1.81	0	0.49	38
291	0.15	1.32	1.65	0	0.25	35.8
294	0	1.32	1.49	0	0	33.5
297	0	1.15	1.8	0	0.65	35
300	0	0.98	2.1	0	1.29	36.6

GILT #3306

72 µg/kg MCYST-A iv

Time = minutes in relation to the dose of MCYST-A.

Kid1, Kid2, and Kid3 = kidney perfusion measured from 1 TPD (temperature pulse decay) probe in ml/min gm.

Liv1, Liv2, and Liv3 = liver perfusion measured from 3 TPD probes in ml/min gm.

AoM = aortic mean pressure in mmHg.

-- = data not available.

Note: Six-minute means for hepatic and renal perfusion and arterial mean pressure were calculated from this raw data.

Time	Kid1	Liv1	Liv2	Liv3	AoM
-27	3.1	2.43	3.25	3.33	113.7
-24	2.66	2.79	3.2	3.33	114.5
-21	3.83	2.22	4.66	3.05	111.1
-18	2.3	2.67	2.67	2.49	114.3
-15	2.93	2.5	2.98	3.14	113.6
-12	2.73	2.3	3.19	2.67	114.7
-9	2.99	2.59	3.48	3.61	114
-6	2.38	2.61	2.98	1.17	116.9
-3	1.72	3.61	2.61	1.88	116.5
0	4.18	2.41	4.08	--	116.2
3	1.17	3.17	1.65	1.71	124.2
6	3.58	1.32	3.38	2.16	120.9
9	--	2.62	2.67	2.11	119.1
12	2.55	2.43	3.84	3.26	120.2
15	3.19	2.92	2.97	4.1	117.3
18	2.83	3.06	2.59	2.47	116.1
21	1.33	3.84	2.06	2.16	110.9
24	0	3.86	1.51	1.89	108.1
27	0	2.93	1.48	0	96.2
30	2.74	2.99	1.04	1.17	84.9
33	1.34	3.09	0	0.16	70.3
36	1.32	4.63	0.94	2.37	76.1
39	0	3.23	0	1.06	56.7
42	1.77	3.5	2.33	0.99	63.3
45	0	2.96	0	0	50.7
48	0	3.05	0.18	0	45
51	0.09	2.1	0.42	0	42.2
54	0	1.87	0.56	0	43.8
57	0	2.17	0.24	1.48	41.1
60	0.36	1.44	0.51	1.02	39.6
63	0.21	0.82	0.03	0.27	35.2
66	0	0.76	0.44	0.09	34.6

Time	Kid1	Liv1	Liv2	Liv3	AoM
69	0	1.32	0.39	0	32.8
72	0	0.9	0	0	29.9
75	0	0.72	0	0	28.4
78	0	0.63	0	0	26.4
81	0	0.43	0	0	23.9
84	0	0.37	0	0	19.8

VRB:11b/37
12/12/88

APPENDIX TO SECTION XIII

NT = no treatment.

NA = not available.

TOX = 55 µg/kg of microcystin-A ip on 3/30/87.

TOX = 75 µg/kg of microcystin-A ip on 4/2/87.

VEH = vehicle at equivalent amounts as toxin-treated mice.

TRT GRP = treatment group

WT = weight.

SURV TIME (min) = survival time in minutes.

g = grams.

%-bw = organ weight as a percentage of live body weight.

ln-bw = natural log of the %-bw.

IDENT = identification (cage and color).

Means \pm SD = column mean plus or minus the standard deviation.

CONTROL

IDENT	3/30/87		4/2/87		SURV TIME (min)	KIDNEY WEIGHTS			LIVER WEIGHTS		
	TRT GRP	WT (g)	TRT GRP	WT (g)		grams	%-bw	ln-bw	grams	%-bw	ln-bw
15-GRE	NT	NA	VEH	32.34	1445	0.39	1.21	0.187	1.70	5.26	1.659
15-BLU	NT	NA	VEH	29.97	1449	0.35	1.17	0.155	1.66	5.54	1.712
15-ORA	NT	NA	VEH	36.83	1452	0.45	1.22	0.200	2.07	5.62	1.726
15-PUR	NT	NA	VEH	35.07	1455	0.45	1.28	0.249	1.95	5.56	1.716
15-BRO	NT	NA	VEH	35.68	1458	0.45	1.26	0.232	1.65	4.62	1.531
15-RED	NT	NA	VEH	31.42	1463	0.37	1.18	0.163	1.53	4.87	1.583
14-GRE	VEH	31.49	VEH	32.76	5992	0.36	1.10	0.094	1.67	5.10	1.629
14-ORA	VEH	32.28	VEH	34.46	6003	0.39	1.13	0.124	2.04	5.92	1.778
14-PUR	VEH	30.52	VEH	32.73	6005	0.45	1.37	0.318	1.82	5.56	1.716
14-BRO	VEH	32.28	VEH	34.46	6011	0.50	1.45	0.372	1.86	5.40	1.686
14-RED	VEH	31.44	VEH	34.14	6015	0.38	1.11	0.107	1.72	5.04	1.617
13-GRE	VEH	29.15	VEH	30.96	1467	0.38	1.30	0.265	1.56	5.04	1.617
13-BLU	VEH	31.19	VEH	33.42	1470	0.41	1.23	0.204	1.94	5.80	1.759
13-ORA	VEH	30.94	VEH	32.75	1474	0.41	1.25	0.225	1.74	5.31	1.670
13-PUR	VEH	29.21	VEH	30.49	1478	0.37	1.21	0.194	1.54	5.05	1.620
13-BRO	VEH	29.89	VEH	30.95	1480	0.34	1.10	0.094	1.79	5.78	1.755
13-RED	VEH	30.96	VEH	33.03	1483	0.35	1.06	0.058	1.79	5.42	1.690
Means						0.191			1.674		
± SD						± 0.0833			± 0.0676		

PERACUTE DEATH

IDENT	3/30/87		4/2/87		SURV TIME (min)	KIDNEY WEIGHTS			LIVER WEIGHTS		
	TRT GRP	WT (g)	TRT GRP	WT (g)		grams	%-bw	ln-bw	grams	%-bw	ln-bw
19-GRE	NT	NA	TOX	30.00	149	0.49	1.63	0.491	2.39	7.97	2.075
19-BLU	NT	NA	TOX	29.83	151	0.45	1.51	0.411	2.27	7.61	2.029
19-ORA	NT	NA	TOX	33.95	158	0.52	1.53	0.426	2.88	8.48	2.138
19-PUR	NT	NA	TOX	31.74	149	0.51	1.61	0.474	2.46	7.75	2.048
19-BRO	NT	NA	TOX	31.83	145	0.40	1.25	0.228	2.30	7.23	1.978
19-RED	NT	NA	TOX	31.95	133	0.47	1.47	0.386	2.60	8.14	2.097
18-GRE	NT	NA	TOX	31.45	98	0.53	1.69	0.522	2.71	8.62	2.154
18-BLU	NT	NA	TOX	34.62	109	0.46	1.33	0.284	2.82	8.15	2.097
18-ORA	NT	NA	TOX	30.86	121	0.40	1.30	0.259	2.49	8.07	2.088
18-PUR	NT	NA	TOX	31.48	151	0.41	1.30	0.264	2.60	8.26	2.111
18-BRO	NT	NA	TOX	31.55	117	0.43	1.36	0.310	2.42	7.67	2.037
18-RED	NT	NA	TOX	32.36	119	0.47	1.45	0.373	2.72	8.41	2.129
17-GRE	NT	NA	TOX	31.23	162	0.44	1.41	0.343	2.44	7.81	2.056
17-BLU	NT	NA	TOX	34.16	200	0.52	1.53	0.423	2.55	7.49	2.013
17-ORA	NT	NA	TOX	31.52	119	0.48	1.52	0.421	2.86	9.07	2.205
17-PUR	NT	NA	TOX	30.73	175	0.43	1.40	0.336	2.39	7.78	2.051
17-BRO	NT	NA	TOX	32.54	138	0.50	1.54	0.430	2.67	8.21	2.105
17-RED	NT	NA	TOX	33.73	145	0.45	1.33	0.288	2.45	7.26	1.983
16-GRE	NT	NA	TOX	32.52	165	0.44	1.35	0.302	2.57	7.90	2.067
16-BLU	NT	NA	TOX	30.57	129	0.48	1.57	0.451	2.68	8.77	2.171
16-ORA	NT	NA	TOX	34.18	102	0.49	1.43	0.360	2.82	8.25	2.110
16-PUR	NT	NA	TOX	34.44	147	0.43	1.25	0.222	2.73	7.93	2.070
16-BRO	NT	NA	TOX	30.46	116	0.46	1.51	0.412	2.44	8.01	2.081
16-RED	NT	NA	TOX	29.79	150	0.52	1.75	0.557	2.55	8.56	2.147
Mean										2.085	
± SD										± 0.0566	
03-ORA	TOX	31.51	--	---	121	0.46	1.46	0.378	2.30	7.30	1.988
03-BRO	TOX	30.52	---	---	152	0.37	1.21	0.193	2.07	6.78	1.914
03-RED	TOX	29.42	---	---	158	0.41	1.39	0.332	2.32	7.89	2.065
02-ORA	TOX	30.46	---	---	162	0.41	1.35	0.297	2.37	7.78	2.052
06-BRO	TOX	31.32	---	---	163	0.46	1.47	0.384	2.50	7.98	2.077
08-ORA	TOX	28.48	---	---	171	0.44	1.54	0.435	2.29	8.04	2.085
08-RED	TOX	31.55	---	---	179	0.48	1.52	0.420	2.46	7.80	2.054
07-GRE	TOX	28.17	---	---	197	0.37	1.31	0.273	2.05	7.28	1.985
05-BLU	TOX	32.22	---	---	287	0.46	1.43	0.356	2.35	7.29	1.987
Mean										2.023	
± SD										± 0.0572	

PERACUTE DEATH (continued)

IDENT	3/30/87		4/2/87		SURV TIME (min)	KIDNEY WEIGHTS			LIVER WEIGHTS		
	TRT GRP	WT (g)	TRT GRP	WT (g)		grams	%-bw	ln-bw	grams	%-bw	ln-bw
09-GRE	VEH	31.99	TOX	33.54	126	0.53	1.58	0.455	2.68	7.97	2.075
09-BLU	VEH	30.16	TOX	31.19	154	0.44	1.41	0.344	2.41	7.73	2.045
09-ORA	VEH	27.61	TOX	28.84	129	0.44	1.53	0.422	2.23	7.73	2.045
09-PUR	VEH	31.59	TOX	34.43	139	0.46	1.34	0.290	2.62	7.61	2.029
09-BRO	VEH	28.30	TOX	31.26	156	0.45	1.44	0.364	2.45	7.84	2.059
09-RED	VEH	32.18	TOX	35.74	165	0.47	1.32	0.274	2.83	7.92	2.069
10-BLU	VEH	29.96	TOX	32.07	135	0.50	1.56	0.444	2.43	7.58	2.025
10-ORA	VEH	33.82	TOX	36.64	134	0.50	1.36	0.311	2.51	6.85	1.924
10-BRO	VEH	31.90	TOX	36.08	138	0.42	1.16	0.152	2.70	7.48	2.013
10-RED	VEH	28.07	TOX	31.00	137	0.45	1.45	0.373	2.38	7.68	2.038
11-GRE	VEH	29.55	TOX	32.16	192	0.48	1.49	0.400	2.47	7.68	2.039
11-BLU	VEH	29.29	TOX	34.00	182	0.52	1.53	0.425	2.79	8.21	2.105
11-ORA	VEH	31.21	TOX	33.25	169	0.49	1.47	0.388	2.66	8.00	2.079
11-BRO	VEH	29.28	TOX	32.82	137	0.45	1.37	0.316	2.49	7.59	2.026
12-GRE	VEH	29.00	TOX	31.26	148	0.47	1.50	0.408	2.41	7.71	2.042
12-ORA	VEH	27.59	TOX	30.13	137	0.49	1.63	0.486	2.42	8.03	2.083
12-PUR	VEH	30.38	TOX	33.01	154	0.45	1.36	0.310	2.57	7.79	2.052
12-BRO	VEH	29.11	TOX	30.99	133	0.46	1.58	0.458	2.82	9.10	2.208
12-RED	VEH	26.73	TOX	27.82	155	0.45	1.62	0.481	2.28	8.20	2.104
Mean										2.056	
± SD										± 0.0540	
06-PUR	TOX	27.42	TOX	29.09	263	0.44	1.51	0.414	2.30	7.91	2.068
06-BLU	TOX	29.47	TOX	31.20	181	0.47	1.51	0.410	2.85	9.13	2.212
08-BLU	TOX	29.42	TOX	30.89	194	0.52	1.68	0.521	2.78	9.00	2.197
08-PUR	TOX	30.41	TOX	33.05	172	0.51	1.54	0.434	2.71	8.20	2.104
05-GRE	TOX	30.28	TOX	32.10	192	0.43	1.34	0.292	2.73	8.50	2.141
05-ORA	TOX	28.20	TOX	29.04	229	0.43	1.48	0.393	2.59	8.92	2.188
05-PUR	TOX	30.30	TOX	31.62	174	0.42	1.33	0.284	2.82	8.92	2.188
03-PUR	TOX	28.69	TOX	30.32	319	0.49	1.62	0.480	2.40	7.92	2.069
01-GRE	TOX	31.34	TOX	33.42	184	0.45	1.35	0.298	2.86	8.56	2.147
01-ORA	TOX	29.80	TOX	31.38	189	0.44	1.40	0.338	2.74	8.73	2.167
02-GRE	TOX	29.23	TOX	29.12	192	0.49	1.68	0.520	2.38	8.17	2.101
02-PUR	TOX	30.29	TOX	32.37	286	0.50	1.54	0.435	2.80	8.65	2.158
04-GRE	TOX	31.97	TOX	33.31	197	0.49	1.45	0.368	2.99	8.82	2.177
04-ORA	TOX	33.42	TOX	34.91	203	0.51	1.46	0.379	3.31	9.48	2.249
04-RED	TOX	30.89	TOX	32.43	246	0.44	1.36	0.305	2.63	8.11	2.093
Means							0.373		2.151		
± SD							± 0.0844		± 0.0541		

ACUTE DEATH

IDENT	3/30/87		4/2/87		SURV TIME (min)	KIDNEY WEIGHTS			LIVER WEIGHTS		
	TRT GRP	WT (g)	TRT GRP	WT (g)		grams	%-bw	ln-bw	grams	%-bw	ln-bw
02-BLU	TOX	29.23	---	---	370	0.40	1.37	0.314	1.93	6.60	1.887
06-GRE	TOX	31.93	---	---	1524	0.45	1.41	0.343	2.04	6.39	1.855
Mean										1.871	
± SD										± 0.0226	
10-PUR	VEH	31.08	TOX	34.45	1280	0.40	1.16	0.149	2.21	6.42	1.859
11-PUR	VEH	28.05	TOX	30.10	1255	0.46	1.53	0.424	2.10	6.98	1.943
Mean										1.901	
± SD										± 0.0594	
03-GRE	TOX	28.16	TOX	29.68	414	0.41	1.38	0.323	2.26	7.61	2.030
01-PUR	TOX	30.33	TOX	31.61	686	0.45	1.42	0.353	2.43	7.69	2.040
01-RED	TOX	30.81	TOX	32.48	833	0.48	1.48	0.391	2.47	7.60	2.029
05-RED	TOX	32.53	TOX	35.03	1208	0.48	1.37	0.315	2.60	7.42	2.004
07-RED	TOX	32.46	TOX	34.92	1237	0.53	1.52	0.417	2.55	7.30	1.988
08-BRO	TOX	29.81	TOX	30.23	2005	0.40	1.32	0.280	2.31	7.64	2.034
06-ORA	TOX	28.59	TOX	29.61	2645	0.45	1.52	0.419	2.18	7.36	1.956
Means							0.339		2.017		
± SD							± 0.0798		± 0.0207		

SUBACUTE DEATH

IDENT	3/30/87		4/2/87		SURV TIME (min)	KIDNEY WEIGHTS			LIVER WEIGHTS		
	TRT GRP	WT (g)	TRT GRP	WT (g)		grams	%-bw	ln-bw	grams	%-bw	ln-bw
02-BRO	TOX	30.71	TOX	32.54	2928	0.40	1.23	0.206	2.02	6.21	1.826
04-BLU	TOX	28.54	TOX	30.48	2953	0.42	1.38	0.321	2.17	7.12	1.963
04-BRO	TOX	30.94	TOX	32.26	3217	0.41	1.27	0.240	2.24	6.94	1.938
06-RED	TOX	30.20	TOX	33.05	3391	0.39	1.18	0.166	2.28	6.90	1.931
03-BLU	TOX	31.08	TOX	30.75	3830	0.40	1.30	0.263	1.87	6.08	1.805
04-PUR	TOX	29.85	TOX	32.10	3909	0.39	1.21	0.195	2.46	7.66	2.036
05-BRO	TOX	29.46	TOX	31.65	4864	0.50	1.58	0.457	2.03	6.41	1.858
02-RED	TOX	30.68	TOX	32.21	5357	0.37	1.15	0.139	1.92	5.96	1.785
Means								0.248			1.893
± SD								± 0.1018			± 0.0878

SURVIVOR

IDENT	3/30/87		4/2/87		SURV TIME (min)	KIDNEY WEIGHTS			LIVER WEIGHTS		
	TRT GRP	WT (g)	TRT GRP	WT (g)		grams	%-bw	ln-bw	grams	%-bw	ln-bw
11-RED*	VEH	28.02	TOX	28.94	5951	0.38	1.31	0.272	1.81	6.25	1.833
12-BLU*	VEH	27.75	TOX	30.66	5911	0.40	1.30	0.266	1.79	5.84	<u>1.764</u>
Mean											1.799
± SD											± 0.0488
01-BLU	TOX	30.28	TOX	30.59	5830	0.31	0.98	-0.019	2.08	6.80	1.917
07-BLU	TOX	32.15	TOX	34.27	5904	0.43	1.25	0.227	2.39	6.97	1.942
07-ORA	TOX	28.68	TOX	31.57	5907	0.35	1.11	0.103	2.58	8.17	2.101
07-PUR	TOX	28.85	TOX	31.57	5910	0.37	1.17	0.159	2.46	7.79	2.053
07-BRO	TOX	30.97	TOX	34.61	5913	0.42	1.21	0.194	2.77	8.00	2.080
08-GRE	TOX	31.27	TOX	35.58	5951	0.40	1.12	0.117	2.70	7.59	2.027
01-BRO*	TOX	29.76	TOX	29.53	5829	0.40	1.35	<u>0.303</u>	1.74	5.85	<u>1.766</u>
Means								0.180			1.984
± SD								± 0.1021			± 0.1178

* = did not show any ill effects

14-BLU VEH 30.26 VEH 31.17 5996 0.28 0.90 -0.107 1.28 4.11 1.413
Removed from study due to a visibly small kidney.

10-GRE VEH 27.91 TOX 30.11 5984 0.43 1.43 0.350 1.54 5.11 1.632
Removed from study due to highly suspected toxin injection into urinary bladder.

VRB:11b/37
12/12/88

DISTRIBUTION LIST

4 copies	Commander US Army Medical Research Institute of Infectious Diseases ATTN: SGRD-UII-M Fort Detrick, Frederick, MD 21701-5011
1 copy	Commander US Army Medical Research and Development Command ATTN: SGRD-RMI-S Fort Detrick, Frederick, MD 21701-5012
2 copies	Defense Technical Information Center (DTIC) ATTN: DTIC-DDAC Cameron Station Alexandria, VA 22304-6145
1 copy	Dean School of Medicine Uniformed Services University of the Health Sciences 4301 Jones Bridge Road Bethesda, MD 20814-4799
1 copy	Commandant Academy of Health Sciences, US Army ATTN: AHS-CDM Fort Sam Houston, TX 78234-6100
